UNIVERSITÀ DEGLI STUDI DI MESSINA

DIPARTIMENTO DI SCIENZE CHIMICHE, BIOLOGICHE, FARMACEUTICHE ED AMBIENTALI

DOTTORATO DI RICERCA IN SCIENZE CHIMICHE
XXXIV CICLO
S.S.D. CHIM/01

STUDY OF THE THERMODYNAMIC PROPERTIES OF SOME MOLECULES OF BIOLOGICAL INTEREST

PhD thesis of:
Antonio GIGLIUTO

Supervisor:
Prof. Francesco CREA

PhD Coordinator:
Prof.ssa Paola DUGO

Academic year 2020/2021

Index

Chapter 1

Introduction

1.1 Speciation

In recent years, a big attention has been paid to the study of molecules such as metals, organic and inorganic compounds, that play fundamental roles in the human body and in the environment. It is already known that the biological and chemical activity of these substances can be attributed only to some of the chemical forms in which they are present in the biological and natural fluids [1]. To understand better their mechanism of action, it is necessary to know not only their analytical concentration, but also their "*speciation*". This term, also used in natural science but with a different meaning, indicates the distribution of the different physical and chemical forms (isotopic composition, electronic or oxidation state, inorganic compounds and complexes, organometallic compounds, organic and macromolecular complexes) in which a component is present in a system, where it can participate to various processes of formation of chemical species through different types of reactions (strong and weak interactions, complex formations, etc), to the effect of parameters such as temperature, pH, ionic strength and ionic medium [2]. In this context it is possible to obtain important information on the behavior of molecules, such as their transport, adsorption, desorption, dissolution, metal-complexation and toxicity, bioavailability.

Examples of applications of the speciation studies, diffused in the fields of food, clinical and environmental chemistry, biogeochemistry, medicine, pharmacy, and industry, are reported in **Table 1.1**.

Due to the incredible variety and diversity of biological (blood, plasma, urine) and natural (seawater, fresh water) fluids and to the high number of species that we can find on Earth, performing speciation studies in conditions like these multi-component systems could appear a relevant issue. Considering a drug, it can be transported, adsorbed, and performing its function if it is present in a specific pharmacological form in the human body. On the other hand, if we focus our attention on a particular neurotransmitter that must bind a specific receptor, its action could be speeded up, slowed down or even blocked in the presence of a metal with which the neurotransmitter could form metal-ligand complex species. A further example concerns the presence of potentially toxic metals (in ionic or complexed form) that induce reactions leading to the formation of free radicals that can be harmful from many points of view for the human body and in environmental matrices.

Table 1.1. Examples of applications of the speciation studies.

Element (Symbol)	Application area of speciation analysis
Aluminium (Al)	Polymerization products. Forms of aluminium (*e.g.*, labile, complexed) in serum.
Antimony (Sb)	Redox forms and organoantimony compounds in the environment and food products.
Arsenic (As)	Redox forms and organoarsenic compounds in the environment. Arsenic-bound proteins in serum and hemoglobin. Arsenic in food products. Forms of arsine AsH_3 (arsenious hydride) in indoor air at the workplace.
Cadmium (Cd)	Complex organic cadmium compounds, metallothionine.
Chromium (Cr)	Redox forms of chromium, Cr(VI) in the environment. Chemical forms of chromium coupled with proteins.
Iodine (I)	Iodine forms in the environment and biological fluids.
Lead (Pb)	Forms of lead compounds in the environment, *e.g.*, trialkylated Pb compounds.
Phosphorus (P)	Phosphine (hydrogen phosphides) in indoor air at workplace
Mercury (Hg)	Forms of mercury compounds in the environment and food products (in particular methylmercury).
Platinum (Pt)	Inorganic forms in the environment. Metal-organic forms of cis-platinum in medicine (therapeutic).
Selenium (Se)	Inorganic and organometallic selenium compounds in the environment and food products (*e.g.*, potatoes).
Tin (Sn)	Organometallic forms in the environment and food products (*e.g.*, shellfish)
Actinide series	Chemical forms of compounds in the environment and in radioactive waste storage places.

Furthermore, a chemical substance, at certain doses or concentrations or in different oxidation states, could cause disturbances or damage to living organisms (animals or plants) to which it has been administered or with which they have come into contact. For example, a high-dose mercury is very toxic, but it can become even more dangerous if it is found in the organometallic form as

organomercury (methylmercury, ethylmercury, etc.). Furthermore, Cr(III) is essential and participates in the metabolism of glucose, while Cr(VI) is highly toxic and carcinogenic [3]. Therefore, different "species" or chemical forms of the same element can have different toxicity levels.

Using new instrumentation and analytical methods such as potentiometry (ISE-H^+), UV-Vis spectrophotometry, spectrofluorimetry, calorimetry, nuclear magnetic resonance (NMR), voltammetry, electrophoresis, gas chromatography (GC), high performance liquid chromatography (HPLC), hyphenated methods (*e.g.* GC-MS, LC-MS, GC-ICP-MS) is therefore possible to detect and quantify the species present in a particular system.

The approach used by the research group where the PhD work presented in this thesis was performed, to carry out speciation studies, has a thermodynamic nature, based on the determination of thermodynamic properties (*e.g.* equilibrium constants K_{eq}, dependence of thermodynamic parameters on ionic strength and temperature) related to the formation of the species in the considered system.

In this thesis, although the investigated molecules are very different from each other in term of molecular structures and have different functions, they are essential or have healthy or therapeutical effects for the human body.

The ligands under study can be divided into three categories:

- neurotransmitters: Dopamine;
- antibacterials: Ornidazole and Ofloxacin;
- amino acids: Tryptophane and Histidine.

The investigated metal cations can be classified based on their position on the periodic table and on their metallic or organometallic nature. Along the text the following three groups will be considered:

- group A metals: Ca^{2+}, Mg^{2+}, Sn^{2+};
- group B metals: UO_2^{2+}, Cd^{2+}, Cu^{2+}, Mn^{2+}, Zn^{2+};
- organometals: CH_3Hg^+, $(CH_3CH_2)_2Sn^{2+}$.

1.2 Neurotransmitters

1.2.1 Dopamine

Dopamine, also known as 4-(2-aminoethyl)benzene-1.2-diol as IUPAC name, is an important molecule for the nervous system. It is part of the family of catecholamines, molecules featured by a structure containing a catechol, an aromatic ring with two hydroxy groups in position 1 and 2 (**Figure 1.1**) and a lateral amino chain in position 4 [4].

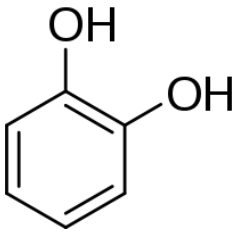

Figure 1.1. Catechol structure

In the human body, the most abundant catecholamines, in addition to dopamine, are epinephrine (or adrenaline) and norepinephrine

Catecholamines are synthesized starting from precursors such as phenylalanine or tyrosine (synthesis shown in **Figure 1.2**, are 50% water-soluble and are found bound to plasma proteins in blood vessels.

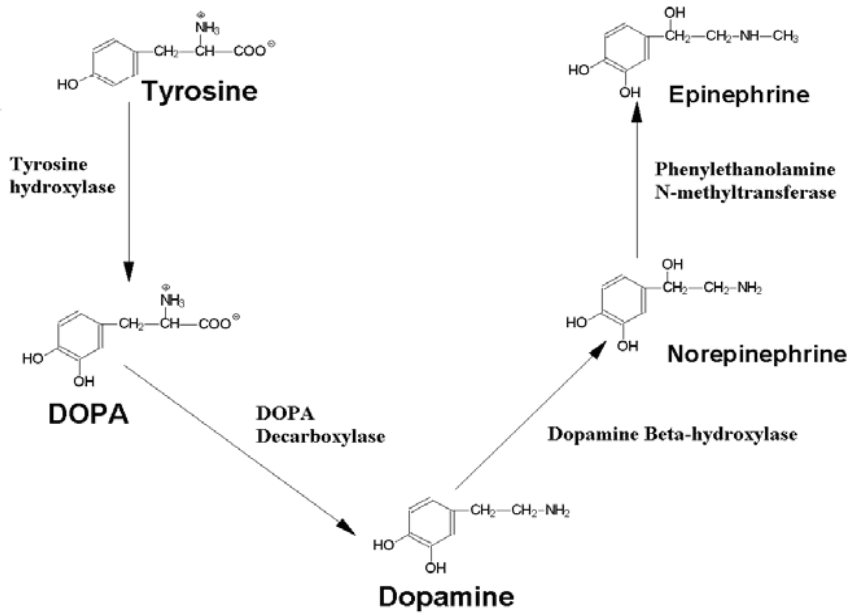

Figure 1.2. Catecholamine synthesis

Catecholamines such as adrenaline and dopamine, act as central nervous system modulators and as hormones in the bloodstream, while the release of adrenaline and norepinephrine from the adrenal medulla of the adrenal glands is part of the fight or flight response [5].

In many cases, stress depends on high levels of catecholamines in the blood, which can be induced by psychological reactions or environmental stressors such as high levels of noise, bright light, or other hormonal response. If the concentrations of catecholamines are extremely high, catecholamine toxicity can occur due to trauma to the central nervous system owing to stimulation and / or damage to the nuclei concerning the sympathetic nervous system, responsible for the person voluntary actions.

Dopamine was for the first time synthesized in 1910 by George Barger and James Ewens at Wellcome Laboratories in London, England [6]. Its structure is reported in **Figure 1.3**.

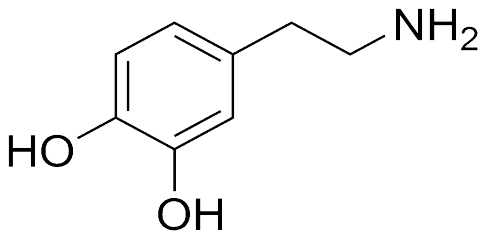

Figure 1.3. Dopamine structure

The neurotransmitter behavior was already known since 1958[7] by Arvid Carlsson and Nils-Åke Hillarp, but only in the 2000s its hormonal action and its biogenic synthesis have been discovered. As a medicinal agent, dopamine is synthesized by demethylation of 2-(3,4-dimethoxyphenyl)ethylamine using hydrobromic acid [8, 9] and following the reaction reported in **Figure 1.4.**

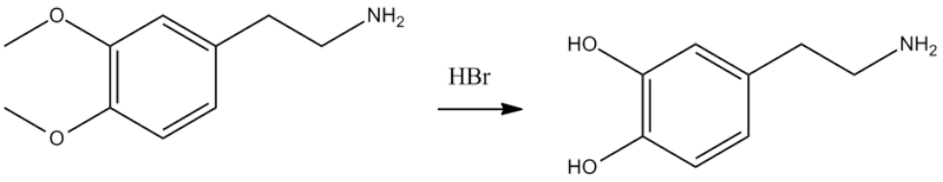

Figure 1.4. Dopamine synthesis

Dopamine is believed to be the primary neurotransmitter of the sympathetic nervous system. Neurotransmitters are ligands used for the transmission of nerve impulses in the human body; they are synthesized by the neurons and are released at the proper moment in different areas of the body to act in a specific way with a postsynaptic cell. Dopamine is the main neuroendocrine inhibitor of prolactin secretion from the anterior pituitary gland [10].

It is produced by neurons in the arcuate nucleus of the hypothalamus, it is secreted into the hypothalamic-hypophysial blood vessels of the median eminence, which supply the pituitary gland. It is also produced in several areas of the brain, including the substantia nigra and the ventral segmental area.

Dopamine is a hormonal regulator of the cardiovascular and urinary system; induces natriuresis (sodium loss) in the kidneys and has a diuretic effect [11, 12]; it is also used in patients with shock or heart failure to increase cardiac output and blood pressure [13].

Diseases of the nervous system, such as Parkinson's one, are associated with a degenerative condition linked to the loss of dopamine-secreting neurons in the substantia nigra. The opposite and widely demonstrated [14, 15] condition occurs in patients with Schizophrenia, who have high levels of dopaminergic activity in the mesolimbic pathway and low in the prefrontal cortex.

It is known that dopamine is also released at the level of the synapses of the central nervous system, where it plays the role of a neurotransmitter by interacting with dopaminergic receptors. For this reason and for being released at the end of a reflex pathway involving both the nervous and endocrine systems, dopamine is one of the neurohormones.

Dopaminergic receptors are coupled to G proteins. There are two types of receptors, different in pharmacological and biochemical characteristics, with a different binding affinity for both dopamine itself and for other agonists and antagonists.

For example, dopaminergic D1 receptors have various functions, such as: the activation of adenylate cyclase and through it they mediate the phosphorylation of some proteins; or they mediate the response of peripheral blood vessels and ultimately activate phospholipases that cause calcium mobilization.

Another example of dopaminergic receptors are those of class D2 coupled to different translation systems that have many fundamental functions, such as: inhibition of adenylate cyclase, reduction of CaAMP which determines the opening or closing of Ca and K channels [16].

Dopamine occurs as a white or almost white, odorless, microcrystalline or granular substance. Exposure to light or air causes darkening. From the data reported in the literature it is clear that dopamine is quite soluble in water and this solubility depends on the pH. The minimum solubility values are obtained at pH≈9.4, but the formation of ionic species following its solubility further increases its solubility. It is a rather unstable compound and susceptible to decomposition in the solid state. Its release is linked to the perception of motor stimuli; all these stimuli are processed at the hypothalamic level, where they evoke a response of the parasympathetic nervous system.

In Parkinson's disease the concentration of dopamine has to be increased, but it cannot be introduced as it is because it would be metabolized, therefore it is administered as L-DOPA and CARBO-DOPA (which has no activity).

Dopamine which has performed its function has to be eliminated from the synaptic cleft and it can be made in two ways: by degradation, by enzymes or by reuptake.

The latter mode is mediated by specific transport proteins. These proteins can be inhibited by creating an increase in dopamine levels (ideal for Parkinson's). An inhibitor is cocaine which has a high affinity for these proteins. Cocaine, depending on how it is administered, has a different action (usually all drugs of abuse increase dopamine levels); it can also act as a local anesthetic if chewed.

Cocaine, when used as an anesthetic, is found in the Na channels blocking the pumping system and consequently blocking nerve impulses.

1.3 Amino acids

Amino acids are the most versatile small biomolecules. They fulfil a number of extremely important roles in biology, such as building block of proteins, they are precursors of hormones and of molecules with specialized physiological function, e.g., the neurotransmitter dopamine and the hormone thyroxine are both derivatives of the Tyrosine [17].

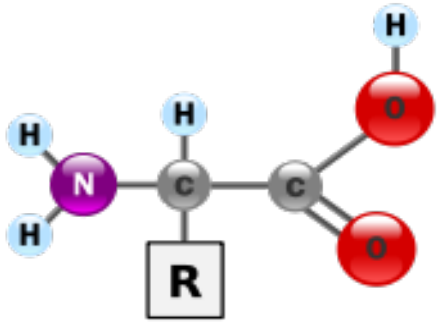

Figure 1.5. Structure of a generic amino acid

The generic structure of an amino acid is based on a central α-carbon, where a carboxyl group, an hydrogen atom, an amino group, and a variable side chain or R group are bound (see **Figure 1.5**).
In **Figure 1.6** the structure of the 20 common amino acids is reported; 8 of them are essential for the human diet since human lack the enzymes to synthesize them from scratch and 2 are semi-essential (required for growth by the young human).

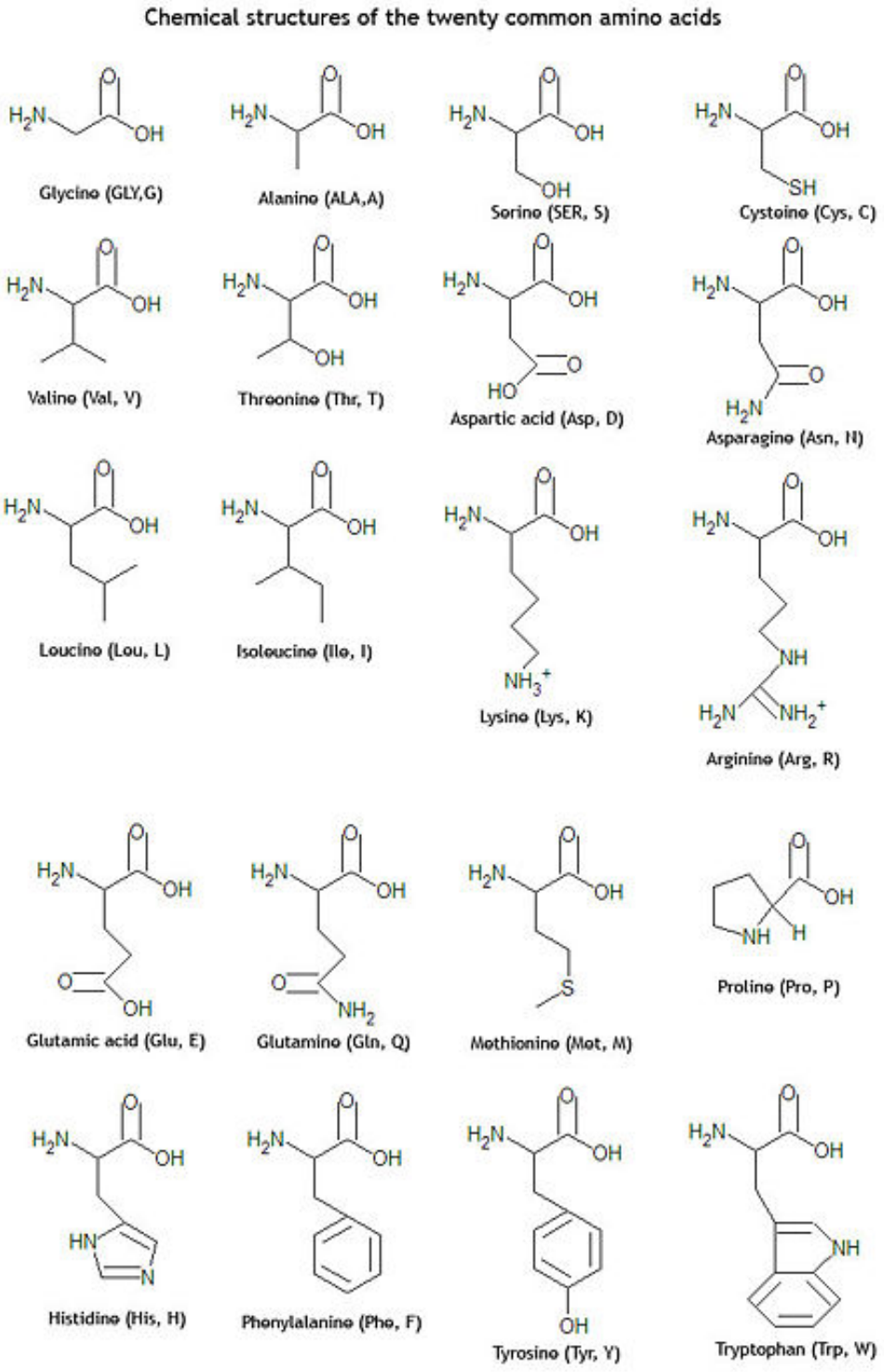

Figure 1.6. Amino acids structure

The essential amino acids are: Phe, Val, Trp, Thr, Ile, met, Lys and Leu; His and Arg are essential during childhood and for the growth and development of the child.

The amino acids are weak polyprotic acids. The carboxyl group is a rather strong carboxylic acid with pK_a around 2.5, whereas the amino groups is a base with pK_a around 9.5. The particularity of the amino acids is that the natural form is represented by the zwitterion ion that forms at a pH value

characteristic for each amino acid; in this form, the amino group is present as $-NH_3^+$, while the carboxylic group is deprotonated (see **Figure 1.7**).

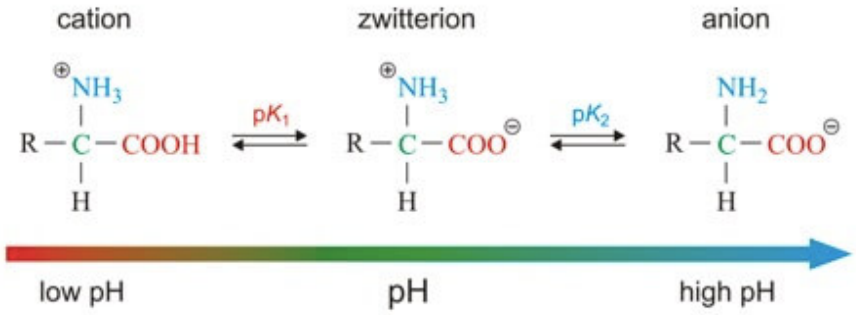

Figure 1.7. Generic amino acid deprotonation

In this thesis, particular attention was paid to the complex properties of Histidine and DL-Tryptophan.

1.3.1 Tryptophan

DL-Tryptophan (Trp, see **Figure 1.8**) is an essential amino acid.

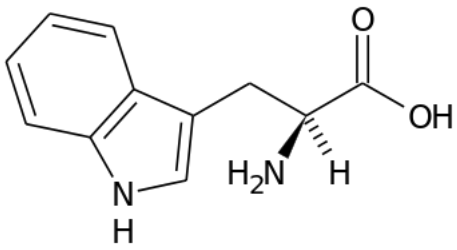

Figure 1.8. Tryptophan structure

The isolation of Tryptophan was for the first time reported by Frederick Hopkins in 1901[18] through hydrolysis of casein. In 1989, the importation of L-Tryptophan was banned in the United States after cases of deadly autoimmune illness called eosinophilia-myalgia syndrome [19]. Since 1994 Tryptophan has been available and marketed as a dietary supplement in the United States, while imported product remains limited by special regulations. From 600 grams of crude casein, it is possible to obtain 4-8 grams of Tryptophan [20]. Plants and microorganisms commonly synthesize Tryptophan from shikimic acid or anthranilate [21]. The latter compound condenses with phosphoribosylpyrophosphate (PRPP), generating pyrophosphate as a bi-product. After ring opening

of the ribose moiety and following reductive decarboxylation, indole-3-glycerinephosphate is produced, which in turn is transformed into indole. In the last step, Tryptophan synthetase catalyses the formation of Tryptophan from indole and the amino acid serine (see **Figure 1.9**).

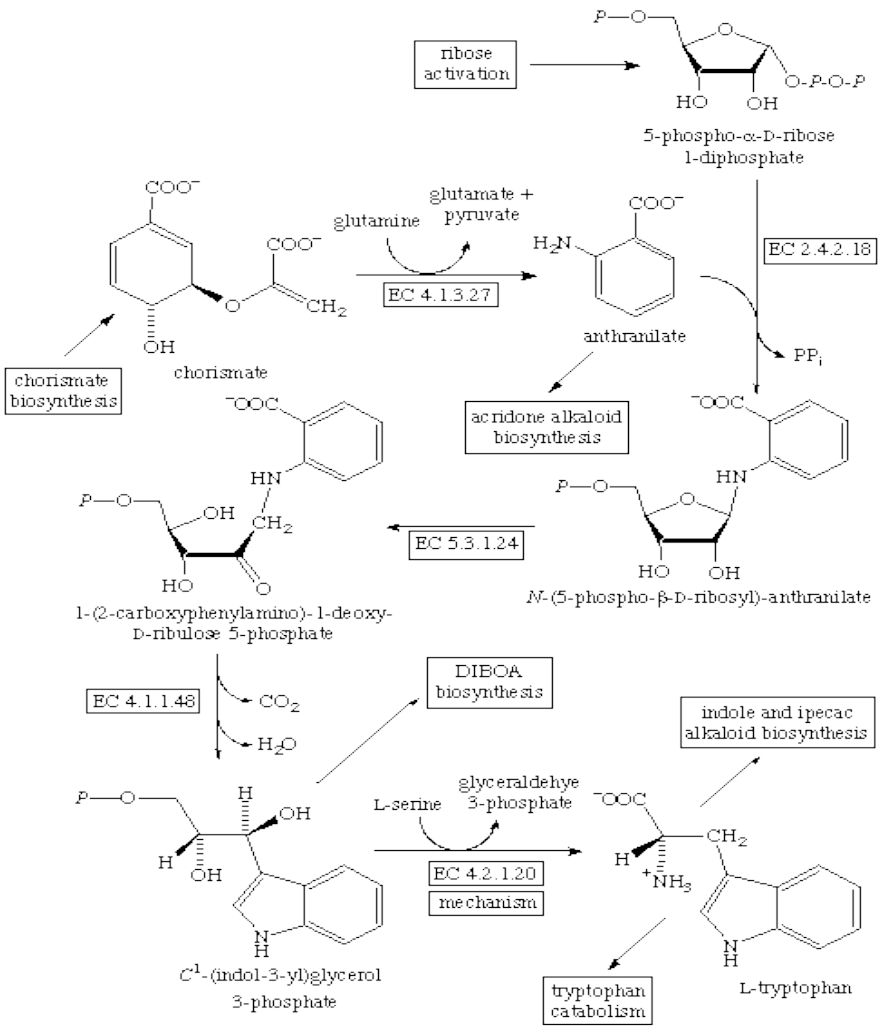

Figure 1.9. Tryptophan synthesis

It is provided by food and transported into the brain through the high affinity LAT1/r4F2hc L-system transporter [22]. It increases the amount of serotonin in the brain, allowing crucial “serotonin neural circuits" to function more effectively and with greater reliability. Tryptophan plays a very important role in many biological processes. For example, it is converted into niacin (vitamin B3) by the liver, but perhaps most importantly, it is, like Tyrosine, an essential precursor of a big number of neurotransmitters in the brain; in fact, it is the only component that can be converted into serotonin, which in turn is converted into melatonin [23, 24]. Some studies have also shown some relations on memory in patient with schizophrenia [25]. Tryptophan and Tyrosine create a delicate balance in the brain, a balance that keeps us on a calm and even emotion keel (see **Figure 1.10**).

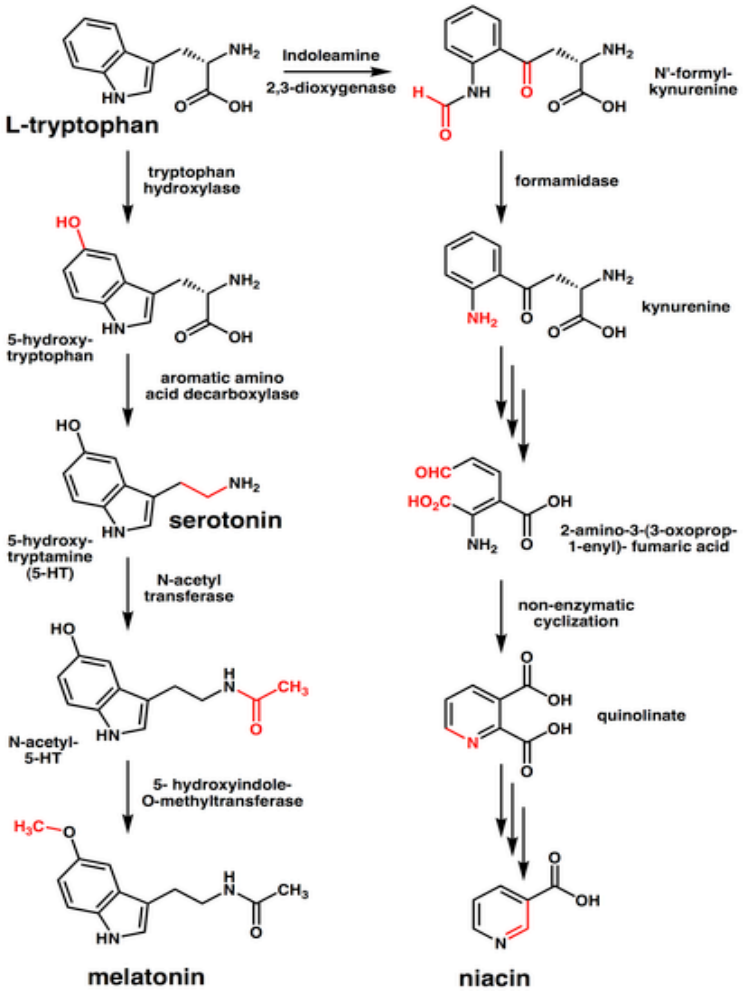

Figure 1.10. Tryptophan conversion

1.3.2 Histidine

Histidine (His, see **Figure 1.11**) is another essential α-amino acid, important for the biosynthesis of proteins and enzymes. Histidine is obtained from the diet. The WHO (World Health Organization)/ FAO (Food and Agriculture Organization of the United Nations) Histidine requirement for adults is 10 mg ·kg body weight^{-1} · d^{-1}.

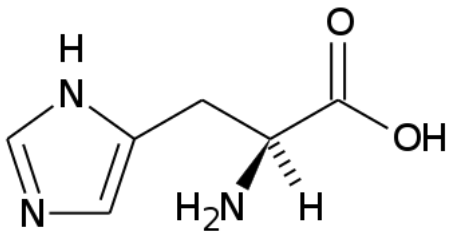

Figure 1.11. Histidine structure

Like all the amino acids, His is featured by a protonated α-amino group and a deprotonated carboxylic group at physiological conditions. In addition, a partially protonated imidazole side chain is bound to the amino acid moiety. The imidazole of the Histidine side chain represents the aromatic part of the molecule; moreover, it is an ionizable group with an acid ionization constant logK_a = 6.5. His has the tendency to coordinate metal cations such as Ca^{2+} and Zn^{2+}, which allow to catalyze many biological processes [26].

Histidine was isolated for the first time by the German physician Albrecht Kossel and Sven Gustaf Hedin in 1896 [27]. Histidine, whose acyl radical is histidyl, is also a precursor of histamine, a vital inflammatory agent in immune responses.

The imidazole side chain of Histidine residue commonly acts as a ligand in metalloproteins. An example is the axial base attached to iron ion in myoglobin and hemoglobin. Immobilized metal-affinity chromatography (IMAC) can be employed to purify recombinant proteins featured by a short affinity tag consisting of polyhistidine residues. This technique exploits the specific amino acid side chains interactions with transition metals, such as Co^{2+}, Ni^{2+}, Cu^{2+}, Zn^{2+}, immobilized on a matrix [28].

Natural polyhistidine peptides found in the venom of the viper Atheris squamigera have been shown to bind Zn^{2+}, Ni^{2+} and Cu^{2+} and affect the function of the venom metalloproteases [29]. Furthermore, low-complexity regions rich in Histidine are found in proteins binding metals such as nickel and cobalt ions [30].

1.4. Antibacterials

1.4.1. Ofloxacin

Ofloxacin with IUPAC name [(±)-9-fluoro-2,3-dihydro-3-methyl-10-(4-methyl-1-piperazinyl)-7-oxo-7*H*-pyrido[1,2,3-*de*][1,4]benzoxazine-6-carboxylic acid) (**Figure 1.12)** is a fluorinated quinolones whose structure is related to Nalidixic acid.

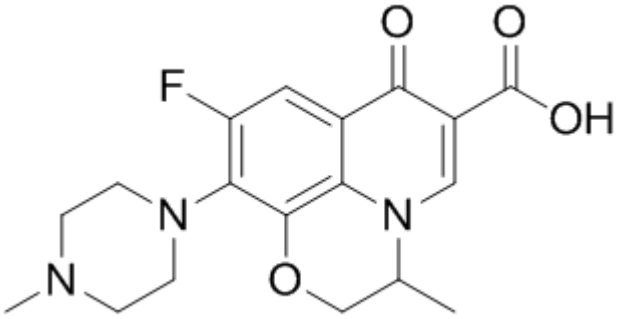

Figure 1.12. Ofloxacin Structure.

Quinolones characterized by the bicyclic basic structure of 4-quinolone (**Figure 1.13**) constitute a large family of antibiotics [31].

Discovered in the early 1960s; have acquired increasing importance for therapeutic use from both community-acquired and severe hospital-acquired infections [32].

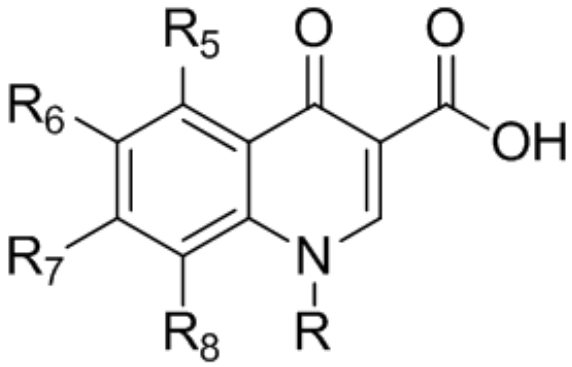

Figure 1.13. Base structure of Quinolone there are 6 important positions for modifications to improve the activity of the drug: R1, R5, R6, R7, R8,

Nalidixic acid is the first antibiotic of this class, synthesized at the Sterling-Winthrop Research Institute in the 1930s [33], although its antibacterial abilities were studied in more detail in the 1950s [31].

Nalidixic acid (like other classes of quinolones) was shown to act by inhibiting the activity of bacterial enzymes of type II topoisomerase, slowing bacterial replication [34], this discovery made its application useful for different types of infections human [35], caused by Gram-positive bacteria.

The negative point of the first quinolones was the restricted spectral action, the bacterial resistance [36] and side effects upon administration, with gastrointestinal reactions, CNS reactions, genotoxicity, phototoxicity and some minor side effects.

For this reason 4 successive generations (**Figure 1.14**) [37] of drugs have been synthesized which, by substituting functional groups, have solved the problems of nalidixic acid.

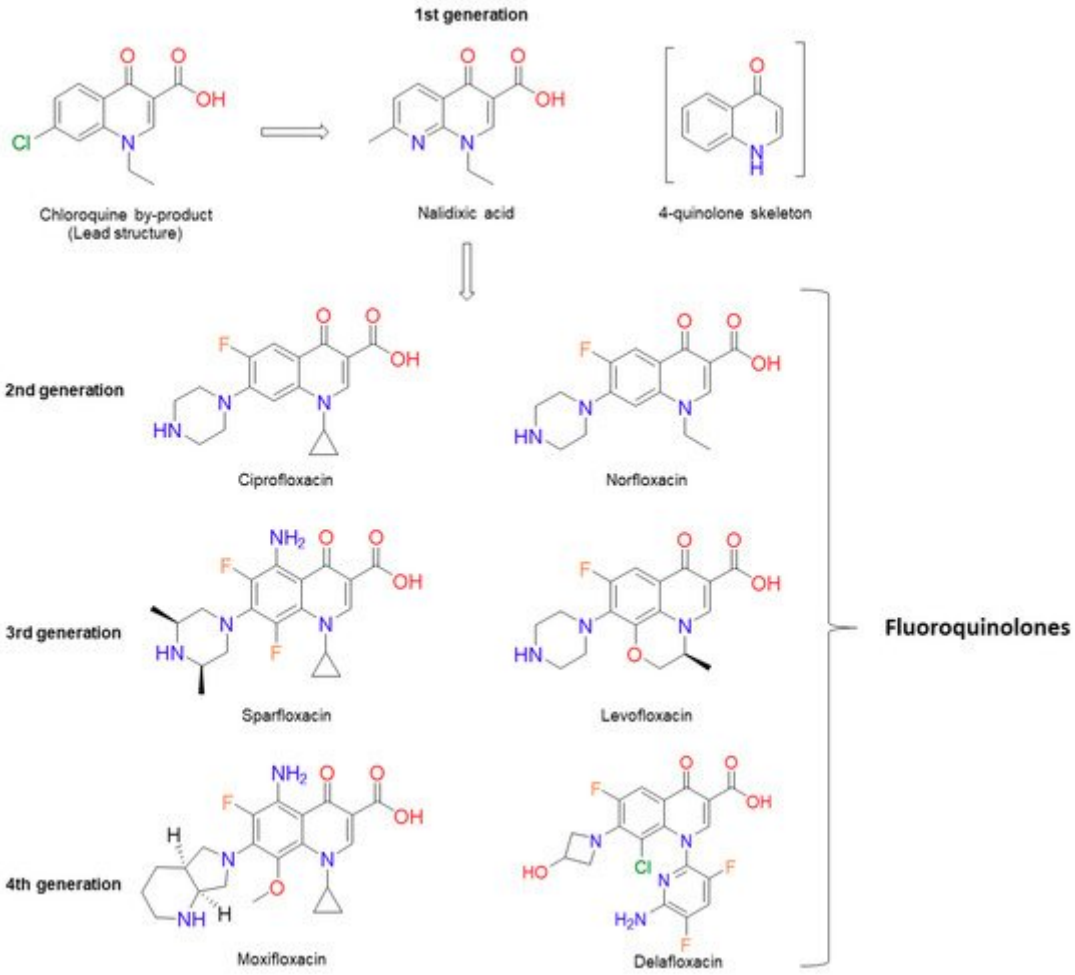

Figure 1.14. The different classes of quinolones

The activity spectrum has been improved by adding a fluorine atom (F) in position R6 [38] and leading to the classification of this new class of drugs as fluoroquinolones.

Furthermore, the addition of a piperazine ring in position R7 allowed to obtain a better bactericidal action against Gram-negative bacteria.

In ofloxacin, the piperazine group is found alkylated, which also allows it to inhibit Gram-positive microorganisms [39].

Ofloxacin is currently considered the most potent of the quinolones as it combines all the new substituents and is still used for clinical treatment. Its enantiomer Levofloxacin is 4 times more active. It can be administered orally or intravenously against a wide range of infections caused by Gram-negative and Gram-positive bacteria from the gastrointestinal tract, Pseudomonas stuartii, Providencia species and Gardnerella vaginalis MIC_{90}.

1.4.2 Ornidazole

Ornidazole [1-Chloro-3-(2-methyl-5-nitro-1H-imidazol-1-yl)propan-2-ol] (see **Figure 1.15**) is a drug belonging to the class of 5-nitro-imidazoles (e.g. Metronidazole, Tinidazole, Secnidazole), initially used for the treatment of trichomonas vaginitis, and then for the fighting of other protozoa such as *Helicobacter pylori* and *Gardnerella vaginalis* and other anaerobic bacteria.

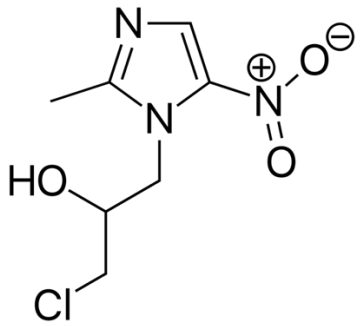

Figure 1.15. Ornidazole structure

The antimicrobial action of nitroimidazoles is attributable to the reduction of the nitro fraction in position 5 to anionic nitro radical and other highly active compounds including nitric and hydroxylamine derivatives [40-44]. Among the 5-nitro-imidazoles class, ornidazole is the only synthetic drug that has a halogen atom in position 1 of the side chain, for this reason it has a longer half-life with respect to the other ligand belonging to the same family[45]. It has also recently been used for patients with Chron's disease [46].

1.5. Metals

1.5.1. Cadmium

Cadmium (symbol Cd) is the chemical element with atomic number 48. Metallic in appearance, it is toxic and is a naturally occurring minor element, one of the metallic components in the Earth's crust and oceans, and present everywhere in our environment.

It was discovered for the first time in Germany in 1817 [47] as a by-product of the zinc refining process.

Cadmium-sulfide based pigments were used as early as 1850 and appeared prominently in the paintings of Vincent Van Gogh in the late 1800s. Thomas A. Edison in the United States and Waldemar Junger in Sweden developed the first nickel-cadmium batteries early in the 20th Century.

Cadmium is a metal with a silvery appearance with bluish reflections; it is malleable, elastic, and soft as it can be cut with a normal knife.
For many aspects it is like zinc but tends to form compounds with a more complex stoichiometry. It has also similar characteristics to strontium but a lower reactivity. Cadmium has an oxidation number of +2, only in some rare cases it assumes the state +1.
Nowadays, the 79% of total cadmium is used in Ni/Cd batteries applications, 11% for pigments, 7% for coatings, 2% for stabilizers and 1% for minor applications (alloys etc.). Tobacco smoking is the most important source of cadmium exposure in the general population. It has been estimated that about 10% of the cadmium content of a cigarette is inhaled through smoking.
Cadmium was also the protagonist of major soil and water pollution in Japan that caused the onset of the itai-itai disease.
Cadmium, when absorbed into plasma, binds mainly to metallothionein, a plasma protein containing several sulfhydryl groups; the cadmium-containing protein is eliminated by glomerular filtration and then reabsorbed by the cells of the proximal tubule, where it causes toxicity.
The large reabsorbed quantity explains the reason why in the initial phases of exposure, cadmium is weakly excreted in the urine (however significant excretion).
Exposure to this metal can also cause toxicity on tubular cells leading to the kidney's inability to reabsorb the excreted cadmium with relative cadmiuria.

1.5.2. Calcium

Calcium (symbol Ca) has been known as an element since 1808 by Sir Davy and by Berzelius and Pontin while in 1898 Moissan was the first person to produce the pure metal [48].
It constitutes about 3% of the Earth's crust essentially in the form of sedimentary rocks of biological origin formed about 3 billion years ago.
Seawater has a calcium concentration that is between 5 and 50 times that of drinking water, which in turn contains a calcium concentration about 10 times than of rainwater.
The amount of this metal on grass and other plants used for the nutrition of the animals such as goats, cows and sheeps is between 1.2 and 17 g kg^{-1} dry weight [49].
An adult man owns in total about 1000 g of calcium distributed in the bone (99%), in the muscle tissue (0.3%), in plasma, in the extracellular fluid and in other cells (0.7%). The calcium in the plasma is represented by free calcium ions (50%), bound to the protein (40%) and complexed with anions (10%) [48].

Calcium has several roles in the human body, such as formation of the structures of bones, activation of enzymes and other molecules in the processes of blood clotting, contraction of the muscles and the heart, thanks to the bonding of calcium with actin and myosin, and participation to the cellular communication, working as intracellular second messenger.

Calcium binds to proteins, possibly a related metal deficiency is the cause of stone formation. Vitamin D3 regulates the absorption of both calcium and phosphate.

It is a hard metal and binds to oxygen with a bond length 0.25-0.3 A shorter than that with nitrogen. The geometry of the bond varies accordingly to the ligands: with the carboxylates it can form monodentate, bidentate and mixed complexes; generally, the preferred coordination number is 8 but 6 is also common. Magnesium can interfere in the binding between the metal and proteins because it is very similar to calcium and is present in higher quantities in the cytosol. If the ligand is monodentate there is not a significant difference in the behavior between calcium and magnesium. As the number of electronic doublets present on the ligand structure increases, like in the case of EDTA, magnesium does not present interferences with calcium.

The Recommended Daily Allowance (RDA) of calcium is 700 mg for children (1-3 years), 1000 mg (4- 8 years), 1300 mg for adolescents, 1000 mg for young adults, 1200 mg for women over 51 and 1200 mg for men and women over 70.

Calcium used clinically is prescribed as a dietary supplement in the form of pills, or like calcium-fortified juices (easier to take, more digestible). They can be used, for example, for the treatment of diseases due to calcium malabsorption, (*e.g.* hypoparathyroidism, malabsorptive bowel disease) and in the case of arising of the osteoporosis [50]. This latter pathology is characterized by symptoms such as muscular and skeletal pain, ache at the ends of the fingers, forearm and lower back, cramps, weakness, and bone fragility, especially in women. In rapidly growing children, the calcium deficiency may provoke rickets. Low concentrations of this metal in the intestine, because of a not correct dietary, is suspected to be associated with the increased risk of kidney stones and colon cancer[51]. This aspect could be due to the decreased binding and increased absorption of oxalic acid, the main constituent of kidney stones and of carcinogens such as bile acids [50].

Other problems linked to the deficiency of calcium are imbalances in the correct activity of thyroid, liver and kidneys and also insomnia and tachycardia.

The decrease of the concentration of calcium ions in the plasma leads to an increase of neuromuscular excitability and a syndrome called tetania [52]. The opposite condition, and so the increase of the total blood calcium, causes symptoms such as anorexia, nausea, constipation, and depression.

1.5.3. Copper

Copper (symbol Cu), even if present in traces, is an essential metal for the growth and development of the human body, in fact it plays important roles in the normal activity of the brain, nervous and cardiovascular systems, and in the protection of cells against oxidation, bone strengthening and the functioning of the immune system.

The human body normally contains copper at a level of about 1.4 to 2.1 mg for each kg of body weight. Copper is widely distributed in the body and occurs in liver, muscles and bone. Copper is transported in the bloodstream on a plasma protein called ceruloplasmin. Copper is found in a variety of enzymes, including the copper centres of cytochrome C oxidase and the enzyme superoxide dismutase (containing copper and zinc). In addition to its enzymatic roles, copper is used for biological electron transport. The blue copper proteins that participate in electron transport include azurin and plastocyanin. The name "blue copper" comes from their intense blue colour arising from a ligand-to-metal charge transfer (LMCT) absorption band around 600 nm. Most molluscs and some arthropods such as the horseshoe crab use the copper-containing pigment hemocyanin rather than iron-containing haemoglobin for oxygen transport, so their blood is blue when is oxygenated rather than red.

It is also necessary for the formation and maintenance of myelin, the protective layer that covers neurons, and through superoxide dismutase it fights cell oxidation, neutralizing free radicals that would otherwise damage the cells themselves. The main manifestations of severe copper deficiency in humans are at the level of the hematopoietic system with the onset of anemia and at the level of the nervous system with the onset of myeloneuropathy: a serious alteration of the spinal cord and peripheral nerves. Side effects due to copper deficiency also include enlarged heart, arteries with degenerated smooth muscle, and aneurysms in the ventricular and coronary arteries. Copper has also an environmental importance, linked to the use of copper-based products as agricultural fungicides, especially since many of them are natural and particularly cheap. However, copper is a heavy metal and as such it can represent a potential threat to human health and the environment, and in this regard it is necessary to consider the dose that does not make it harmful and also the residence time of the substance in the environment and its accumulation in living beings. The biocidal action of copper determines a decrease in the microbial and fungal flora, the greater the accumulation of the same metal in the soil, impoverishing the soil and even more the aquatic ecosystems of these two fundamental components. Furthermore, the use of copper leads to a decrease in the organic substance of the soil, a phenomenon that reduces the quality of the soil itself. In fact, the results obtained from scientific research have shown that this metal has negative effects on most soil species (including

micro and macrofauna), leading to a decrease in the biodiversity of the agricultural environment, an effect that increases over time due to accumulation of copper.
In copper compounds, metal can have different oxidation states, but the most common is +2, where Cu often imparts blue or green colours to natural minerals such as turquoise. Copper have also been used historically widely as pigments. The metal as both metal and pigmented salt, has a significant presence in decorative art. Copper(II) ions are soluble in water, where they function at low concentration as bacteriostatic substances and fungicides.

1.5.4. Magnesium

Magnesium (symbol Mg) is the eighth most abundant element and constitutes 2% of the Earth's crust and it is one of the essential elements for the correct functions and for the health of human body.
Due to its high reactivity, magnesium is not found in nature as a free metal, but in the form of various salts and ionized in water. Although Sir Humphry Davy for the first time isolated magnesium metal in 1808, the medicinal use of magnesium in the form of magnesium-rich mineral waters dates back to ancient times. Indeed, it was during the 17th century that magnesium sulphate was discovered to be the cathartic agent in mineral water. Only in the first part of the twentieth century Willstätter and Stoll proved that magnesium is an essential constituent of the chlorophyll molecule.
However, the full extent of the functions of magnesium, and its regulation in living cells, has been realized only during the past few decades when new analytical techniques have become available [53]. Because of the important interaction between phosphate and magnesium ions, Mg^{2+} is essential to the basic nucleic acid chemistry of life, and thus are essential to all cells of all known living organisms. Over 300 enzymes require the presence of magnesium ions for their catalytic action, including all the enzymes utilizing or synthesizing ATP, or those that use other nucleotides to synthesize DNA and RNA. ATP exists in cells normally as a chelate of ATP and a magnesium ion. Magnesium is a vital component of a healthy human diet.
An adult man owns about 1 mol, namely 24 g of magnesium, distributed in: bone (60 – 65%), muscles (27%), other cells (6 – 7%), extracellular (< 1%), erythrocytes, serum (55% free, 13% complexed with citrate, phosphate, etc., 32% bound, primarily to albumin), mononuclear blood cells, cerebrospinal fluid (55% free, 45% complexed), sweat, secretions [54].
Low levels of magnesium in the body have been associated with the development of human illnesses such as asthma, diabetes, and osteoporosis [55]. Taken in the proper amount, magnesium plays a role in preventing both stroke and heart attack. Excess magnesium in the blood is freely filtered at the kidneys, and for this reason it is difficult to overdose on magnesium from dietary sources alone. With

supplements, overdose is possible, however, particularly in people with poor renal function; occasionally, with use of high cathartic doses of magnesium salts, severe hypermagnesemia has been reported to occur even without renal dysfunction [56].

Magnesium has many therapeutic properties, which can bring benefits to the human body, it is indicated for the treatment of states of depression, anxiety and nervousness because an increase of these symptoms is linked to a higher consumption of this element.

The assumption of magnesium regulates digestion and intestinal functions in case of constipation and diarrhea, it relieves any inflammation and has a mild laxative effect.

It has energizing properties to combat mental and physical fatigue.

1.5.5. Manganese

Manganese (symbol Mn) is a transition metal with atomic number 25. It is found as a free element in nature (often in combination with iron), and in many minerals.

Manganese makes up about 1000 ppm (0.1%) of the Earth's crust, making it the 12th most abundant element there [57]. Soil contains 7–9000 ppm of manganese with an average of 440 [57]. Seawater has only 10 ppm manganese and the atmosphere contains 0.01 μg m^{-3} [57]. Manganese principally occurs as pyrolusite (MnO_2), braunite, $(Mn^{2+}Mn^{3+}{}_6)_6(SiO_{12})$, psilomelane $(Ba,H_2O)_2Mn_5O_{10}$, and to a lesser extent as rhodochrosite ($MnCO_3$).

The cave paintings in Gargas contain manganese as pigments and these cave paintings are 30,000 to 24,000 years old. Manganese compounds were used by Egyptian and Roman glassmakers, either to remove color from glass or add color to it [58]. The use as glassmakers soap continued through the Middle Ages until modern times and is evident in 14th century glass from Venice. Scheele and other chemists were aware that manganese dioxide contained a new element, but they were not able to isolate it. Johan Gottlieb Gahn was the first to isolate an impure sample of manganese metal in 1774, by reducing the dioxide with carbon. In the 20th century, manganese dioxide has seen wide commercial use as the chief cathodic material for commercial disposable dry cells and dry batteries of both the standard (carbon–zinc) and alkaline type.

Manganese is essential to iron and steel production due to its sulfur-fixing, deoxidizing, and alloying properties.

Manganese with +1 oxidation state forms an organometallic compound, namely the methylcyclopentadienyl manganese tricarbonyl, employed as an additive in unleaded gasoline with the aim of boosting octane rating and reducing engine knocking. Manganese(IV) oxide (manganese dioxide, MnO_2) is used as a reagent for the oxidation of benzylic alcohols (i.e. adjacent to an aromatic

ring). Manganese compounds are less toxic than those of metals such as nickel and copper. However, exposure to manganese dusts and fumes should not exceed the ceiling value of 5 mg m^{-3} even for short periods because of its toxicity level. Manganese poses a particular risk for children due to its propensity to bind to CH-7 receptors. Manganese poisoning has been linked to impaired motor skills and cognitive disorders. A form of neurodegeneration similar to Parkinson's Disease called "manganism" has been connected to manganese exposure amongst miners and smelters since the early 19th century. Allegations of inhalation-induced manganism have been made regarding the welding industry.

Manganese is an essential trace nutrient in all forms of life [57]. The classes of enzymes that have manganese cofactors are very broad and include oxidoreductases, transferases, hydrolases, lyases, isomerases, ligases, lectins, and integrins. The reverse transcriptase of many retroviruses (though not lentiviruses such as HIV) contain manganese. The best-known manganese-containing polypeptides may be arginase, the diphtheria toxin, and Mn-containing superoxide dismutase (Mn-SOD). The human body contains about 10 mg of manganese, which is stored mainly in the liver and kidneys. In the human brain the manganese is bound to metalloproteins, most notably glutamine synthetase in astrocytes.

1.5.6. Methylmercury

Organomercury compounds consist of different chemical structures in which divalent mercury forms one (R-Hg-X) or two (R-Hg-R) covalent bond with carbon. These compounds tend to be much more toxic than the inorganic mercury ones and have been implicated in causing brain and liver damage.

Monomethylmercury cation (symbol CH_3Hg^+) is one of the most dangerous pollutant in the Earth; it is formed from inorganic mercury by the action of anaerobic organisms that live in aquatic systems including lakes, rivers, wetlands, sediments, soils and the open ocean [59]. It presents the intrinsic toxicity of the mercury cation and the lipophilicity of the methyl group. The organic part of this molecule confers to methylmercury cation the possibility to pass through the cells' membrane, and readily reacting with biologically important ligands, where, for example, sulfhydryl groups of cysteine [60] strongly interact with CH_3Hg^+ producing toxic effects not only for ingestion but also for contact and inhalation.

Methylation process converts inorganic mercury into methylmercury in the natural environment and, for example, absorbed by fish. At each step of the food chain, the concentration of methylmercury in the organism increases. This concentration in the aquatic predators can reach a level a million times higher than the corresponding one in water. This aspect is because methylmercury has a half-life of

about 72 days in aquatic organisms resulting in its bioaccumulation within these food chains. Organisms, including humans, fish-eating birds and fish-eating mammals, such as otters and whales that consume fish from the top of the aquatic food chain, receive the methylmercury that has been accumulated through this process. Fish and other aquatic species are the only significant source of human methylmercury exposure.

Ingested CH_3Hg^+ is readily and completely absorbed by the gastrointestinal tract. In the adults, methylmercury exposition may cause cardiovascular diseases [61], heart attacks and, despite no confirmation have been published, also autoimmune diseases.

1.5.7. Tin

Tin (symbol Sn) is a silvery – white, soft and malleable metal and it is the 24th element as abundance on the Earth's crust, [62] with a concentration of 2 – 3 ppm compared with 94 ppm for zinc, 63 ppm for copper and 12 ppm for lead.

Tin is mainly obtained from the mineral cassiterite, where it occurs as tin dioxide, SnO_2. The first alloy used in large scale since 3000 BC was bronze, an alloy of tin and copper. An important application of tin is corrosion-resistant tin plating of steel. Because of its low toxicity, tin-plated metal is also used for food packaging, giving the name to tin cans, which are made mostly out of aluminium or tin-plated steel.

It is a versatile metal and its compounds can be divided in two categories:

- metal and inorganic tin salts, with oxidation number of tin +2, in the stannous form, and +4, in the stannic one;
- organotin compounds, with one to four atoms of carbon directly bound to the Sn atom, giving the general formula R_nSnX_{4-n}, where R is an alkyl or phenyl group and X an ionic species in the form of chloride, fluoride, oxide, hydroxide, carboxylate or thiolate [63].

Focusing on the inorganic tin, it can be mostly released to the environment from anthropogenic sources, such as smelting and refining processes, industrial uses of Sn, waste incineration and burning of fossil fuels producing gases, dusts and fumes containing this metal [64]. Furthermore, the wind may transfer Sn particles over long distances before their deposition, that depends from the type of emitting source, physical form and properties (*e.g.* size, density), physical or chemical changes that could happen during the transport, adsorption processes and meteorological conditions [65]. In waters, inorganic tin can exist in both its oxidation states under environmental conditions. [66].

Tin concentrations in soil are low, with the exception of areas where tin-containing minerals are present. Sn can also be bioaccumulated by plants, animals and humans. Indeed, marine macroalgae bioconcentrate tin from seawater with concentrations of 0.5 - 101 mg kg^{-1} dry weight [67].
In muscles and liver of juvenile Japanese squids, the inorganic metal reaches maximum 0.13 mg kg^{-1} dry weight [68], more than 0.9 mg kg^{-1} dry weight in fishes from the Great Lakes in North America [69].
The bioaccumulation of inorganic tin on humans could be mostly due to the use of canned foods because of the dissolution of the tin coating or tin plate [66].
The corrosion of tin-plated food cans by acidic food and beverages has caused several intoxications due to soluble tin compounds. Nausea, vomiting and diarrhoea have been reported as symptoms occurring after ingesting canned food containing 200 mg kg^{-1} of tin [70]. This observation led the Food Standards Agency in the UK to propose upper limits of 200 mg kg^{-1}. A study showed that 99.5% of the controlled food cans containing tin present lower Sn levels with respect to the mentioned limit. Irritation of the skin or the eyes could occur for Sn intoxication.
Besides the packaging of food products and beverages, inorganic tin is used for holding paints, motor oil, disinfectants, polishes and in the pharmaceutical industry in the fields of dentary, veterinary medicine, radiopharmacology and chemotherapy.
The occupational exposure limit of inorganic tin compounds can cause diseases such as syndrome of metal fume fever, stannosis, bronchial syndrome and hemolysis.

1.5.8. Diethyltin (IV)

As already mentioned in the previous paragraph, tin can be also found in organic form.
The first systematic studies on organotin compounds were performed by Sir Edward Frankland (1825-1899) who synthesized diethyltin-diiodide and tetraethyltin in 1853 and 1859, respectively [71].
Other investigations followed and today more than 800 organotin compounds are known. Most of them are of anthropogenic origin except methyltins, which can also be produced by biomethylation [72].
"Organotin(IV)" are defined as all those compounds which have from one to four alkyl (or aryl) groups covalently bonded to a central atom of Sn with oxidation state IV.
Chemically, these compounds are represented by the general formula $R_nSnX_{(4-n)}$, where R symbolizes the organic group, X an anion (often halides, hydroxyls, acetates, etc.) and with $1 \leq n \leq 4$. The number and nature of C-Sn bonds and the substituents influence the electronegativity of tin and consequently the chemical and physical properties of its compounds.

For example, tetrabutyltin is soluble in non-polar solvents and is insoluble and non-reactive in water, while monobutyltin trichloride is soluble in polar solvents and in water.

The synthesis of the alkyltin(IV) compounds (industrial scale and laboratory), is carried out from $SnCl_4$ for full alkylation with an organometallic reagent (RMgX), with the classical method of Friedel-Crafts alkylation; other derivatives are obtained from R_4Sn and $SnCl_4$ with the right proportions, by heating to 200 °C.

Organotin compounds have a wide range of applications: dialkyltin is mainly used as a stabilizer for plastics because the PVC polymer becomes unstable under the influence of heat and light, resulting in discoloration and embrittlement [73]; the trisubstituted organotin compounds are used as biocides, for example as active components of marine antifouling paints for boats and ships, in the agricultural field as fungicides and acaricides, as additives in antifouling paints in order to avoid the attack to the hulls of ships by algae and shellfish, as homogeneous catalysts, etc.

As for most of the organometallic compounds, the presence of organotin derivatives in the environment is attributable to anthropogenic locations due, in particular, to industrial and agricultural applications.

Numerous organotin compounds have been shown to be toxic: there is the growing concern that their widespread use may cause adverse effects in both environmental and biological systems [74].

The biological effects of these substances depend on both the nature and the number of the organic groups bound to the Sn cation.

Trimethyltin and triethyltin compounds are the most toxic ones and are well absorbed from the gastrointestinal tract. Triethyltins produce specific edema in the white matter of the central nervous system in several species, including humans. Diethyltin dichloride was found to be generally irritant with the ability to produce nasal irritation and headache, but it also has an emetic action on the intestine [71]. In particular, di- and trisubstituted organotins cause carcinogenic and neurotoxic effects. Human exposure to organotin compounds can occur through the consumption of contaminated fish and seafood.

Although the organotin compounds are mostly toxic, some of them have proved to be active *in vitro* against human tumor cells. For this reason, in the last decade the interest in the possible interactions between alkyltin cations and biologically relevant compounds increased a lot.

1.5.9. Uranyl

The uranyl ion, (symbol UO_2^{2+}), represents the form of uranium existing in aqueous solution in the oxidation state of +6. It is a well-characterized chemical species, which has a linear structure with short double uranium-oxygen bonds. The compounds that contain this ion are characterized by a yellow color. As examples, the uranyl dinitrate, more simply called uranyl nitrate, $UO_2(NO_3)_2$, is a crystalline substance with lemon-yellow color, while the uranyl acetate $UO_2(Ac)_2$, is a yellow powder. The uranyl ion is stable in water and retains its identity in many reactions, but its chemistry is difficult, due to the presence of numerous complexation and hydrolysis reactions. Owing to the hydrolysis reactions, the aqueous solutions of the uranyl ion are acidic, and the equilibria related to these reactions are rather complicated, with the formation of polymeric species, influenced by the pH and the presence of other ions. The UO_2^{2+} salts are toxic for humans and can cause severe renal failure and acute tubular necrosis. Its accumulation in gonocytes causes congenital diseases, while its accumulation in white blood cells provokes damage to the immune system. Studies carried out at the Northern Arizona University have established that cells exposed to water-soluble uranyl salt, particularly uranyl acetate, are prone to genetic mutations, resulting in tumors and other diseases, however independent of its radioactive properties. Contamination by uranyl ions detected in the vicinity of targets affected by depleted uranium can cause, regardless of the uranium, damages to the kidneys and organs of the digestive system, but also to the lungs and the brain, showing cytotoxic and carcinogenic effects in animals and causing teratogenic effects in humans.

1.5.10. Zinc

Zinc (symbol Zn) is a transition metal and an essential trace element for the life. It is a white-blue metal, fragile and crystalline at room temperatures but ductile and malleable when heated between T = 383.15 K and 423.15 K.

The abundance of this metal in the Earth's crust is about 70 g ton^{-1} [75]. Zinc is a chalcophilic element, together with copper and lead and a trace constituent of most rocks. The amount of Zn in soils and rocks is, for example, 10 – 30 mg kg^{-1} in sand, 50 mg kg^{-1} in granitic rocks, 95 mg kg^{-1} in basalt [76, 77]. Sphalerite (zinc blende, ZnS) is the main ore mineral and the principal source for Zn production, while the main impurities in zinc ores are iron (1 – 14%), cadmium (0.1 – 0.6%) and lead (0.1 – 2%), changing on the base of the location of the deposit.

Zinc is the fourth most common metal in the use technological after iron, aluminum and copper. It is estimated that about 50% of world production is used for anticorrosive coatings of steel, 30% is used

for alloys (mostly brass), and the remaining for chemicals, pigments, coinage and other minor uses. The galvanized products, that are obtained after the galvanizing process, are found in a wide variety of industries (construction, transportation, machinery), while the remaining Zn compounds are widely used in agriculture (fertilizer additive and dietary supplement livestock) in the chemical, pharmaceutical, and rubber industry fields. ZnO is widely used as a pigment in paints and in the cosmetics industry. ZnS is employed in devices that exploit the phenomena of electroluminescence and photoconductivity as cathode ray tubes connected to the TV screen, $ZnCl_2$ as wood preservative agent.

In recent years, its concentration in air, water and soil, is increasing due to the massive and unregulated use of the metal in the industries.

In waters, the amount of this metal depends on factors such as biological and physical - chemical conditions, from the seasonal variations and from the nature and the age of the geological formations through which the water flows [75]. The ocean waters contain a concentration of zinc between 0.002 and 0.1 $\mu g\ kg^{-1}$, with higher amounts at bigger depth and a lower ones in the surface [78]. Wastewater can contain big amount of this metal, while in drinking waters its concentration is lower than 0.2 mg L^{-1}. Anthropogenic sources of zinc can be the following: mining, zinc and metal production facilities, corrosion of galvanized structures, coal and fuel combustion, waste disposal and incineration, use of fertilizers and agrochemicals which containing Zn, zinc smelters.

In plants the concentration of zinc depends on their vegetation state and by the geological origin of the material for soil formation. The age of plants is also important because the amount of the metal decreases with increasing the lifetime of the plant [79].

In animals, Zn is present in sea fish and mollusks with an average concentration of about 25 mg kg^{-1}, in crustaceans between 7 and 50 mg kg^{-1}. In mammals, the bones contain 75- 170 mg kg^{-1} of zinc, while the white muscle tissue about 240 mg kg^{-1} [75].

In the human body, zinc is the second most abundant transition element after iron; a man of 70 kg body weight contains about 2 g variously distributed in different parts of the body, and the daily dose to be introduced in the diet is equal to 15 mg [80].

Zinc has various biological functions within the human body such as regulation of immune functions [81], wound healing, in particular leg ulcer healing [82], has antioxidant function [83], regulates insulin production, helps for problems of memory and learning and it is important for the proper growth and delopment of human body.

Zinc deficiency can be due to various factors such as an inadequate diet, or gastrointestinal problems, leading to symptoms that could be anorexia, lethargy, diarrhea, delayed bone maturation, reduced immune function and susceptibility to infections and, in severe cases, including sexual retardation of

maturation, impotence, alopecia, dermatitis, intellectual disability, nerve conduction disturbance and nerve damage, weight loss, altered taste, smell and wound healing [84].
In contrast, an excess of zinc in the diet prevents the absorption of other essential trace elements such as iron and copper [85].

1.6. Aim of the thesis

The main objective of this thesis is to implement a systematic study on dopamine speciation in electrolyte solutions that simulate biological fluids, both in terms of average and saline concentration, and in terms of temperature. The complexing capacities of dopamine against various metal cations of industrial, biological and pharmaceutical interest will be studied. The speciation of the system will be defined through the determination of the formation constants, after which it will be possible to determine the ionic strength dependence parameters and the specific interaction parameters by means of the Specific Ion Interaction Theory (SIT), as well as determining the corresponding gradients of formation constants with respect to temperature.
The probable formation of mixed species of the MM'L type by dopamine (L) with uranyl (M) and copper (M') or cadmium (M') and the mixed species of MLL' type by dopamine (L) with zinc (M) and tryptophan (L') or histidine (L') will be studied.
Furthermore, the solubilities and acid-base properties of two antibacterial drugs, Ofloxacin and Ornidazole will be studied.
The possible knowledge of these properties, for the two antibacterials, it will allow us to carry out speciation studies in the presence of metal cations.
The final stage of the work will be to calculate the objective sequestering capacity of the ligands studied against the aforementioned metals. This will be possible by using the parameter $pL_{0.5}$ already extensively tested on a wide range of ligands. This parameter makes it possible to uniquely compare the different sequestering abilities of different ligands towards a metal or of a ligand towards different metals. Through the parameter $pL_{0.5}$ it will be possible to quantify the sequestering ability as the conditions of (pH, temperature, ionic strength) vary, determining the concentration of ligand necessary to sequester the 50% initial concentration of metal present in traces.
The modeling of thermodynamic parameters will allow to predict and model the behavior of these components in environmental matrices.

Chapter 2

Experimental part

In this thesis many analytical techniques were used in order to gain the expected information. In this chapter all common analytical techniques, procedures and computer program are described.

2.1. Potentiometry

Potentiometry is one of the most reliable and well-known analytical technique and its application fields include acid-base, precipitation, complexation and redox titrations [1].
Potentiometric measurements are based upon the determination of the cell potential, i.e., the e.m.f. between two electrodes in an electrochemical cell under equilibrium conditions (zero current conditions), between two electrodes which are plunged into a sample solution:

- the external reference electrode, that is the electrochemical reference half- cell for which the potential is constant with respect to that of the sample solution, once ionic strength and temperature are fixed;
- the indicator electrode, also known as the working electrode, whose potential varies as a function of the concentration of a single ion. It is separated from the sample solution by a membrane, selectively permeable to the analyte being studied [86].

Figure 2.1 reports a generic potentiometric apparatus.

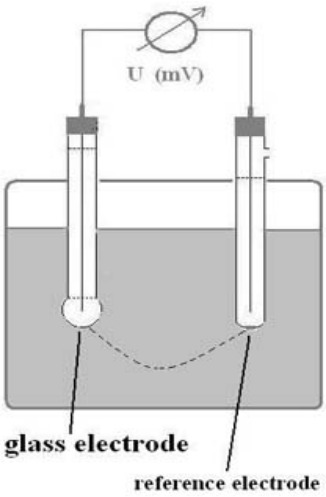

Figure 2.1. Potentiometric cell

The solution inside the electrode contains a known concentration of H^+ ion, either as dilute HCl or a buffer solution. The solution is saturated in AgCl. The activity of H^+ inside the electrode is constant and keeps the internal potential fixed. An internal reference electrode is sealed inside the tube and is attached to one terminal of the potentiometer. The glass pH electrode is used in combination with a reference electrode, either a separate Ag/AgCl electrode [87].

Both electrodes are immersed in a solution of unknown pH and the cell potential developed, caused by the addiction of the titrant, is a measure of the hydrogen ion concentration in the solution on the outside of the glass membrane of the pH electrode, since all other potentials are fixed.

In the measurements performed during this thesis work in the laboratory, an ISE-H^+ combined glass electrode was used, which includes both the reference electrode and the indicator electrode, such as the one shown in **Figure 2.2.**

This particular electrode, also called glass electrode, is specific to H^+ ions and highly selective.

It consists of a thin hydrogen ion-sensitive glass membrane, often shaped like a bulb, sealed onto a glass or polymer tube.

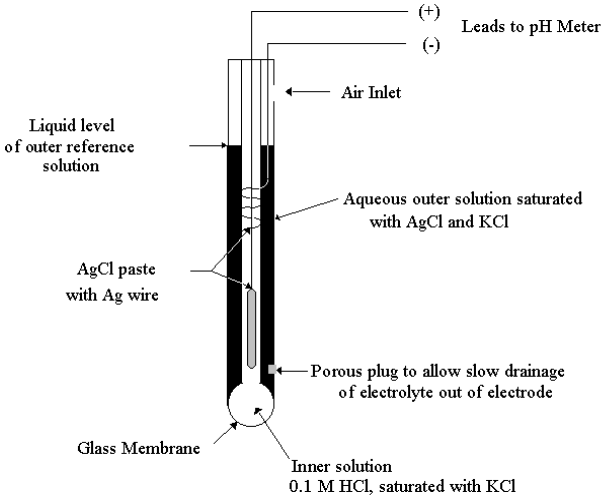

Figure 2.2. Glass electrode

The glass electrodes have a Nernstian slope up to pH ≈ 11 as described by the Nernst equation:

$$E = E^0 - s \log \frac{a_{H^+}(\text{intern})}{a_{H^+}(\text{extern})} \qquad (2.1)$$

where E is the measured potential, E^0 is the formal potential, and s (the Nernstian slope) is 2.303RT/nF (59.16 and 29.58 mV for monovalent and divalent ions, respectively, at 298 K). The formal potential includes different contributions, such as the standard potentials of the internal and external Ag/AgCl electrodes, the liquid junction potential and the asymmetry potential of the glass membrane. It also includes the term s $\log\gamma_H$, which is constant in the experimental conditions of the study (constant ionic medium).

The typical setup, used during the works carried out in this thesis, for the acid/base potentiometric titrations is schematically represented in **Figure 2.3**, and it basically consists of an automatic burette and a pH-meter interfaced to a PC.

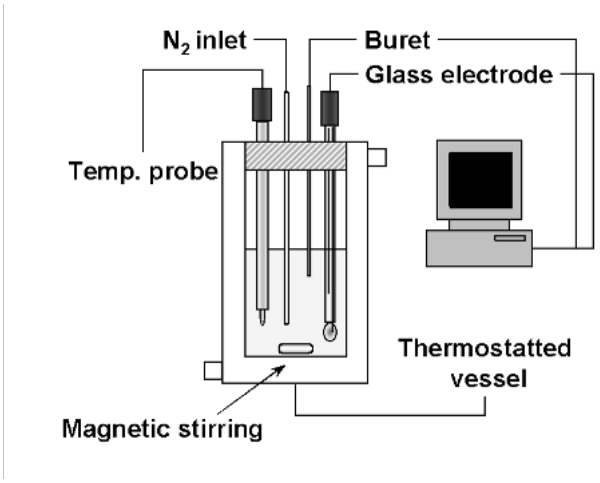

Figure 2.3. Apparatus for a potentiometric titration

2.2. UV-Vis Spectrophotometry

A widely used technique for the study of solution equilibria is spectrophotometry.

The spectrophotometric methods are based on the measurements of the intensity of an electromagnetic radiation absorbed by a molecule.

Electromagnetic radiation is a form of energy whose behavior is described by the properties of both waves and particles. The optical properties of electromagnetic radiation are better explained considering it as a wave. While the interactions between an electromagnetic radiation and the matter, are better described treating the light as a particle or a photon. Electromagnetic radiation consists of oscillating electric and magnetic fields that propagate through space along a linear path and with a constant velocity. The oscillations in the electric and magnetic fields are perpendicular to each other, and to the direction of the wave propagation.

Every wave is described by parameters such as an amplitude A, a wavelength λ, a frequency ν and a velocity of propagation v.

The energy E associated to a wave is proportional to its frequency, according to Planck law:

$$E = \hbar\nu \qquad (2.2)$$

Where $\hbar$ is the Planck constant, and its value is $6.63 \cdot 10^{-34}$ J s.

The range of all the electromagnetic radiations constitutes the electromagnetic spectrum, represented in **Figure 2.4.**

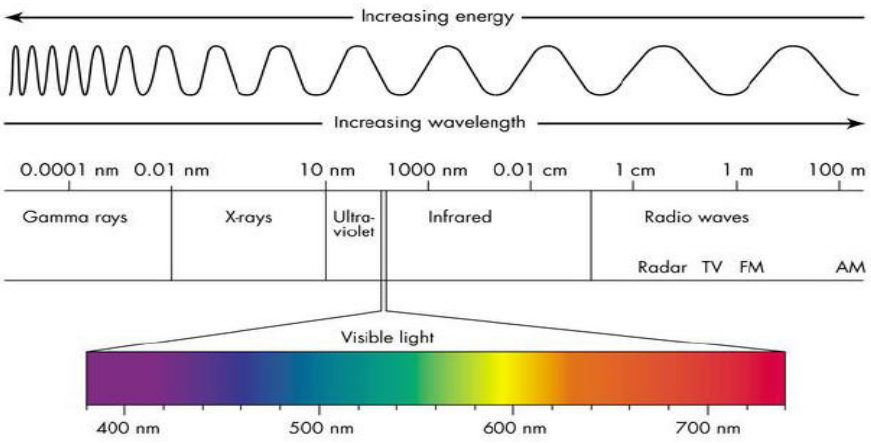

Figure 2.4. Electromagnetic spectrum

Molecular systems can be identified by their characteristic electronic, vibrational and rotational states. At room temperature the substances are mainly in their electronic and vibrational group states. Upon interaction with the appropriate type of electromagnetic radiation, characteristic electronic, vibrational and rotational transitions can be induced in the sample.

When a molecule or ion absorbs ultraviolet or visible radiation it undergoes a change in its valence electron configuration. Four types of transitions between quantized energy levels account for molecular UV-VIS spectra:

$$\sigma \rightarrow \sigma^*$$

$$\pi \rightarrow \pi^* \text{ and } \pi \rightarrow \sigma^*$$

$$n \rightarrow \pi^*$$

$$n \rightarrow \sigma^*$$

These transitions involve functional groups characteristic of the analyte and wavelengths. In particular, the functional groups that absorb ultraviolet and visible radiations are called chromophores, such as for example C = C, C≡C, C = O, N = O, C-X (with X = Br, I).

If an UV-Vis radiation of intensity I_0 strikes an absorbent material perpendicular to the surface, an attenuation of the transmitted radiation will be evidenced and its intensity will become I. Quantitatively, this aspect can be described by the transmittance T and the absorbance A. The equations (2.3) and (2.4) describe the transmittance and absorbance, respectively:

$$T = I / I_0 \qquad (2.3)$$

and

$$A = - \log T = - \log I / I_0 \qquad (2.4)$$

The absorbance, according to the Lambert Beer law, eq. (2.5), is proportional to the concentration, of the analyte with a concentration *c* (mol dm^{-3}), contained in a cell of thickness b (cm):

$$A = \varepsilon\, b\, c \qquad (2.5)$$

Where ε is the molar absorbance or molar absorptivity (mol^{-1} L cm^{-1}), it represents the value of absorbance measured if the optical path and the concentration of the analyte are unitary and depends on the wavelength, the solvent and the type of chemical species which absorbs.

During a titration, the chromophores could produce a bathochromic shift (or red shift), that is shift of the maximum of absorption towards higher wavelengths and lower energy. Differently, an hypsocromic shift (or blue shift) occurs when the maximum of absorption shifts towards lower λ and higher energy. Furthermore, an effect that produces a variation of the ε is defined hyperchromic or hypochromic, depending on whether the change is positive or negative.

2.3. Thermogravimetry

Thermogravimetry (or ThermoGravimetric Analysis, TGA) is based on the determination of the weight variation that a sample undergoes when subjected to a linear variation in temperature.

Thermogravimetric methods can therefore only be applied to reactions in which the change in temperature leads to a change in the mass of the sample. They are therefore limited to the reactions of decomposition, oxidation and physical processes such as evaporation and sublimation.

Weight variations may be due to the loss of moisture retained by the sample or to chemical reactions in which gaseous substances are released.

If the temperature variation is carried out in the presence of gas capable of reacting with the sample, an increase in weight can also be recorded (for example in the case of oxidation of a metal in the presence of O_2).

The graph relating to the variation in weight as a function of temperature is called a thermogram (or thermal decomposition curve).

To more accurately detect weight changes, the differential diagram can be recorded by plotting dW/dT respect to the temperature (T). The differential thermogram (DTG) will be obtained.

From the thermogram it is possible to obtain information on the thermal stability of the substance, on the composition of the test substance, on any intermediate products and on the final product, on the kinetics of a given reaction.

The equipment used in thermogravimetry is known as a thermobalance (**Figure 2.5** block diagram of a thermobalance).

There are different types of thermobalance on the market. The main components are the analytical balance and the oven, connected to a temperature programming system and to a computer for data acquisition and display.

The system is generally connected to a device that allows the delivery of an inert gas during the measurement.

The balance must continuously evaluate changes in mass, and the main characteristics, that it must possess, are: accuracy, sensitivity, reproducibility, stability and response speed. There are several types of thermobalance commercially available that can provide quantitative information on samples whose mass is between 1 and 100 mg. The most common type of scale has a range of 5-20 mg. The balance must be thermally insulated.

The oven is equipped with a thermocouple device for measuring the temperature. The temperature range for most ovens is from room temperature to 1873 K. The heating rate can typically be varied from just over zero to 473 K/min. The oven must have good thermal insulation because the escaping heat can alter the functioning of the scale.

The temperature is recorded by placing a small thermocouple as close as possible to the sample container (not directly in the sample, to avoid contamination and weighing errors resulting from contact of the sample with the thermocouple wires).

We usually operate in an inert gas environment, such as nitrogen or argon, to purge the furnace and prevent oxidation of the sample. Measurements can be made by keeping the atmosphere static or by bubbling gas.

In some cases, it is preferable to change the gases as the analysis proceeds.

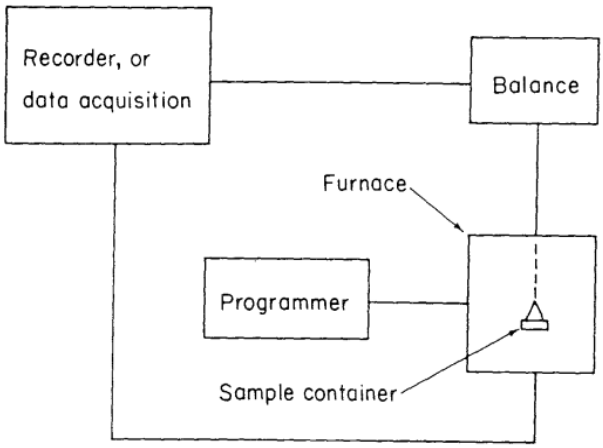

Figure 2.5. Block diagram of a thermobalance

2.4. Computer programs

The experimental data collected from the different instrumental techniques were processed by different computer programs; that allow us to obtain both the thermodynamic parameters necessary to model the behaviour of the analytes taken into account, and their corresponding parameters for the dependence on the ionic strength and temperature.
The computer programs used are described as follows:

- STACO and BSTAC [88, 89] : both of them use the nonlinear least square minimization method and allow the refinement of all the analytical parameters of a potentiometric titration at constant or different ionic strength. The program considers also the variation of the ionic strength during a titration and allow the refinement of the stoichiometric and thermodynamic equilibrium constants. The programs can refine also the ionic strength dependence of the stability constants on ionic strength by means of Debye-Hückel equation [90]. Concerning the refinement procedure, STACO minimizes the sum of squares of the residuals relatives to the volume delivering, while BSTAC [88, 89] do the same operation on the e.m.f. readings:

$$U_V = \sum_n w_n (v_n^{\exp} - v_n^{calc})^2 \qquad \text{(STACO)} \qquad (2.6)$$

$$U_E = \sum_n w_n (E_n^{\exp} - E_n^{calc})^2 \qquad \text{(BSTAC)} \qquad (2.7)$$

where:

$$w_n = 1/\sigma_n^2 \qquad (2.8)$$

$$\sigma_n^2 = \sigma_V^2 + (\delta v_i / \delta E_i)^2 \sigma_E^2 \qquad \text{(STACO)} \qquad (2.9)$$

$$\sigma_n^2 = \sigma_E^2 + (\delta E_i / \delta v_i)^2 \sigma_v^2 \qquad \text{(BSTAC)} \qquad (2.10)$$

Alternatively, $w_n = 1$, usually this last assumption is made when using STACO, because the partial derivative in eq. (2.9) is null. For both programs, it is possible to perform two refinements processes, the first one with weight = 1, and the second one by eq. (2.8), where σ is taken from the first refinement cycle. The possibility to perform two cycles allows the operator to give minor weight, in the second cycle, to the data points affected by higher errors (σ).

- ESAB2M (Equilibria in Solution, Acid Base titrations, program n° 2) [91]: it uses the nonlinear least square minimization method; it can refine the stoichiometric protonation constants and the analytical parameters of an acid-base system. It is often used to calculate

the purity of the reagents. In an acid-base titration, the mass balance equations can be resolved to obtain an explicit function of the titrant concentration and number of protons bound to it. By minimizing the sum of squares of the residuals on the volume (analogously to STACO), it is possible to refine all the parameters involved in the titration, for example: the analytical concentrations of reagents, the standard electrode potential E^0, K_w, liquid junction potential coefficient j_a, and the protonation constants.

$$U_V = \sum_n w_n \left(v_n^{exp} - v_n^{calc}\right)^2 \qquad \text{(ESAB2M)} \qquad (2.11)$$

Another possibility is to minimize the sum of squares of the residuals on the e.m.f. readings:

$$U_E = \sum_n w_n \left(E_n^{exp} - E_n^{calc}\right)^2 \qquad \text{(ESAB2M)} \qquad (2.12)$$

Analogously to BSTAC and STACO, the weight can be calculated by variance propagation as reported in the eqs. (2.9-2.10). Usually, by using ESAB2M, the minimization of the eq. (2.11), as objective function, is faster. The algorithm used for the refinement is the Gauss-Newton one, with the Levenberg-Marquardt as protection algorithm from divergence. Although ESAB2M, BSTAC and STACO can appear identical, they have different options that, push the operator to use ESAB2M in the case of the refinement of strong acid-base titrations or when dealing with a single titration; whilst the other two programs are preferred when dealing with more than one titration systems with complex formation systems and measured at different ionic strength, since ESAB2M does not take into account the ionic strength variation during a titration.

- LIANA (Linear and Nonlinear Analysis) [92] : this is a very flexible computer program, written in Pascal code, used for general fitting and optimization of experimental data, with some peculiarities that make it suitable for application to chemical sciences:
    - it can be used for the calculation of the parameter of linear and nonlinear equations;
    - the equations can be written by operator;
    - the equation can be splitted into several partial equations;
    - several equations can be written in the same input and the parameters can be present in several equations;

- it is possible to give different weights to different variables and multi variables fitting can be solved;
- some graphics can be displayed for a more rapid evaluation of the results;
- it is possible to solve linear systems, two or more problematic in the same time;
- it has a great number of library equations.

- ES4ECI [89]: this program is useful for the calculation of the formation percentage of the species present in a multicomponent solution at the equilibrium. The program allows to draw, from stability constants and analytical concentrations of the components., the speciation diagrams,
- HYPERQUAD [93]: This program allows to treat the experimental data from various instruments (potentiometric, UV / Vis and fluorimetric, NMR), as well as determine the speciation model, although the formation constants and the distribution of the species. The advantage of this program compared to BSTAC and STACO, is that it allows to treat simultaneously the potentiometric and spectrophotometric data. The spectrophotometric data were analysed by the program Hyperquad 2006, which allows to calculate the values of the molar extinction coefficients of each species, knowing experimental spectra (absorbance, A, versus wavelength, λ / nm), the analytical concentrations of the reagents and identifying the speciation model (stoichiometric coefficients and stability constants of the complexes) that best allows fitting the experimental data. The spectra are obtained by means of deconvolution procedures for each species in solution (molar extinction coefficients, ε/mol^{-1} L cm^{-1}, versus wavelength, λ / nm), assuming the additivity of absorbances in the concentration range investigated (Beer-Lambert law). At this point, the experimental spectra are again reconstructed from those calculated using the concentration of the species calculated according to their distribution. This program, however, does not take into account the shape of the possible curves, as well as the nature of the electronic transitions.

2.5. Chemicals

For the investigation carried out, all products were purchased from Sigma-Aldrich Italy. All solutions were prepared with analytical grade water (ρ = 18 MΩ cm^{-1}) using grade A glassware and preserved from atmospheric CO_2 by means of soda lime traps.

Further details on the chemicals used for the investigation here carried out are reported in **Table 2.1**.

For metals Ca^{2+}, Cd^{2+}, CH_3Hg^+, Cu^{2+}, Mg^{2+}, Mn^{2+}, UO_2^{2+}, Zn^{2+}, $(CH_3CH_2)_2Sn^+$ and Sn^{2+}, were prepared from the corresponding chloride salts and were used without further purification. The standard stock solutions of $SnCl_2$ were acidified with HCl to pH~2 and a piece of metallic tin was added to the solutions after the preparation, to prevent the oxidation of Sn^{2+} to Sn^{4+} and to hamper the formation of soluble and sparingly soluble hydrolytic species.

The concentration of the metal ions in the aqueous solutions were determined by means of complexometric titrations with EDTA (Ethylenediaminetetraacetic acid sodium salt) [94].

The acid (HCl) and base (NaOH) solutions were prepared by dilution from the relative Fluka® concentrated vials and standardized respectively with sodium carbonate and potassium acid phthalate (Fluka puriss.), Previously dried in an oven at T = 383.15 K. The soda was stored in dark bottles and protected from atmospheric CO_2 by soda lime traps.

The NaCl solution was prepared by weighing the corresponding Fluka® product of analytical purity, even after drying.

Dopamine hydrochloric salt, Ofloxacin, Ornidazole, L-Histidine and Tryptophan (Sigma Aldrich products) were used; the solutions were prepared by weighing the chemical without further purification.

The purity of the chemicals was checked potentiometrically by alkalimetric titrations and resulted to be > 99 %.

Table 2.1. Chemicals used in this work, purchased from Sigma-Aldrich Italy

Chemical	CAS Number	Purification method	Purity (% wt.)	Purity check
Hydrochloric acid	7647-01-0	none	≥99%	Volumetric titrations with Na_2CO_3
Potassium phthalate monobasic	877-24-7	none	≥99.5%	-
Sodium carbonate	497-19-8	none	≥99.5%	-
Sodium chloride	7647-14-5	none	≥99%	-
Sodium hydroxide	1310-73-2	none	≥99%	Volumetric titrations with potassium phthalate monobasic
$CaCl_2 \cdot 2H_2O$	10035-04-8	none	≥99%	Volumetric titrations with EDTA
$CdCl_2$	10108-64-2	none	98%	Volumetric titrations with EDTA
$CuCl_2 \cdot 2H_2O$	10125-13-0	none	≥99%	Volumetric titrations with EDTA
CH_3HgCl	115-09-3	none	≥99%	-
$MgCl_2 \cdot 6H_2O$	7791-18-6	none	≥99%	Volumetric titrations with EDTA
$MnCl_2 \cdot 4H_2O$	12446-34-9	none	≥99%	Volumetric titrations with EDTA
$SnCl_2 \cdot 2H_2O$	10025-69-1	none	≥99%	Volumetric titrations with EDTA
$(CH_3CH_2)_2SnCl \cdot$	866-55-7	none	≥99%	Volumetric titrations with EDTA
$UO_2(Ac)_2$	541-09-3	none	≥99%	Volumetric titrations with EDTA
$ZnCl_2$	7646-85-7	none	≥99%	Volumetric titrations with EDTA
Dopamine·HCl	62-31-7	none	≥99.5%	Potentiometric titrations
L- Histidine	71-00-1	none	≥99%	Potentiometric titrations
Tryptophan	73-22-3	none	≥99%	Potentiometric titrations
Ofloxacin	82419-36-1	none	≥99%	Potentiometric titrations
Ornidazole	16773-42-5	none	≥99%	Potentiometric titrations

2.6. Procedures

2.6.1. Solubility measurements

Saturated solutions of Ofloxacin and Ornidazole were prepared by adding an excess of ligands in appropriate flasks (total volume 1.5-2.5 cm^3), to solutions containing NaCl as supporting electrolytes at a constant ionic strength value of I = 0.15 $mol \cdot dm^{-3}$. These solutions were stirred for 24 h (time sufficient to reach the equilibrium) in a thermostated room at different temperatures [T = 288.15, 295.15, 310.15 K (standard uncertainties: u(T) = 1 K)]. The saturated solutions were centrifuged at 12000 rpm and filtered through a cellulose membrane filter (Ø = 0.45 μm)**.**

An aliquot of each filtered solution was inserted in the UV-Vis measurements cell for selected the bands of maximum absorbance.

For the measurements of the solubility of Ofloxacin and Ornidazole, the filtered saturated solutions were diluted at a volume ratio of 1:500; in order to maintain the same ionic strength values of the saturated solutions, the dilutions were carried out with sodium chloride aqueous solutions (I = 0.15 $mol \cdot dm^{-3}$).

The concentration of Ofloxacin and Ornidazole, in the diluted solutions, was calculated from the slope of calibration straight lines obtained measuring the absorbance of the standard solutions having concentrations from 0.00099 to 0.099 mmol·dm^{-3}.
The solubility of the ligands at each experimental condition was then calculated taking into account the dilution previously carried out on the saturated solutions.

2.6.2. Spectrophotometry measurements

The spectrophotometric measurements were carried out by a Varian Cary 50 UV–VIS spectrophotometer (**Figure 2.6**) equipped with an optic fibre probe with a fixed 1 cm path length; preliminary absorbing spectra were recorded in order to know the wavelength interval where the ligands absorb. On the basis of the obtained results, measurements were carried out in different wavelength range for different ligands. The spectrophotometer was connected to a PC and the acquisition of the couple of data absorbance (A) vs. wavelength (λ/nm) was made by the Varian Cary WinUV (version 3.00) software. During these measurements, we introduced in the thermostated measurement cell (total volume of 25 or 50 ml), a 602 Biotrode combined glass electrode by Metrohm, that was connected to a potentiometric apparatus (see previous section). In this order, we are able to record simultaneously the couple of data A vs. λ (nm), and e.m.f. (mV) vs. volume of titrant (ml) for each alkalimetric titration point. The combined glass electrode was standardized before each experiment in terms of pH = –log[H^+]. Spectrophotometric titrations were made at different temperature. The titrant was delivered in the measurement cell by means of a Metrohm 665 automatic burette, and the homogeneity of the solutions during the titration was performed with a stirring bar. Before each experiment, $N_{2(g)}$ was bubbled in the solutions for at least 5 minutes in order to exclude the presence of $CO_{2(g)}$ and $O_{2(g)}$.

Figure 2.6. Spectrophotometer apparatus

2.6.3. Potentiometry measurements

Potentiometric measurements were carried out by using a Metrohm model 809 Titrando, a potentiometer connected to an automatic burette, and equipped with a combined glass electrode (Ross type 8102, from Thermo-Orion). The apparatus was linked to a PC and automatic titrations were performed using the MetrohmTiAMO 1.2 software to control titrant delivery, data acquisition and to check for e.m.f. stability. Estimated accuracy was ±0.15 mV and ±0.003 mL for e.m.f. and titrant volume readings, respectively.

Potentiometric titrations were performed at different conditions of temperature ($288.15 \leq T / K \leq 318.15$) and ionic strength ($0.10 \leq I$ / mol dm$^{-3} \leq 1.0$) in ionic medium NaCl.

The measurements were performed in thermostated cells under magnetic stirring and bubbling purified presaturated $N_{2(g)}$ through the solution to exclude $O_{2(g)}$ and $CO_{2(g)}$ inside.

For each experiment, independent titrations of strong acid with standard base solutions were performed, at the same experimental conditions of ionic medium, ionic strength (I) and temperature (T) of the investigated systems, to determine the value of electrode potential (E^0), the acidic junction potential ($E_j = j_a[H^+]$), and the ionic product of water (K_w). The pH scale used was the free scale and pH≡ -log[H^+], where [H^+] is the free proton concentration. For each titration, 80 – 100 data points were collected, and the equilibrium state during titrations was checked by adopting precautions, such as to check the necessary time to reach equilibrium and performing back titrations.

During a strong acid – strong base titration, the graph obtained is a sigmoid curve from which, through the method of the first derivative or even the method of the second derivative, more precise than the graphical extrapolation methods, it is possible to calculate the equivalence point.

In **Figure 2.7** some examples of an acid-base titration curve, the curve obtained by the methods of the first and the second derivative, respectively, are shown.

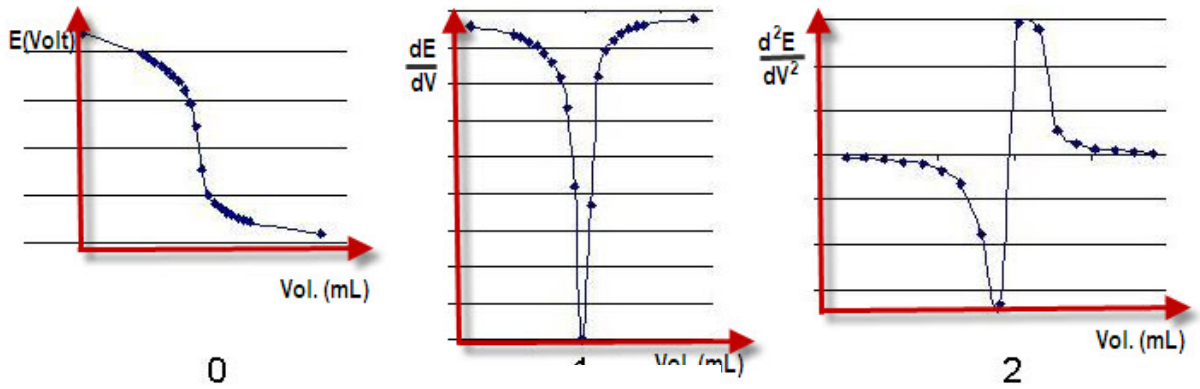

(a) (b) (c)

dE / dV *vs.* V (b) in the first derived method

and d^2E / dV^2 *vs.* V (c) in the second derivative method.

In the case of the systems investigated, the titration curves were more complicated than a strong acid – strong base reaction, and they were characterized by the presence of more flex points due to the presence of different protonable sites.

Potentiometric measurements for the different systems were carried out using NaCl as ionic medium, following the conditions expressed in **Tables 2.2 – 2.6**:

Table 2.2 Experimental conditions investigated for the M^{n+}/Dop^- systems in NaCl aqueous solutions

C_M (mmol dm^{-3})	C_L (mmol dm^{-3})	M:L
1	1.5	1:1.5
1.5	3	1:2
1.5	5	1:3
2	5	1:2.5

M = Ca^{2+}, Mg^{2+}, Sn^{2+}, Cd^{2+}, Cu^{2+}, Mn^{2+}, Zn^{2+}, UO_2^{2+}, $CH_3Hg^+$and $(CH_3CH_2)_2Sn^{2+}$;L= Dopamine.

Table 2.3 Experimental conditions used for ternary complexes M-M'/Dop^- systems in NaCl aqueous solutions

C_M (mmol dm^{-3})	$C_{M'}$ (mmol dm^{-3})	C_L (mmol dm^{-3})	M:M':L
5	5	10	1:1:2
2	6	6	1:3:3
4	6	10	1:1.5:1.6
2	7	11	1:3.5:5.5
6	6	10	1:1:1.6
6	3	10	2:1:3

M = Uranyl; M' = Cadmium or Copper; L= Dopamine.

Table 2.4 Experimental conditions used for ternary complexes Zn^{2+}/L'/Dop^- systems in NaCl aqueous solutions

C_M (mmol dm^{-3})	$C_{L'}$ (mmol dm^{-3})	C_L (mmol dm^{-3})	M:L':L
2	2	2	1:1:1
2	4	2	1:2:1
2	2	4	1:1:2
2	4	6	1:2:3
2	6	4	1:3:2

M = Zinc; L= Dopamine; L' = Histidine or Tryptophan.

Table 2.5 Experimental conditions investigated for the M^{n+}/$Oflox^-$ systems in NaCl aqueous solutions

C_M (mmol dm^{-3})	C_L (mmol dm^{-3})	M:L
1.5	1.5	1:1
1.5	4	1:2.5
1	3	1:3
1	2	1:2

M = Calcium or Zinc; L= Ofloxacin.

Table 2.6 Experimental conditions investigated for the M^{n+}/Orn systems in NaCl aqueous solutions

C_M (mmol dm^{-3})	C_L (mmol dm^{-3})	M:L
1	1.5	1:1.5
1.5	3	1:2
1.5	5	1:3.3
2	5	1:2.5

M = Calcium; L= Ornidazole.

Chapter 3

Modelling of the thermodynamic parameters

3.1. Equilibrium constants

For a correct study of speciation of organic and inorganic ligands in aqueous solution, it is necessary to pay particular attention to the equilibria with which the formation of species are related, described by means of stepwise (3.1) or overall (3.2) equilibrium constants.
In the various chapters of this thesis, the equilibrium constants are expressed in their decimal logarithm scale. In particular as regards the protonation constants of all the ligands (generally indicated with L) considered, they are given according to the equilibria:

$$H^+ + H_{r-1}L^{(n-r+1)} = H_rL^{(n-r)-} \qquad logK_r^H \qquad (3.1)$$

$$rH^+ + L^{(n-)} = H_rL^{(n-r)-} \qquad log\beta_r^H \qquad (3.2)$$

where r represents the r-th protonation step and n is the charge of the different ligands.
The hydrolysis takes into account the following generic equilibrium:

$$pM^{n+} + rH_2O = M_p(OH)_r{}^{(np-r)} + rH^+ \qquad \log\beta_{Mp(OH)r\ (np-r)} \qquad (3.3)$$

Some of the considered metals (Cd^{2+} or Sn^{2+}) tend to form with chloride (anion of the supporting electrolyte) stable complexes and ternary hydrolytic species (MClOH); in these cases, the equilibrium of formation can be expressed by:

$$M^{n+} + jCl^- + H_2O = MCl_j(OH)^{(n-j-1)} + H^+ \qquad \log\beta_{MClj(OH)(n-j-1)} \qquad (3.4)$$

As regards the formation constants of all the ligands (L), with the metal (M) systems, they are based on the following equilibria:

$$pM^{n+} + qL^{z-} + rH^+ = M_pL_qH_r{}^{(np-zq+r)} \qquad \log\beta_{pqr} \qquad (3.5)$$

$$pM^{n+} + qL^{z-} + rH_2O = M_pL_q(OH)_r{}^{(np-zq-r)} + rH^+ \qquad \log\beta_{pq-r} \qquad (3.6)$$

3.2. Dependence of equilibrium constants on ionic strength

The necessity to perform experimental measurements at different ionic strengths is due to the fact that the thermodynamic parameters such as the protonation and hydrolysis constants as well as the stability constants of the metal – ligand complexes are related to the activity coefficient of the species which are present in solution. It depends on the ionic strength, temperature, pressure, chemical characteristics of the species and properties of the solvent.

The activity coefficient is related to the ionic strength through the Limited Debye – Hückel theory, based on the description of the different physical-chemical interactions between the ions and of their interactions with the molecules of the solvent. This theory takes into account only the electrostatic interactions between ions of opposite charge and the ions are considered as point charges. The Limited Debye – Hückel law, valid for solution with $0 \leq I$ / mol kg$^{-1} \leq 0.001$, is:

$$\log \gamma_i = -A\,|z^+ z^-|\,\sqrt{I} \qquad (3.7)$$

where

γ_i = activity coefficient of the i-th ion;

z = charge of the ion;

A = constant dependent from temperature and solvent (in water at T = 298.15 K, A = 0.51);

I = ionic strength in the molal scale.

In a successive elaboration of the law, Debye and Hückel considered the ions of finite dimensions and interacting with each other at distances not lower than the sum of their radii. The Extended Debye – Hückel law, valid for solutions characterized by $0.001 \leq I$ / mol kg$^{-1} \leq 0.01$, is:

$$\log \gamma_i = (-A\,|z^+ z^-|\,\sqrt{I}) / (1+\text{å}\,B\,\sqrt{I}) \qquad (3.8)$$

where

B = constant dependent from temperature, pressure and dielectric constant of the solvent (in water at T = 298.15 K, B = 0.32);

å = the maximum distance of approach between oppositely charged ions expressed in Angstrom (Å).

For ionic strength values up to 0.2 mol kg^{-1}, the Extended Debye – Hückel law is substituted by the [95] eq. (3.9). It is more suitable and takes into account only the charge of the ions and not their individual features.

$$\log \gamma_i = -0.51\,z^2\,((\sqrt{I} / (1+\sqrt{I}) - 0.3I) \qquad (3.9)$$

Many different approaches were proposed to model the dependence of the equilibrium constants on ionic strength and to extend its validity at higher values of ionic strength, typical of a lot of natural fluids. The extended Debye - Hückel equation, implemented by a term L(*I*), is:

$$\log \gamma_i = (-A\,|z^+ z^-|\,\sqrt{I}) / (1+å\,B\,\sqrt{I}) + L(I) \qquad (3.10)$$

where

L(*I*) represents the specific short-range interactions.

A modified model, was proposed by the research group, eq. (3.11) [96], in which this thesis was developed:

$$\log K_i = \log {}^{T}K_i - z^* DH + C\,I + D\,I^{3/2} + E\,I^2 \qquad (3.11)$$

where

K_i = equilibrium constant of the i-th species at a given *I* value;

${}^{T}K_i$ = thermodynamic equilibrium constant of the i-th species at infinite dilution.

$z^* = \Sigma\,(z)^2_{reactants} - \Sigma\,(z)^2_{products}$

$DH = 0.51\,(\sqrt{I} / (1+1.5\sqrt{I}))$;

$C = (c_o\,p^* + c_1\,z^*)$;

$D = (d_o\,p^* + d_1\,z^*)$;

$E = (e_o\,p^* + e_1\,z^*)$;

c_o, c_1, d_o, d_1, e_o, e_1 = empirical parameters for the dependence on ionic strength;

$p^* = \Sigma\,(p)^2_{reactants} - \Sigma\,(p)^2_{products}$ (p = stoichiometric coefficients).

The empirical parameters C, D and E can be considered constants, or independent of the stoichiometry of the complex considered. When $I >> 1$ mol dm^{-3}, it is necessary to use one or both the terms D $I^{3/2}$ and E I^2. Furthermore, the use of one or more linear terms depends also on the supporting electrolyte. For $I \leq 1$ mol L^{-1} only one term (C *I*) in NaCl aqueous solutions has been used, while for tetraethyl ammonium iodide (Et_4NI) aqueous solutions it has been necessary to fit the data with two empirical parameters, C and D. Moreover, the Eq. (3.11) can be used with both molar and molal concentration scales.

Concerning SIT model used to study the dependence of the stability constants on the ionic strength, the concentrations and the stability constants were converted from the molar to the molal scale.

The c/m ratio can be determined by the following formula:

$$c/m = d_0 + a_1 c + a_2 c_2 \qquad (3.12)$$

where d_0 is the water density at $T = 273.15$ K, $d_0 = 0.99987$ g/cm^3. The dependence of water density on temperature can be modelled by the following equation:

$$d(T/K) = [(d_0 + p_1 \ T/K - p_2 (T/K)^2)/(p_3 (T/K) + 1))] \ 10^{-3} \quad (3.13)$$

where $d(T/K)$ is the water density at the desired temperature; $p_1 = 8.119$, $p_2 = 7.8735 \cdot 10^{-3}$ and $p_3 = 8.0574 \cdot 10^{-3}$ are empirical parameters obtained by modelling the data pair pure water density (g/cm^3) vs. T / K and derived from literature data [97].

The knowledge of the density of water at the desired temperature and the molarity and molality of the electrolytic solution (NaCl in our case) at a given saline concentration, allows the calculation of the c/m value. Using Eq. (3.12), the following parameters have been calculated: $a_1 = -0.017765$, $a_2 = -6.525 \cdot 10^{-4}$. The range of validity for conversion in NaCl is: $0 \leq I$ (NaCl)/mol kg$^{-1} \leq 6$. The stability constants converted in the molal concentration scale, by using the above approach, are reported in Tables S1-10 of the Supplementary Material section.

Once obtained the equilibrium constants in concentration scale, Eq. (3.11) becomes equivalent to the one used for SIT (Specific ion Interaction Theory) with a first order linear term, where $C \equiv \Delta\varepsilon$ (ε = specific interaction parameter).

The SIT has the advantages of requiring a much simpler mathematical treatment; according to this theory only linear interactions between oppositely charged ions are taken into account. These interactions are believed to cause deviations from the criteria of the ideality. Scientists who follow this theory propose expressions based on the extensions of the Debye-Hückel equation [98-101].

Since 1960, many speciation models have been proposed, and in many cases, they improved the applicability to multicomponent solutions and up to high ionic strength values (> 6 mol kg^{-1}).

The SIT approach [102-108] is very useful and quite simple model, is on the basis of this model, the activity coefficients of the ions are calculated considering all their interactions with only ions of opposite charge. It is a physical-chemical approach according to which the term L(I) added to the Debye-Hückel equation, can be explained in the following way:

$$\log \gamma_{\pm} = -\frac{A \cdot z^2 \sqrt{I}}{1 + \overset{0}{a} B\sqrt{I}} + \Delta\varepsilon_i (I) \quad (3.14)$$

$\Delta\varepsilon$ is the specific ionic interaction coefficient in molal concentration scale.

For a generic equilibrium constant, we can write:

$$\log\beta_{pqr} = \log \beta^0_{pqr} - z^* (A\sqrt{(I_m)})/(1+1.5\cdot\sqrt{I_m}) + \Delta\varepsilon \cdot I_m + j \log a_w \quad (3.15)$$

Moreover, I_m is the ionic strength expressed in the molal concentration scale, log a_w is the activity coefficient of water (log a_w = 0.015), j = number of water molecules involved in the equilibrium.
The $\Delta\varepsilon$ parameter can be expressed by

$$\Delta\varepsilon = \sum \varepsilon_{react} - \sum \varepsilon_{prod} \quad (3.16)$$

And ε are the SIT coefficients for the interaction of all ionic species involved in the considered equilibrium with all the ions (of opposite sign) of the ionic medium.
For equilibria involving uncharged species, their activity coefficients must be expressed by the Setschenow equation [109]:

$$\log \gamma = k_{c,m} \cdot I \quad (3.17)$$

where k_c and k_m are the Setschenow coefficients of the neutral species in a given ionic medium, in the molar (c) or molal (m) concentration scales, respectively.
If all the interactions between the ligand and the metal ion are taken into account, the generic $\Delta\varepsilon$ parameter of Equation (3.16) can explicated to obtain the $\varepsilon(M_pL_qH_r^{(np-zq+r)}, Na^+/Cl^-)$ ion-pair SIT coefficients for all the species involved in the equilibrium of formation of the complexes.

3.3. Dependence of equilibrium constants on Temperature

Formation constants at different temperatures allowed to calculate the enthalpy values by applying the Van't Hoff equation, assuming that the contribution of ΔCp in a small temperature range, as in our case 283.15-318.15 K, is negligible:

$$\log K_T = \log K_\theta + (\Delta H_\theta / 2.303R)\,(1/\theta - 1/T) \quad (3.18)$$

where
θ = reference temperature (298.15 K);
T = temperature in Kelvin;
ΔH_θ = enthalpy change at reference temperature;
R = 8.314 J K^{-1} mol^{-1} and is the universal gas constant.
The dependence on ionic strength of the enthalpy changes was modeled by a modified Debye - Hückel type equation:

$$\Delta H = (\Delta H^0 - z^* 1.5\sqrt{I} / (1 + 1.5\sqrt{I}) + C_T \cdot I) \cdot 52.23 \quad (3.19)$$

where

ΔH^0 = enthalpy change at infinite dilution;

C_T = dependence parameter on ionic strength of the enthalpy changes;

52.23 = 1/(R ln10) in kJ mol^{-1}.

It is necessary to consider that the enthalpy changes here mentioned, is not really the state function, in such concentration scale used (namely the molar one), therefore it was obtained a gradient of the temperature.

Furthermore, the Gibbs free energy can be calculated from the equilibrium constants as reported by Eq. (3.20):

$$\Delta G = -RT \ln K \quad (3.20)$$

From the knowledge of the enthalpy changes and the Gibbs free energy, the $T\Delta S$ values can be calculated in the same experimental conditions:

$$T\Delta S = \Delta H - \Delta G \quad (3.21)$$

The knowledge of the parameters for the dependence on ionic strength and temperature gives a complete thermodynamic picture of these systems, whose equilibrium constants can therefore be predicted for any experimental condition.

Chapter 4

Results

4.1 Metal-Dopamine System

Experimental measurements were carried out to determine the formation constants of the considered metal complexes with dopamine using different metal-ligand concentration ratios. For each measurement, the potentiometric system was calibrated by titrating a strong acid solution under the same ionic strength and temperature conditions as the measurement solution. This operation allows to calculate the value of the standard potential of the electrode.

In all the systems studied, in order to identify the speciation model that would allow to obtain the best statistical parameters in terms of standard deviation and mean deviation, different speciation models were tested, and the best model was chosen based on precise selection criteria:

- Simplicity of the model compared to other tested models;
- Significant formation percentage (≥10%) for each species present in the speciation model and in various conditions of component concentration, ionic strength and temperature;
- Analyze the relationship between the variances of the different models obtained.

All the models obtained in the different systems are based on the following equilibria:

$$pM^{n+} + qL^{z-} + rH^{+} = M_pL_qH_r^{(np-zq+r)} \qquad \log\beta_{pqr} \qquad (4.1)$$

$$pM^{n+} + qL^{z-} + rH_2O = M_pL_q(OH)_r^{(np-zq-r)} + rH^{+} \qquad \log\beta_{pq-r} \qquad (4.2)$$

Figure 4.1 shows as an example the comparisons between the titration curves of dopamine and in the presence of the different investigated metal ions; the different titration curves were obtained under the same experimental conditions and component concentrations. A quick comparison between the different titration curves highlights in many cases different profiles of the curves, due to both the different speciation of the system, and the different acid-base properties of the metal.

For example, the titration curves of the systems containing Ca^{2+}, Cd^{2+}, Mg^{2+}, Mn^{2+}, and CH_3Hg^{+} are quite similar to each other, especially up to the neutralization of the proton resulting from the addition of inorganic acid HCl. Similar trend, but with a significant shift in the pH jump, occurs for Cu^{2+} and Zn^{2+} due to hydrolytic properties which are significantly different from other metals.

The profiles of the titration curves for Sn^{2+} and $(CH_3CH_2)_2Sn^{2+}$ (or indicate DET^{2+}) appear completely different, while in the case of the UO_2^{2+} ion, the anomalous titration curve of the dopamine system is explained considering that the use of the acetate salt instead of the nitrate one. This, as we will see in the section dedicated to this system, significantly affects the speciation of the entire binary system.

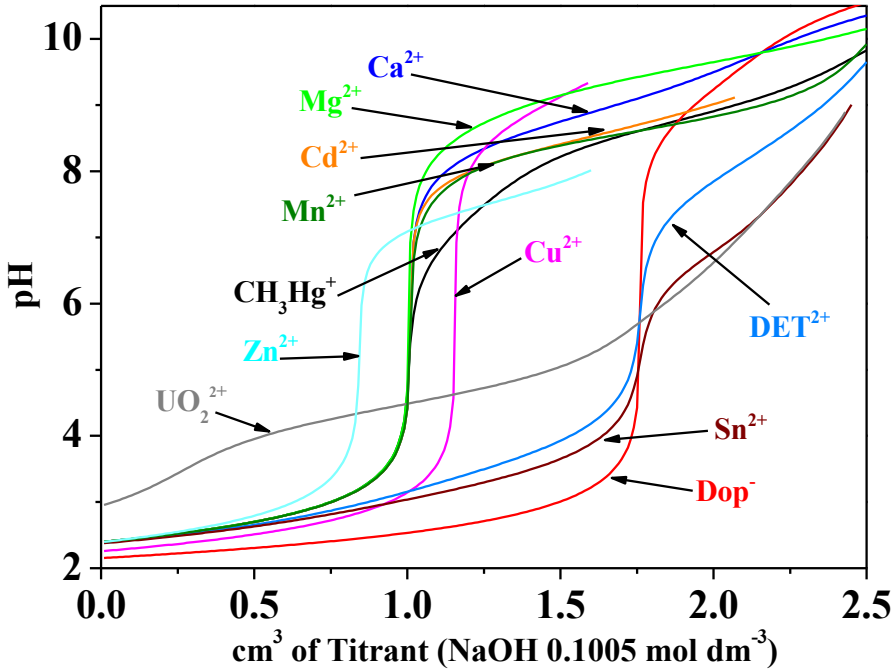

Figure 4.1. Titration curves of dopamine and of the different M^{n+}/Dop^- systems at T = 298.15 K, I = 0.15 mol dm^{-3}.
Experimental conditions: C_L = 3 mmol dm^{-3}; C_M = 1.5 mol dm^{-3}. Titrant solution: NaOH 0.1005 mol dm^{-3}.

4.1.1 Acid-Base properties of Dopamine.

Considering the importance of this molecule, our research group has been involved in a systematic investigation on the thermodynamic properties in aqueous solutions and on the interaction with metals.

In particular, the studies already done regards the determination of the solubility in different solvents, by means of distributions measurements, and of the protonation in NaCl aqueous solutions at different ionic strengths and temperatures. Investigations were carried out by potentiometry, UV spectrophotometry / ISE H^+ and spectrofluorimetry / ISE H^+.

The protonation constants of this molecule refer to the following equilibria:

$$H^+ + L^- = HL^0 \qquad logK_1^H \qquad (4.3)$$

$$H^+ + HL^0 = H_2L^+ \qquad logK_2^H \qquad (4.4)$$

In general:

$$nH^+ + L^- = H_nL^{(n-1)} \qquad log\beta_2^H \qquad (4.5)$$

The first protonation constant refers to the amine group of the lateral chain (log $K^H{}_1$) whilst the second to the phenolic group presents in the para position respect to the lateral chain (log $K_2{}^H$).

The other phenolic group (meta position) has a logK^H value > 13 and is less important from a biological point of view.

In **Table 4.1** the literature protonation constants at different ionic strengths and temperatures are reported [110].

Table 4.1. Literature protonation constants of dopamine at different ionic strengths and temperatures in NaCl aqueous solutions

***I*/mol mol^{-3}**	**logK_1^H** a)	**logK_2^H** a)	***I*/mol mol^{-3}**	**logK_1^H** a)	**logK_2^H** a)
	***T* = 288.15 K**			***T* = 298.15 K**	
0.147	10.687	9.496	0.162	10.566	9.209
0.491	10.743	8.923	0.197	10.573	8.963
0.747	10.941	8.951	0.491	10.440	9.066
0.982	11.029	9.018	0.504	10.399	9.119
			0.735	10.307	8.971
			0.980	10.262	8.8.78
	***T* = 310.15 K**			***T* = 318.15 K**	
0.148	9.989	8.376	0.148	9.519	8.144
0.165	9.988	8.690	0.493	9.136	8.257
0.495	9.904	8.470	0.749	9.213	8.307
0.743	10.002	8.514	0.986	8.798	8.312
0.989		8.513			

a)Refer to the equilibria in Eqs. 4.3-4.4

The knowledge of the protonation constants allows to obtain information about the chemical behavior of this molecule at the investigated experimental conditions and it is necessary for the studies on the interaction with the metal ions.

These investigations were carried out in the presence of different metal ions and in aqueous solutions containing sodium chloride as supporting electrolyte, since it is the main inorganic component of natural and biological.

4.1.2 Acid-Base properties of Metals A, B and Organometals Groups.

Below, the literature acid-base properties of the investigated metal ions are reported; for simplicity, the metal ions were divided in three main groups as in **Table 4.2**.

The hydrolytic constants reported in the next tables refer to the experimental conditions used to investigate the interaction with dopamine, namely NaCl solutions, $0.15 \leq I$ / mol dm$^{-3} \leq 1$ and $288.15 \leq T$ / K ≤ 318.15.

Table 4.2. Metals investigated

Metals		
A	**B**	**Organometals**
Ca^{2+}	UO_2^{2+}	CH_3Hg^+
Mg^{2+}	Cd^{2+}	$(CH_3CH_2)_2Sn^{2+}$
Sn^{2+}	Cu^{2+}	
	Mn^{2+}	
	Zn^{2+}	

The hydrolysis constants of the various metals have been collected, processed and tabulated below. The data here reported for the hydrolysis of the metal ions has been obtained from the literature, or from experimental investigations carried out by this research group.

As regards the metals of A group: the hydrolysis constants of Ca^{2+} were taken from the data literature [111] while for Mg^{2+} from [112]. The hydrolytic constants of Sn^{2+} were already published by this group, and obtained both from experimental investigations and from an accurate analysis of previous literature data at different conditions (*i.e.*, *I*/mol dm^{-3}, *T*/K, etc.) in NaCl aqueous solutions [62]. Investigations carried out in NaCl aqueous solutions allowed the determination of the stability constants of the weak complexes with chloride anion.

Group B is composed by the metals Cd^{2+}, Zn^{2+} and UO_2^{2+}; the hydrolysis constants in NaCl aqueous solutions at different ionic strengths and temperatures are reported in previous studies and published. For Cd^{2+} [113] investigations in NaCl allowed the determination of the $CdCl_i$ (i= 1-4) and CdOHCl complexes.

For UO_2^{2+}, the hydrolytic constants were taken from our previous investigations [114]; moreover, since the UO_2(Acetate)$_2$ salt was used, the speciation and the formation constants of the UO_2/Ac system in NaCl were considered [115].

For Zn^{2+}, hydrolytic constants obtained from careful analysis of literature data were used (unpublished data).

For Cu^{2+} and Mn^{2+}, the hydrolytic constants were taken from the literature [111, 116].

For the last group, the organometals, the hydrolysis constants of CH_3Hg^+ in NaCl at $0 < I/\text{mol dm}^{-3} \leq 1.0$ were taken from previous investigations [117, 118]. In chloride media, the acid-base behavior of methylmercury(II) is characterized by the formation of a stable CH_3HgCl complex that forms in significant amount and represents the main species up to pH~7–8.

The hydrolytic constants for $(CH_3CH_2)_2Sn^{2+}$ were taken by literature data [119].

As it already reported, the hydrolysis reactions of the metal ions can be expressed by means of the following general equilibrium:

$$pM^{n+} + rH_2O = M_p(OH)_r^{(np-r)} + rH^+ \qquad \log\beta_{Mp(OH)r\,(np-r)} \qquad (4.6)$$

Some of the considered metal (Cd^{2+} or Sn^{2+}) tend to form with chloride (anion of the supporting electrolyte) stable complexes and ternary hydrolytic species (MClOH); in these cases, the equilibrium of formation can be expressed by:

$$M^{n+} + jCl^- + H_2O = MCl_j(OH)^{(n-j-1)} + H^+ \qquad \log\beta_{MClj(OH)(n-j-1)} \qquad (4.7)$$

Table 4.3. Literature hydrolytic constants of Mg^{2+} ,Ca^{2+} and Sn^{2+}ions in NaCl aqueous solutions at different ionic strengths and temperatures

Group A												
Metals	**Mg^{2+}**		**Ca^{2+}**	**Sn^{2+}**								
	$\log\beta_{pr}$		**$\log\beta_{pr}$**	**$\log\beta_{pr}$**								
Species	**$MgOH^+$**	**$Mg_4(OH)_4^+$**	**$CaOH^+$**	**$SnOH^+$**	**$Sn(OH)_2^0$**	**$Sn(OH)^{3-}$**	**$Sn2(OH)_2^{2-}$**	**$Sn_3(OH)_4^{2+}$**	**$SnCl^+$**	**$SnCl_2^0$**	**$SnCl_3^-$**	**$SnCl(OH)^0$**
I/mol dm^{-3}	***T* = 288.15 K**		***T* = 288.15 K**	***T* = 288.15 K**								
0.15	-11.21 [a);b)]	-37.46	-13.14 [a);c)]	-3.96 [a);d)]	-6.67	-16.53	-5.36	-7.00	0.7	1.44	1.38	-2.11
0.5	-11.22	-37.83	-	-	-	-	-	-	-	-	-	-
0.75	-11.27	-37.97	-	-	-	-	-	-	-	-	-	-
1	-11.33	-38.09	-	-	-	-	-	-	-	-	-	-
	***T* = 298.15 K**		***T* = 298.15 K**	***T* = 298.15 K**								
0.15	-11.22	-37.46	-12.98	-3.78	-6.53	-16.97	-5.06	-6.39	0.76	1.5	1.46	-2.07
0.5	-11.23	-37.85	-12.98	-3.91	-6.68	-17.05	-5.2	-6.63	0.58	1.23	1.19	-2.36
0.75	-11.28	-38.00	-12.98	-3.96	-6.75	-17.1	-5.26	-6.72	0.52	1.15	1.11	-2.5
1	-11.33	-38.13	-12.97	-4.00	-6.81	-17.15	-5.32	-6.8	0.49	1.09	1.05	-2.61
	***T* = 310.15 K**		***T* = 310.15 K**	***T* = 310.15 K**								
0.15	-11.22	-37.47	-12.56	-3.56	-6.36	-17.5	-4.7	-5.66	0.77	1.76	1.71	2.98
0.5	-11.23	-37.88	-	-	-	-	-	-	-	-	-	-
0.75	-11.28	-38.04	-	-	-	-	-	-	-	-	-	-
1	-11.34	-38.18	-	-	-	-	-	-	-	-	-	-

a) Equilibria are expressed as $\log\beta pr$ according to the equilibria considered in equations 4.6 – 4.7; b) [112]; c) [111]; d) [62].

Table 4.4. Literature hydrolytic constants of Cd^{2+} ions in NaCl aqueous solutions at different ionic strengths and temperatures

Group B											
Metals	**Cd^{2+}**										
	$\log\beta_{pr}$										
Species	**$CdOH^{+}$**	**$Cd(OH)_2^{0}$**	**$Cd(OH)_3^{-}$**	**$Cd(OH)_4^{2-}$**	**$Cd_2(OH)^{3+}$**	**$Cd_4(OH)_4^{4+}$**	**$CdCl^{+}$ b)**	**$CdCl_2^{0}$ b)**	**$CdCl_3^{-}$ b)**	**$CdCl_4^{2-}$ b)**	**$CdCl(OH)^{0}$ b)**
I/mol dm^{-3}	***T* = 288.15 K**										
0.15	-10.36 a);b)	-	-	-	-9.1	-32.28	-	-	-	-	-
	***T* = 298.15 K**										
0.15	-10.36	-20.63	-33.3	-46.78	-9.1	-32.28	1.51	1.92	1.49	0.9	-7.89
0.5	-10.05	-20.77	-33.3	-46.5	-8.98	-32	1.35	1.74	1.38	0.82	-7.89
0.75	-10.55	-20.82	-33.3	-46.4	-8.92	-31.9	1.31	1.71	1.4	0.83	-7.85
1	-10.59	-20.86	-33.3	-46.33	-8.88	-31.83	1.33	1.76	1.5	0.9	-7.8
	***T* = 310.15 K**										
0.15	-10.35	-	-	-	-9.09	-32.27	-	-	-	-	-

a) Equilibria are expressed as $\log\beta pr$ according to the equilibria considered in equations 4.6 – 4.7; b)[113].

Table 4.5. Literature hydrolytic constants of Cu^{2+}, Mn^{2+} and Zn^{2+}ions in NaCl aqueous solutions at different ionic strengths and temperatures

Group B											
Metals	**Cu^{2+}**			**Mn^{2+}**		**Zn^{2+}**					
	$\log\beta_{pr}$			**$\log\beta_{pr}$**		**$\log\beta_{pr}$**					
Species	**$CuOH^{+}$**	**$Cu_2(OH)^{3+}$**	**$Cu_2(OH)_2^{2+}$**	**$Mn(OH)^{+}$**	**$Mn_2(OH)^{3+}$**	**$Zn(OH)^{+}$**	**$Zn(OH)_2^{0}$**	**$Zn(OH)_3^{-}$**	**$Zn(OH)_4^{2-}$**	**$Zn_2(OH)^{3+}$**	**$Zn_2(OH)_6^{2-}$**
I/mol dm^{-3}	***T* = 288.15 K**			***T* = 288.15 K**		***T* = 288.15 K**					
0.15	-7.90 [a);b)]	-6.42	-11.19	-10.6 [a);b)]	-26.35	-9.50 [a);c)]	-17.64	-29.12	-41.67	-9.27	-58.91
0.5	-7.80	-6.39	-11.18	-	-	-9.42	-17.60	-29.05	-41.39	-9.62	-58.70
0.75	-7.80	-6.39	-11.18	-	-	-9.33	-17.53	-29.00	-41.29	-9.92	-58.60
1	-7.70	-6.38	-11.17	-	-	-9.21	-17.44	-28.95	-41.21	-10.23	-58.51
	***T* = 298.15 K**			***T* = 298.15 K**		***T* = 298.15 K**					
0.15	-7.70	-6.10	-10.72	-10.46	-24.47	-9.16	-17.11	-28.37	-40.63	-8.92	-57.48
0.5	-7.60	-6.07	-10.79	-10.70	-24.69	-9.08	-17.07	-28.30	-40.35	-9.28	-57.28
0.75	-7.55	-6.90	-10.78	-10.82	-24.80	-8.98	-17.00	-28.25	-40.25	-9.58	-57.18
1	-7.50	-6.11	-10.77	-10.95	-24.92	-8.87	-16.91	-28.20	-40.18	-9.89	-57.09
	***T* = 310.15 K**			***T* = 310.15 K**		***T* = 310.15 K**					
0.15	-7.50	-5.80	-10.34	-9.20	-23.51	-8.78	-16.52	-27.54	-39.47	-8.54	-55.90
0.5	-7.50	-5.86	-10.40	-	-	-8.70	-16.48	-27.47	-39.20	-8.90	-55.69
0.75	-7.40	-5.90	-10.40	-	-	-8.60	-16.41	-27.42	-39.10	-9.20	-55.59
1	-7.40	-5.90	-10.38	-	-	-8.49	-16.32	-27.37	-39.02	-9.51	-55.50
	***T* = 318.15 K**										
0.15	-7.30	-5.77	-9.96								
0.5	-7.30	-5.76	-10.10								
0.75	-7.30	-5.76	-10.01								
1	-7.20	-5.80	-9.99								

a) Equilibria are expressed as $\log\beta pr$ according to the equilibria considered in equations 4.6 – 4.7; b) [111, 116]; c) unpublished data

Table 4.6. Literature hydrolytic constants of UO_2^{2+} ions in NaCl aqueous solutions at different ionic strengths and temperatures.

Group B					
Metals	**UO_2^{2+}**				
	$\log\beta_{pr}$				
Species	**$UO_2(OH)^+$**	**$UO_2[(OH)_2]^{2+}$**	**$(UO_2)_3[(OH)_4]^{2+}$**	**$(UO_2)_3[(OH)_5]^+$**	**$(UO_2)_3[(OH)_7]^-$**
I/mol dm^{-3}			***T* = 288.15 K**		
0.15	-5.74 [a);b)]	-6.29	-12.86	-17.34	-30.77
0.5	-5.96	-6.42	-12.96	-17.63	-30.85
0.75	-6.07	-6.46	-12.97	-17.72	-30.84
1	-6.18	-6.5	-12.95	-17.79	-30.82
			***T* = 298.15 K**		
0.15	-5.5	-6.02	-12.27	-16.64	-29.72
0.5	-5.72	-6.14	-12.4	-16.95	-29.84
0.75	-5.84	-6.19	-12.41	-17.05	-29.86
1	-5.96	-6.24	-12.4	-17.13	-29.85
			***T* = 310.15 K**		
0.15	-5.22	-5.7	-11.62	-15.85	-28.56
0.5	-5.46	-5.84	-11.77	-16.18	-28.72
0.75	-5.59	-5.9	-11.79	-16.3	-28.76
1	-5.71	-5.94	-11.79	-16.39	-28.77
			***T* = 318.15 K**		
0.15	-5.05	-5.51	-11.22	-15.36	-27.83
0.5	-5.3	-5.65	-11.37	-15.71	-28.02
0.75	-5.43	-5.7	-11.41	-15.84	-28.07
1	-5.55	-5.76	-11.41	-15.93	-28.09

a) all equilibria are expressed as logβpr according to the equilibria considered in equations 4.6 – 4.7; b) [114].

Table 4.7. Literature hydrolytic constants of UO_2^{2+} - Acetate ions in NaCl aqueous solutions at different ionic strengths and T = 298.15K

Group B				
Metals	**UO_2^{2+} - acetate**			
	$\log\beta_{pAcOH}$			
Species	**$UO_2(ac)^+$**	**$UO_2(ac)_2^0$**	**$UO_2(ac)_3^-$**	**$(UO_2)_3(ac)_3(OH)^{2-}$**
I/mol dm^{-3}				
0	2.86 [a);b)]	4.62	7.22	2.14
0.119	2.44	4.02	6.58	1.92
0.504	2.38	4.09	6.44	1.79
0.734	2.36	4.02	6.43	1.77
0.975	2.33	4.24	6.40	1.78
C[c)]	0.31	0.82	0.47	0.02

a) Equilibria are expressed as logβ according to the equilibria considered in equations 4.1 – 4.2; b) [115] c) parameter for the dependence on ionic strength of the formation constants.

Table 4.8. Literature hydrolytic constants of CH_3Hg^+ and $(Et)_2Sn^{2+}$and ions in NaCl aqueous solutions at different ionic strengths and temperatures

Organometals Group							
Metals	**CH_3Hg^+**		**$(CH_3CH_2)_2Sn^{2+}$**				
	$\log\beta_{pr}$		**$\log\beta_{pr}$**				
Species	**CH_3HgOH**	**CH_3HgCl**	**$(CH_3CH_2)_2Sn(OH)^+$**	**$(CH_3CH_2)_2Sn(OH)_2$**	**$(CH_3CH_2)_2Sn(OH)_3^-$**	**$(CH_3CH_2)_2Sn_2(OH)_2^{2+}$**	**$(CH_3CH_2)_2Sn_2(OH)_3^+$**
I/mol dm^{-3}	***T* = 288.15 K**		***T* = 288.15 K**				
0.15	-4.52 [a);b)]	5.33	-2.99 [a);b)]	-8.13	-18.86	-4.92	-9.19
0.5	-4.48	5.31	-	-	-	-	-
0.75	-4.45	5.32	-	-	-	-	-
1	-4.42	5.34	-	-	-	-	-
	***T* = 298.15 K**		***T* = 298.15 K**				
0.15	-4.54	5.25	-3.57	-8.98	-19.97	-4.96	-10.20
0.5	-4.58	5.16	-3.83	-9.36	-20.20	-5.19	-10.70
0.75	-4.64	5.13	-3.93	-9.54	-20.37	-5.31	-10.90
1	-4.64	5.13	-4.02	-9.69	-20.51	-5.39	-11.10
	***T* = 310.15 K**		***T* = 310.15 K**				
0.15	-4.50	5.34	-4.22	-9.93	-21.21	-5.00	-11.33
0.5	-4.46	5.31	-	-	-	-	-
0.75	-4.44	5.32	-	-	-	-	-
1	-4.41	5.34	-	-	-	-	-
	***T* = 318.15 K**						
0.15	-4.50	5.33					
0.5	-4.46	5.30					
0.75	-4.43	5.31					
1	-4.40	5.33					

a) Equilibria are expressed as logβpr or logβpCl according to the equilibria considered in equations 4.4 – 4.5; b)[117, 118]; c) [120].

4.1.3. Metal group A/Dopamine systems

The procedures used to identify the best speciation model for the metal/dopamine systems follow some general rules, namely: 1. the simplicity of the model; 2. the agreement with similar metal-ligand systems; 3. the significant formation percentages of each species in all the experimental conditions; 4. the differences in variance between the accepted model and other checked ones.
These procedures were applied at each of the experimental conditions (*i.e.* ionic strength and temperature) investigated, better described in the dedicated sections.
The measurements were performed by potentiometric titrations at different ionic strengths: $0.15 \leq I$ / mol $dm^{-3} \leq 1.00$ in NaCl, different metal - ligand molar ratios and temperatures $288.15 \leq T$ / K ≤ 310.15.
For some metal-dopamine systems (Ca^{2+}/Dop^{-}, Sn^{2+}/Dop^{-}, Cd^{2+}/Dop^{-}; see also the next sections) the dependence of the stability constants on the temperature, in the interval $288.15 \leq T$ / K ≤ 310.15, was studied only at $I = 0.15$ mol dm^{-3}.
The next sections report an accurate discussion on the main obtained results, where the stability constants are expressed as it already reported in the Eqs. (4.1-4.2).

4.1.3.1. Ca^{2+}/Dop^{-} system

For the interactions of calcium with dopamine, the speciation model that gave the best results in terms of statistical parameters was characterized only by the MLH and MLOH species. However, having available a large number of experimental data at $T = 298.15$ K, it was also possible to determine the ML species which, compared with the other two species MLH and MLOH, is formed in lower amount, independent of the experimental conditions (ionic strength and temperature) and concentrations or metal:ligand molar ratios.
The formation constants for Ca^{2+}/Dop^{-} species are shown in **Table 4.9**, in the molar concentration scale, at the investigated ionic strengths and temperatures; from the data here reported we can affirm that the stability of the complexes formed by dopamine with Ca^{2+} are fairly weak. This is one of possible reason how the interaction occurs over pH ~ 7.5.
From the distribution diagram reported in **Figure 4.2**, we can observe this evidence, and that the equilibrium in aqueous solution can be considered reliable up to pH ~ 10; after this pH we observed the formation of sparingly soluble species, that were collected and characterized by thermogravimetric analysis.

An analysis of the effect of the ionic strength on the distribution of the species, highlight that increasing the ionic strength, the complex species tend to form at lower pHs; as an example, at I = 1.0 mol dm^{-3}, we observed the presence of the MLH at pH ~ 6, reaching about 50% of formation at pH = 8.

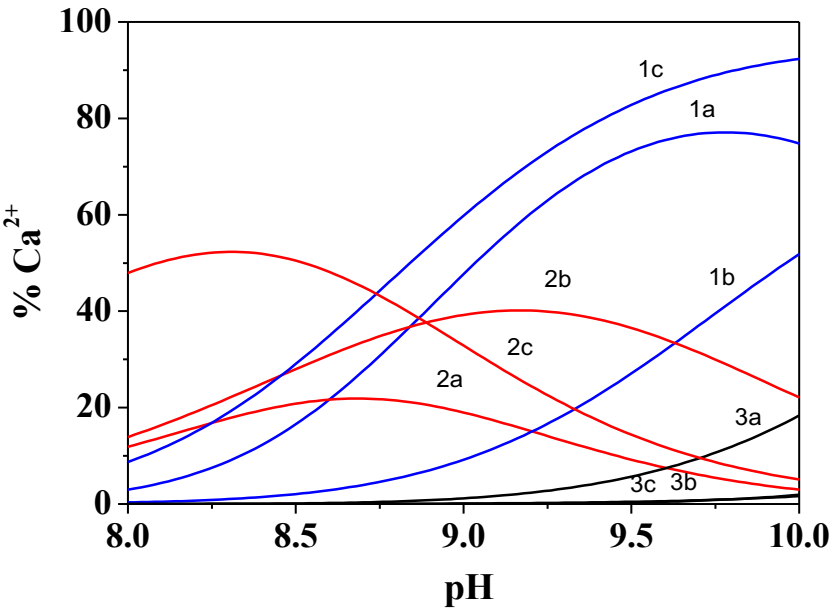

Figure 4.2. Distribution diagram for the Ca^{2+}/Dop^- species at T = 298.15 K and different ionic strengths. Species: 1 ML; 2 MLH; 3 MLOH. [M = Ca^{2+}; L = Dop^-]
a: I = 0.15 mol dm^{-3}; b: I = 0.50 mol dm^{-3}; c: I = 1.00 mol dm^{-3}
(Experimental Conditions: C_{Ca2+} = 1.5 mmol dm^{-3}; C_{DOP-} = 5 mmol dm^{-3})

The effect of the temperature on the distribution of the Ca^{2+}/Dop^- species can be observed from **Figure 4.3**; in this case a significant variation on the distribution of the species, both in term of pH of maximum formation and formation percentages was obtained; we remind that only the ionic strength I = 0.15 mol dm^{-3} was investigated at different temperatures.

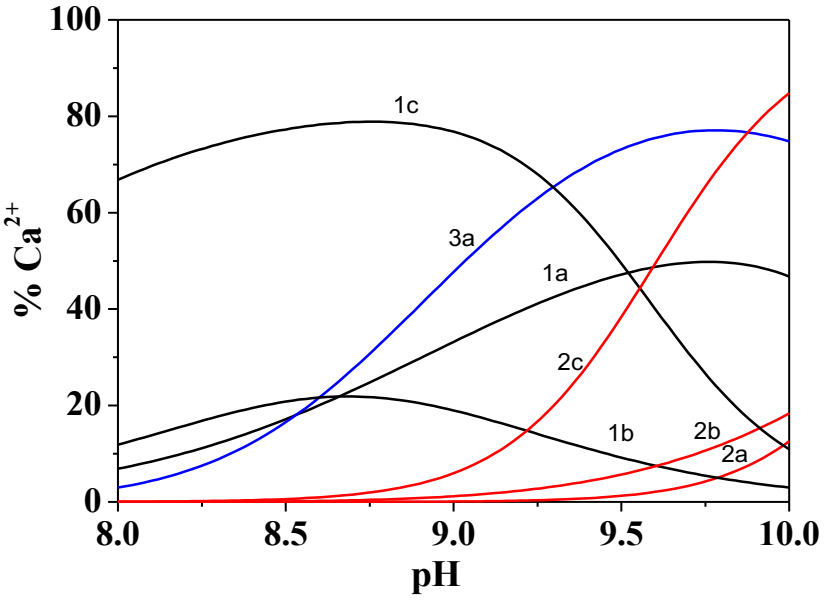

Figure 4.3. Distribution diagram for the Ca^{2+}/Dop^- species at I = 0.15 mol dm^{-3} and different temperatures.
Species: 1 MLH; 2 MLOH; 3 ML. [M = Ca^{2+}; L = Dop^-]
a: T = 288.15 K; b: T = 298.15 K; c: T = 310.15 K
(Experimental Conditions: C_{Ca2+} = 1.5 mmol dm^{-3}; C_{DOP-} = 5 mmol dm^{-3})

Table 4.9. Experimental formation constants of the Ca^{2+}/Dop^- species in NaCl aqueous solutions

T/K	I/mol dm^{-3}	$\log\beta_{ML}$ a)	$\log\beta_{MLH}$ a)	$\log\beta_{MLOH}$ a)
288.15	0.150	-	13.60 ± 0.03 b)	-6.97 ± 0.08 b)
298.15	0.143	4.83 ± 0.08 b)	13.43 ± 0.08	-5.78 ± 0.16
298.15	0.472	3.65 ± 0.07	13.28 ± 0.06	-7.78 ± 0.10
298.15	0.692	3.95 ± 0.07	13.65 ± 0.05	-6.69 ± 0.09
298.15	0.933	5.26 ± 0.10	14.44 ± 0.06	-6.49 ± 0.15
310.15	0.150	-	13.51 ± 0.23	-5.60 ± 0.22

a)$\log\beta_{pqr}$ refer to Eqs. 4.1 – 4.2; b) ± Std. Dev

From the potentiometric measurements where the formation of a sparingly soluble species has been obtained; the precipitates were recovered, filtered on 0.45µm cellulose filters, washed with ultrapure water and finally dehydrated under vacuum. In particular, three different Ca^{2+}/Dop^- precipitates, identified with A, B, C, obtained at different metal/ligand molar ratios were analyzed.

Thermogravimetric analyses were performed from T = 293.15 to T = 1073.15 K (gradient temperature; more details are reported in the footnote of **Figure 4.4**) and the diagram in **Figure 4.4**, highlights the different decomposition steps for each sample (more details in **Figure 4.5** for the sample Ca^{2+}/Dop^- B).

At the end of the thermogravimetric analyses, it is visible how the amount of the metal oxide is different for the three samples.

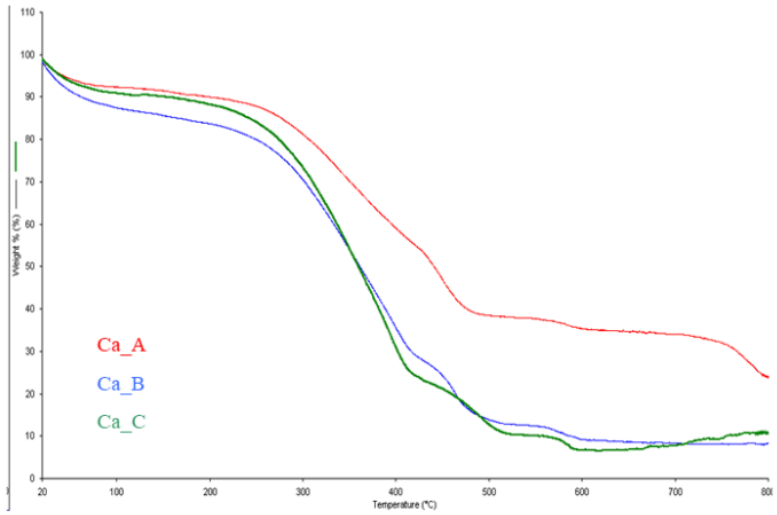

Figure 4.4. Thermogravimetric curve for the Ca^{2+}/Dop^- precipitates obtained at different metal:ligand molar ratios, at I = 0.15 mol dm^{-3}. Component concentration in the solution: C_{Ca2+} = 1.5 mmol dm^{-3} and C_{Dop-} = 1.5-7.5 mmol dm^{-3}. Atmosphere of air (gaseous mixture of nitrogen and oxygen with 80 and 20%, v/v, respectively) at a flow rate of 100 mL min^{-1} and a scanning rate of 10 K min^{-1}.

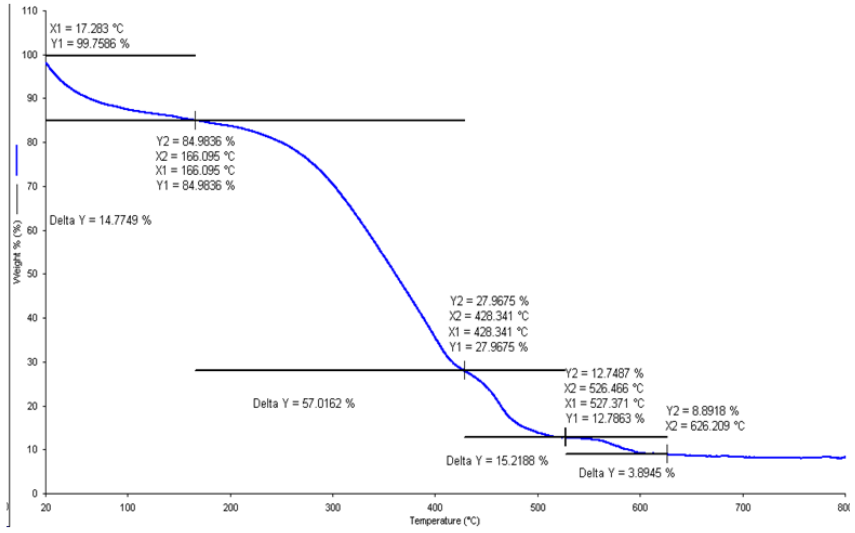

Figure 4.5. Thermogravimetric profile of the percentage weight loss for Ca^{2+}/Dop^- B.

Table 4.10 reports the percentage weight loss for each Ca^{2+}/Dop^- system, calculated from the thermal decomposition of the precipitates. Considering these experimental data, the stoichiometry of the precipitates was calculated, assuming that the residual of the decomposition process is CaO. As it can be observed, the stoichiometry of the precipitate changes between a metal:ligand molar ratios of 1:3 to 1:5, in dependence on the initial concentrations of the components in the vessel.

Table 4.10. Thermal decomposition steps for the Ca^{2+}/Dop precipitates

system	*Percentages by weight at the beginning of the process*	*Percentage loss of weight during the decomposition process*
Ca-Dop(A)		
1° process	99.8 %	9.45 %
2° process	90.31 %	34.49 %
3° process	55.82 %	17.96 %
4° process	37.82%	3.10%
5° process	34.77%	10.56%
Stoichiometry (M:L)	**1:1**	
Ca-Dop(B)		
1° process	99.76%	14.77%
2° process	84.98%	57.02%
3° process	27.97%	15.22%
4° process	12.75%	3.89%
Stoichiometry (M:L)	**1:3**	
Ca-Dop(C)		
1° process	99.86%	10.01%
2° process	89.85%	67.93%
3° process	21.92%	11.79%
4° process	10.12%	3.48%
Stoichiometry (M:L)	**1:5**	

4.1.3.2 Mg^{2+}/Dop^{-} system

The interactions of Mg^{2+} with Dopamine were investigated at different of ionic strengths (from I = 0.15 to 1.0 mol dm^{-3}) and temperatures (from T = 288.15 to 310.15 K). As for the Ca^{2+} system, the speciation model and the stoichiometry are characterized by simple mononuclear complexes. The model that gave the best results is featured by the ML and MLOH species.

Table 4.11 reports the corresponding formation constants of the Mg^{2+}/Dop^- complexes determined at different temperatures and ionic strengths in NaCl aqueous solutions.

As it is possible to observe from **Figure 4.6**, the formation of the metal-ligand species occurs at pH~8.5 and up to this pH value, magnesium is present as free metal ion. Only at higher pH, the $MLOH^0_{(aq)}$ complex becomes the predominant one and ML reaches ~10%.

This evidence reported in **Figure 4.6**, it refers to the experimental conditions: T = 310.15 K and I = 0.15 mol dm^{-3}; similar results were observed at also different conditions, obtaining only slightly shift of the maximum of formation, changing the ionic strength or the temperature.

Unlike to the Ca^{2+}/Dop^- system, the formation of the MLH species was not observed. This can be probably due to the different behavior of the two metals in terms of hydrolytic constants.

From the distribution diagrams of the two metal/Dop systems we observe as an example, that the interaction between Ca^{2+} and dopamine begins at pH ~ 7.5, whilst for Mg^{2+} at about 8.5; this aspect can be explained because in the second case, we did not obtain the formation of the MLH species.

Table 4.11. Experimental formation constants of the Mg^{2+}/Dop^- species in NaCl aqueous solutions at different ionic strengths and different temperatures

I/mol dm^{-3}	$\log\beta_{ML}$ a)	$\log\beta_{MLOH}$ a)
	T = 288.15 K	
0.15	3.459±0.068 b)	-6.278±0.040 b)
0.50	3.259±0.078	-6.676±0.030
0.75	3.267±0.084	-6.905±0.032
1.00	3.467±0.092	-7.336±0.012
	T = 298.15 K	
0.15	3.034±0.044	-6.111±0.026
0.50	2.797±0.052	-6.531±0.020
0.75	2.777±0.056	-6.825±0.022
1.00	2.951±0.092	-7.324±0.008
	T = 310.15K	
0.15	2.561±0.064	-5.926±0.040
0.50	2.281±0.074	-6.369±0.030
0.75	2.232±0.082	-6.736±0.034
1.00	2.375±0.092	-7.311±0.012

a) $\log\beta_{pqr}$ refer to Eqs. 4.1 – 4.2; b) ± Std. Dev

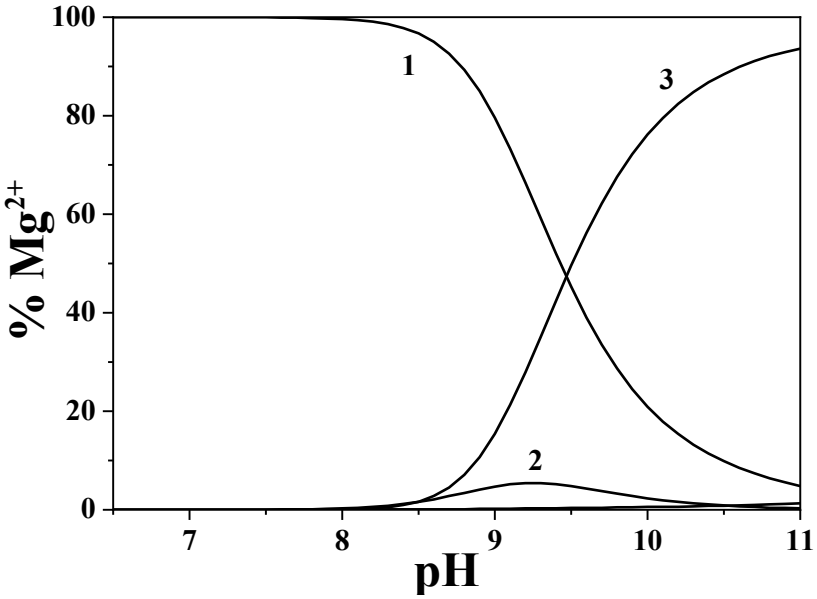

Figure 4.6. Distribution diagram for the Mg^{2+}/Dop^- species at I = 0.15 mol dm^{-3} and T = 310.15 K. Species: 1 M, 2 ML, 3 MLOH. [M = Mg^{2+}; L = Dop^-] (Experimental Conditions: C_{Mg2+} = 1.0 mmol dm^{-3}; C_{DOP-} = 1.0 mmol dm^{-3})

4.1.3.3 Sn^{2+}/Dop^- system

A quite different behavior with respect to calcium and magnesium, was observed for the Sn^{2+}/Dop^- system, both in term of speciation model, stoichiometry, and stability of the species. This can be explained taking into account both the different acid-base properties of Sn^{2+} with respect to calcium and magnesium, and its tendency of forming in chloride solution $SnCl_i$ (i = 1-3) species, together with SnOHCl hydrolytic complex [121-124]. Moreover, another different behavior of Sn^{2+} respect to the other two cations forms, is the formation of polynuclear complexes as reported in **Table 4.12**. Moreover the limits of this investigation is the formation of the $Sn(OH)_{2(s)}$ sparingly soluble species [62], whose formation is observed at pH values dependent on the metal concentration, ionic medium and ionic strength and temperature. Applying the already cited criteria of selection of the best speciation model, the model that gave the better statistical parameter is featured by the M_2L_2, ML_2, MLOH and M_2LOH species, whose stability constants are reported in **Table 4.12**.

Table 4.12. Experimental formation constants of the Sn^{2+}/Dop^- species in NaCl aqueous solutions

T/K	I/mol dm^{-3}	$\log\beta_{M2L2}$ a)	$\log\beta_{ML2}$ a)	$\log\beta_{MLOH}$ a)	$\log\beta_{M2LOH}$ a)
288.15	0.150	35.21 ± 0.09 b)	24.51 ± 0.01 b)	9.54 ± 0.01 b)	15.43 ± 0.06 b)
298.15	0.147	34.83 ± 0.01	24.12 ± 0.01	9.49 ± 0.01	15.67 ± 0.03
298.15	0.472	34.35 ± 0.01	23.10 ± 0.01	9.10 ± 0.01	15.55 ± 0.02
298.15	0.709	33.95 ± 0.01	22.51 ± 0.01	8.74 ± 0.01	15.96 ± 0.01
298.15	0.954	31.68 ± 0.07	20.75 ± 0.03	7.63 ± 0.02	15.60 ± 0.05
310.15	0.150	32.54 ± 0.09	20.89 ± 0.02	8.47 ± 0.06	14.90 ± 0.01

a)$\log\beta_{pqr}$ refer to Eqs. 4.1 – 4.2; b) ± Std. Dev

All the species reported in the speciation model are formed in high amount, covering the entire range of pH investigated, as highlighted by **Figure 4.7**. Moreover, the free metal ion is present in very lower percentages (~5% and at pH < 4). The M_2L_2 species covers almost all the investigated pH range, representing the main complexes up to pH ~ 6.5, beyond which the species MLOH and ML_2 become the most important ones. The same Figure also evidence the effect of the ionic strength variation on the distribution of the species; in particular, **Figure 4.7** reports the distribution of the species at the lower and higher investigated ionic strengths, obtaining a significant shift of the maximum of formation in term of percentage and of pH value.

Analysis of **Figure 4.7**. evidence two other important aspects; the first one is the formation of the $SnCl_i$ (i = 1-3) complexes at low pH values. The second is that the strength of the Sn^{2+}/Dop^- complexes avoids the formation of the $Sn_p(OH)_q$ species in high amounts, that reach about 5% of formation (not reported in **Figure 4.7**.), even if the SnOHCl one at I = 0.15 mol dm^{-3} and pH ~ 3, achieves about 20% of formation. The pH limit investigated (pH~ 8-9) is bound to the formation of an insoluble species in turn dependent on the experimental conditions investigated.

Similar observation can be made for the effect of the temperature; in this case, for the overall stability constants of M_2L_2 and ML_2 species, differences of about 3 orders of magnitudes between T = 288.15 and 310.15 K at I = 0.15 mol dm^{-3} are observed. For the overall stability constants of MLOH and M_2LOH, the differences are smaller, about 1 and 0.5 order of magnitudes, respectively.

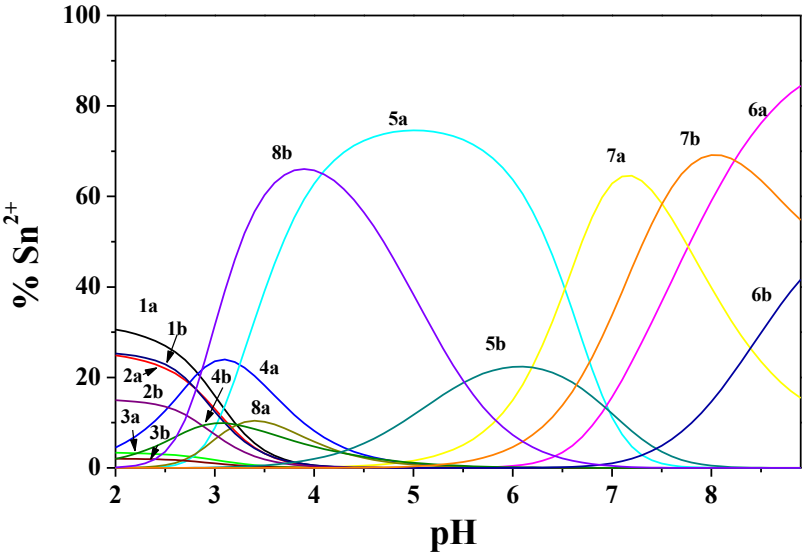

Figure 4.7. Distribution diagram for the Sn^{2+}/Dop^- species a T = 298.15 K and different ionic strengths. Species: 1. MCl; 2. MCl_2; 3. MCl_3; 4. MCl(OH); 5. M_2L_2; 6. ML_2; 7. MLOH; 8. M_2LOH. [M = Sn^{2+}; L = Dop^-] a: I = 0.15 mol dm^{-3}; b: I = 1.00 mol dm^{-3}.
(Experimental Conditions: C_{sn2+} = 2.0 mmol dm^{-3}; C_{DOP-} = 5.0 mmol dm^{-3})

4.1.3.4 Dependence on ionic strength and temperature of complexes with metals of Group A

The dependence of the formation constants, determined in NaCl aqueous solutions, on the ionic strength and temperature was modelled by using two approaches: the first one applying an extended Debye-Hückel equation (EDH), the second, the Specific ionic Interaction Theory (SIT). They allow the calculation of the stability constants at infinite dilution, in the molar concentration scale the first one, and in the molal concentration scale the second. Moreover, the EDH allows to model the variation of the stability constants, when the ionic strength changes, by the calculation of simple empirical parameters, in turn dependent on the stoichiometry of the reaction, on the charge of the components and on the formed species involved in the reaction. The SIT approach allows the determination of the specific ion interaction parameters of the ion-pairs involved in the formation of the given species.

Equation (4.8) reports the extended Debye-Hückel equation used to model the variation of the stability constants; it is possible to observe that with respect to the classical model, this equation reports an additive term for the dependence on the temperature:

$$\log\beta_{pqr} = \log^{T}\beta_{pqr} - z^{*}\cdot A\cdot \sqrt{I}/(1+1.5\cdot\sqrt{I}) + C\cdot I + L\cdot (1/298.15 - 1/T)\cdot 52.23 \qquad (4.8)$$

where 52.23 is 1/(R·ln10) and C is the adjustable parameter for the dependence of formation constants on ionic strength, in the molar concentration scale; in turn, the C parameter can be expressed by the following equation: $C = c_0\, p^{*} + c_1\, z^{*}$ with $p^{*} = \Sigma p_{reactants} - \Sigma p_{products}$ and $z^{*} = \sum z react^2 - \sum z prod^2$; z and p are the charge and the stoichiometric coefficient, respectively. $\log^{T}\beta_{pqr}$ is the formation constant at infinite dilution and A is the Debye-Hückel term expressed with respect to its dependence on the temperature, as reported in the Eq. (4.9), where 0.856 and 0.00385 are empirical parameters, T = 298.15 K is the reference temperature and T' the desired temperature expressed in Kelvin (K):

$$A = (0.51 + (0.856\cdot (T' - 298.15) + 0.00385\cdot (T - 298.15)^2)/1000) \qquad (4.9)$$

Moreover,

$$L = (\Delta H_n^0 - z^{*}\cdot (1.5 + 0.024\cdot (T' - 298.15)\cdot \sqrt{I})/(1 + 1.5\cdot \sqrt{I})) \qquad (4.10)$$

By using the Eq. (4.10), it is possible to calculate, in the investigated ΔT range, the enthalpy change value of formation of a given species at infinite dilution ΔH_n^0.

For the investigations where the dependence of the stability constants on the ionic strength has been carried out at only a single temperature, the applied Debye-Hückel equation used to model the dependence of the stability constants on the ionic strength is the version reported in equation (3.11). The formation enthalpy change values were calculated only at the ionic strengths where the measurements were carried out at different temperatures, by using the equation (3.18), and assuming as reference temperature (T = 298.15 K).

However, this approach, *i.e.* Eq. (3.11)., has also been applied at each single temperature, allowing the determination of the stability constants at infinite dilution as reported in **Table 4.13**, for Mg^{2+}.

Tables 4.13 - 4.15 report the results obtained for the Ca^{2+}, Mg^{2+} and Sn^{2+}/Dop^{-} systems. The results reported in **Table 4.14**, allow as to observe that the formation reactions of the metal/dopamine species are all exothermic, except for the MLOH ones of the calcium and magnesium systems. Moreover, it is possible to confirm that, as for the specie formed by electrostatic interaction, the entropy can be considered the driving force of the reactions.

Table 4.13. Formation constants, at infinite dilution and at different temperatures, of the Mg^{2+}/Dop^{-} species

	$\log \beta^{T}_{ML}$ [b)]	$\log \beta^{T}_{MLOH}$ [b)]
	T = 288.15 K	
$I \rightarrow 0$ [a)]	3.895±0.040 [c)]	-5.291±0.090
C [d)]	0.190±0.072	-0.692±0.144
	T = 298.15 K	
$I \rightarrow 0$	3.560±0.036	-5.366±0.108
C	0.140±0.090	-0.612±0.152
	T = 310.15 K	
$I \rightarrow 0$	3.007±0.170	-4.796±0.094
C	-0.007±0.223	-1.239±0.146

a) I/mol dm^{-3}; b) refer to the Eqs. (4.1 – 4.2); c) ±Std. Dev.; d) parameter for the dependence of $\log\beta_{pqr}$ on I/mol dm^{-3}

Table 4.14. Formation constant, enthalpy and entropy change values of the M^{n+}/Dop^- species at infinite dilution and at $T = 298.15$ K

Species	$\log\beta^{T}_{pqr}$ [a)]	C[b)]	ΔH[c)]	$T\Delta S$[c)]
		Ca^{2+}/Dop^-		
ML	5.30 ± 0.07[d)]	-0.88 ± 0.12	-	
MLH	13.80 ± 0.06	0.33 ± 0.15	-58±25 [d,e)]	20±25 [d,e)]
MLOH	-6.18 ± 0.06	-0.06± 0.09	99±43	64±43
		Mg^{2+}/Dop^-		
ML	3.560±0.036 [d)]	0.07±0.04	-72±2 [d,f)]	52±2
MLOH	-5.366±0.108	-1.03±0.03	24±3	-7±3
		Sn^{2+}/Dop^-		
M_2L_2	36.40 ± 0.29 [d)]	-2.90 ± 0.50	-211±28 [d,e)]	-4±28 [d,e)]
ML_2	25.56 ± 0.20	-3.33 ± 0.36	-286± 35	-141±35
MLOH	10.43 ± 0.19	-1.75 ± 0.33	-84± 20	-24±21
$M_2L(OH)$	16.11 ± 0.04	0.30 ± 0.06	-42± 21	50±21

a) $\log\beta_{pqr}$ refer to eqs. (4.1 – 4.2); b) parameter for the dependence on I/mol dm^{-3}; c) enthalpy and entropy change values of formation in kJ/mol ; d) ±Std.Dev. ; e) calculated at $I = 0.15$ mol dm^{-3} and $T = 298.15$ K ; f) at infinite dilution

By using the two different applications of the SIT approach (Eq. 3.15) and considering the specific ion interaction coefficients of the following ion-pairs: $\varepsilon(H^+,Cl^-) = 0.12$ [125]; $\varepsilon(Dop^-,Na^+) = -0.228$ [110]; $\varepsilon(Ca^{2+},Cl^-) = 0.14$ [126]; $\varepsilon(Mg^{2+},Cl^-) = 0.209$ [126] and $\varepsilon(Sn^{2+},Cl^-) = 0.032$ [62], it was possible to calculate both the $\Delta\varepsilon$ and the single $\varepsilon(M_pL_qH_r^{-/+}, Na^+/Cl^-)$ coefficients.

The specific ion interaction coefficients (ε and $\Delta\varepsilon$) of the ionic species and the Setschenow coefficients for the neutral ones for the metal/dopamine species are reported in **Table 4.15.**

Table 4.15. Specific ion interaction and Setschenow coefficients for the species of the metal/dopamine systems.

		Ca^{2+}		
	$\Delta\varepsilon_{ML}$ a)		**$\Delta\varepsilon_{MLH}$ a)**	**$\Delta\varepsilon_{MLOH}$ a)**
***T* = 298.15 K**	-1.11±0.07 b)		0.19±0.09 b)	-0.16±0.06 b)
		Mg^{2+}		
***T* = 288.15 K**	0.26±0.06			-1.22±0.04
***T* = 298.15 K**	0.06±0.07			-1.02±0.06
***T* = 310.15 K**	0.11±0.06			-1.63±0.02
		Sn^{2+}		
	$\Delta\varepsilon_{M_2L_2}$ a)	**$\Delta\varepsilon_{ML_2}$ a)**	**$\Delta\varepsilon_{MLOH}$ a)**	**$\Delta\varepsilon_{M_2LOH}$ a)**
***T* = 298.15 K**	-2.88±0.19 b)	-3.29±0.14	-1.72±0.13	0.30±0.02
Species		**Ca^{2+}**	**Mg^{2+}**	**Sn^{2+}**
***T* = 298.15 K**				
$\varepsilon_{(ML+,Cl-)}$ c)		1.03±0.07 b)	-0.20±0.07	-
$\varepsilon_{(MLH2+,Cl-)}$ c)		-0.16±0.09	-	-
k_{MLOH} c,d)		-0.06±0.01	0.99±0.05	1.39±0.13
$\varepsilon_{(M2L22+,Cl-)}$ c)		-	-	2.49±0.19
k_{ML2} c, d)		-	-	2.90±0.14
$\varepsilon_{(M2LOH2+,Cl-)}$ c)		-	-	-0.60±0.02

a) Calculated by means of Eq. (3.15); b) ±Std. Dev.; c) Specific ion Interaction coefficient of the ion-pair; d) Setschenow coefficient for the neutral species calculated by means of Eq. (3.17).

4.1.4 Metal Group B/Dopamine systems

The Group B includes as already reported, the following metals: Cd^{2+}, Cu^{2+}, Mn^{2+}, Zn^{2+} and UO_2^{2+}. The interactions of dopamine [2-(3,4-Dihydroxyphenyl)ethylamine, (Dop^-)] with cadmium, copper and dioxouranium(VI) were studied in $NaCl_{(aq)}$ at different ionic strengths ($0 \leq I$ / mol $dm^{-3} \leq 1.0$) and temperatures ($288.15 \leq T$ / K ≤ 318.15).

4.1.4.1 Cd^{2+}/Dop^- system

For the cadmium(II) interactions towards dopamine, the speciation model, used as input in the BSTAC program, includes the protonation constants of the ligand, the hydrolytic species of the metal and the $CdCl_i$ (i = 1-4) and the CdOHCl species formed with the ion of the supporting electrolyte (i.e.

NaCl), that in some conditions (*i.e.* high chloride concentration) reaches formation percentages higher than 30% [113].

The interactions of dopamine towards cadmium(II) was investigated in quite wide experimental conditions, I = 0.15 mol dm^{-3} from T = 288.15 to 318.15 K. Measurements at T = 298.15 K were also carried out at different ionic strengths from I = 0.15 to 1.0 mol dm^{-3}, at the metal:ligand molar ratios already reported in **Table 2.2** of Experimental part.

Table 4.16 reports the stability constants of the Cd^{2+}/Dop^{-} species at different experimental conditions; the speciation model is formed by only the ML, MLH and ML_2 (M = Cd; L = dopamine; charge omitted) mononuclear species.

Table 4.16. Experimental formation constants of the Cd^{2+}/Dop^{-} species in NaCl aqueous solutions

***T*/K**	***I*/mol dm^{-3}**	**logβ_{ML} a)**	**logβ_{MLH} a)**	**logβ_{ML2} a)**
288.15	0.15	6.66 ± 0.03 b)	14.90 ± 0.09 b)	11.62 ± 0.08 b)
298.15	0.148	6.48 ± 0.03	14.08 ± 0.02	10.88 ± 0.02
298.15	0.488	6.06 ± 0.07	14.18 ± 0.01	10.31 ± 0.02
298.15	0.730	6.41 ± 0.02	14.71 ± 0.05	10.35 ± 0.07
298.15	0.956	6.30 ± 0.09	14.10 ± 0.05	9.13 ± 0.06
310.15	0.15	4.61 ± 0.04	12.56 ± 0.10	9.26 ± 0.02

a) logβ_{pqr} refer to Eqs. (4.1 – 4.2); b) ± Std. Dev

From the stability constants shown in **Table 4.16**, it can be observed that the cadmium complexes have approximately the same order of magnitude of the Ca^{2+}/Dop system (**Table 4.9**), with differences on the ML species of just one logarithmic unit. The difference between the stability constants of the two systems can also be justified considering that the Ca^{2+}/Dop^{-} complexes must be considered as conditional formation constants, whilst for Cd^{2+} we considered the interaction of the metal ion with the anion of the supporting electrolyte (Cl^{-}).

Another comparison between the different stability of complexes of the two systems can be carried out calculating the stepwise formation constants of the MLH species, taking into account the following equilibrium of formation: M + LH = MLH; for the Cd^{2+} we have a logK_{MLH} = 3.514 and of 2.864 for Ca^{2+}.

Considering the distribution diagrams reported in the **Figures 4.8 - 4.10**, some considerations can be done: 1. the importance of the $CdCl_i$ species is highlighted in **Figure 4.8**, where the distribution and the formation percentages of the species are calculated at I = 0.15 mol dm^{-3} and T = 298.15 K at metal:ligand molar ratio of 1:2, but similar results were also obtained at the other experimental conditions.

The $CdCl^{-}$ species reaches about 60% of formation at pH values lower than 6, contributing to reduce the amount of Cd^{2+} free. The others Cd(II)/chloride species are formed in lower amount and in

dependence on the chloride concentration (*i.e.* ionic strength) in solution. Interesting is also the presence of the ternary CdOHCl species that at pH ~ 8 reaches the maximum of formation. 2. Up to pH ~ 7, the interaction of dopamine towards cadmium does not occur; over this pH we observe the formation of the MLH species (~10% at pH ~ 8.5), whilst the ML and ML_2 form at higher pH and in higher amount, ~80%. 3. Although cadmium forms some mono and polynuclear hydrolytic species, and the "weakness" of its complexes with dopamine, the hydrolysis of the metal is inhibited by complexation at alkaline pH values and by the formation of the chloride species at acid pHs. 4. The effect of the ionic strength on the stability and distribution of the species is reported in **Figure 4.9**, where the distribution of the Cd^{2+}/Dop^- species follows different trend: the formation percentages of MLH and ML_2 species increase from I = 0.15 to 0.50 mol dm^{-3} and decrease from I = 0.50 to 1.00 mol dm^{-3}; for ML species the formation percentage decreases from I = 0.15 to 0.50 mol dm^{-3} and increases from I = 0.50 to 1.00 mol dm^{-3}. 5. Concerning the effect of the temperature reported in **Figure 4.10**, we can observe a net decreasing trend of the formation constant with increasing the temperature, with a difference of about 2 order of magnitude between values at T = 288.15 and 310.15 K.

At pH ~ 10-10.5, we observed the formation of a sparingly soluble species. The precipitate, collected at the end of some measurements (at different metal:ligand molar ratios, see here after), were washed sometimes with few amount of ultra-pure water and then dried under vacuum and characterized by TGA (see hereafter).

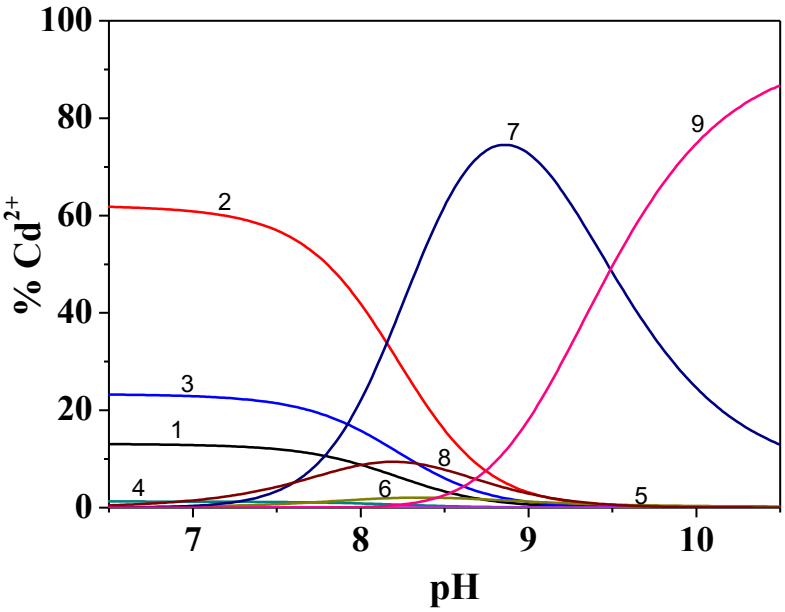

Figure 4.8. Distribution diagram for the Cd^{2+}/Dop^- system at I= 0.15 mol dm^{-3} and T = 298.15K (the percentages of formation of the $CdCl_i$ species are also reported)
Species 1 Cd free; 2 CdCl; 3 $CdCl_2$; 4 $CdCl_3$; 5 $CdCl_4$; 6 CdClH; 7 CdDop; 8 CdDopH; 9 $CdDop_2$.
(Experimental Conditions: C_{Cd2+} = 1.5mmol dm^{-3}; C_{DOP} = 3.0 mmol dm^{-3})

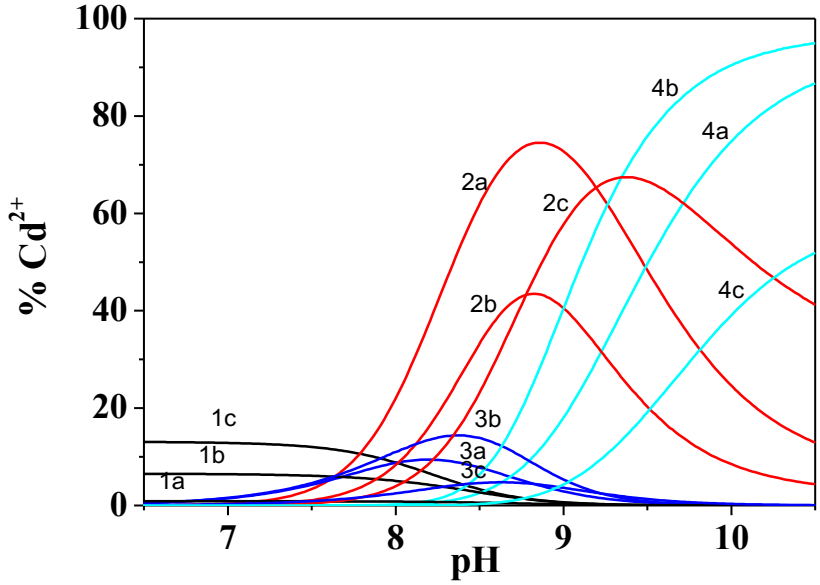

Figure 4.9. Distribution diagram for the Cd^{2+}/Dop^- system at different ionic strengths and T = 298.15 K.
Species 1 Cd^{2+} free; 2 CdDop;3 CdDopH;4 $CdDop_2$.
a I = 0.15 mol dm^{-3}; b I = 0.50 mol dm^{-3}; c I = 1.00 mol dm^{-3}.
(Experimental Conditions: C_{Cd2+} =1.5 mmol dm^{-3}; C_{DOP} = 3.0 mmol dm^{-3})

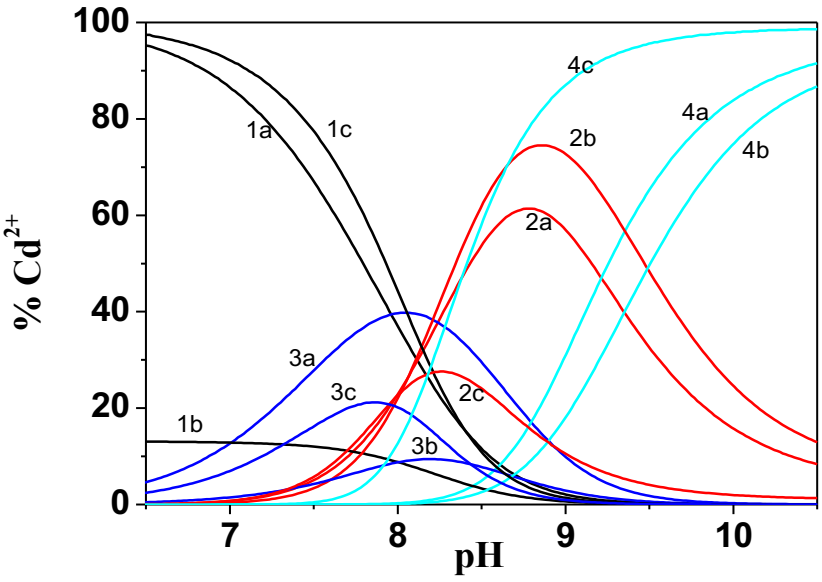

Figure 4.10 Distribution diagram for the Cd^{2+}/Dop^- system at I = 0.15 mol dm^{-3} and at different temperatures T= 288.15, 298.15, 310.15 K
Species 1 Cd^{2+} free; 2 CdDop; 3 CdDopH; 4 $CdDop_2$
a T= 288.15 K; b T = 298.15 K; c T = 310.15 K
(Experimental Conditions: C_{Cd2+} = 1.5 mmol dm^{-3}; C_{DOP} = 3.0 mmol dm^{-3})

Thermogravimetric analysis was performed with an air flow (mixed oxygen and nitrogen, 20% and 80% respectively) and with a temperature range of 293.15 - 1073.15 K, as for the Ca^{2+}/Dop^- precipitates.

The thermogravimetric spectra reported in **Figure 4.11**. concern two recovered samples, in which the ratios between metal and ligand in the initial aqueous solution were different.

Significant differences can be observed for the different precipitates, in term of amount of metal oxide at the end of the measurements.

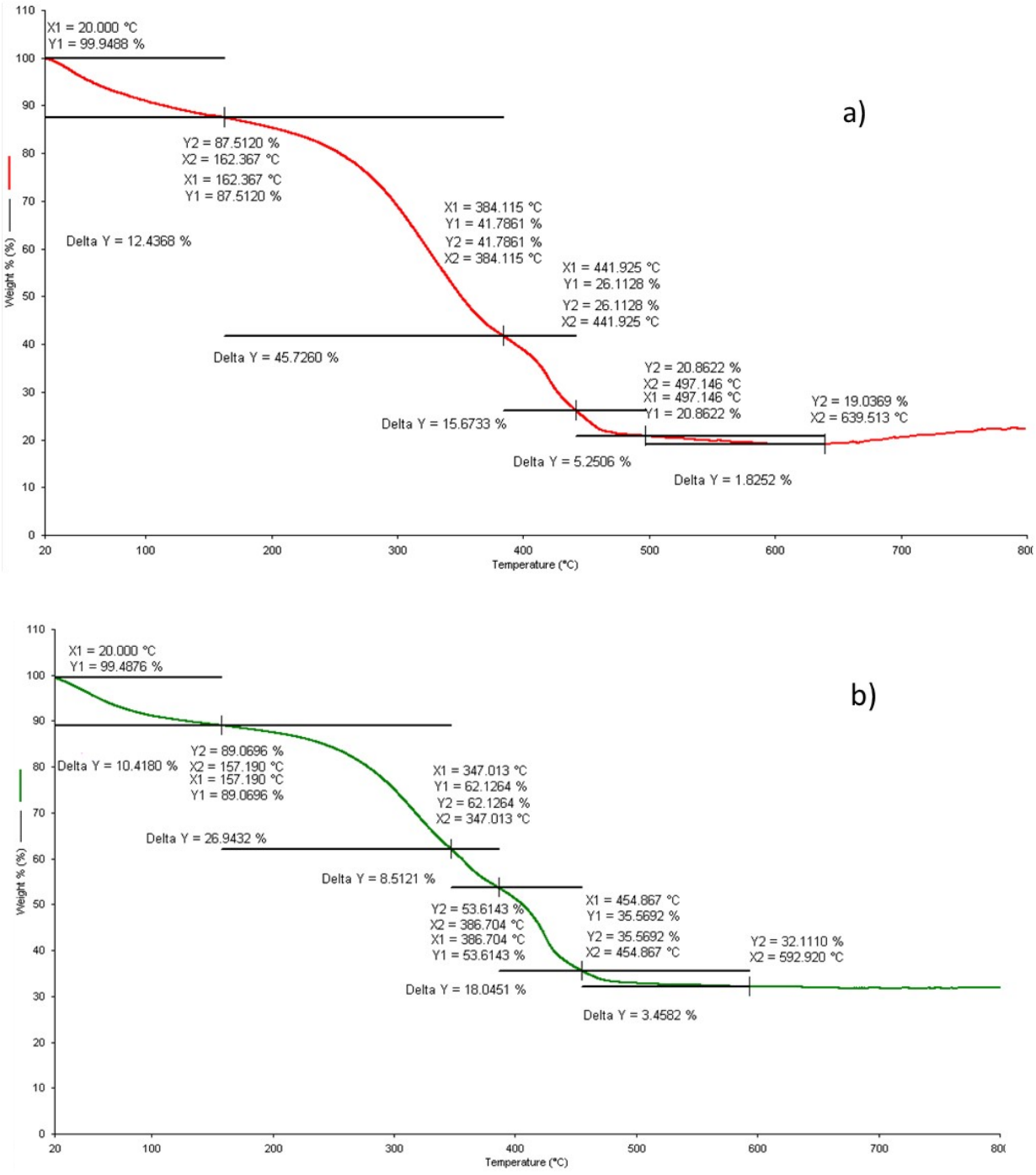

Figure 4.11. Thermogravimetric curves for the Cd^{2+}/dop^{-} system. Experimental condition: Air flow (gaseous mixture of nitrogen and oxygen with 80% and 20%, v/v, respectively) and in the temperature range 293.15-1073.15 K. Flow rate: 100 mL min^{-1}; scanning rate 10 K min^{-1}. Sample ~8-10 mg.

The curves reported in **Figure 4.11**. and the data in **Table 4.17**. highlight the different decomposition processes.

The initial decomposition process concerns the loss of the aromatic ring(s) also accompanied by the loss in some cases of a phenolic group of the ring itself. Subsequently, the other fragments of the side chain are decomposed up to the metal oxide.

Table 4.17. Thermic decomposition step of Cd^{2+}/Dop^{-} precipitates.

Cd-Dop(A)	% weight start process	% Weight loss during the decomposition process
1st decomposition process	99.95 %	12.44 %
2nd decomposition process	87.51 %	45.73 %
3rd decomposition process	26.11 %	15.67 %
4th decomposition process	20.86%	5.25%
5th decomposition process	19.04%	1.82%
stoichiometry metal:ligand	**1:3**	

Cd-Dop(B)		
1st decomposition process	99.49%	10.42%
2nd decomposition process	89.07%	26.94%
3rd decomposition process	62.12%	8.51%
4th decomposition process	35.57%	18.04%
5th decomposition process	32.11%	3.46%
stoichiometry metal:ligand	**2:3**	

4.1.4.2 Cu^{2+}/Dop^- system

The speciation of the Cu^{2+}/Dop^- system is much more complex with respect to the corresponding system with Cd^{2+}. In fact, in this case the best results were obtained when the formation of the ML_2, M_2L, M_2L_2, $M_2L_2OH_2$, M_2LOH and ML_2OH was considered. In this case, we observe the prevalence of simple binary and ternary hydrolytic binuclear complexes. On the contrary of that obtained for Cd^{2+}, the formation of the ML and MLH species does not occur.

Table 4.18. Experimental formation constants of the Cu^{2+}/Dop^- species in NaCl aqueous solutions at different ionic strengths and temperatures

			$\log\beta$			
***I*/mol dm^{-3}**	**ML_2 [a)]**	**M_2L [a)]**	**M_2L_2 [a)]**	**$M_2L_2(OH)_2$ [a)]**	**M_2LOH [a)]**	**ML_2OH [a)]**
			***T* = 288.15 K**			
0.161	21.02±0.08[b)]	15.21±0.06	27.34±0.08	13.40±0.08	8.87±0.02	11.38±0.06
0.492	20.50±0.06	15.33±0.04	26.86±0.04	12.68±0.06	9.02±0.02	11.25±0.04
0.743	20.21±0.05	15.42±0.03	26.60±0.02	12.26±0.04	9.21±0.03	10.22±0.03
0.995	19.95±0.06	15.52±0.04	26.38±0.04	11.89±0.04	9.42±0.04	10.20±0.03
			***T* = 298.15 K**			
0.171	19.36±0.06	14.57±0.04	25.66±0.06	11.72±0.05	8.86±0.02	11.01±0.05
0.474	18.88±0.04	14.68±0.02	25.22±0.03	11.04±0.03	9.00±0.02	10.88±0.03
0.738	18.57±0.04	14.78±0.03	24.94±0.03	10.60±0.03	9.19±0.02	10.85±0.02
0.965	18.33±0.05	14.87±0.04	24.74±0.05	10.26±0.04	9.38±0.04	10.84±0.03
			***T* = 310.15 K**			
0.145	17.58±0.01	13.85±0.02	23.87±0.06	9.95±0.03	8.85±0.03	10.63±0.04
0.482	17.02±0.05	13.98±0.02	23.35±0.05	9.16±0.02	8.99±0.02	10.47±0.03
0.728	16.73±0.05	14.07±0.04	23.09±0.06	8.74±0.04	9.16±0.03	10.43±0.03
0.982	16.46±0.10	14.16±0.06	22.85±0.08	8.36±0.07	9.37±0.04	10.42±0.04
			***T* = 318.15 K**			
0.161	16.40±0.06	13.41±0.01	22.67±0.06	8.73±0.02	8.84±0.04	
0.505	15.83±0.05	13.54±0.03	22.15±0.07	7.94±0.04	8.98±0.03	10.20±0.04
0.732	15.56±0.07	13.62±0.05	21.91±0.08	7.55±0.06		
0.994	15.28±0.09	13.72±0.08	21.66±0.11	7.16±0.09	9.36±0.04	10.15±0.06

a) $\log\beta_{pqr}$ refer to Eqs. (4.1 – 4.2); b) ± Std. Dev.

Table 4.18 reports the formation constants of the species obtained at the different experimental conditions (*i.e.* ionic strengths and temperatures). In the case of the Cu^{2+}/Dop^- system, we did not observe the formation of precipitate up to pH ~ 10.

The interaction between Cu(II) and dopamine begin at pH ~ 4, where the formation of the M_2L species occurs; in particular, the distribution diagram reported in **Figure 4.12** evidences that the formation percentages of the all complexes species of the Cu^{2+}/Dop^- system reach significant formation percentages in the pH range between 4.5-10.0. Moreover, the same diagram shows the effect of the

ionic strength on the formation percentage of the species. This effect is different for each complex species, and, for the CuL_2, Cu_2L_2, $Cu_2L_2(OH)_2$ the percentage of formation decreases increasing the ionic strength, while in the case of the Cu_2L and Cu_2LOH species an opposite effect was observed. For the CuL_2OH species, the same formation percentage (50% at pH = 8.5) was obtained at the two experimental conditions, but we observe at I = 1.00 mol dm^{-3}, a shifted versus low pH (pH~7.5).

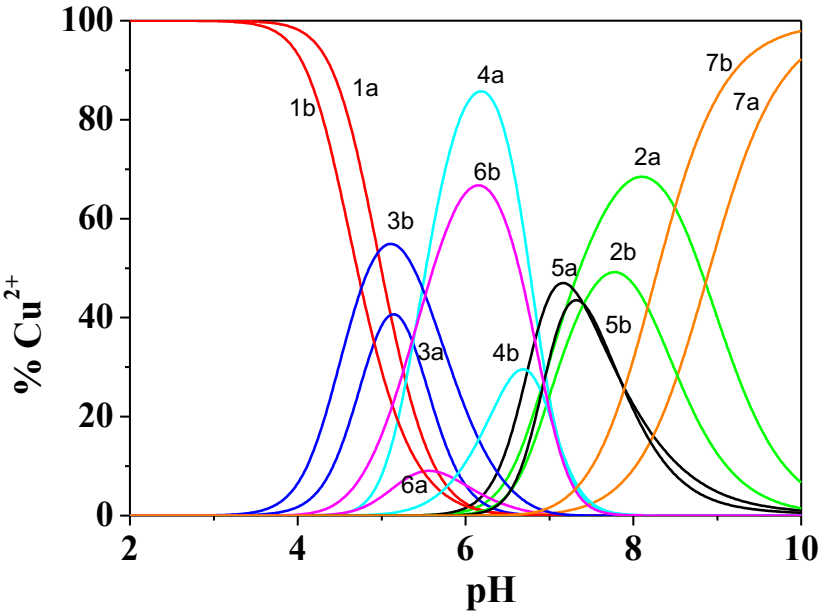

Figure 4.12. Distribution diagram for the Cu^{2+}/Dop^- system at different ionic strengths and T = 298.15 K
Species 1 Cu^{2+} free; 2 $CuDop_2$; 3 Cu_2Dop; 4 Cu_2Dop_2; 5 $Cu_2Dop_2OH_2$; 6 Cu_2DopOH; 7 $CuDop_2OH$.
a) I = 0.15 mol dm^{-3}; b I = 1.00 mol dm^{-3}
Experimental Conditions: C_{Cu2+} = 0.05 mmol dm^{-3}, C_{Dop-} = 1.5 mmol dm^{-3}.

Concerning the dependence of the formation percentages on the temperature, better information can be obtained from **Figure 4.13**, where the distribution of the species at I = 0.5 mol dm^{-3} and different temperatures has been drawn. The distribution diagram in **Figure 4.13** demonstrates the important effect of temperature on the formation of the Cu^{2+}/Dop^- complex. For some of them we observe a significant variation on the formation percentage, such as for the ML_2 that at T = 288.15 K achieves about 85% and at T = 318.15 K, only 8%. Similar behaviour has been observed for the M_2L_2, whilst in the case of $M_2L_2(OH)_2$ and M_2LOH, the formation percentages at T = 318.15 K do not exceed 5%.

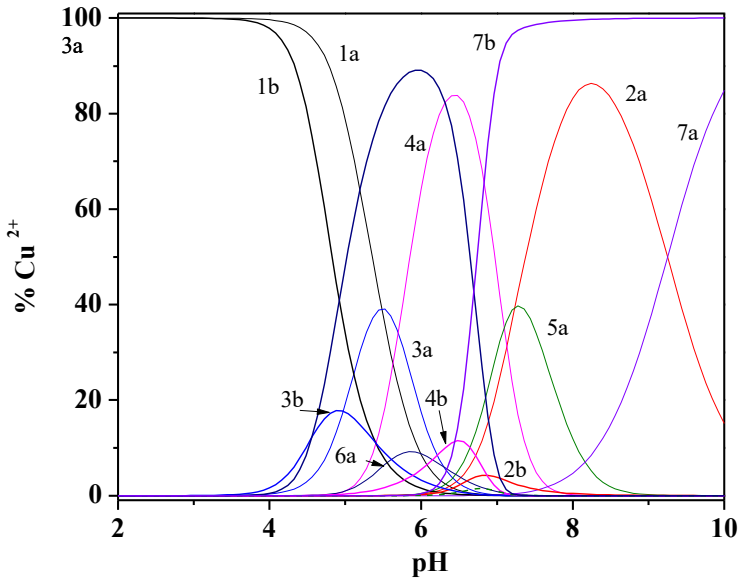

Figure 4.13 Distribution diagram for the Cu^{2+}/Dop^- system at I = 0.50 mol dm^{-3} and different temperatures
Species 1 Cu^{2+} free; 2 $CuDop_2$; 3 Cu_2Dop; 4 Cu_2Dop_2; 5 $Cu_2Dop_2OH_2$; 6 Cu_2DopOH; 7 $CuDop_2OH$.
a T = 288.15K; b T = 318.15K.
Experimental Conditions: C_{Cu2+} = 0.5 mmol dm^{-3}, C_{Dop-} = 1.5 mmol dm^{-3}.

Similar investigations carried out on the precipitates of the Ca^{2+}/Dop^- and Cd^{2+}/Dop^- systems were performed on the Cu^{2+}/Dop^- precipitate as reported in **Figure 4.14**. For the Cu^{2+}/Dop^- precipitate, we observe five main decomposition processes, with weight loss different between them, as reported in **Table 4.19**; calculation allowed to calculate a stoichiometry of 1:1.

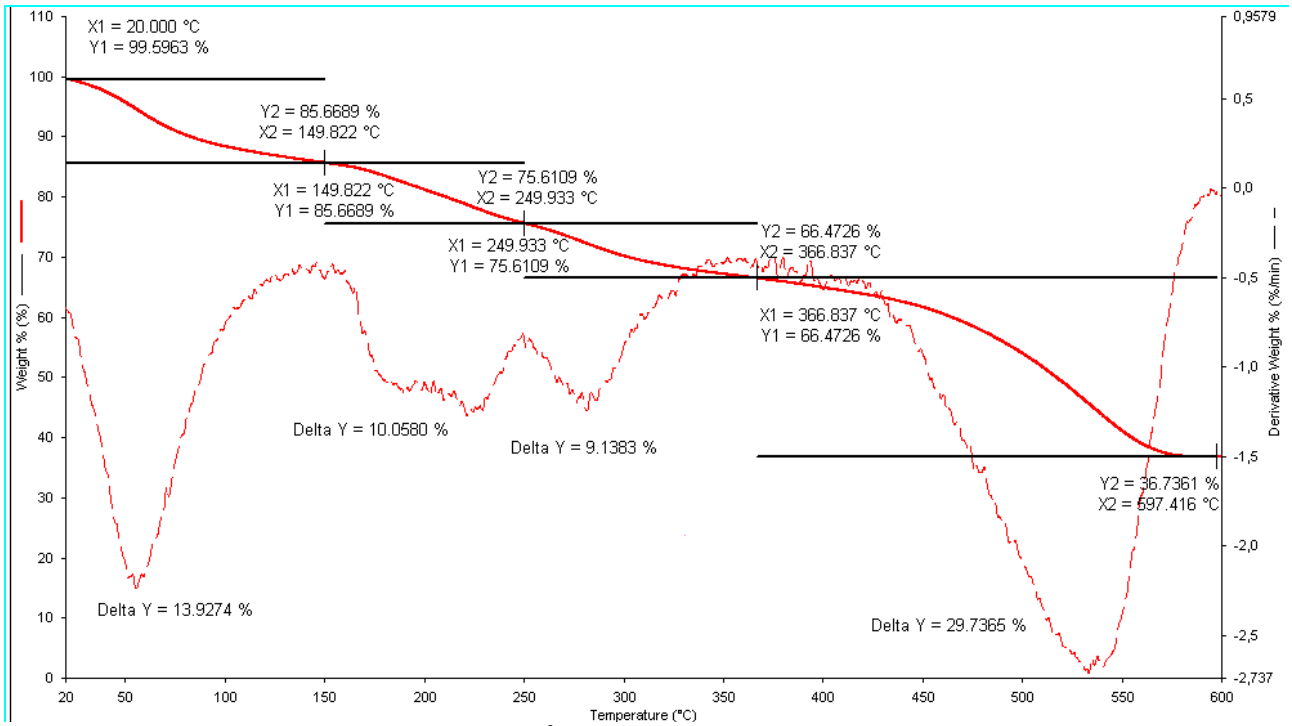

Figure 4.14. Thermogravimetric curves for the Cu^{2+}/dop^- system. Experimental condition: Air flow (gaseous mixture of nitrogen and oxygen with 80% and 20%, v/v, respectively) and in the temperature range 293.15-1073.15 K. Flow rate: 100 mL min^{-1}; scanning rate 10 K min^{-1}. Sample ~8-10 mg.

Table 4.19. Thermic decomposition step of Cu^{2+}/Dop^- precipitates.

Cu-Dop	% weight start process	% Weight loss during the decomposition process
1st decomposition process	99.59 %	13.99 %
2nd decomposition process	85.67 %	10.06 %
3rd decomposition process	75.61 %	10.11 %
4th decomposition process	66.50%	9.11%
5th decomposition process	36.7%	29.8%
stoichiometry metal:ligand	**1:1**	

4.1.4.3 Mn^{2+}/Dop^- system

Concerning the interaction of manganese with dopamine, the investigations were carried out at $0.15 \leq I/\text{mol dm}^{-3} \leq 1.00$, and $T = 288.15$, 298.15 and 310.15 K. The speciation model that gave the best results is featured by the following species: ML, MLH, ML_2. This speciation model is like the one obtained for Cd^{2+}. **Table 4.20** reports the corresponding stability constants at the investigated experimental conditions.

Table 4.20. Experimental formation constants of the Mn^{2+}/Dop^- species in NaCl aqueous solutions

T/K	I/mol dm^{-3}	$\log\beta_{ML}$ a)	$\log\beta_{MLH}$ a)	$\log\beta_{ML2}$ a)
288.15	0.140	6.65 ± 0.02b)	14.40 ± 0.04b)	11.40 ± 0.14b)
298.15	0.144	5.42 ± 0.07	13.87 ± 0.04	10.78 ± 0.10
298.15	0.459	5.09 ± 0.02	13.22 ± 0.03	9.54 ± 0.04
298.15	0.685	5.13 ± 0.03	13.54 ± 0.02	9.87 ± 0.03
298.15	0.919	4.58 ± 0.04	12.98 ± 0.05	8.73 ± 0.09
310.15	0.138	4.48 ± 0.04	12.34 ± 0.07	8.96 ± 0.03

a) $\log\beta_{pqr}$ refer to Eqs. (4.1 – 4.2); b) ± Std. Dev

The first consideration that can be done, is the similar strength in term of stability of the Mn^{2+}/Dop^- and Cd^{2+}/Dop^- complexes, independent on the experimental condition.

Figure 4.15 reports the distribution of the Mn^{2+}/Dop^- species at $T = 298.15$ K and $I = 0.15$ mol dm^{-3}. As already observed for other cations, up to pH ~ 8, the metal is mainly present as free Mn^{2+}; the distribution of the complex species occurs in a pH interval of 1.5-2 units. The MLH species reaches the maximum of formation (~40%) at pH = 8, while the ML one is formed at higher pH values and with a maximum of 30% at pH = 8.4; for the ML_2 we have 85% at pH = 9.

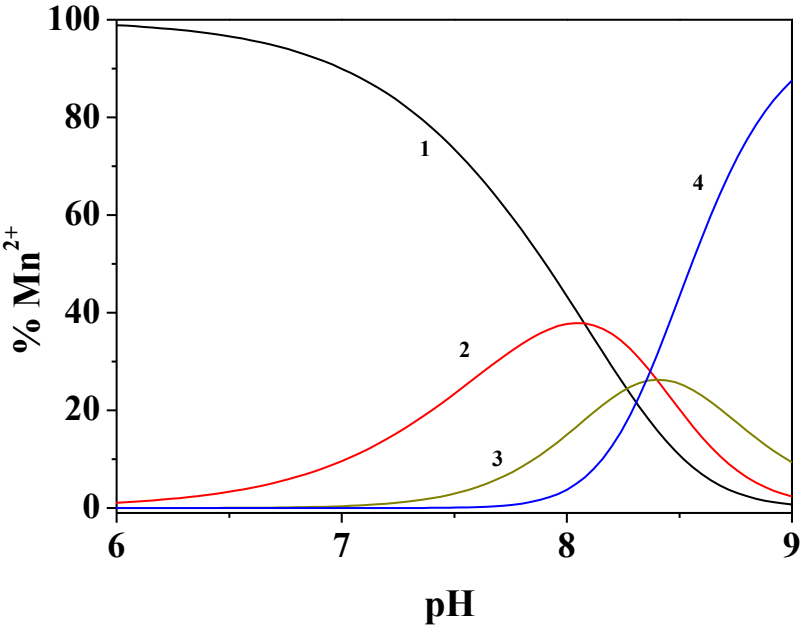

Figure 4.15. Distribution diagram for the Mn^{2+}/Dop^- system at T = 298.15 K and I = 0.15 mol dm^{-3}.
Species: 1. Mn^{2+}free; 2. MLH; 3. ML; 4. ML_2; M = Mn^{2+}; L = Dop^-.
Experimental Conditions: C_{Mn2+} = 2.0 mmol dm^{-3}; C_{DOP-} = 8.0 mmol dm^{-3}.

The effect of the ionic strength on the distribution of the species is highlighted in **Figure 4.16**, where for the MLH and ML_2 species we observe a lowering of the maximum percentage of formation with a slight shift towards more alkaline pH increasing the higher ionic strength.

The opposite trend was obtained for the ML species, whose formation percentage tends to increase with the ionic strength. Moreover, we observe a shift of the curve versus more alkaline pH (from 8.4 to 8.7) and a significant increment of the formation percentage up to 40%.

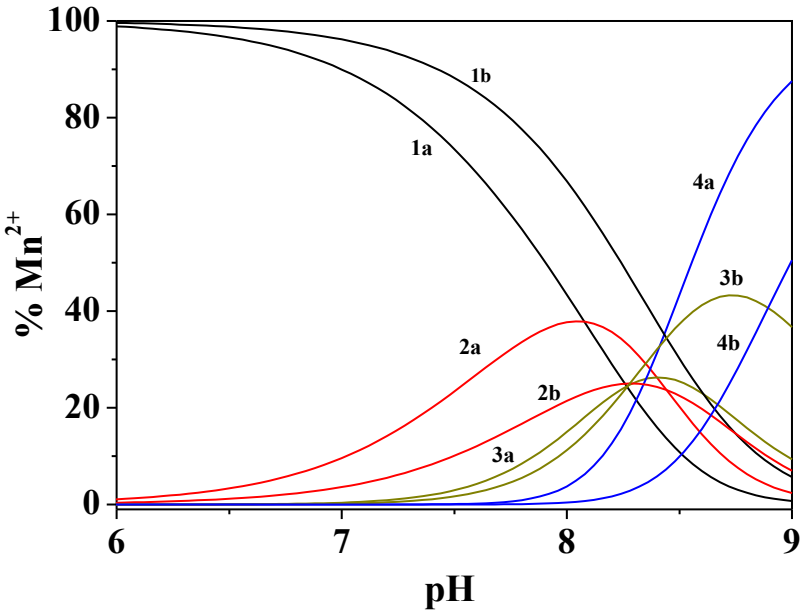

Figure 4.16. Distribution diagram for the Mn^{2+}/Dop^- system at T = 298.15 K and different ionic strength.
Specie: 1. Mn^{2+}free; 2. MLH; 3. ML; 4. ML_2; M = Mn^{2+}; L = Dop^-.
a: I = 0.15 mol dm^{-3}; b: I = 1.00 mol dm^{-3}.
Experimental Conditions: C_{Mn2+} = 2.0 mmol dm^{-3}; C_{DOP-} = 8.0 mmol dm^{-3}.

The effect of the temperature is shown in **Figure 4.17**; it is possible to highlight how for the MLH and ML species there is a lowering of the percentage of formation with increasing temperature, as consequence of the lowering of the stability constants increasing T/K.

The opposite trend was observed for the ML_2 species, that at pH = 9 and T = 310.15 K reaches a percentage of formation of ~ 90%.

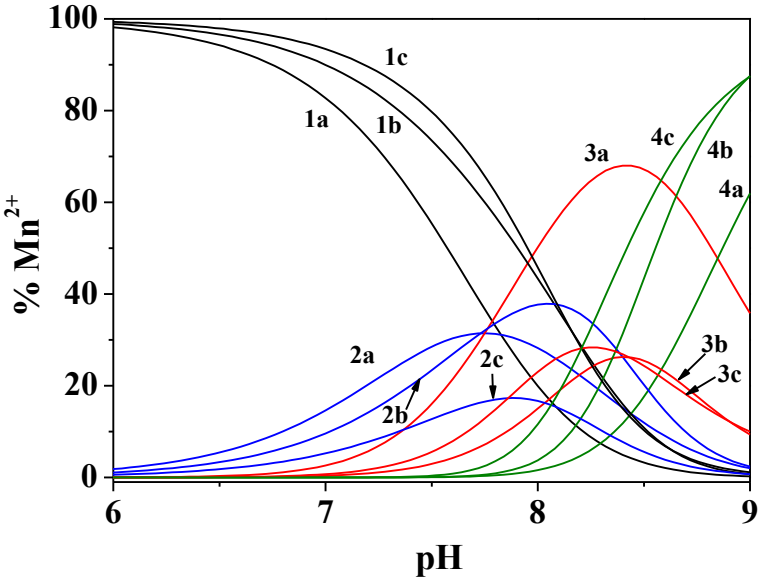

Figure 4.17. Distribution diagram for the Mn^{2+}/Dop^- system at I = 0.15 mol $dm^{-3}$and different T= 288.15, 298.15, 310.15 K.
Species: 1. Mn^{2+}free; 2. MLH; 3. ML; 4. ML_2; M = Mn^{2+}; L = Dop^-.
a) T = 288.15 K; b) T = 298.15 K; c) T = 310.15 K.
Experimental Conditions: C_{Mn2+} = 2.0 mmol dm^{-3}; C_{DOP-} = 8.0 mmol dm^{-3}.

4.1.4.4 Zn^{2+}/Dop^- system

Similar investigation were also carried out on the Zn^{2+}/Dop^- system and at the same experimental conditions of the Mn^{2+}/Dop^- ones.

The best results were obtained when the following species were considered: ML, MLH, MLOH and ML_2H; **Table 4.21** reports the corresponding formation constants at different ionic strengths and temperatures.

Table 4.21. Experimental formation constants[a)] of the Zn^{2+}/Dop^- species in NaCl aqueous solutions

T/K	I/mol dm^{-3}	$\log\beta_{ML}$ [a)]	$\log\beta_{MLH}$ [a)]	$\log\beta_{MLOH}$ [a)]	$\log\beta_{ML2H}$ [a)]
288.15	0.148	7.22 ± 0.02[b)]	14.80 ± 0.02[b)]	-1.32 ± 0.09[b)]	22.20 ± 0.02[b)]
298.15	0.148	7.40 ± 0.01	14.51 ± 0.02	-0.64 ± 0.02	21.64 ± 0.04
298.15	0.471	6.934 ± 0.009	14.24 ± 0.01	-1.23 ± 0.01	21.26 ± 0.01
298.15	0.929	6.648 ± 0.008	13.85 ± 0.02	-1.61 ± 0.02	20.24 ± 0.03
310.15	0.150	6.61 ± 0.01	13.13 ± 0.04	-1.31 ± 0.03	19.23 ± 0.10

a) $\log\beta_{pqr}$ refer to Eqs. (4.1 – 4.2); b) ± Std. Dev

In the pH range investigated, it has been seen that the free metal is the predominant species up to about pH 7; after this value, the formation of ML and MLH species is favored, whilst the MLOH and

ML_2H are formed at higher pH values, as it can be observed from the distribution diagram of the species reported in **Figure 4.18**.

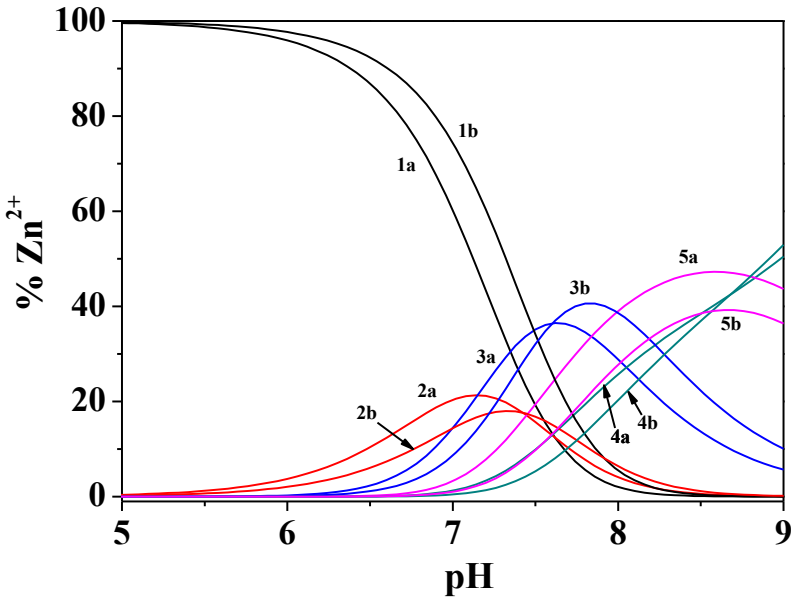

Figure 4.18. Distribution diagram for the Zn^{2+}/Dop^- species at T = 298.15 K and different ionic strengths.
Species: 1. Zn^{2+}free; 2. MLH; 3. ML; 4. MLOH; 5. ML_2H; M = Zn^{2+}; L = Dop^-.
a: I = 0.15 mol dm^{-3}; b: I = 1.00 mol dm^{-3}.
Experimental Conditions: C_{Zn2+} = 2.0 mmol dm^{-3}; C_{DOP-} = 6.0 mmol dm^{-3}.

As it already done for the other investigated systems, a distribution diagram has been drawn to highlight the effect of the temperature on the distribution of the species.

From this figure it is possible to observe how for the ML and ML_2H species, the lower temperatures favor their formation, whilst the opposite trend is observed for the other two species.

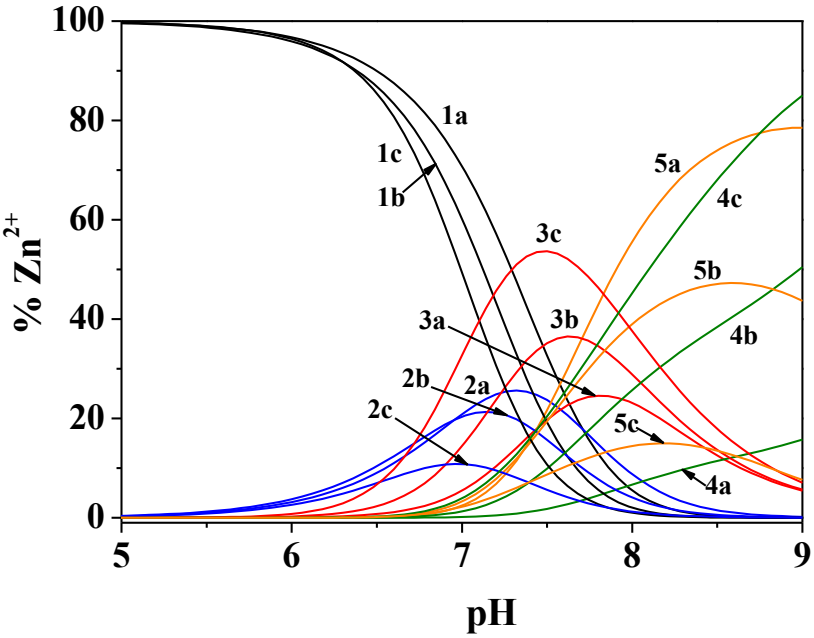

Figure 4.19. Distribution diagram for the Zn^{2+}/Dop^- species at I = 0.15 mol dm^{-3} and different temperatures.
Species: 1. Zn^{2+}free; 2. MLH; 3. ML; 4. MLOH; 5. ML_2H; M = Zn^{2+}; L = Dop^-.
a) 288.15K; b) 298.18K; c) 310.15K.
Experimental Conditions: C_{Zn2+} = 2.0 mmol dm^{-3}; C_{DOP-} = 6.0 mmol dm^{-3}.

4.1.4.5 UO_2^{2+}/Dop^- system

Investigation of the interaction between uranyl(VI) and dopamine resulted different with respect to the other two systems, in part due to the different acid-base behavior of UO_2^{2+} with respect to Cd^{2+} and Cu^{2+}, and to the fact that for our investigation the $UO_2(Acetate)_2$ product during our studies.
For this reason, the speciation model used as input in the BSTAC program contains, the protonation constants of dopamine, the hydrolytic species of uranyl(VI) and the formation constants of the UO_2^{2+}/Ac^- system already studied [115] (see **Table 4.7**). By using the criteria of selection already reported, different mononuclear and binuclear species were tested, but the best results were obtained when the ML_2 and MLOH species were introduced in the speciation model. With respect to other systems involving the interaction of UO_2^{2+} towards different classes of organic ligands [127], in this case we did not observe the formation of protonated, hydrolytic or polynuclear species. Moreover, a significant improvement of the statistical parameters was obtained when the MLAc (Ac = acetate)

was introduced in the speciation model, together with the other two species, as reported in T**able 4.22**, where we also reported the stability constant of the complexes.

The presence of this ternary complex can be explained considering that at the beginning of the potentiometric titrations, the metal is mainly present as acetate salt, forming species of significant stability along the pH interval of investigation where simultaneously there is the interaction with Dopamine. In fact, as reported in the distribution diagrams of the species (**Figures 4.20 - 4.21**) at different ionic strengths and temperatures, we observe that up to pH ~ 5-5.5, the MLAc can be considered the main species in solution, due also to the high stability of the complex, that has a log β value of ~ 16-17. To better evaluate the stability of this complex, we can calculate the stepwise formation constants considering the following equilibrium of formation: MAc + L = MLAc, where M = UO_2^{2+}, Ac = acetate and L = dopamine (charge omitted). At I = 0.15 mol dm^{-3} and T = 298.15 K, we have: log K_{MAc} = 2.44 and log β_{MLAc} = 16.14, for the formation of the logK_{MLAc} = 16.14 – 2.44 = 13.70. The strength of the complex formed by the interaction of uranyl(VI) with dopamine justify the absence of possible other species with higher stoichiometric coefficient.

The high stability of this species supports the hypothesis made about its existence and its predominant role in the speciation of the UO_2-dopamine system.

The percentage of formation of this species also confirms what has already been observed in many works published by our research group, regarding the stability of mixed species, favoring their formation compared to simple binary species.

As already observed for the other two systems, we observe from the distribution diagrams significant shift of the maximum of formation changing the experimental conditions (i.e. ionic strength and temperature). In the case of the UO_2^{2+}-Ac/Dop^- system, the ML_2 and MLAc species can be considered the main ones, since the MLOH form always in lower amounts and over pH ~6.5. The effect of the variables I/mol dm^{-3} and T/K on the stability of each complexes can be better observed form the following diagrams (**Figure 4.22**), where the variation of the logβ of each UO_2^{2+}-Ac/Dop^- species is reported.

Table 4.22. Experimental formation constants of UO_2^{2+}/Dop^- system in NaCl aqueous solutions at different ionic strengths and temperatures.

I /mol dm^{-3}	$\log\beta_{ML2}$ [a)]	$\log\beta_{MLAc}$ [a)]	$\log\beta_{MLOH}$ [a)]
		***T*=288.15 K**	
0.161	22.20 ± 0.12[b)]	16.11 ± 0.11	6.66 ± 0.07
0.526	21.87 ± 0.11	15.88 ± 0.10	6.71 ± 0.05
0.742	22.26 ± 0.12	15.83 ± 0.11	6.83 ± 0.06
0.994	22.67 ± 0.15	15.81 ± 0.12	6.96 ± 0.09
		***T*=298.15 K**	
0.165	21.69 ± 0.10	16.14 ± 0.09	7.09 ± 0.06
0.504	21.35 ± 0.07	15.66 ± 0.06	6.83 ± 0.04
0.74	21.23 ± 0.08	15.44 ± 0.06	6.73 ± 0.05
0.992	21.13 ± 0.11	15.24 ± 0.07	6.64 ± 0.08
		***T*=310.15 K**	
0.160	22.15 ± 0.10	16.58 ± 0.10	7.48 ± 0.06
0.505	21.88 ± 0.05	16.28 ± 0.06	7.29 ± 0.03
0.738	21.80 ± 0.06	16.17 ± 0.04	7.23 ± 0.04
0.990	21.75 ± 0.09	16.10 ± 0.04	7.20 ± 0.07
		***T*=318.15 K**	
0.159	22.12 ± 0.12	17.22 ± 0.12	7.49 ± 0.06
0.502	21.97 ± 0.07	16.81 ± 0.08	7.51 ± 0.04
0.739	21.98 ± 0.07	16.63 ± 0.06	7.60 ± 0.05
0.988	22.02 ± 0.09	16.48 ± 0.05	7.71 ± 0.07

a) $\log\beta_{pqr}$ refer to Eqs. (4.1 – 4.2); b) ± Std. Dev

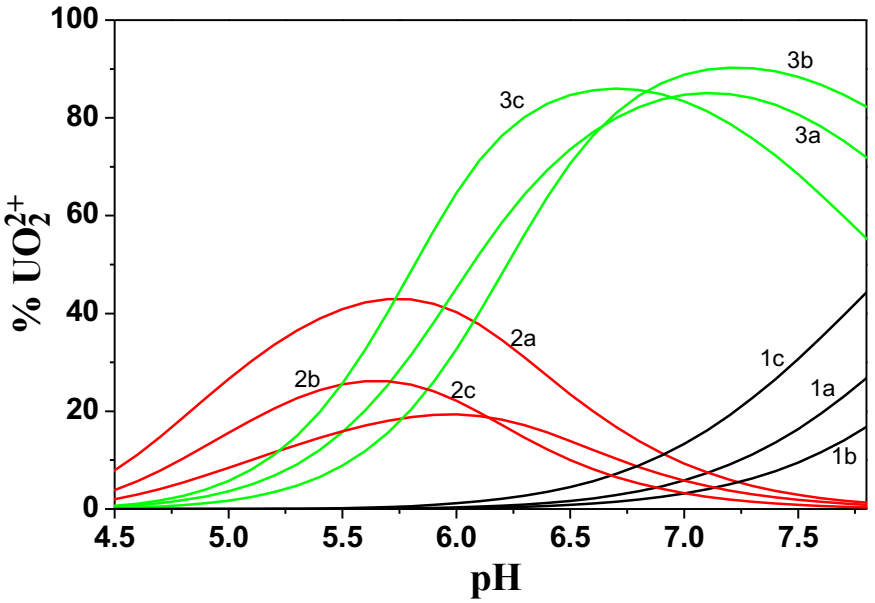

Figure 4.20. Distribution diagram of the species for UO_2-Ac/Dop^- system at T = 298.15 K and different ionic strengths.
Species: 1. MLOH; 2. MLAc; 3. ML_2; M = UO_2^{2+} L = Dop^-
a: I = 0.15 mmol dm^{-3}; b: I = 0.50 mmol dm^{-3}; c: I = 1.00 mmol dm^{-3}.

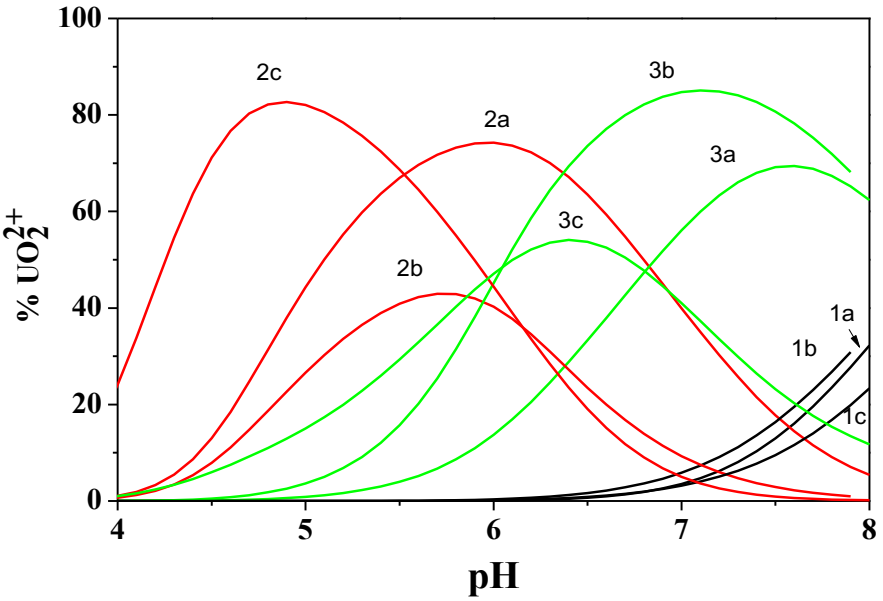

Figure 4.21. Distribution diagram of the species for UO_2-Ac/Dop^- system at I = 0.15 mol dm^{-3} and different temperatures.
Species: 1. MLOH; 2. MLAc; 3. ML_2;M = UO_2^{2+} L = Dop^-
a: T = 288.15 K; b: T = 298.15 K; c: T = 310.15 K

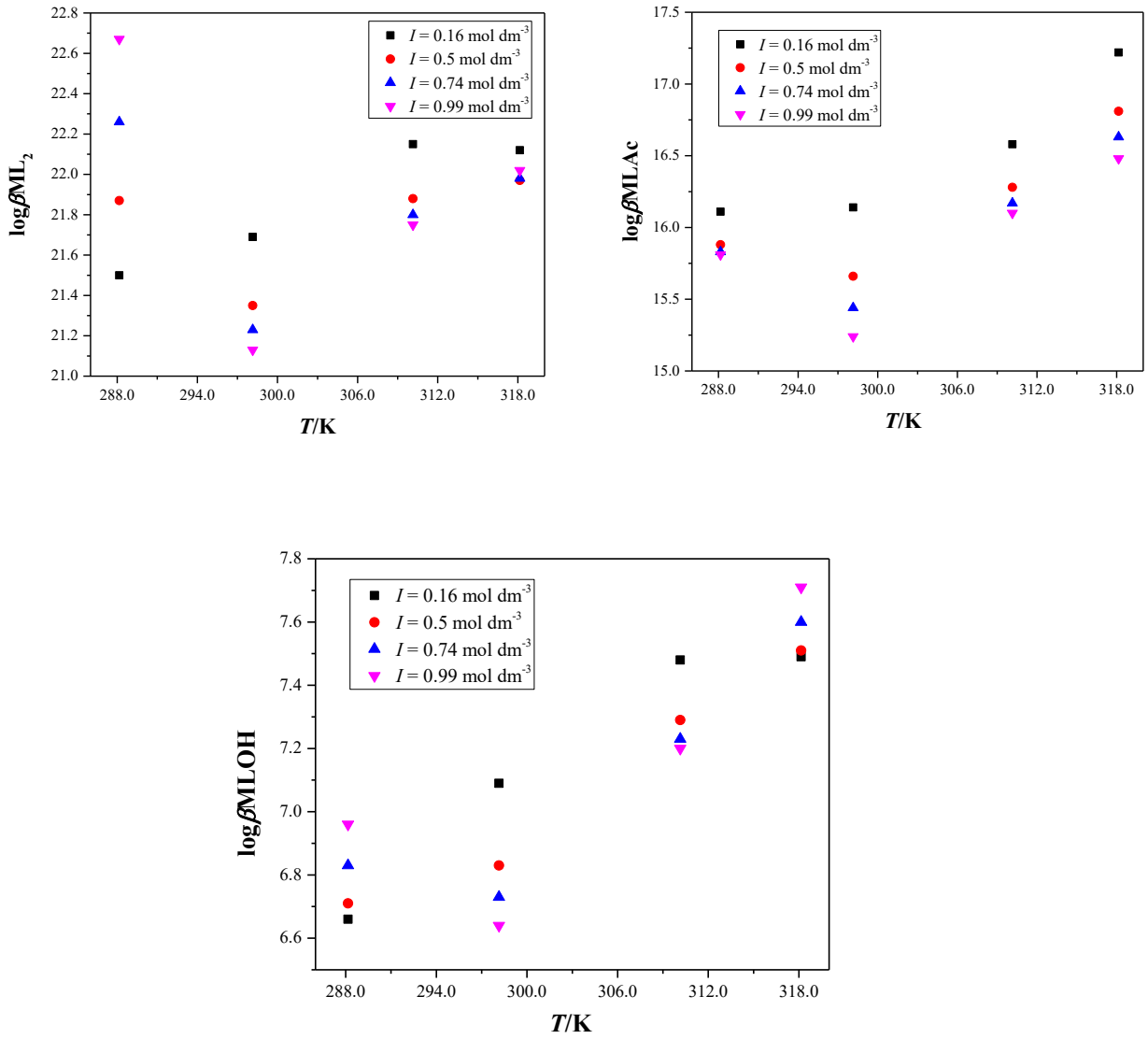

Figure 4.22. Trend of the experimental formation constants of the UO_2^{2+}/Dop$^-$ complex species, at different temperature and ionic strength values: a) ML_2; b) MLAc species; c) MLOH species.

4.1.4.6 Dependence on ionic strength and temperature of complexes with metals of group B

As already seen in paragraph 4.1.4, the dependence on ionic strength and temperature of the formation constants determined has been modeled by means of an extended Debye-Hückel equation (EDH), and of the Specific ion Interaction theory (SIT).

For the Cd^{2+}, Mn^{2+} and Zn^{2+} systems, the dependence on the ionic strength was only investigated at T = 298.15 K, and for this reason the modelling of the stability constants with respect to the ionic strength was performed by using a Debye-Hückel equation where the term for the dependence on T/K was neglected.

For the same systems, the modelling of the dependence on the temperature of the stability constants, that allows to calculate the enthalpy change values of the complex formation, was performed by using

a classical Van't Hoff equation (Eq. 3.18). For this reason, the calculated ΔH/kJmol^{-1} and TΔS/kJ mol^{-1}, are valid at the single ionic strength investigated at the different temperatures, namely I = 0.15 mol dm^{-3}.

Table 4.23 reports both the stability constants and the empirical parameters for the dependence on I/mol dm^{-3} (at T = 298.15 K) and the enthalpy and entropy change values of the complex formation at I = 0.15 ml dm^{-3}.

Table 4.23. Formation constant, entropy and enthalpy change values at infinite dilution of M^{n+} /Dop$^-$ species

Species	$\log\beta^T_{pqr}$ a)	C b)	ΔH c)	$T\Delta S$ c)
		Cd^{2+}/Dop$^-$		
MLH	14.33 ± 0.04 d)	0.19 ± 0.05	-183±26 d,e)	-103±26 d,e)
ML	6.87 ± 0.06	0.21 ± 0.08	-162±43	-125±43
ML_2	11.93 ± 0.06	-1.63± 0.08	-185±29	-123±29
		Mn^{2+}/Dop$^-$		
MLH	14.22 ± 0.09 d)	-0.89 ± 0.14	-162±28 d,e)	-80±28 d,e)
ML	6.02 ± 0.08	-0.55 ± 0.16	-168± 18	-133±17
ML_2	11.78 ± 0.09	-1.93 ± 0.18	-191± 30	124±30
		Zn^{2+}/Dop$^-$		
MLH	14.86 ± 0.02 d)	-0.66 ± 0.03	-138±62 d,e)	-55±62 d,e)
ML	7.95 ± 0.03	-0.55 ± 0.04	-54± 57	-12±57
MLOH	-0.05 ± 0.04	-0.83 ± 0.05	-9± 69	-13±69
ML_2H	22.66 ± 0.06	-1.26 ± 0.08	-246± 84	-122±84

a) $\log\beta_{pqr}$ refer to eqs. (4.1 – 4.2); b) parameter for the dependence on I/mol dm^{-3}; c) enthalpy and entropy change values of formation in kJ/mol ; d) ±Std.Dev. ; e) calculated at I = 0.15 mol dm^{-3} and T = 298.15 K .

For the uranyl and copper systems, the dependence of the stability constants on the ionic strength and temperature was investigated by using the Eq. (4.8), considering as reference temperature T = 298.15 K. For this reason, the $\log\beta^T_{pqr}$, C, ΔH/kJmol^{-1} and $T\Delta S$/kJ mol^{-1} values were calculated at infinite dilution and are valid at the reference temperature.

Table 4.24 reports these thermodynamic parameters for the UO_2^{2+} and Cu^{2+}/Dop$^-$ systems.

Table 4.24. Formation constant, entropy and enthalpy change values at infinite dilution of M^{n+} /Dop^- species

Species	$\log\beta^{T}_{pqr}$ [a,b]	C[b]	ΔH[c]	$T\Delta S$[c]
		Cu^{2+}/Dop^-		
ML_2	20.27 ± 0.07[d]	-0.75 ± 0.11 [d]	-265.5 ± 5.5 [d]	150±6 [d]
M_2L	14.51 ± 0.05	0.37 ± 0.09	-105.1 ± 3.8	22±4
M_2L_2	26.55 ± 0.08	-0.62 ± 0.13	-267.9 ± 5.1	116±5
$M_2L_2(OH)_2$	12.95 ± 0.07	-1.10 ± 0.11	-266.7 ± 5.1	193±5
$M_2L(OH)$	9.21 ± 0.02	1.01± 0.06	1.6±2.5	-54±3
$ML_2(OH)$	11.51 ± 0.06	0.14± 0.08	-56.6±3.8	-9±4
		UO_2^{2+}/Dop^-		
ML_2	22.05 ± 0.12 [d]	0.16 ± 0.19	15.0 ± 8.9 [d,e]	-141 ± 9 [d,e]
MLAc	16.66 ± 0.10	-0.51 ± 0.13	54.8 ± 8.8	-150 ± 9
MLOH	7.01 ± 0.08	-0.06 ± 0.14	47.6 ± 4.1	-88 ± 4

[a] $\log\beta^{T}_{pqr}$ valid at T = 298.15 K, refer to eqs. (4.1 – 4.2); [b] parameter for the dependence on I/mol dm^{-3}; [c] enthalpy and entropy change values of formation in kJ mol^{-1}; [d] ±Std. Dev.

By the conversion of the concentration (i.e., the ionic strength) and stability constants from the molar to the molal concentration scale (see paragraph 3.2), the two different forms of the SIT approach were applied; in the first case (Eq. 3.15) it was possible to calculate the Δε values of the formation reactions. In the second case, considering all the possible interactions that occur in the solution between the components or the metal ion/ligand species, with the ion of opposite charge of the supporting electrolyte, it was possible to calculate the single specific ion interaction coefficient.

To obtain this goal, it is necessary to consider the following literature data of the specific ionic interaction coefficients $\varepsilon(H^+,Cl^-)$ = 0.12 [125]; $\varepsilon(Dop^-,Na^+)$ = -0.228 [110]; $\varepsilon(Cd^{2+},NO_3^-)$ = 0.09 [126]; $\varepsilon(Cu^{2+},Cl^-)$ = 0.08 [126], $\varepsilon(Zn^{2+},Cl^-)$ = 0.16 [126], $\varepsilon(Mn^{2+},Cl^-)$ = 0.13[126], and $\varepsilon(UO_2^{2+},Cl^-)$ = 0.25[115].

The specific ion interaction coefficients (ε and $\Delta\varepsilon$) of the ionic species and the Setschenow coefficients for the neutral ones for the metal/dopamine species are reported in **Table 4.25**.

Table 4.25. Specific ion interaction parameters and Setschenow coefficients for the species of the metal/dopamine systems.

			Cd^{2+}			
Δε	**MLH[a)]**	**ML[a)]**	**ML_2[a)]**			
***T* = 298.15 K**	0.95±0.09 [b)]	0.34±0.11 [b)]	-0.68±0.10 [b)]			
			Cu^{2+}			
Δε	**ML_2[a)]**	**M_2L[a)]**	**M_2L_2[a)]**	**$M_2L_2(OH)_2$[a)]**	**$M_2L(OH)$[a)]**	**$ML_2(OH)$[a)]**
***T* = 288.15 K**	-0.725±0.001[b)]	0.346±0.002[b)]	-0.607±0.001[b)]	-1.060±0.001[b)]	0.998±0.003[b)]	0.149±0.002[b)]
***T* = 298.15 K**	-0.740±0.002	0.344±0.001	-0.623±0.002	-1.080±0.002	0.983±0.002	0.137±0.001
***T* = 310.15 K**	-0.763±0.006	0.341±0.002	-0.647±0.005	-1.108±0.006	0.962±0.002	0.120±0.003
***T* = 318.15 K**	-0.78±0.02	0.34±0.02	-0.66±0.02	-1.13±0.02	0.95±0.02	0.12±0.06
			Mn^{2+}			
Δε	**MLH[a)]**	**ML[a)]**	**ML_2[a)]**			
***T* = 298.15 K**	-0.88±0.28 [b)]	-0.56±0.30 [b)]	-1.93±0.35 [b)]			
			UO_2^{2+}			
Δε	**ML_2[a)]**	**$MLAc$[a)]**	**$MLOH$[a)]**			
***T* = 288.15 K**	1.54±0.06 [b)]	-0.19±0.07 [b)]	0.35±0.06 [b)]			
***T* = 298.15 K**	-0.50±0.07	-0.90±0.07	-0.54±0.07			
***T* = 310.15 K**	-0.31±0.07	-0.41±0.07	-0.34±0.07			
***T* = 318.15 K**	0.04±0.07	-0.71±0.07	0.24±0.06			
			Zn^{2+}			
Δε	**MLH[a)]**	**ML[a)]**	**$MLOH$[a)]**	**ML_2H[a)]**		
***T* = 298.15 K**	-0.65±0.02 [b)]	-0.55±0.12 [b)]	-0.80±0.14 [b)]	-1.25±0.22 [b)]		
Species		**Cd^{2+}**	**Cu^{2+}**	**Mn^{2+}**	**UO_2^{2+}**	**Zn^{2+}**
$\varepsilon_{(M^{2+},Cl^-)}$ [c)]		0.09(NO_3^-)	0.08	0.13	0.25	0.16
$\varepsilon_{(Na^+,L^-)}$ [c)]	-0.228					
$\varepsilon_{(M^{2+},Ac^-)}$ [c)]					0.01	
$\varepsilon_{(Na^+,Ac^-)}$ [c)]	0.08					
$\varepsilon_{(H^+,Cl^-)}$ [c)]	0.12					
$\varepsilon_{(ML^+,\ Cl^-)}$ [c)]		-0.34±0.10		0.450±0.001		0.48±0.12
$\varepsilon_{(MLH^{2+},\ Cl^-)}$ [c)]		-0.46±0.20		0.906±0.0022		0.70±0.08
k_{MLAc} [c);d)]					1.00±0.07	
k_{MLOH} [c);d)]					0.42±0.07	0.60±0.14
k_{ML2} [c);d)]		0.87±0.25	0.364±0.002	1.580±0.002	0.29±0.07	
k_{MAcL} [c);d)]					0.67±0.07	
$\varepsilon_{(M2L^{3+},\ Cl^-)}$ [c)]			-0.412±0.001			
$\varepsilon_{(ML2H^+,\ Cl^-)}$ [c)]						1.07±0.22
$\varepsilon_{(M2L2^{2+},\ Cl^-)}$ [c)]			0.327±0.002			

$k_{M2L2(OH)2}$ c);d)	0.514±0.002
$\varepsilon_{(M2LOH^{2+}, Cl^-)}$ c)	-1.186±0.002
$\varepsilon_{(ML2OH^-, Na^+)}$ c)	-0.648±0.001

a) Calculated by means of Eq. (3.18); b) ±Std. Dev.; c) Specific ion interaction coefficient of the single ion-pair; d) Setschenow coefficient for the neutral species calculated by means of Eq. (3.17).

4.1.5 Organometals group /Dopamine systems

The interaction between the OrganoMetals and Dopamine were investigated by means of the potentiometric titrations. The criteria of selection already adopted for other systems were also here used to obtain the best speciation model. For CH_3Hg^+/Dop^- system it has been possible to investigate a wide temperature range between $288.15 \leq T / K \leq 318.15$ at different ionic strengths between $0.15 \leq I /$ mol $dm^{-3} \leq 1$ in aqueous NaCl solution.

For $(CH_3CH_2)_2Sn^{2+}$/Dop^-, the investigations were carried out at different ionic strengths, but only at $T = 298.15$ K; the dependence on T/K, from $T = 288.15$ to 310.15 K was investigated only at $I = 0.15$ mol dm^{-3}.

4.1.5.1 CH_3Hg^+/Dop^- system

Investigations regarding the methylmercury/dopamine system resulted to be complex for two main reasons; the first one associated to investigation carried out in chloride medium, and the second to the tendency of this metalloid to form with the chloride a CH_3HgCl neutral species of high stability, avoiding the hydrolysis of CH_3Hg^+, up to rather high pH values (~8).

Investigations carried out at the experimental conditions above reported, allowed to studies the metal:ligand system up to pH ~ 10; over this pH, the formation of a sparingly soluble species has been observed. Moreover, the pH spectra of investigation was limited to this range, since from the literature and from an our previous investigation resulted that at higher pH the degradation of dopamine occurs [110].

The speciation model that gave the best results was featured by the following species: ML, MLH, MLCl, MLOH, whose formation constants are reported in **Table 4.26**.

Table 4.26. Experimental formation constants of the CH_3Hg^+/Dop^- species in NaCl aqueous solutions at different ionic strengths and temperatures

I /mol dm^{-3}	$\log\beta_{ML}$ [a)]	$\log\beta_{MLH}$ [a)]	$\log\beta_{MLCl}$ [a)]	$\log\beta_{MLOH}$ [a)]
		***T*=288.15 K**		
0	11.08±0.05 [b)]	19.69±0.08 [b)]	11.62±0.04[b)]	1.99±0.06[b)]
0.15	10.89±0.05	19.48±0.08	11.42±0.04	1.99±0.06
0.5	10.87±0.05	19.36±0.09	11.32±0.04	1.97±0.06
0.75	10.91±0.06	19.33±0.11	11.31±0.05	1.96±0.06
1	10.95±0.07	19.31±0.13	11.30±0.06	1.95±0.07
		***T*=298.15 K**		
0	10.62±0.04	19.65±0.05	11.42±0.02	2.00±0.04
0.15	10.43±0.03	19.43±0.05	11.21±0.02	1.99±0.04
0.5	10.40±0.03	19.30±0.07	11.10±0.03	1.98±0.04
0.75	10.44±0.04	19.27±0.09	11.09±0.04	1.97±0.05
1	10.48±0.06	19.25±0.11	11.08±0.05	1.96±0.06
		***T*=310.15 K**		
0	10.11±0.06	19.59±0.04	11.18±0.01	2.01±0.03
0.15	9.91±0.05	19.37±0.03	10.96±0.01	2.01±0.02
0.5	9.88±0.05	19.24±0.06	10.86±0.03	1.99±0.03
0.75	9.91±0.06	19.20±0.09	10.84±0.04	1.98±0.03
1	9.95±0.07	19.18±0.12	10.83±0.05	1.97±0.05
		***T*=318.15 K**		
0	9.79±0.08	19.56±0.04	11.04±0.02	2.02±0.02
0.15	9.58±0.07	19.33±0.04	10.81±0.02	2.01±0.02
0.5	9.54±0.07	19.19±0.06	10.70±0.03	1.99±0.02
0.75	9.57±0.07	19.16±0.09	10.68±0.04	1.99±0.03
1	9.61±0.08	19.13±0.12	10.67±0.06	1.98±0.05

a) $\log\beta_{pqr}$ refer to Eqs. (4.1 – 4.2); b) ± Std. Dev

The formation of the ternary chloride species is bound to the existence in chloride medium of the MCl species, that reaches at each experimental conditions, significant formation percentages, as reported in **Figure 4.23**, where the dependence of the ionic strength on the distribution of the species is reported.

In particular, we observe an increase of the formation percentage of the $MLCl^-$ species with increasing the chloride concentration (i.e. the ionic strength) in the solution, reaching at I = 1.0 mol dm^{-3} a formation percentage of ~20%. The other CH_3Hg^+/Dop^- species form with a yield of 15-20% for the ML in dependence on the ionic strength, and of ~90-95% for the MLOH at pH~9.5-10.

At I = 0.15 mol dm^{-3}, and between pH ~ 6-9, the MLH is the main species, reaching a formation 55-65% at pH~8. Increasing the ionic strength, the maximum of formation of MLH shifts at lower pH, reaching ~70% at I = 1.0 mol dm^{-3}. The profile of the MLOH curves is instead almost unchanged.

This could seem strange, but it can be easily explained considering that the overall formation constant of this species is characterized by having both values of z* and p* equal to zero.

As already mentioned, the hydrolytic capacities of the metal justify the formation of the ternary species MLOH and MLCl visible in the distribution diagram of **Figure 4.15** together with the ML and MLH species.

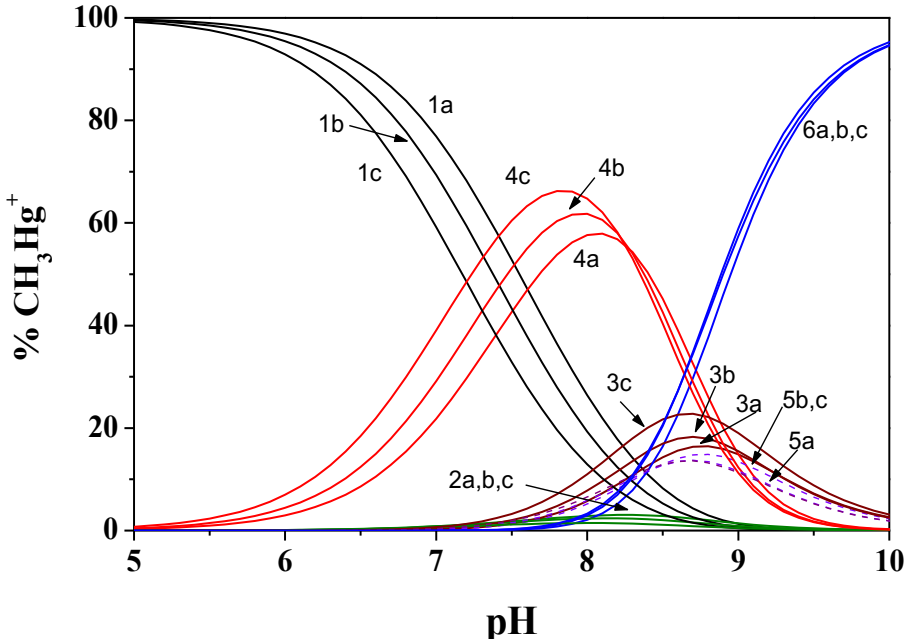

Figure 4.23. Distribution diagram for the CH_3Hg^+/Dop^- species at T = 298.15 K and different ionic strengths.
Species: 1. MCl; 2. MOH; 3. ML; 4. MLH; 5 MLCl; 6. MLOH; [M = CH_3Hg^+; L = Dop^-]
a: I = 0.15 mol dm^{-3}; b: I = 0.5 mol dm^{-3}; c: I = 1.0 mol dm^{-3}
(Experimental Conditions: C_{CH3Hg+} = 0.5 mmol dm^{-3}; C_{DOP-} = 1.5 mmol dm^{-3})

The effect of the temperature on the speciation and distribution of the CH_3Hg^+/Dop^- species is shown in the **Figure 4.24.**

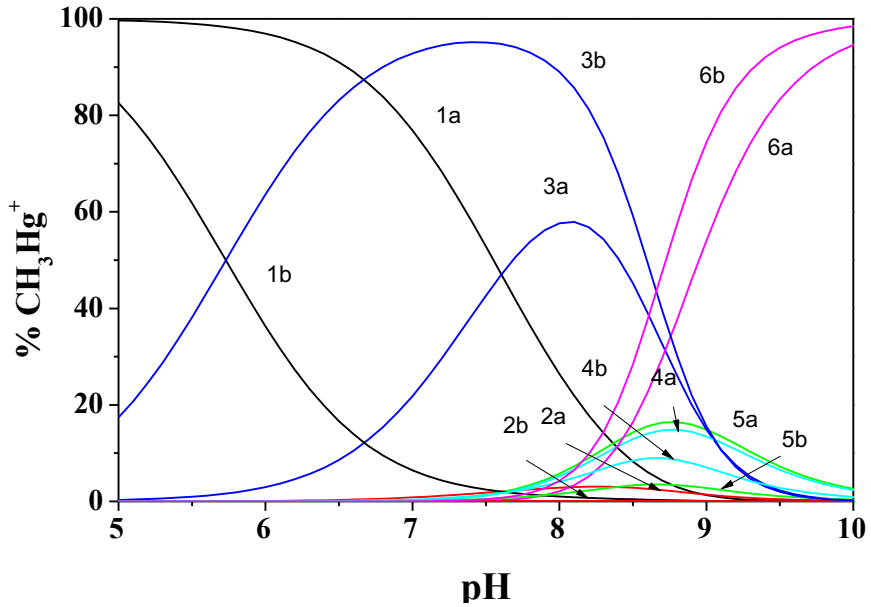

Figure 4.24. Distribution diagram for the CH_3Hg^+/Dop^- species at I = 0.15 mol dm^{-3} and different temperatures.
Species: 1. MCl; 2. MOH; 3. MLH; 4. ML; 5 MLCl; 6. MLOH; [M = CH_3Hg^+; L = Dop^-]
a: T = 298.15 K; b: T = 318.15 K [M = CH_3Hg^+; L = Dop^-]
(Experimental Conditions: C_{CH3Hg+} = 0.5 mmol dm^{-3}; C_{DOP^-} = 1.5 mmol dm^{-3})

Among the important aspects that we can comment on is that the MCl species undergoes a considerable shift on the maximum of formation, modifying the temperature, and therefore the corresponding percentage of formation.

The same considerations can be made for the ternary species MLOH and MLH. While for the ML and MLCl species the pH formation intervals remain almost unchanged, while the percentages change significantly as the temperature varies.

4.1.5.2 $(CH_3CH_2)_2Sn(IV)/Dop^-$ system

The speciation studies of the $(CH_3CH_2)_2Sn(IV)/Dop^-$ system were conducted in aqueous solution of NaCl, in an ionic strength range of $0.15 \leq I$ / mol $dm^{-3} \leq 1$ and T = 288.15 , 298.15 and 310.15 K. The best speciation model consists of the species: ML, MLOH, ML_2 and M_2LOH. The formation constants expressed according to the equilibria (4.1 – 4.2), are reported in **Table 4.27**.

Table 4.27. Experimental formation constants of the $(CH_3CH_2)_2Sn^{2+}$/Dop^- species in NaCl aqueous solutions

T/K	I/mol dm^{-3}	$\log\beta_{ML}$ [a)]	$\log\beta_{MLOH}$ [a)]	$\log\beta_{ML2}$ [a)]	$\log\beta_{M2LOH}$ [a)]
288.15	0.139	15.96 ± 0.01[b)]	8.37 ± 0.02[b)]	22.30 ± 0.03[b)]	15.55 ± 0.02[b)]
298.15	0.148	15.11 ± 0.06	7.32 ± 0.02	20.95 ± 0.02	15.38 ± 0.02
298.15	0.468	14.881 ± 0.06	7.38 ± 0.01	20.88 ± 0.02	13.76 ± 0.04
298.15	0.702	14.589 ± 0.004	6.958 ± 0.008	19.78 ± 0.02	12.10 ± 0.08
298.15	0.936	14.188 ± 0.005	6.62 ± 0.02	18.90 ± 0.07	11.05 ± 0.07
310.15	0.138	14.33 ± 0.04	7.04 ± 0.06	19.75 ± 0.05	14.08 ± 0.03

a) $\log\beta_{pqr}$ refer to Eqs. (4.1 – 4.2); b) ± Std. Dev

Data reported in **Table 4.27** refer to each of the investigated experimental conditions above described; independent of the temperature or ionic strength variation, we observed a systematic decreasing trend of the stability constants, with difference of about one order of magnitude for the ionic strength variation between $0.15 \leq I$ / mol dm$^{-3} \leq 1$ and $288.15 < T/K < 310.15$ K.

The effect of these variables on the distribution of the species can be observed analyzing the distribution diagram drawn by using the experimental conditions reported in **Figures 4.25. - 4.27.**

The species that reaches the highest percentages of formation is the species ML, with a maximum of 90% at pH = 6.2, while the species M_2L, MLOH and ML_2 reaches a percentage of 60% at pH = 3.7, 8.0 and 9.0, respectively.

The other M_2L, MLOH and ML_2 species reach a percentage of 60% at pH = 3.7, 8.0 and 9.0, respectively.

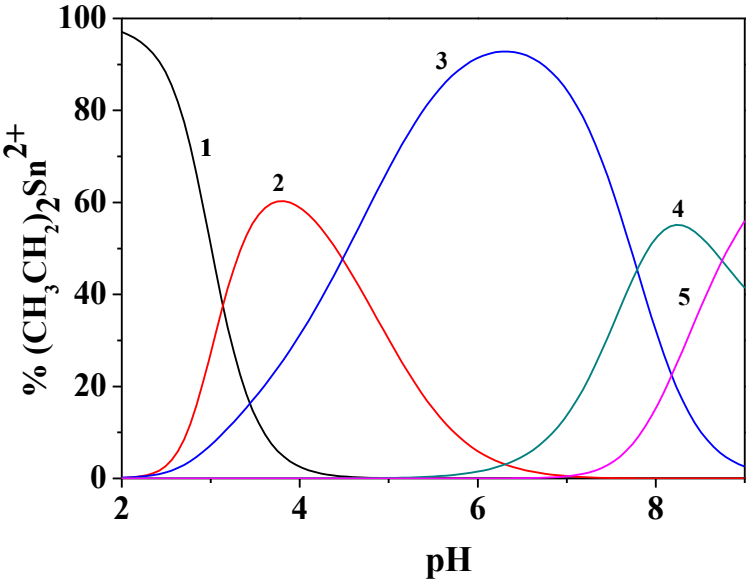

Figure 4.25. Distribution diagram for the $(CH_3CH_2)_2Sn^{2+}$/Dop^- system at T = 298.15 K and I = 0.15 mol dm^{-3}.
Species: $1M_{Free}$; 2. M_2LOH; 3. ML; 4. MLOH; 5. ML_2 ; M = $(CH_3CH_2)_2Sn^{2+}$; L = Dop^-.
Experimental Conditions: $C_{(CH3CH2)2Sn2+}$ = 2.0 mmol dm^{-3}; C_{DOP-} = 6.0 mmol dm^{-3}.

In particular, **Figure 4.26** evidences the effect of the ionic strength variation on the distribution of species in interval investigated; it is evident that the species 3 must be considered as the main species in the pH interval betwwen 4 and 8, whilst the others three species formed in same amount (about 60% of formation) become predominant at different pH values.

As it can be seen from the graph, the percentage of free metal decreases as the ionic strength increases; the percentage of formation of the species $(CH_3CH_2)_2Sn^{2+}/Dop^-$ is almost equal in the conditions of I = 0.468 and 0.936 mol dm^{-3} with a maximum of 96% at pH = 5.5 while at I = 0.148 mol dm^{-3} the maximum% formation, decreases slightly, moving towards pH = 6.0.

In the case of the species $(CH_3CH_2)_2SnDop(OH)$, the percentage of formation increases as the ionic strength increases, reaching a value of 80% at I = 0.936 mol dm^{-3}; the opposite trend is observed for the $[(CH_3CH_2)_2Sn]_2Dop(OH)$ species which, reaches at I = 1.00 mol dm^{-3} a formation percentage of 3.7%.

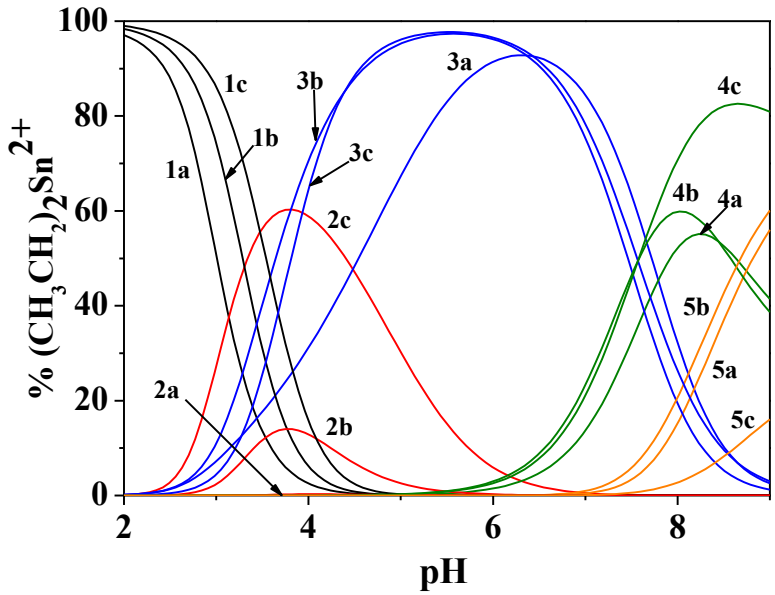

Figure 4.26. Distribution diagram for the *$(CH_3CH_2)_2Sn^{2+}/Dop^-$ system at T = 298.15 K and different* ionic strengths.
Species: $1M_{Free}$; 2. M_2LOH; 3. ML; 4. MLOH; 5. ML_2 ; M = *$(CH_3CH_2)_2Sn^{2+}$*; L = Dop^-.
a) I = 0.15 mol dm^{-3}; b) I = 0.5 mol dm^{-3} ; c) I = 1.00 mol dm^{-3}
Experimental Conditions: $C_{(CH3CH2)2Sn2+}$ = 2.0 mmol dm^{-3}; C_{DOP-} = 6.0 mmol dm^{-3}.

Figure 4.27 reports the effect of the temperature on the distribution of species; it is evident to observe the significant variations of the percentage of formation of the species and a shift of the maximum of formation towards higher of lower pHs in depedence of their different stoichiometry.

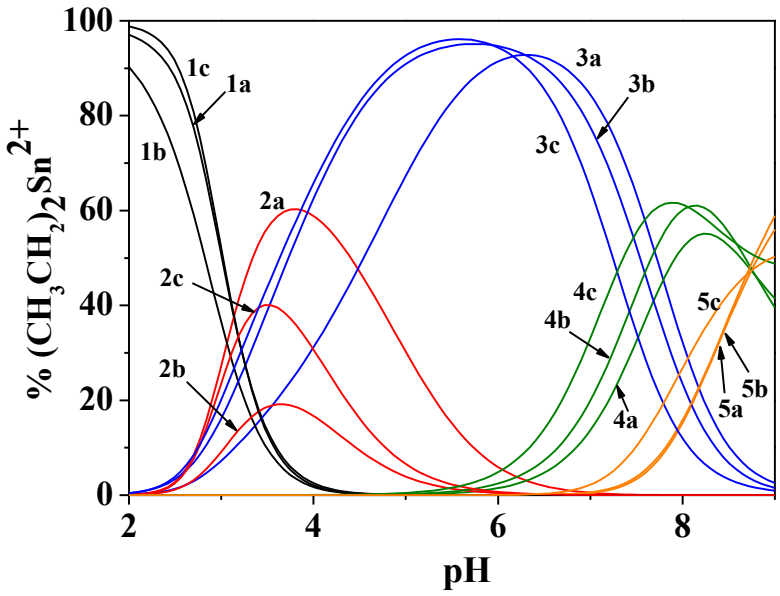

Figure 4.27. Distribution diagram for the $(CH_3CH_2)_2Sn^{2+}$/Dop^- system *at* I = 0.15 mol dm^{-3} and different Temperatures.
Species: $1M_{Free}$; 2. M_2LOH; 3. ML; 4. MLOH; 5. ML_2; M = $(CH_3CH_2)_2Sn^{2+}$; L = Dop^-.
a) T = 288.15 K; b) T = 298.15 K ; c) T = 310.15 K
Experimental Conditions: $C_{(CH3CH2)2Sn2+}$ = 2.0 mmol dm^{-3}; C_{DOP-} = 6.0 mmol dm^{-3}.

4.1.5.3 Dependence on ionic strength and temperature of complexes with Organometals.

As already done for the metal/dopamine systems, the dependence on the ionic strength and temperature of the formation constants was modelled by using the approaches hereafter described (Eq.s 4.8 and 3.11 - 3.18).

Table 4.28. and **4.29**. report the calculated stability constants at infinite dilution and at the different investigated temperatures for the CH_3Hg^+/Dop^- and $(CH_3CH_2)_2Sn^{2+}$/Dop^- systems, respectively. The same tables also report the C parameter that account for the variation of the stability constants with the ionic strength; these values were calculated applying the equation (3.11).

Table 4.28. Formation constants at infinite dilution and different temperatures of the CH_3Hg^+/Dop^- species

	CH_3Hg^+/Dop^-			
	$\log\beta^T_{ML}$ [b]	$\log\beta^T_{MLH}$ [b]	$\log\beta^T_{MLCl}$ [b]	$\log\beta^T_{MLOH}$ [b]
	***T* = 288.15 K**			
$I \rightarrow 0$ [a]	10.80±0.02 [c]	19.52±0.03 [c]	11.44±0.02 [c]	1.99±0.06 [c]
C [d]	0.158±0.04	-0.40±0.03	1.68±0.04	-0.16±0.03
	***T* = 298.15 K**			
$I \rightarrow 0$	10.62±0.04 [c]	19.65±0.05 [c]	11.42±0.02 [c]	2.00±0.04 [c]
C	0.30±0.02	2.18±0.11	0.07±0.06	0.99±0.14
	***T* = 310.15 K**			
$I \rightarrow 0$	10.48±0.02 [c]	19.43±0.01 [c]	11.16±0.02 [c]	2.01±0.03 [c]
C	-0.62±0.02	0.49±0.04	-0.49±0.03	-0.24±0.04
	***T* = 318.15 K**			
$I \rightarrow 0$	9.79±0.08 [c]	19.56±0.02 [c]	11.50±0.02 [c]	2.02±0.02 [c]
C	-0.68±0.10	-0.49±0.03	-0.38±0.02	-0.10±0.01

a) *I*/mol dm^{-3}; b)refer to the Eqs. (4.1 – 4.2); c) ±Std. Dev.; d) parameter for the dependence of $\log\beta_{pqr}$ on *I*/mol dm^{-3}

Table 4.29. Formation constants at infinite dilution and different temperatures of the $(CH_3CH_2)_2Sn^{2+}/Dop^-$ species

	$(CH_3CH_2)_2Sn^{2+}/Dop^-$			
	$\log\beta^T_{ML}$ [b]	$\log\beta^T_{MLOH}$ [b]	$\log\beta^T_{ML2}$ [b]	$\log\beta^T_{M2LOH}$ [b]
	***T* = 298.15 K**			
$I \rightarrow 0$ [a]	15.81±0.02 [c]	7.99±0.03 [c]	21.59±0.06 [c]	16.21±0.06 [c]
C [d]	-0.70±0.03	-0.28±0.03	-0.32±0.04	-4.16±0.03

a) *I*/mol dm^{-3}; b)refer to the Eq. (4.1 – 4.2); c) ±Std. Dev.; d) parameter for the dependence of $\log\beta_{pqr}$ on *I*/mol dm^{-3}

The next step consisted in the calculation of the standard enthalpy change value of formation of the complex species; two different approaches were used for the two organometals; in the case of CH_3Hg^+/Dop^-, it was possible to apply the Debye-Hückel type equation expressed by means of the equation (4.8); in this case both the calculated stability constants and the standard enthalpy change values refer to infinite dilution. For $(CH_3CH_2)_2Sn^{2+}/Dop^-$ system, whose dependence of the stability constants on the temperature has been only investigated at I = 0.15 mol dm^{-3}, the standard enthalpy change values were calculated by means of the classical Van't Hoff equation (eq. 3.18). These data are reported in **Table 4.30**., together with the standard entropy change values of formation.

Table 4.30. Formation constant, enthalpy and entropy change values at infinite dilution for the M^{n+}/Dop^- species, at $T = 298.15$K

Species	$\log\beta^T_{pqr}$ a)	C b)	ΔH c)	$T\Delta S$ c)
		CH_3Hg^+/Dop^-		
ML	10.62 ± 0.03 d)	0.27 ± 0.06 d)	-76 ± 5 d)	-15±5 d)
MLH	19.64 ± 0.05	0.01 ± 0.10	-8 ± 5	104±5
MLCl	11.41 ± 0.02	0.08± 0.05	-34±2	31±2
MLOH	2.00 ± 0.04	-0.04± 0.05	2±3.3	13±3
		$(CH_3CH_2)_2Sn^{2+}/Dop^-$		
ML	15.81±0.02 d)	-0.70 ± 0.03	-126.4 ± 10.5 d,e)	-39.8±10.5 d,e)
MLOH	7.99±0.03	-0.28 ± 0.03	-102.0 ± 24.4	-58.3±24.4
ML_2	21.59±0.06	-0.32± 0.04	-197.8±14.2	-77.6±14.2
M_2LOH	16.21 ± 0.06	-4.16± 0.03	116.0±27.2	-30.6±27.2

a) $\log\beta_{pqr}$ refer to eqs. (4.1 – 4.2); b) parameter for the dependence on I/mol dm^{-3}; c) enthalpy and entropy change values of formation in kJ/mol ; d) ±Std.Dev. ; e) calculated at $I = 0.15$ mol dm^{-3} and $T = 298.15$ K .

From the data there reported, it can be observed that the formation of the methylmercury(II) complexes is assocaited at a more exothermic process, with respect to the ones of diethyltin(VI).
Since both for methylmercury and diethyltin, the specific ion interaction coefficient with chloride anion is unknown, the only SIT approach that can be applied is that reported in the equation (3.15), allowing the calculation of the Δε parameter (see **Table 4.31**).

Table 4.31. Specific ion interaction parameters and Setschenow coefficients for the species of the metal/dopamine systems.

		CH_3Hg^+		
	$\Delta\varepsilon_{ML}$ a)	$\Delta\varepsilon_{MLH}$ a)	$\Delta\varepsilon_{MLCl}$ a)	$\Delta\varepsilon_{MLOH}$ a)
***T* = 288.15 K**	1.53±0.02 b)	-0.88±0.06	1.61±0.02	-0.15±0.03
***T* = 298.15 K**	0.38±0.02	2.43±0.15	0.48±0.04	0.99±0.15
***T* = 310.15 K**	-0.64±0.02	0.31±0.04	-0.52±0.02	-0.24±0.03
		$(CH_3CH_2)_2Sn^{2+}$		
	$\Delta\varepsilon_{ML}$ a)	$\Delta\varepsilon_{MLOH}$ a)	$\Delta\varepsilon_{ML2}$ a)	$\Delta\varepsilon_{M2LOH}$ a)
***T* = 298.15 K**	-0.74±0.32 b)	-0.50±0.40	-2.02±0.58	-6.15±0.55

a) Calculated by means of Eq. (3.15); b) ±Std. Dev.

4.1.6 Mixed systems with Dopamine.

As it is known, in multicomponent solutions where there is the simultaneous presence of different components (metals and organic or inorganic ligands) at different concentrations and molar concentrations ratios, it is necessary for a correct speciation study, to consider the possible formation of ternary MLL' or MM'L species. The literature usually reports information for complexes of the MLL' type, while there is very little information on the formation of complexes mixed with the metal. In previous works, this research group investigated the formation of mixed hydrolytic species formed by UO_2^{2+}/Cu^{2+} and UO_2^{2+}/Cd^{2+} [128].

As a possible further contribution to this type of investigation, during the work of this thesis it was decided to verify what can happen when a ligand such as dopamine is also present in solution.

Investigations were carried out at a single ionic strength, namely I = 0.15 mol dm^{-3} and T = 298.15 K.

Simultaneously, also the mixed Zn^{2+}/Dop^-/Tryptophan and Zn^{2+}/Dop^-/ Histidine systems has been investigated but in the ionic strength range $0.15 \leq I$ / mol $dm^{-3} \leq 1$ and T = 298.15K.

The speciation models used as input are characterized by many different species, 28 and 32 for the $UO_2^{2+}/Cu^{2+}/Dop^-$ and $UO_2^{2+}/Cd^{2+}/Dop^-$ systems, respectively. As an example, in the case of the $UO_2^{2+}/Cd^{2+}/Dop^-$ systems, the speciation model consists of the following species (in parenthesis number of species): ionic product of water (1); dopamine protonation constants (2); Cd^{2+} hydrolysis (6); $CdCl_i$ complexes (5); UO_2^{2+} hydrolysis (5); acetate protonation constant (1); UO_2^{2+}/Ac^- complexes (4); UO_2^{2+}/Cd^{2+} hydrolysis (2); UO_2^{2+}/Dop^- species (3); Cd^{2+}/Dop^- species (3).

For the $UO_2^{2+}/Cu^{2+}/Dop^-$ system, the model that gave the best results is featured by the species: MM′L, $M_2M'L_2OH$, $M_2M'L_2(OH)_2$, $MM'L_2OH$ (with M = UO_2^{2+} , M '= Cu^{2+} and L = Dop); in the case of the $UO_2^{2+}/Cd^{2+}/Dop^-$ system, by the species: MM′L, $M_2M'L_2OH$, and $MM'_2L_2(OH)_2$ (with M = UO_2^{2+} , M '= Cd^{2+} and L = Dop).

The speciation models have two common species, the MM'L and $M_2M'L_2OH$ ones, but characterized by different stability, about 4 orders of magnitude.

The corresponding overall stability constants of the mixed species are reported in **Table 4.32**.

Table 4.32. Experimental formation constants of the UO_2^{2+}- Cu^{2+}- Dop^- and UO_2^{2+}- Cd^{2+}- Dop species in NaCl aqueous solutions at I = 0.15 mol dm^{-3} and T = 298.15K

	$\log\beta$[a]				
I/mol dm^{-3}	MM'L	$M_2M'L_2OH$	$M_2M'L_2(OH)_2$	$MM'L_2OH$	$MM'_2L_2(OH)_2$
			UO_2^{2+}- Cu^{2+}- Dop^-		
0.150	22.51 ± 0.11[b]	34.72 ± 0.10[b]	30.34 ± 0.12[b]	31.56 ± 0.11[b]	
			UO_2^{2+}- Cd^{2+}- Dop^-		
0.150	26.58 ± 0.06	38.57 ± 0.13			36.35 ± 0.08[b]

a) Refer to the general equilibria p M + q M' + m L = $M_pM'_qL_mOH_r$ + r H^+ (charge omitted); b)± Std. Dev.

Generally, when the formation of mixed species is observed, the calculation of the "extra-stability" of formation can be obtained by using the formation constants of the corresponding homo-polynuclear complexes, as discussed by Beck and Nagypàl [129] for the statistical prediction of the strength of complex formation constants for mixed species.

However, in our case, the stoichiometry of the mixed species does not correspond to the stoichiometry of the homo-polynuclear complexes, and for this reason, the only way to estimate the stability of this species is to calculate the corresponding stepwise formation constants; as an example, this calculation can be done for the following species reported in **Table 4.33**, where the possible reaction of formation of the mixed species are proposed.

Table 4.33. Stepwise formation constants of some mixed species at I = 0.15 mol dm^{-3} and T = 298.15 K

Species	Proposed formation reaction[a]	log$K$
	UO_2^{2+}/Cu^{2+}/Dop^- system	
$M_2M'L_2OH$	$\log\beta_{MLOH} + \log\beta_{M_2'L} = \log\beta_{M_2M'L_2OH}$	$\log K_{M_2M'L_2OH} = 22.51 - 7.09 - 14.57 = 9.90$
$M_2M'L_2(OH)_2$	$\log\beta_{MLOH} + \log\beta_{M_2'LOH} = \log\beta_{M_2M'L_2(OH)_2}$	$\log K_{M_2M'L_2(OH)_2} = 30.34 - 7.09 - 8.86 = 14.39$
	UO_2^{2+}/Cd^{2+}/Dop^- system	
$MM'_2L_2(OH)_2$	$\log\beta_{M'OH} + \log\beta_{M'L} + \log\beta_{MLOH} = \log\beta_{MM'_2L_2(OH)_2}$	$\log K_{MM'_2L_2(OH)_2} = 36.35 + 10.36 - 6.48 - 7.09 = 33.14$

a) M = UO_2^{2+}; M' = Cu^{2+} or Cd^{2+}; L = Dop^-.

To better highlight the pH value ranges where the mixed species form and where they coexist with the binary complexes, some distribution diagram were drawn, as reported in **Figures 4.28.- 4.29**. some important aspects can be highiligthed; i) the first one is that, as already observed from the other similar investigations, the mixed species form in very high amounts and are in each case the main complexes in the pH ranges investigated; ii) the strength of the mixed complexes avoid in the Cd^{2+} containing system the formation of the hydrolytic species both for UO_2^{2+} and Cd^{2+} and of the corresponding mixed hydrolytic species; iii) this behaviour does not occur in the mixed system

containing Cu^{2+}, where we observed the coexistence of the $(UO_2)_2(OH)_2$ and $(UO_2)_3(OH)_5$ species that reach about the 6-8%; iv) the formation of the species of the binary systems is avoided by the formation of the mixed ones, except for the UO_2LAc complex that in each case (namely, $UO_2^{2+}/Cd^{2+}/Dop^-$ and $UO_2^{2+}/Cu^{2+}/Dop^-$ systems) forms in significant amount, starting from pH ~ 3, and reaching about the 10 % and 20% of formation in the mixed containing Cd^{2+} and Cu^{2+} systems; v) as already observed for the binary UO_2^{2+}/Dop^- system, also for the mixed ones, the use of the chemical $UO_2(Ac)_2$ salt has a great influence on the formation and distribution of the binary and ternary complexes; in fact in each cases, the $UO_2(Ac)_i$ (i = 1-3) and the $UO_2(Ac)_3OH$ complexes are the main complexes of the system.

It is important to stress, that distribution of the mixed species and the corresponding formation percentages are related to the component concentration and metal:metal':ligand molar ratios; as an example, in the distribution diagram reported in **Figure 4.28**, we can observe the absence of the $MM'_2L_2(OH)_2$ ($M = UO_2^{2+}$; $M' = Cd^{2+}$), but if the experimental condition are changed with respect to the one reported in the same figure, as an example: $C_{UO_2^{2+}} = 4.0$ mmol dm^{-3}; $C_{Cd^{2+}} = 6.0$ mmol dm^{-3}; $C_{Dop^-} = 10$ mmol dm^{-3} , we have the $MM'_2L_2(OH)_2$ reach about the 54% of formation at pH = 5.4.

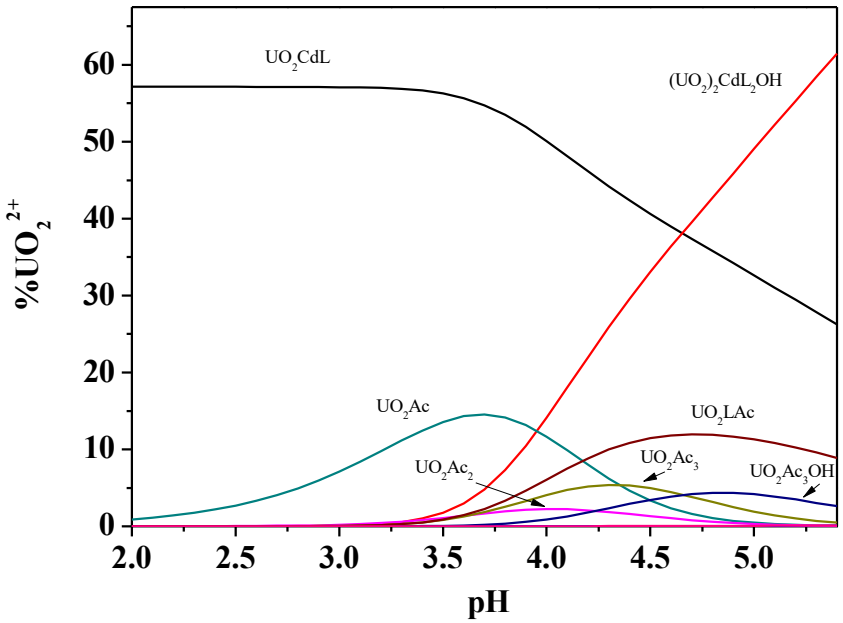

Figure 4.28. Distribution diagram of the $UO_2^{2+}/Cd^{2+}/Dop^-$ system at $I = 0.15$ mol dm^{-3} and $T = 298.15$ K. Experimental conditions: $C_{UO22+} = 14.0$ mmol dm^{-3}; $C_{Cd2+} = 8.0$ mmol dm^{-3}; $C_{Dop-} = 16$ mmol dm^{-3}. Charges omitted for simplicity.

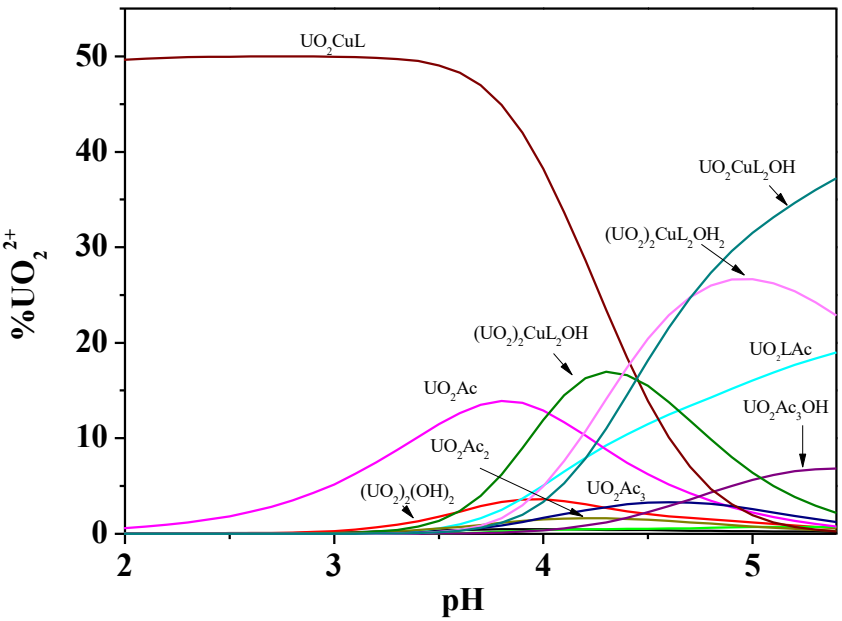

Figure 4.29. Distribution diagram of the $UO_2^{2+}/Cu^{2+}/Dop^-$ system at $I = 0.15$ mol dm^{-3} and $T = 298.15$ K. Experimental conditions: $C_{UO22+} = 8.0$ mmol dm^{-3}; $C_{Cd2+} = 4.0$ mmol dm^{-3}; $C_{Dop-} = 10$ mmol dm^{-3}. Charges omitted for simplicity.

As regards the mixed metal-ligand1-ligand2 system, it is necessary to know in advance not only the hydrolysis constants of the metal, but also the protonation constants of the two ligands [130, 131], and the formation constants of the metal-ligand binary system, under the same experimental conditions than those adopted in the studies of the ternary system. In the case of the zinc-histidine-tryptophan system, the interactions of the metal with histidine are well known, while those with tryptophan are not reported in the literature, at least at the experimental conditions used in these investigations.

For this reason, the first step was to investigate the speciation of the Zn^{2+}/Tryptophan system in NaCl aqueous solutions at different experimental conditions ($0.15 \leq I$ / mol dm^{-3} ≤ 1.00 and $T = 298.15$K and at temperatures between $288.15 \leq T$/ K ≤ 310.15 and at $I = 0.15$ mol dm^{-3}).

The selected model that gave the best results in term of statistical parameters is featured by the following species: ML, ML_2 and $ML(OH)_2$ species, whose stability constants are reported in **Table 4.34**, for each of the experimental condition investigated. The knowledge of the stability constants of the Zn^{2+}/Tryptophan system is prodromal to the investigation of the mixed system.

As for the other systems, and as usual, the dependence of the stability constants on the ionic strength and temperature has been modelled by means of the equations (3.11) and (3.18). The stability constants at infinite dilution, the parameter for the dependence on the ionic strength and the standard enthalpy change values of formation are reported in **Table S.11** of the Supplementary material.

Table 4.34. Experimental formation constants of the Zn^{2+}/$Tryp^{-}$ species in NaCl aqueous solutions

T/K	I/mol dm^{-3}	$\log\beta_{ML}$ [a)]	$\log\beta_{ML(OH)2}$ [a)]	$\log\beta_{ML2}$ [a)]
288.15	0.149	4.302 ± 0.008[b)]	-12.16 ± 0.01[b)]	8.06 ± 0.01[b)]
298.15	0.148	4.61 ± 0.05	-11.75 ± 0.02	9.008 ± 0.06
298.15	0.470	4.63 ± 0.01	-11.21 ± 0.02	8.75 ± 0.02
298.15	0.928	4.66 ± 0.01	-11.44 ± 0.03	8.80 ± 0.02
310.15	0.145	5.19 ± 0.01	-10.48 ± 0.02	10.053 ± 0.008

a) $\log\beta_{pqr}$ refer to Eqs. (4.1 – 4.2); b) ± Std. Dev

Concerning the mixed MLL' ternary systems, the speciation model used as input for the processing of the potentiometric experimental data is composed by 21 – 25 species.

Investigations were carried out at the same experimental condition of the Zn^{2+}/Tryp system, but only at T = 298.15 K.

Different speciation models were checked, obtaining many different species, in many cases formed in very low percentage of formations, whlst other chcked species were reject by the BSTAC program. The model that allowed to obtain the results is characterized by the species MLL'H, MLL_2'H, MLL_2' and ML_2L'H (where L = Tryp and L' = Dop), whose formation constants are reported in **Table 4.35**

Table 4.35. Experimental formation constants of the Zn^{2+}/Trip/Dop species in NaCl aqueous solutions

	$\log\beta$[a)b)]			
I/mol dm^{-3}	MLL'H	MLL_2'H	MLL_2'	ML_2L'H
0.144	18.32 ± 0.17[c)]	25.78 ± 0.02 [c)]	16.80 ± 0.01 [c)]	23.78 ± 0.01 [c)]
0.461	18.84 ± 0.05	25.45 ± 0.03	15.88 ± 0.16	23.43 ± 0.02
0.915	19.50 ± 0.03	25,68 ± 0.06	17.02 ± 0.05	23.34 ± 0.03

a) $\log\beta_{pqr}$ refer to Eq. (4.1 – 4.2); b) refer to T = 298.15K c) ± Std. Dev

As an example, **Figure 4.30** reports the distribution diagram of the species for the mixed Zn^{2+}/Tryp/Dop system. It can be observed that there is a coexistence of both the ternary and binary complexes species formed by Zn^{2+} with the two ligands. The ternary mixed species tend to form at higher pH value (>7-7.5) with respect to simple binary ones, that form from pH ~ 5. We can observe that ternary mixed species reach high formation percentages, except for the MLL'H that in the experimental conditions used to draw **Figure 4.30** is present with a percentage of formation of ~5%.

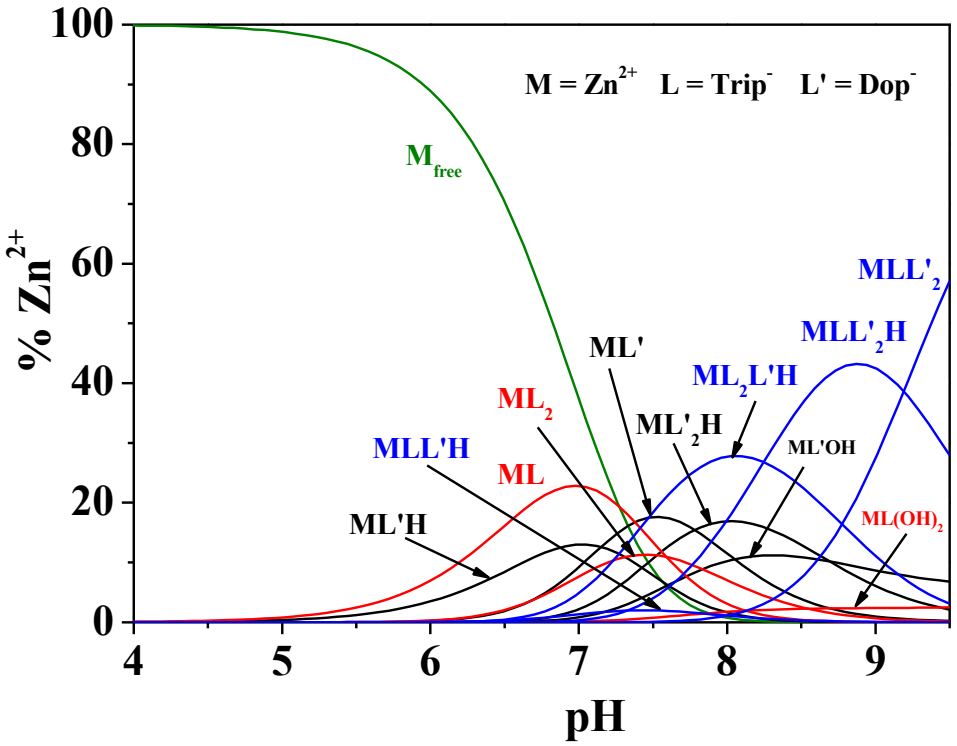

Figure 4.30. Distribution diagram for the Zn^{2+}/$Trip^{-}$/ Dop^{-} species at I = 0.15 mol dm^{-3} and T = 298.16K. Species: green line Metal free; red line ML, MLH, MLOH, ML_2H; black line ML', ML'_2, $ML'(OH)_2$; Blue line MLL'H, MLL'_2H, MLL'_2, $ML_2L'H$.
(Experimental Conditions: $C_{Zn^{2+}}$ = 2 mmol dm^{-3}; $C_{Trip^{-}}$ = 4 mmol dm^{-3},$C_{DOP^{-}}$ = 6 mmol dm^{-3}) [M = Zn^{2+}; L = $Trip^{-}$, L' = Dop^{-}]

Concerning the other mixed Zn^{2+}/His/Dop (His = Histidine) system [132-136], the literature already reports several papers were the interactions of zinc with histidine were investigated; for this reason and by using this data, it was possible to directly check the mixed interaction between Zn^{2+} and the two ligands (dopamine, histidine).

As usual, by using the criteria of selection for the best speciation model, based on the ratio between the variance of the accepted model and the other ones, we selected the following species reported in the **Table 4.36**. As it can be observed, the speciation model is featured by many simple ternary, protonated and hydrolytic complexes. The same Table also reports the corresponding formation constants at the investigated ionic strengths.

Table 4.36. Experimental formation constants of the Zn^{2+}/His/Dop species in NaCl aqueous solutions

	$\log\beta^{a)b)}$					
***I*/mol dm^{-3}**	**MLL'**	**MLL'_2**	**$ML_2L'H$**	**ML_2L'**	**$ML_2L'(OH)$**	**$ML_2L'(OH)_2$**
0.133	13.58 ± 0.01 c)	16.50 ± 0.05 c)	24.74 ± 0.07 c)	16.13 ± 0.02 c)	6.23 ± 0.02 c)	-7.29 ± 0.01 c)
0.444	13.41 ± 0.01	16.26 ± 0.06	25.01 ± 0.05	16.17 ± 0.02	6.09 ± 0.02	-7.36 ± 0.02
0.893	12.680 ± 0.08	15.74 ± 0.02	25.03 ± 0.03	15.89 ± 0.02	4.57 ± 0.2	-8.00 ± 0.01

a) $\log\beta_{pqr}$ refer to Eqs. (4.1 – 4.2); b) refer to T = 298.15K c) ± Std. Dev

Figure 4.31. reports the distribution of the Zn^{2+}/His/Dop species at I = 0.15 mol dm^{-3}, but similar evidence can be obtained at the other ionic strengths. As for the previous ternary Zn^{2+}/Tryp/Dop system, the mixed species tend to form in significant percentages over pH = 7, reaching about 40-50% of formation.

An important aspect that can be observed from the same distribution diagram is that the MLL' species, inhibits the formation of the binary Zn^{2+}/Dop^{-} species that, at least in the condition of **Figure 4.31**. are present in very low percentages of formation. On the contrary, the Zn^{2+}/His species are formed, especially at pH values lower with respect to the formation of the MLL' complexes, in higher amounts; as an example, the ML and ML_2 reach about 60% of formation.

It is important to stress that the data reported in **Table 4.36** were obatined processing separately the experimental data obtained at each ionic strength.

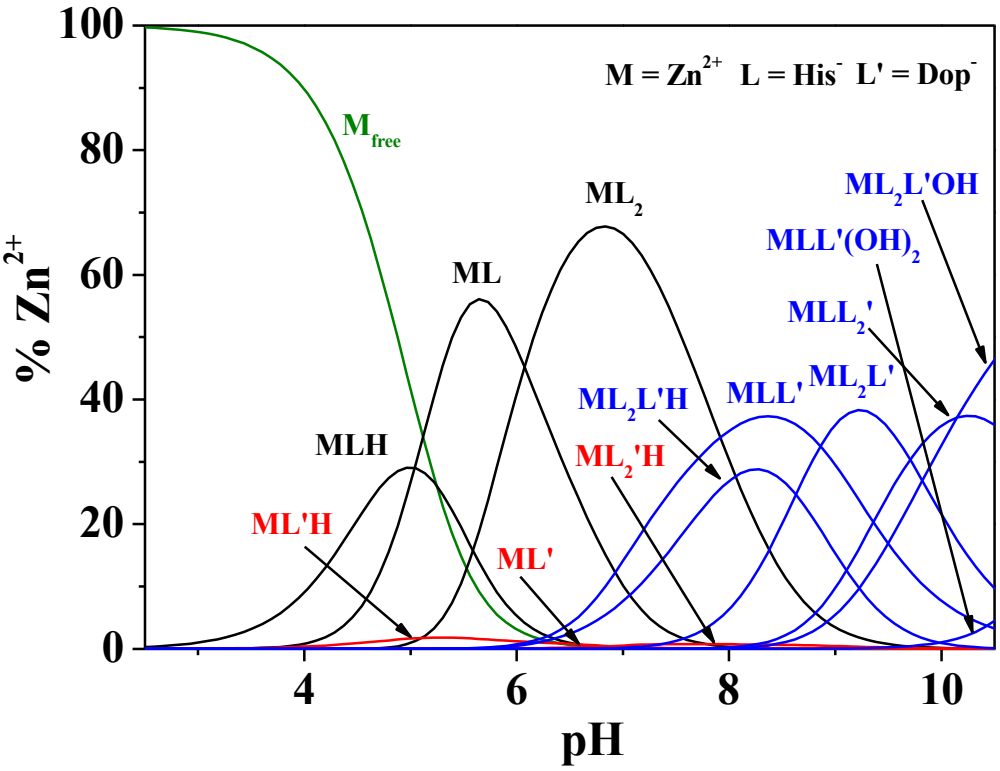

Figure 4.31. Distribution diagram for the Zn^{2+}/His^{-}/ Dop^{-} species at I = 0.15 mol dm^{-3} and T = 298.16K.
Species: green line Metal free; black line ML, MLH, ML_2; red line ML', ML'H, ML'$_2$H; blue line MLL', MLL'$_2$, $ML_2L'H$, ML_2L'; $ML_2L'OH$; MLL'(OH).
(Experimental Conditions: $C_{Zn^{2+}}$ = 2 mmol dm^{-3}; $C_{His^{-}}$ = 4 mmol dm^{-3},$C_{DOP^{-}}$ = 6 mmol dm^{-3}) [M = Zn^{2+}; L = His^{-} , L' = Dop^{-}]

4.1.6.1 Dependence on ionic strength of Mixed system with Dopamine.

As for the binary systems, the dependence of the formation constants of the ternary mixed Zn^{2+}/His/Dop and Zn^{2+}/Tryp/Dop complexes on the ionic strength was investigated by means of the extended Debye-Hückel equation (EDH) expressed by mean of the equation (3.11).
Table 4.37 reports the formation constants at inifinite dilution and the C parameter that account for the variation with the ionic strength.

Table 4.37. Formation constants at infinite dilution and different temperatures for the Mixed system with Dopamine species.

Species	$\log\beta^{T}_{pqr}$ a)	C b)
	Zn^{2+}/His/Dop	
MLL'	14.47 ± 0.08 c)	-0.62 ± 0.13 c)
ML_2'	17.32 ± 0.06	-0.41 ± 0.10
$ML_2L'H$	25.63 ± 0.08	1.16 ± 0.12
ML_2L'	16.88 ± 0.07	0.26 ± 0.11
$ML_2L'(OH)$	6.91 ± 0.11	-2.09 ± 0.17
$ML_2L'(OH)_2$	-7.10 ± 0.07	-0.98 ± 0.11
	Zn^{2+}/Tryp/Dop	
MLL'H	18.79±0.06 c)	2.10 ± 0.08 c)
$ML_2'H$	26.62±0.06	0.70 ± 0.09
ML_2'	17.13±0.15	1.05± 0.22
$ML_2L'H$	24.72 ± 0.06	0.24± 0.04

a) $\log\beta_{pqr}$ refer to eq. (4.1 – 4.2); b) parameter for the dependence on *I*/mol dm^{-3}; c) ±Std.Dev.

4.2 Ofloxacin

4.2.1 Solubility of Ofloxacin

Solubility studies allow to quantify the maximum amount of ligand that can dissolve in a defined amount of solvent (natural or biological fluids, industrial site waters, etc.). By means of ligand mass balance equations, from the knowledge of the ligand protonation constants determined at the same experimental conditions, and from the knowledge of the pH of the saturated solutions, it is possible to calculate the concentration of the ligand neutral species and the corresponding activity coefficients. In the past, our research group has been involved in this kind of investigation, for the determination

of both the acid-base properties, solubility and neutral species concentration of many different ligands of biological or pharmaceutical interest [98-101, 137-150].

For Ofloxacin, experimental investigations were carried out by spectrophotometric technique allowing the determination of the solubility (S^T) of the molecule in aqueous solutions of $NaCl_{(aq)}$ at ionic strength I = 0.15 mol·dm^{-3} and three different temperatures T = 288.15, 295.15, and 310.15 K.

By using the mass balance equations reported in Eqs. (4.11 – 4.17), it was also possible to calculate the concentration of the ofloxacin neutral species.

The total solubility is given by the sum of the concentrations of the different free, protonated and deprotonated species:

$$S^T = [HL^0] + [L^-] + [H_2L^+] \quad (4.11)$$

If we indicate the concentration of the HL^0 neutral species with S^0, from the equilibria reported in the Eqs. (4.12 – 4.14) we have that:

$$H^+ + L^- = HL^0 \qquad logK_1^H \quad (4.12)$$

$$H^+ + HL^0 = H_2L^+ \qquad logK_2^H \quad (4.13)$$

$$2H^+ + L^- = H_2L^+ \qquad log\beta_2^H \quad (4.14)$$

We have:

$$K_1^H = \frac{[HL^0]}{[H^+]\cdot[L^-]} \quad \text{and} \quad [L^-] = S^0 \cdot \frac{1}{K_1^H \cdot [H^+]} \quad (4.15)$$

$$K_2^H = \frac{[H_2L^+]}{[H^+]\cdot[HL^0]} \quad \text{and} \quad [H_2L^+] = S^0 \cdot K_2^H \cdot [H^+] \quad (4.16)$$

Rearranging Eq. (4.11), we obtain:

$$S^T = S^0 \cdot \left(1 + \frac{1}{K_1^H \cdot [H^+]} + K_2^H \cdot [H^+]\right) \quad (4.17)$$

The calculation of S^0, which expresses the concentration of the neutral species of Ofloxacin at the already mentioned experimental conditions, can be performed by means of Eq. (4.17), if S^T, K_i^H (i = 1-2) and the pH of solubilization are known.

The solubility of Ofloxacin at the selected conditions was calculated from the slope of the calibration straight lines constructed from the absorbance of the standard solutions measured at two different wavelengths (287-331.5 nm) and at different concentrations (from 0.00099 to 0.099 mmol·dm^{-3}), starting from a stock solution C = 1.24 mmol·dm^{-3}.

Independent of the selected wavelengths, the obtained calibration lines follow the Lamber-Beer law, although, as it already mentioned, between the first and last point there is a difference in concentration of about two orders of magnitude.

The obtained results are visible from **Figure 4.32**, and **Table 4.38** It can be observed that the solubility of ofloxacin increases with increasing temperature.

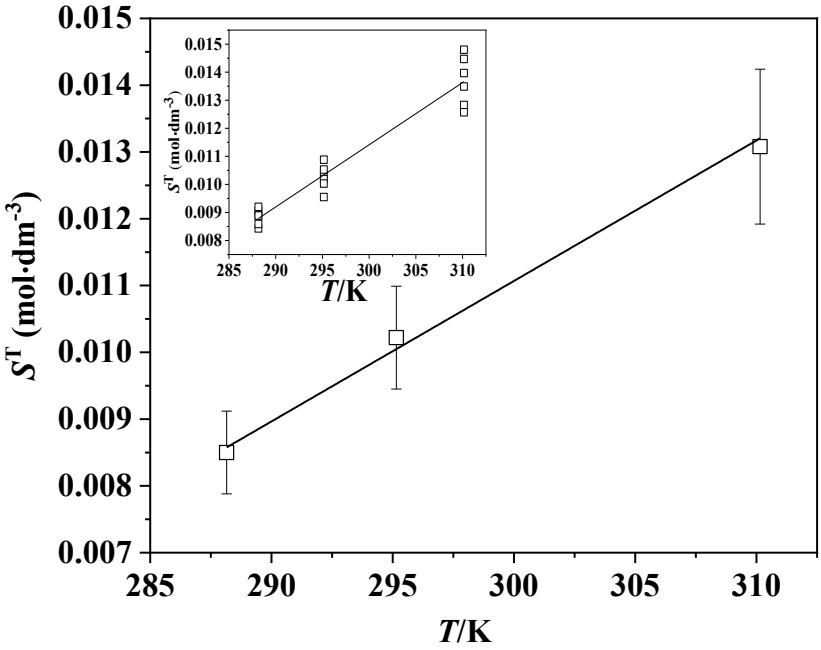

Figure. 4.32. Mean solubility (S^T) of Ofloxacin in molar concentration scale at different temperatures, in aqueous solutions of sodium chloride at I = 0.15 mol·dm^{-3}. (In the small box, the same correlation is reported, taking into account all the experimental solubility data; coefficient of correlation R^2 = 0.932).

This figure shows the average values of the solubility, together with the respective standard deviations, while in the smaller box, all the experimental solubility values are reported.

It is possible to observe an almost linear variation of S^T *vs* T/K, with a positive slope and an increase of the value with increasing temperature, with a R-squared value of 0.996.

Table 4.38 also reports the pH values of the saturated solutions that correspond to the pH of formation of the neutral species (zwitterion).

Table 4.38. Solubility and neutral species concentrations of Ofloxacin in $NaCl_{(aq)}$, at I = 0.15 mol·dm^{-3} and at different temperatures.

	S^{T} a)		ln x b)		S^{0} c)		pH d)	S^{0}% e)
				T = 288.15 K				
				Wavelengths (λ (nm))				
	287 nm	331.5 nm	287 nm	331.5 nm	287 nm	331.5 nm		
	0.00905	0.00709	-8.723	-8.967	0.00771	0.00604	7.08	85
	0.00889	0.00819	-8.740	-8.822	0.00759	0.00699	7.09	85
	0.00843	0.00837	-8.793	-8.801	0.00719	0.00714	7.08	84
	0.00920	0.00900	-8.706	-8.728	0.00782	0.00765	7.06	85
	0.00859	0.00874	-8.775	-8.757	0.00734	0.00746	7.08	85
	0.00889	0.00761	-8.740	-8.896	0.00754	0.00645	7.08	85
Mean value	0.00850±0.00062 f)		8.79±0.08 f)		0.00724±0.00053			85
				T = 295.15 K				
				Wavelengths (λ (nm))				
	287 nm	331.5 nm	287 nm	331.5 nm	287 nm	331.5 nm		
	0.00955	0.00836	-8.669	-8.802	0.00822	0.00720	7.10	86
	0.01036	0.01018	-8.588	-8.605	0.00892	0.00876	7.11	86
	0.01088	0.01077	-8.539	-8.549	0.00938	0.00928	7.11	86
	0.01019	0.00981	-8.604	-8.642	0.00874	0.00842	7.10	86
	0.01053	0.01135	-8.571	-8.496	0.00905	0.00976	7.09	86
	0.01003	0.01062	-8.620	-8.563	0.00866	0.00917	7.12	86
Mean value	0.01022±0.00077		-8.60±0.08		0.00880±0.00066			86
				T = 310.15 K				
				Wavelengths (λ (nm))				
	287 nm	331.5 nm	287 nm	331.5 nm	287 nm	331.5 nm		
	0.01283	0.01169	-8.374	-8.467	0.01090	0.00994	7.15	85
	0.01397	0.01269	-8.289	-8.385	0.01188	0.01079	7.13	85
	0.01447	0.01117	-8.254	-8.512	0.01234	0.00953	7.13	85
	0.01480	0.01446	-8.231	-8.254	0.01262	0.01233	7.14	85
	0.01349	0.01253	-8.324	-8.397	0.01148	0.01066	7.13	85
	0.01257	0.01223	-8.394	-8.422	0.01070	0.01042	7.11	85
Mean value	0.01308±0.00116		-8.36±0.09		0.01113±0.00099			85

a)solubility of Ofloxacin (S^{T}) expressed in the molar concentration scale (mol·dm^{-3}); b) (x) solubility expressed as mole fraction calculated from the experimental solubility at different wavelengths; c) concentration of the neutral species (S^{0}) expressed in the molar concentration scale (mol·dm^{-3}); d) pH of dissolution; e) mole fraction percentage of the neutral species; f) ±Std. Dev.

The pH of the solution in equilibrium is fairly similar to the physiological pH (pH ~ 7.4), and from the calculation of the S^{0} concentration, it was observed that at those conditions, ofloxacin is present approximately for 85% (as mole fraction percentage) in zwitterionic form.

As regards the dissolution of substances at different temperatures, the literature reports different approaches that relate the mole fraction solubility to its temperature dependence. As an example, the

standard molar enthalpy of solution ($\Delta H^0_{\mathrm{sol}}$) can be calculated by using the following Van't Hoff equation modified by Apelblat [151, 152]

$$\ln x = -\frac{\Delta H^0_{sol}}{R \cdot T} + \frac{\Delta S^0_{sol}}{R} \tag{4.18}$$

where x is the solubility (expressed as mole fraction) at a given temperature, R is the gas constant (8.314 $J \cdot K^{-1} \cdot mol^{-1}$) and T is the thermodynamic temperature expressed in kelvin (K), respectively. The $\Delta H^0_{\mathrm{sol}}$ can be obtained from the slope of the solubility straight line in the Van't Hoff plot, where ln x is plotted versus $1/T$ (the ln x values, at each temperature, have already been reported in **Table 4.38**). By using Eq. (4.18), the $\Delta S^0_{\mathrm{sol}}$ can be calculated from the intercept of the Van't Hoff plot.
The standard molar Gibbs energy of solution can be calculated by the Gibbs−Helmholtz equation:

$$\Delta G^0_{\mathrm{sol}} = \Delta H^0_{\mathrm{sol}} - T\Delta S^0_{\mathrm{sol}} \tag{4.19}$$

The trend of the ln x *vs.* $1/T$ is reported in **Fig. 4.33**. From the $\Delta H^0_{\mathrm{sol}}$ and $\Delta S^0_{\mathrm{sol}}$ of Ofloxacin in $NaCl_{(aq)}$ at I = 0.15 $mol \cdot dm^{-3}$ and by using the Eq. (4.19), the corresponding $\Delta G^0_{\mathrm{sol}}$ value (see **Table 4.39**) was calculated.
It can be inferred from $\Delta H^0_{\mathrm{sol}} > 0$ that the dissolution process is endothermic. The value of enthalpy is higher than those of entropy, which suggests that more energy is necessary to overcome the strength between the solute and the solvent in the dissolution process.

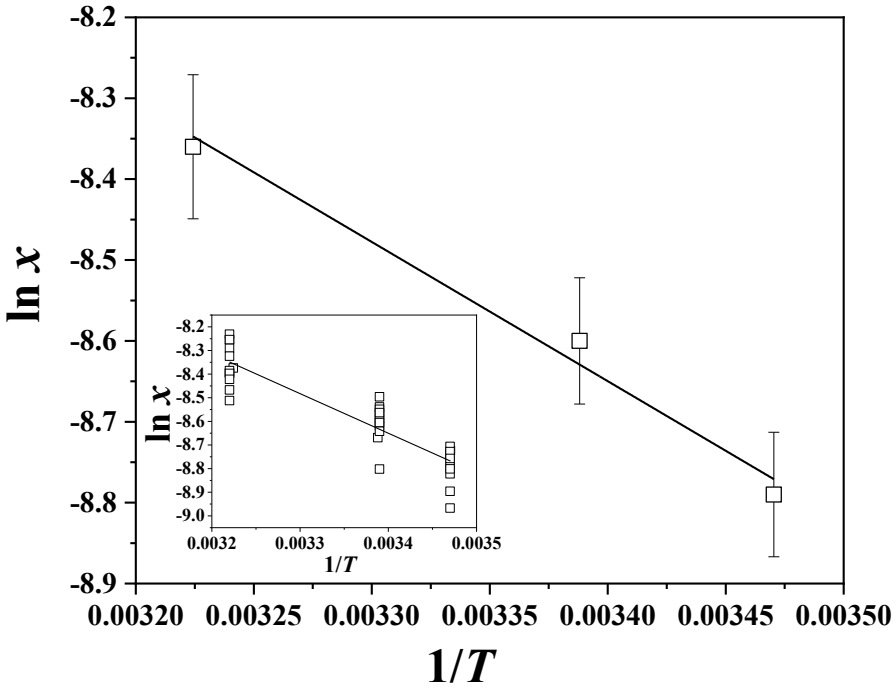

Figure 4.33. Mean mole fraction (ln x) of Ofloxacin (calculated from the experimental S^T values at each temperature) together with the corresponding standard deviation *vs* $1/T$ in $NaCl_{(aq)}$ at $I = 0.15$ mol·dm^{-3}. Coefficient of correlation $R^2 = 0.983$. (In the smaller box all the ln x values calculated from the experimental solubility are reported).

Table 4.39. Standard Gibbs energy, enthalpy and entropy changes of solution of Ofloxacin in $NaCl_{(aq)}$, at $I = 0.15$ mol·dm^{-3} [a)] and $T = 298.15$ K[a)]

Solution		
ΔG^0_{sol}/(J·mol^{-1})	ΔH^0_{sol}/(J·mol^{-1})	ΔS^0_{sol}/(J·mol^{-1})
308±21[b)]	213±15[b)]	-0.32±0.02[b)]

a) Standard uncertainties u are: u(T) = 0.1 K; u (p) = 1 KPa; u(I) = 0.01 mol·dm^{-3}; b) ±Std. Dev. The combined expanded uncertainties u are $u_c(\Delta X_d) = 0.070 \cdot \Delta X_d$

4.2.2. Protonation constants of Ofloxacine

The protonation constants of Ofloxacin, were in a first step investigated at the same experimental condition of the solubility measurements by potentiometric and spectrophotometric titrations.

A usual, and taking into account the general formula of ofloxacin, the protonation constants can be expressed both by the overall and stepwise equilibria:

$$H^+ + L^- = HL^0 \qquad logK_1^H \qquad (4.20)$$

$$H^+ + HL^0 = H_2L^+ \qquad logK_2^H \qquad (4.21)$$

$$2H^+ + L^- = H_2L^+ \qquad log\beta_2^H \qquad (4.22)$$

The obtained protonation constants at I = 0.15 mol dm^{-3} are reported in **Table 4.40**; a fairly linear decreasing trend of the log K^{H}_{n} values with respect to the increase of the temperature is observed, as reported in **Figure 4.34**.

The trends observed can be associated to the lowering of the activity coefficients of the Ofloxacin species with increasing the temperature.

As an example, **Figure 4.35** reports a potentiometric titration curve (electrode potential (mV) *vs.* volume of NaOH (cm^3)) of Ofloxacin at T = 298.15 K, where the experimental (square symbol) and calculated (solid line) values are reported. In the same graph, the first derivative ($(\partial E / \partial V)$ *vs.* volume (cm^3) of titrant) curve is reported, where three different equivalent points can be observed. The first one refers to the neutralization of the HCl added in the solution, whilst the others, to the displacement of the hydrogen from the carboxylic and piperazinic groups, respectively.

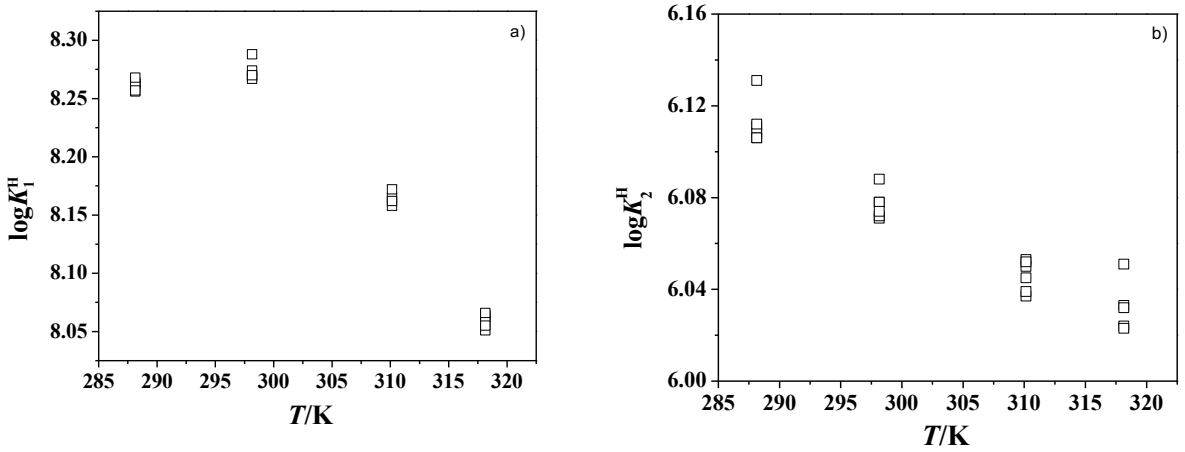

Fig. 4.34. Variation of the: a) log K^{H}_{1} and b) log K^{H}_{2} of Ofloxacin in NaCl(aq), at I = 0.15 mol·dm^{-3} and different temperatures.

Table 4.40. Experimental protonation constants of Ofloxacin at $I = 0.15$ mol·dm^{-3} in $NaCl_{(aq)}$ obtained at different temperatures from potentiometric and spectrophotometric titrations

Pot[a)]	UV[b)]	Pot [a)]	UV [b)]	Pot [a)]	UV [b)]
		$T = 288.15$ K			
$\log K_1^{Hc)}$	$\log K_1^{Hc)}$	$\log \beta_2^{Hd)}$	$\log \beta_2^{Hd)}$	$\log K_2^{He)}$	$\log K_2^{He)}$
8.262±0.001[f)]	8.256±0.002	14.373±0.001	14.368±0.002	6.111	6.112
8.264±0.003	8.268±0.001	14.372±0.002	14.374±0.003	6.108	6.106
8.263±0.002	8.257±0.003	14.369±0.001	14.388±0.004	6.106	6.131
		$T = 298.15$ K			
8.269±0.002	8.267±0.004	14.340±0.004	14.355±0.003	6.071	6.088
8.274±0.003	8.270±0.001	14.352±0.003	14.348±0.003	6.078	6.078
8.274±0.003	8.288±0.005	14.346±0.004	14.362±0.003	6.072	6.074
		$T = 310.15$ K			
8.158±0.001	8.165±0.002	14.208±0.002	14.204±0.004	6.050	6.039
8.165±0.001	8.162±0.003	14.218±0.003	14.207±0.005	6.053	6.045
8.165±0.002	8.172±0.004	14.202±0.005	14.224±0.002	6.037	6.052
		$T = 318.15$ K			
8.051±0.002	8.059±0.003	14.102±0.003	14.108±0.004	6.051	5.959
8.064±0.003	8.066±0.002	14.097±0.004	14.089±0.005	6.033	6.023
8.062±0.004	8.055±0.001	14.086±0.003	14.087±0.003	6.024	6.032

a)Protonation constants calculated from potentiometric titrations carried out titrating the fresh solutions;
b) Protonation constants calculated from the titrations of the diluted solutions obtained from the solubility measurements and collecting simultaneously the spectrophotometric and potentiometric data; c) equilibrium refers to Eq. (4.20); d) equilibrium refers to Eq. (4.22); e) equilibrium refers to Eq. (4.21); f) ±Std. Dev. Standard. uncertainties u are: u(T) = 0.1 K; u (p) = 1 KPa; u(I) = 0.01 mol·dm^{-3}

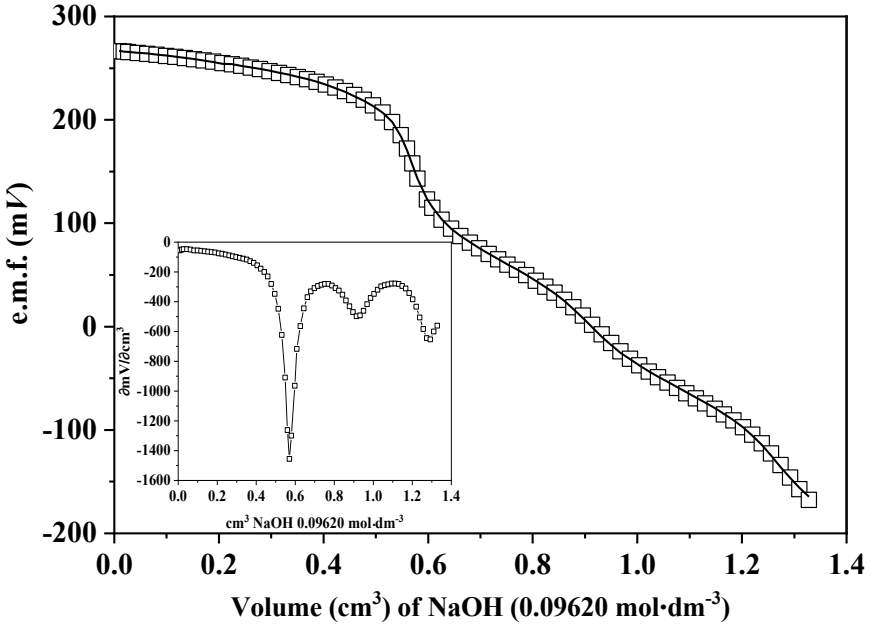

Fig. 4.35. Potentiometric titration curve of Ofloxacin in aqueous solutions of sodium chloride at $I = 0.15$ mol·dm^{-3} and $T = 298.15$ K. Concentrations: Ofloxacin 2.33 mmol·dm^{-3}; NaOH 0.09620 mol·dm^{-3}. Symbols: □, experimental points; solid line, calculated values.

The spectrophotometric titration curves of Ofloxacin at some different pH values and T = 298.15 K are reported in **Figure 4.36** It is possible to observe that at acid pHs, the shape of UV spectra shows no significant variations, but differs only for the intensity, owing to the less dissociation. When the pH increases (pH ≥ 6-6.5), the UV spectra show a decrease, in particular of the intensity of the band with maximum absorption at $\lambda \sim 287$ nm and, at the same time, a hypsochromic shift of about 5-10 nm, owing to the deprotonation of the molecule[153].

From the deconvolution of the spectrophotometric titrations curves and by using HySpec computer program, the molar absorption coefficients (ε / (cm^{-1}·mol^{-1}·dm^3)) of the L^-, HL^0 and H_2L^+ species was determined along the wavelength range of investigation. As an example, a graphical representation of the ε values determined for each species is reported in **Figure 4.37** at T = 298.15 K.

As reported in the literature [154-156], the first protonation constant is attributable to the protonation of a nitrogen atom of the piperazinic ring, while the second equilibrium to the protonation of the carboxylic group of Ofloxacin.

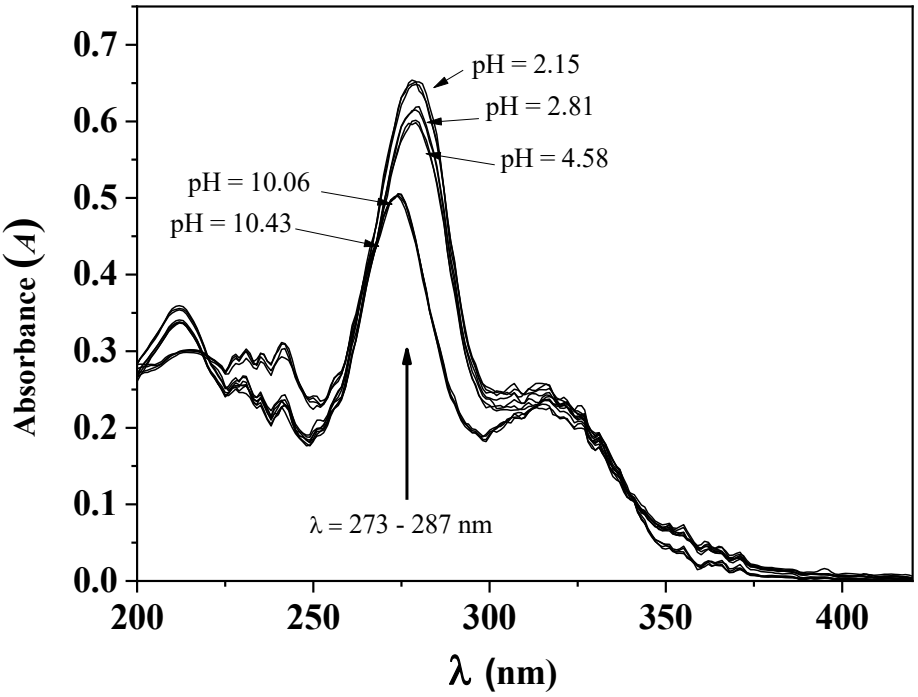

Fig. 4.36. Absorbance (A) spectra of Ofloxacin in aqueous solutions of sodium chloride, at I = 0.15 mol·dm^{-3} for several pH and T = 298.15 K. Ofloxacin concentration: 0.001 mmol·dm^{-3}.

A classic distribution diagram of the species is reported in **Figure 4.38**, where it is possible to observe the pH ranges of existence of each species, as well as the corresponding mole fraction percentage of formation. An albeit modest shift towards lower pH of the species formation, with temperature

increase, is observed; this is a consequence of its influence on the protonation constants. At pH values close to the neutrality, there is a clear prevalence of the HL^0 species.

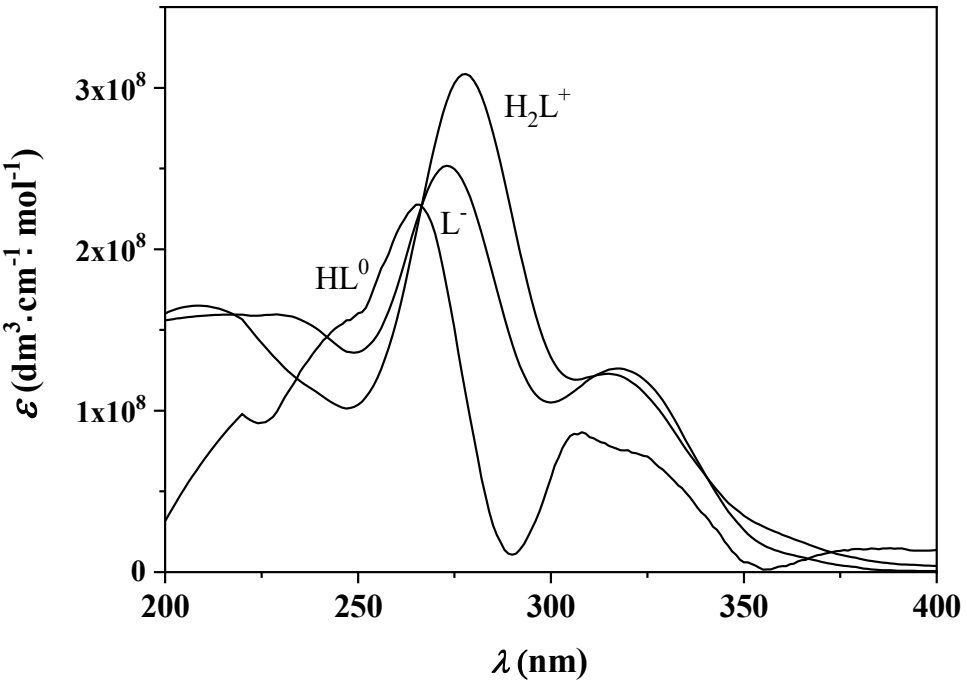

Fig. 4.37. Molar absorption coefficients (ε ($dm^3 \cdot cm^{-1} \cdot mol^{-1}$)) of the $H_nL^{(n-1)}$ species of Ofloxacin in aqueous solutions of sodium chloride at I = 0.15 mol·dm^{-3} and T = 298.15 K.

The information gained from the distribution diagram is in perfect agreement with those obtained from the solubility measurements (see **Table 4.38**), namely ~85% (as mole fraction percentage) of formation of the zwitterion. The pH of formation of the HL^0 species had already been experimentally observed by measuring, the pH of the saturated solutions at different temperatures (see **Table 4.38**), by using an ISE-H^+ electrode suitably calibrated using buffers at pH = 4.0 and 7.0.

The knowledge of the protonation constants at I = 0.15 mol dm^{-3} and different temperatures, allowed the calculation of the enthalpy and entropy change values for the two protonation steps of ofloxacin.

Table 4.41. Standard Gibbs energy, enthalpy and entropy changes of protonation of Ofloxacin in $NaCl_{(aq)}$, at I = 0.15 mol·dm^{-3} [a)], T = 298.15 K[a)]

	Protonation		
	ΔG^0/(kJ·mol^{-1})[b)]	ΔH^0/(kJ·mol^{-1})[b)]	$T\Delta S^0$/(kJ·mol^{-1})[b)]
log K^H_1	- 47.19±0.04[c)]	-16.3±1.8[c)]	30.9±1.8 [c)]
log K^H_2	-34.66±0.05	-4.3±0.7	30.4±0.7

a) Standard uncertainties u are: u(T) = 0.1 K; u (p) = 1 KPa; u(I) = 0.01 mol·dm^{-3}; b) refer to eqs. 4.20.-4.21.; c) ±Std. Dev. The combined expanded uncertainties u are $u_c(\Delta X_d) = 0.070 \cdot \Delta X_d$

Considering the promising results obtained both from the potentiometric and spectrophotometric titrations, we decided to also investigate the dependence of the protonation constants of ofloxacin on the ionic strength in NaCl aqueous solution in the ionic strength range $0.15 \leq I$ / mol dm$^{-3} \leq 1.00$ and by means of ISE-H^+ measurements.

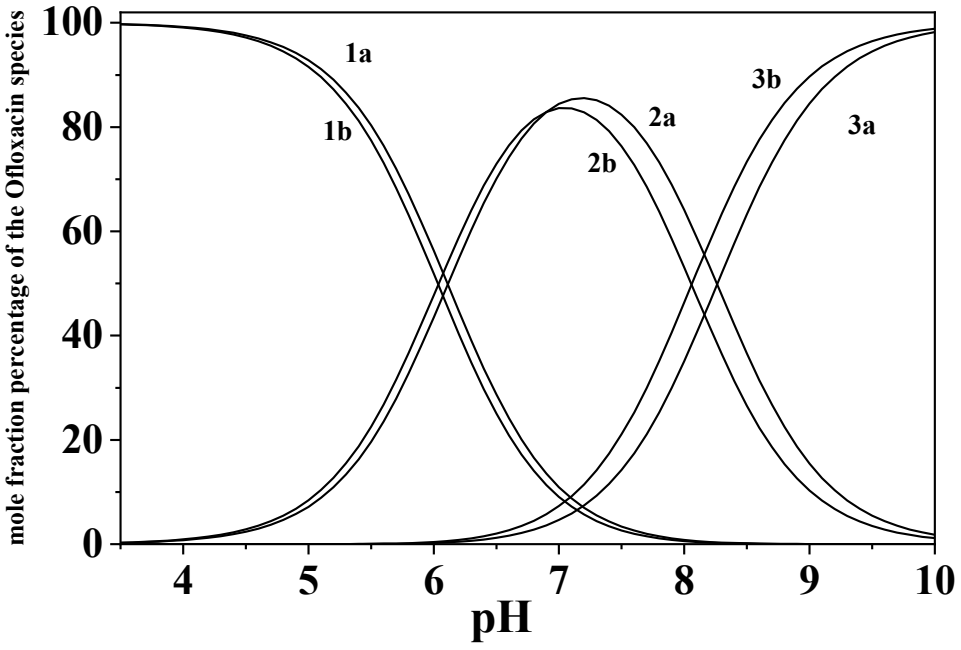

Fig. 4.38. Distribution diagram of Ofloxacin species (as mole fraction percentage (x $H_nL^{(n-1)}$ × 100)) in aqueous solutions of sodium chloride, at I = 0.15 mol·dm^{-3} and different temperatures.
Species: 1) H_2L^+; 2) HL^0; 3) L^-. Index: a) T = 288.15 K; b) T = 318.15 K.

The protonation constants investigated at different ionic strengths and temperatures are reported in **Table 4.42** The data reported in this table, are within the experimental error, in agreement with those previously obtained.

Table 4.42. Experimental protonation constants of Ofloxacin obtained from potentiometric titrations at different ionic strength in $NaCl_{(aq)}$ and different temperatures.

I /mol dm^{-3}	logK_1[Ha)]	logβ_2[Hb)]	logK_2[Ha)]
		T=288.15 K	
0.147	8.308±0.006	14.441±0.009	6.133
0.461	8.542±0.003	14.714±0.003	6.172
0.716	8.660±0.003	14.843±0.004	6.183
0.943	8.750±0.005	14.952±0.007	6.202
		T=298.15 K	
0.144	8.296±0.008	14.38±0.01	6.084
0.47	8.378±0.002	14.456±0.003	6.078
0.707	8.443±0.003	14.510±0.005	6.067
0.940	8.558±0.004	14.646±0.006	6.088
		T=310.15 K	
0.146	8.054±0.003	14.066±0.004	6.012
0.457	8.276±0.005	14.313±0.004	6.037
0.716	8.304±0.006	14.32±0.08	6.016
0.935	8.400±0.009	14.42±0.01	6.020
		T=318.15 K	
0.150	8.059±0.004	14.095±0.005	6.036

a)equilibrium refers to Eq. 4.20.; b) equilibrium refers to Eq. 4.22.; c)equilibrium refers to Eq. 4.21.; d) ±Std. Dev. Standard. uncertainties u are: u(T) = 0.1 K; u (p) = 1 KPa; u(I) = 0.01 mol·dm^{-3}

As already done for other systems, the dependence of the protonation constants on the ionic strength and temperature was investigated by means of the Eq. (4.8); by using T = 298.15 K as reference temperature, the protonation constants at infinite dilution and the parameter for the dependence on I/mol dm^{-3} were calculated.

Eq. (4.8), reports also the Van't Hoff term for the dependence on T/K, allowing the calculation of the standard enthalpy change values of protonation at infinite dilution.

Table 4.43 reports the overall protonation constant of ofloxacin at infinite dilution and the corresponding standard enthalpy and entropy change values. As it can be seen, the protonation steps are exothermic, whilst the entropic contribution constitutes the driving force of the processes.

The ΔH/kJ mol^{-1} values at infinite dilution, are in agreement with those already calculated at I = 0.15 mol dm^{-3}, considering the different ionic strength values and that the ΔH/kJ mol^{-1} values reported in **Table 4.41** refer to the stepwise protonation processes.

Table 4.43. Protonation constants at infinite dilution of Ofloxacin and enthalpy and entropy change values.

	$\log K_1^{HT}$ a)	$\log \beta_2^{HT}$ b)
T = 298.15 K		
$I \rightarrow 0$ c)	8.42±0.03 f)	14.50±0.03 f)
C d)	0.61±0.04	0.64±0.04
ΔH e)	-23.57±1.81	-36.27±2.38
$T\Delta S$ e)	24.50±1.81	46.51±2.39

a) $\log K_1^{HT}$ refers to eq. (4.20); b) $\log \beta_2^{HT}$ refers to eq. (4.22.); c) protonation constants at infinite dilution; d)parameter for the dependence on I/mol dm^{-3}; e) enthalpy and entropy change values of formation in kJ/mol ; f) ±Std.Dev.

4.2.3 Ca^{2+}/Oflox$^-$ system

As regards the study of the interactions of ofloxacin with calcium and zinc, the experimental conditions used are like the ones used for the acid-base properties investigations.

The processing of the potentiometric data allowed to obtain different speciation models for the two metals, even if featured by only mononuclear species.

It is possible to observe from the titration curves reported in **Figure 4.39**, that the systems behave differently, even if we can evidence two inflection points.

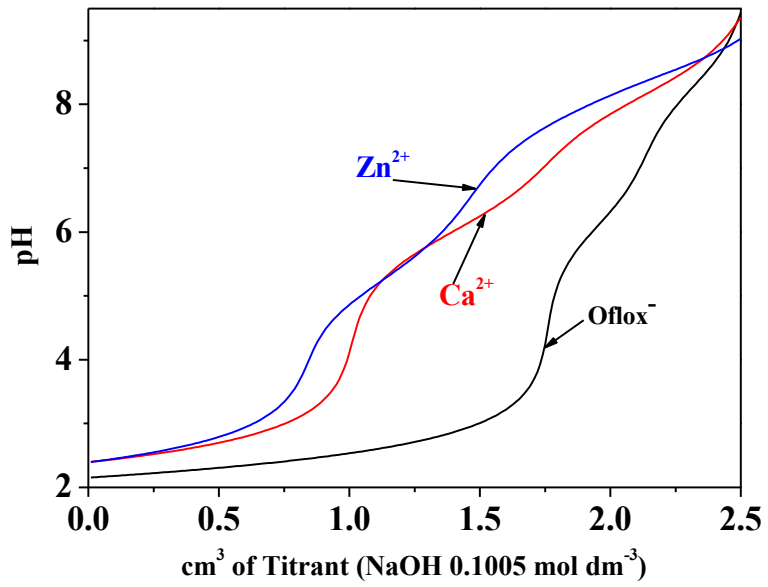

Figure 4.39.Titration curves of Ofloxacine and of the different metal/Oflox$^-$ systems at T = 298.15 K, I = 0.15 mol dm^{-3}. Experimental conditions: C_L = 3 mmol dm^{-3}; C_M = 1.5 mol dm^{-3}. Titrant: NaOH 0.1005 mol dm^{-3}.

In the case of the calcium system, the best results were obtained when the ML, MLH, ML_2 and MLOH species were considered in the speciation model. **Table 4.44** reports the formation constants of the Ca^{2+}/Dop$^-$ species at each of the investigated experimental. The first consideration that can be done,

is that the strength of the interactions is fairly weak, as generally observed for complex species formed by this cation. The second is the effect of the ionic strength and temperature on the stability of the species; in fact, as observed from the results reported in **Table 4.44**, we obtain $\Delta\log\beta_{pqr}$ values generally lower of one order of magnitude between the two extreme values of I/mol dm^{-3} and T/K.

This is better highlighted in the distribution diagrams here reported; **Figure 4.40** shows the distribution diagram of the Ca^{2+}/Ofloxacin species at different ionic strengths and T = 298.15 K, where we observe that the formation percentage of each species tends to increase with increasing the NaCl concentration (i.e. the ionic strength), except for the MLOH. Moreover, at physiological pH ~ 7.4 and up to pH ~ 8, the protonated MLH species in the main form of the system. The other species are formed in higher amount at pH value > 8 up to pH = 10-10.5. At this pH value, the interaction occurs between the calcium cation and the protonated form of ofloxacin that in this condition has the piperazinic protonated.

Concerning the dependence of the distribution of the Ca^{2+}/ofloxacin species on the temperature, we can observe from **Figure 4.41**, that the formation percentages tend to decrease increasing T/K, except for the ML one, that has an opposite trend. Moreover, we can observe a shift of the maximum of formation of the species towards lower pH values increasing the temperature; also in this case, the ML has an opposite trend.

Table 4.44. Experimental formation constants of the Ca^{2+}/Ofloxacine system in NaCl aqueous solutions at different ionic strengths and temperature

I /mol dm^{-3}	$\log\beta_{ML}$	$\log\beta_{MLH}$	$\log\beta_{MLOH}$	$\log\beta_{ML2}$
		T=288.15 K		
0.150	2.74±0.01 [a)b)]	10.74±0.01 [a)b)]	-7.98±0.02 [a)b)]	4.13±0.07 [a)b)]
0.455	2.70±0.02	10.70±0.02	-8.40±0.02	4.30±0.07
0.706	2.81±0.02	10.97±0.02	-8.34±0.03	4.45±0.09
0.927	2.95±0.02	11.11±0.02	-8.12±0.03	5.05±0.02
		T=298.15 K		
0.148	2.86±0.07	10.63±0.06	-7.41±0.03	4.86±0.05
0.455	2.77±0.05	10.91±0.03	-7.78±0.02	4.95±0.07
0.706	2.82±0.05	11.05±0.03	-7.78±0.02	5.16±0.09
0.936	2.99±0.04	11.25±0.03	-7.84±0.02	4.95±0.02
		T=310.15 K		
0.151	2.27±0.04	9.77±0.05	-7.95±0.02	4.57±0.03
0.451	2.68±0.04	10.54±0.03	-7.53±0.02	5.03±0.03
0.701	2.97±0.04	10.89±0.04	-7.40±0.03	5.12±0.04
0.887	3.09±0.07	11.96±0.06	-7.26±0.04	5.20±0.05

a) $\log\beta_{pqr}$ refer to Eqs. (4.1 – 4.2); b) ± Std. Dev

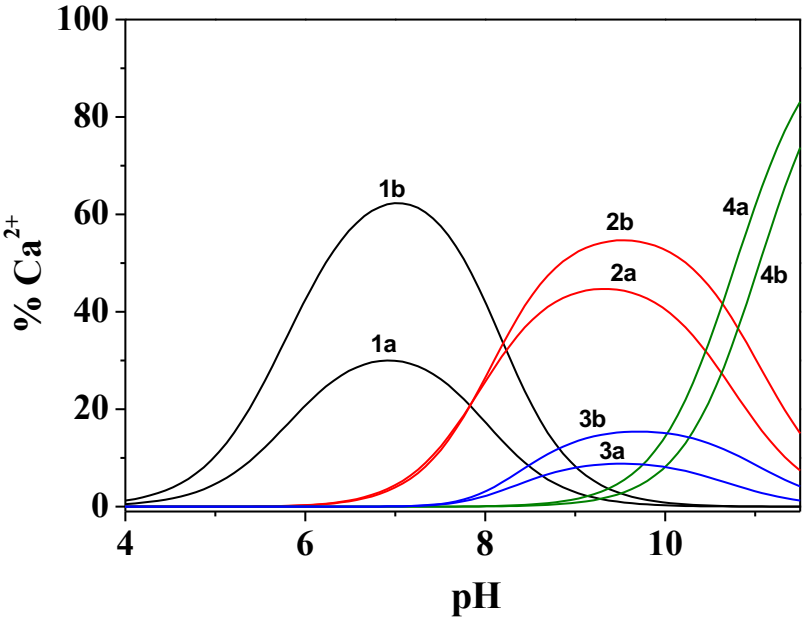

Figure 4.40. Distribution diagram of the species for Ca^{2+}/Oflox system at T = 298.15 K and different ionic strength. Species: 1.MLH; 2. ML; 3. ML_2; 4. MLOH;
a) I = 0.15 mol dm^{-3}; b) I = 1.00 mol dm^{-3}.
(Experimental Conditions: $C_{Ca^{2+}}$ = 2 mmol dm^{-3}; C_{Oflox^-} = 4 mmol dm^{-3}) [M = Ca^{2+}; L = $Oflox^-$]

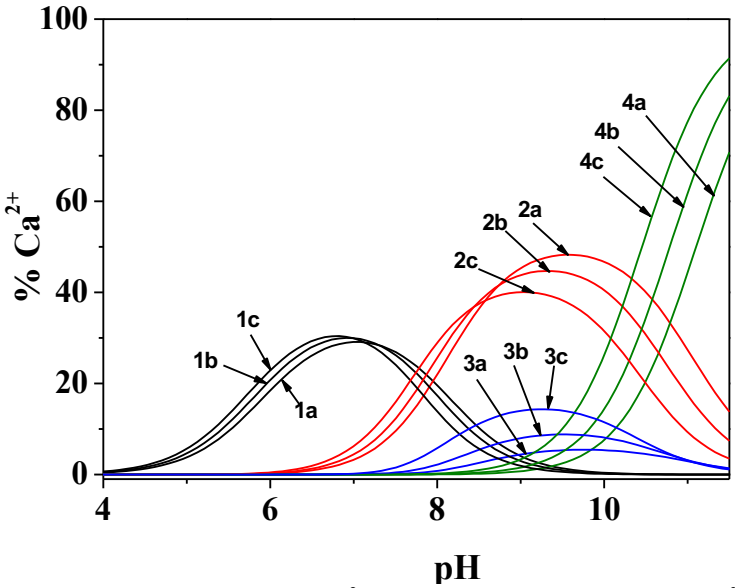

Figure 4.41. Distribution diagram of the species for Ca^{2+}/Oflox system at I = 0.15 mol dm^{-3} and different temperatures. Species: 1.MLH; 2. ML; 3. ML_2; 4. MLOH;
a)T = 288.15 K; b) T = 298.15 K; c) T = 310.15 K.
(Experimental Conditions: $C_{Ca^{2+}}$ = 2 mmol dm^{-3}; C_{Oflox^-} = 4 mmol dm^{-3}) [M = Ca^{2+}; L = $Oflox^-$]

4.2.4 Zn^{2+}/Oflox$^-$ system

Concerning the Zn^{2+}/ofloxacin system, the speciation model is featured, as for calcium, by mononuclear complexes; in particular, we observe both a simple binary metal-ligand species and protonated and ternary hydrolytic species. The proposed speciation model, is also in good agreement with data already reported in the literature, it consists of the ML, MLH, MLOH, $ML(OH)_2$, ML_2H_2 and ML_2H species. The difference in the speciation model with respect to calcium is justified considering the quite different acid-base properties of the two metals and in particular that: i) calcium tend to hydrolyze at high pH values (>10) forming only a simple MOH species; ii) Zn^{2+}, tend to hydrolyze at lower pH values, forming both mono and polynuclear $M_p(OH)_r$ species.

Table 4.45 reports the experimental formation constants of the species at the investigated conditions. From a simple comparison between the two here discussed systems, we observe as an example for the common ML, MLH and MLOH species, that the zinc complexes have a higher stability; in fact if the stepwise formation constants are calculated on the basis of the formation equilibria considered, we have for the ML species a higher stability of about 1-2 order of magnitudes in dependence of the ionic strength or temperature considered; for MLH, considering the following equilibrium of formation M + HL = MLH, log K_{MLH} = 0.06 and 1.09 for Ca^{2+} and Zn^{2+} systems, respectively; for MLOH, considering the formation equilibrium MOH + L =MLOH, we have, log K_{MLOH} = 5.6 and 5.8, respectively.

From the diagram of **Figure 4.42**, that reports the distribution of the species at the lower and higher ionic strength values investigated and T = 298.15 K, it is possible to observe the same evidence already observed for the Ca^{2+}/Dop$^-$ system, namely a significant variation of the maximum of formation of the species with the ionic strength variation. Moreover, significant different percentages of formations and shift at higher or lower pH in dependence on the stoichiometry of the species has been observed.

Table 4.45. Experimental formation constants of the Zn^{2+}/Ofloxacin system in NaCl aqueous solutions at different ionic strengths and temperatures

I /mol dm^{-3}	log β_{ML}	log β_{MLH}	log β_{MLOH}	log $\beta_{ML(OH)2}$	log β_{ML2H2}	log β_{ML2H}
			***T*=288.15 K**			
0.150	4.43±0.07[a)b)]	11.63±0.04	-3.44±0.04	-12.49±0.09	23.96±0.02	16.53±0.04
0.458	4.50±0.05	11.99±0.02	-3.88±0.05	-12.24±0.05	23.34±0.02	16.65±0.03
0.715	4.58±0.04	11.8±0.4	-3.75±0.04	-11.13±0.03	24.52±0.01	16.82±0.02
0.950	4.80±0.05	11.6±0.1	-4.0±0.1	-12.03±0.05	24.71±0.02	16.91±0.04
			***T*=298.15 K**			
0.151	3.4±0.4	11.66±0.03	-3.35±0.02	-12.37±0.07	23.57±0.02	16.36±0.03
0.470	3.7±0.2	11.54±0.02	-3.53±0.01	-12.52±0.05	23.70±0.01	16.22±0.03
0.719	4.88±0.04	10.9±0.2	-3.46±0.05	-11.88±0.04	24.12±0.01	16.38±0.05
0.934	4.24±0.06	11.70±0.02	-3.63±0.02	-12.45±0.05	24.11±0.01	15.84±0.05
			***T*=310.15 K**			
0.149	3.4±0.8	11.26±0.09	-3.13±0.04	-10.96±0.06	23.31±0.03	16.57±0.03
0.459	5.08±0.05	11.1±0.1	-3.8±0.2	-10.89±0.05	23.43±0.02	16.02±0.07
0.714	3.5±0.4	11.36±0.09	-3.16±0.03	-11.46±0.04	24.57±0.02	16.44±0.04
0.945	3.7±0.2	11.44±0.04	-3.38±0.02	-11.84±0.04	24.61±0.01	16.01±0.03

a) logβ_{pqr} refer to Eqs. (4.1 – 4.2); b) ± Std. Dev

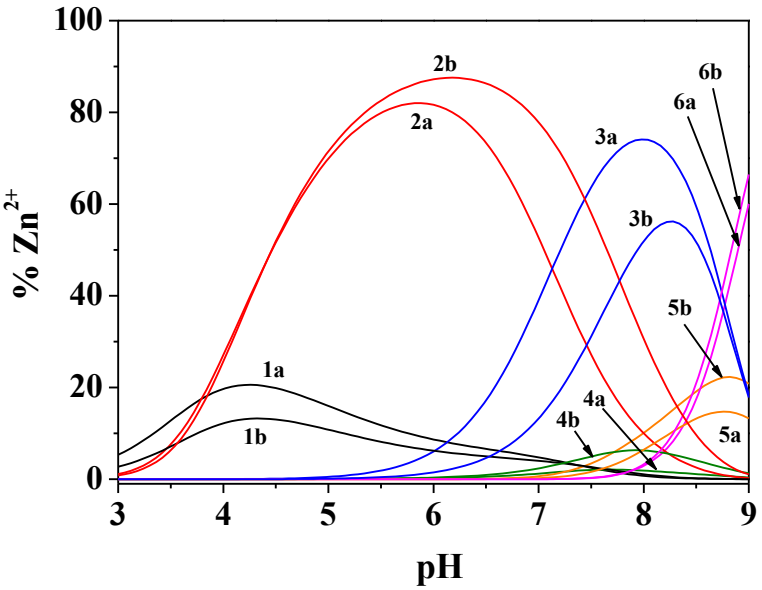

Figure 4.42. Distribution diagram of the species for Zn^{2+}/Oflox system at T = 298.15 K and different ionic strength . Species: 1.MLH; 2. ML_2H_2 ; 3. ML_2H; 4. ML; 5. MLOH; 6. $ML(OH)_2$;
a) I = 0.15 mol dm^{-3}; b) I = 1.00 mol dm^{-3}.
(Experimental Conditions: C_{Zn2^+} = 2 mmol dm^{-3}; C_{Oflox^-} = 4 mmol dm^{-3}) [M = Zn^{2+}; L = Oflox$^-$]

Concerning the distribution of the species at different temperatures, **Figure 4.43**, reports the results obtained at the three investigated temperatures and I = 0.15 mol dm^{-3}.

The consideration that can be done is that the variation of the temperature does not influence significantly the distribution of the species, except for the $MLOH_2$ and ML_2H, even if with an opposite trend, and also a shift towards higher pH.

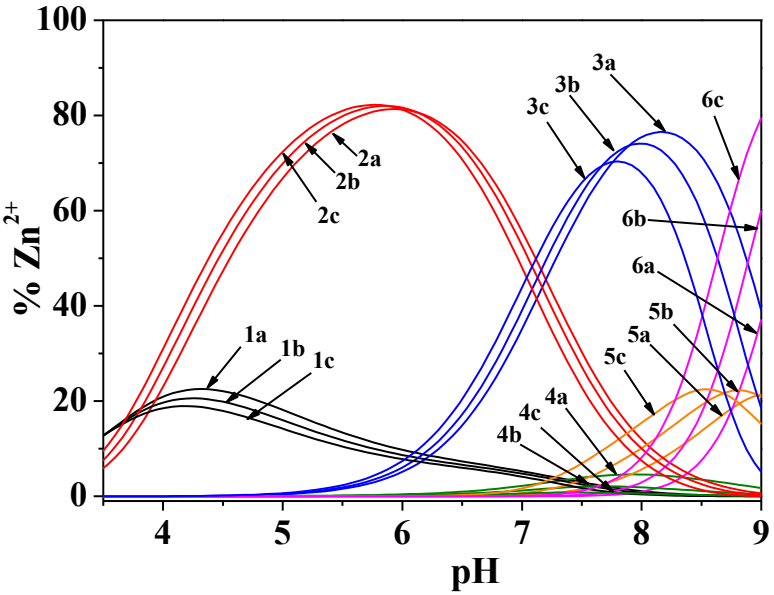

Figure 4.43. Distribution diagram of the species for Zn^{2+}/Oflox system at I = 0.15 mol dm^{-3} and different temperatures. Species: 1.MLH; 2. ML_2H_2 ; 3. ML_2H; 4. ML; 5. MLOH; 6. $ML(OH)_2$;
a) T = 288.15 K; b) T = 298.15 K; c) T = 310.15 K.
(Experimental Conditions: C_{Zn2}^{+} = 2 mmol dm^{-3}; C_{Oflox}^{-} = 4 mmol dm^{-3}) [M = Zn^{2+}; L = Oflox^{-}]

4.2.5 Dependence on ionic strength and temperature of complexes with Ca and Zn.

As for the other investigated systems, the dependence on ionic strength and temperature for the Ca^{2+}/Oflox^{-} and Zn^{2+}/Oflox^{-} systems has been investigated by means of the Debye-Hückel (EDH) reported in Eq. (4.8), allowing the calculation of the stability constants at infinite dilution, of the parameter for the dependence on the ionic strength and the standard enthalpy change values of formation. The obtained parameters are reported in **Table 4.46**.

Table 4.46. Formation constants, parameter for the dependence on the ionic strength, standard enthalpy and entropy change values, at infinite dilution, of the M^{n+}/Oflox$^-$ species.

Species	$\log\beta^T_{pqr}$ a)	C b)	ΔH c)	TΔS c)
		Ca^{2+}/Oflox$^-$		
ML	3.02 ± 0.04 d)	0.83 ± 0.06 d)	2.4 ± 2 d)	19.6±2.4 d)
MLH	10.56 ± 0.04	1.08 ± 0.06	-20.6 ± 2.7	39.6±2.7
MLOH	-7.37 ± 0.05	0.41± 0.07	57±3	15±3.1
ML_2	5.10 ± 0.06	1.27± 0.09	46±3.7	75.4±38
		Zn^{2+}/Oflox$^-$		
ML	4.28±0.15 d)	0.89 ± 0.21	-66.9 ± 12.5 d)	-42.5±12.5 d)
MLH	11.72±0.10	0.28 ± 0.17	-33.3 ± 9.6	33.6±9.6
MLOH	-2.86±0.07	0.04± 0.11	38.1±8.8	21.8±8.8
$ML(OH)_2$	-11.66±0.18	0.14± 0.29	75±12	8.4±12
ML_2H_2	23.92±0.09	1.10± 0.15	-52±10	84.5±9.6
ML_2H	17.13 ± 0.14	0.53± 0.22	-37±11	-60±11.6

a) $\log\beta_{pqr}$ refer to eqs. (4.1 – 4.2); b) parameter for the dependence on I/mol dm^{-3}; c) enthalpy and entropy change values of formation in kJ/mol ; d) ±Std.Dev. .

4.3. Ornidazole

4.3.1. Solubility of Ornidazole

Solubility studies on Ornidazole, as for Ofloxacin, were performed at I = 0.15 mol dm^{-3} in NaCl aqueous solution and 288.15 ≤ T/K ≤ 310.15.

Considering the structure of this ligand, we can assume that it contains only a protonable site, so that the solubility is given by:

$$S^T = [HL^+] + [L^0] \quad (4.23)$$

If the concentration of the L^0 neutral species is indicated with S^0, from the equilibrium reported in the Eqs. 4.23 we have that:

$$H^+ + L^0 = HL^+ \qquad logK^H \qquad (4.24)$$

$$K^H = \frac{[HL^+]}{[H^+] \cdot [L^0]} \quad \text{and} \quad [HL^+] = K^H \cdot [H^+] \cdot [L^0] \qquad (4.25)$$

Rearranging Eq. 4.23, we obtain:

$$S^T = S^0 \cdot (1 + K^H \cdot [H^+]) \qquad (4.26)$$

By means of absorbance measurements of standard solutions of Ornidazole at different concentrations (from 0.00099 to 0.099 mol dm^{-3}), the calibration lines were drawn, observing a linear trend between absorbance and standard concentration in the whole concentration range investigated.

Table 4.47 reports the solubility (experimental and mean value) of Ornidazole in aqueous solutions containing sodium chloride at the ionic strength I = 0.15 mol dm^{-3}.

It appears relevant that the solubility of ornidazole increases linearly with the increase of the temperature, as better highlighted by **Figure 4.44**, that reports the experimental trends of S^T *vs T/K* with an R-square of 0.953.

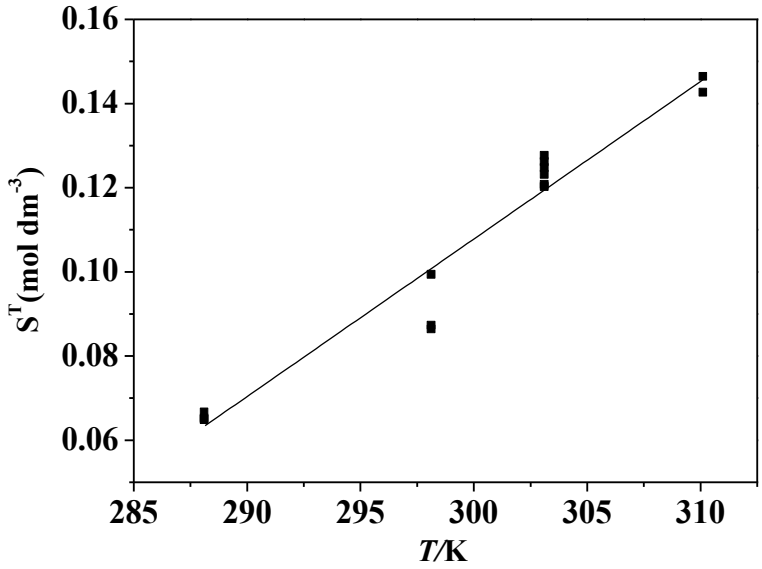

Figure. 4.44 Mean solubility (S^T) of Ornidazole in molar concentration scale at different temperatures, in aqueous solutions of sodium chloride at I = 0.15 mol·dm^{-3}coefficient of correlation R^2 = 0.9531.

From our investigations resulted that at the pH of solubilization, the ligand is totally presents as neutral specie, so that we can assume that $S^T = S^0$. From the pH measurements of the saturated solutions, and also from the potentiometric titrations for the determination of the protonation constant, it was seen that the neutral species is already present at pH = 5, with a percentage of 100%.

Table 4.47. Solubility and neutral species concentrations of Ornidazole in NaCl(aq), at I = 0.15 mol dm^{-3}, different temperatures and p =0.1 MPa

$S^{T\,a)}$ (λ = 320 nm)			
288.15K	**298.15K**	**303.15K**	**310.15K**
0.0646	0.0871	0.1201	0.1425
0.0651	0.0862	0.123	0.1425
0.0665	0.0992	0.1206	0.1462
0.0648		0.1246	
		0.1246	
		0.1275	
		0.126	
0.0653±0.0008[b)]	0.090±0.007	0.124±0.003	0.144±0.002

[a)] solubility of Ornidazole (S^T) expressed in the molar concentration scale (mol·dm^{-3}); [b)] ±Std. Dev. Standard uncertainties u are: u(T) = 0.1 K; u (p) = 1 KPa; u(I) = 0.01 mol·dm^{-3}; u(S^T) = 0.0005 mol·dm^{-3} or lower

4.3.2. Protonation constants of Ornidazole

The acid-base properties of ornidazole were investigated by potentiometry, in solutions aqueous solutions of $NaCl_{(aq)}$ in the of ionic strength range from $0.15 \leq I$ / mol dm$^{-3} \leq 1$ and temperature $288.15 \leq T/K \leq 318.15$.

Table 4.48. Experimental hydronation constants of Ornidazole calculated from potentiometric titrations at different ionic strength in NaCl(aq) and different temperatures.

T = 288.15 K		**T = 298.15 K**	
I /mol dm^{-3}	**log$K_1^{Ha)}$**	**I /mol dm^{-3}**	**log$K_1^{Ha)}$**
0.146	2.459±0.006 b)	0.148	2.556±0.008 b)
0.146	2.302±0.002	0.149	2.345±0.001
0.487	2.610±0.009	0.147	2.280±0.006
0.486	2.60±0.01	0.488	2.4906±0.0007
0.733	2.343±0.008	0.488	2.364±0.002
0.733	2.61±0.01	0.733	2.588±0.003
0.980	2.71±0.03	0.733	2.400±0.002
0.981	2.534±0.003	0.971	2.670±0.002
		0.971	2.500±0.003
T = 310.15 K		**T = 318.15 K**	
I /mol dm^{-3}	**log$K_1^{Ha)}$**	**I /mol dm^{-3}**	**log$K_1^{Ha)}$**
0.146	2.155±0.005 b)	0.150	2.54±0.01 b)
0.146	2.644±0.008	0.150	2.442±0.003
0.497	2.3165±0.0005	0.150	2.325±0.009
0.497	2.323±0.001	0.150	2.194±0.006
0.981	2.894±0.007	0.487	2.410±0.002
0.981	2.601±0.006	0.487	2.22±0.01
		0.487	2.28±0.01
		0.487	2.295±0.006
		0.731	2.74±0.01
		0.731	2.520±0.003
		0.731	2.391±0.005
		0.731	2.33±0.01
		0.976	2.514±0.009
		0.976	2.449±0.009
		0.976	2.547±0.005
		0.976	2.502±0.003

a) refer to Eq. 4.24; b) ± Std. Dev

The data on the protonation constant of Ornidazole, allowed us to model the dependence on ionic strength and temperature by means of the extended Debye-Hückel equation (EDH) and thus determining the C and ΔH/kJ mol^{-1} parameters.

Table 4.49. reports both the stability constants and the empirical parameters for the dependence on I/mol dm^{-3} (at T = 298.15 K) and the standard enthalpy and entropy change values of the protonation constant.

Table 4.49. Protonation constant, enthalpy and entropy change values, at infinite dilution and different temperatures, of Ornidazole.

	$\log K_1^{HT}$	ΔH [c)]	$T\Delta S$ [c)]
		T = 298.15 K	
$I \rightarrow 0$ [a)]	2.40±0.02 [d)]	-6.6±1 [d)]	7.1±2 [d)]
C [b)]	0.21±0.03		

a) $\log K_1^H$ refer to eq. (4.24); b) parameter for the dependence on I/mol dm^{-3}; c) enthalpy and entropy change values of formation in kJ/mol ; d) ±Std.Dev.

4.3.3 Ca^{2+}/Orn System

The interactions of ornidazole with the calcium ion were studied under ionic strength conditions between $0.15 \leq I$ / mol dm^{-3} ≤ 1.00 and temperature $288.15 \leq T$ / K ≤ 310.15 by potentiometric titrations.

For the determination of the best speciation model, the formation of many different species were checked, but the only refined species at each experimental conditions resulted to be ML_2, whose formation constant is reported in **Table 4.50.**

Table 4.50. Experimental formation constants of Ca^{2+}/Orn in $NaCl_{(aq)}$ at different ionic strengths and different temperatures.

	$\log\beta_{ML2}$		
I /mol dm^{-3}	**288.15K**	**298.15K**	**310.15K**
0.15	4.69±0.03 [c)]	4.72±0.05 [c)]	4.12±0.16 [c)]
0.50	3.19±0.02	3.93±0.05	4.32±0.14
0.75	2.11±0.04	3.37±0.04	4.47±0.10
1.00	1.04±0.04	1.68±0.05	4.61±0.20

a) $\log\beta_{pqr}$ refer to eqs. (4.1 – 4.2); b) parameter for the dependence on I/mol dm^{-3}; c) enthalpy and entropy change values of formation in kJ/mol ; d) ±Std.Dev. .

4.3.4 Dependence on ionic strength and temperature of complexes with Ca.

The dependence on ionic strength and temperature for the Ca^{2+}/Orn system has been investigated by means of the Debye-Hückel (EDH) reported in Eq. (4.8), allowing the calculation of the stability constants at infinite dilution, of the parameter for the dependence on the ionic strength and the standard enthalpy change values of formation. The obtained parameters are reported in **Table 4.51.**

Table 4.51. Formation constant, enthalpy and entropy change values, at infinite dilution, dependence parameter on ionic strength of Ca^{2+}/Orn species

	$\log\boldsymbol{\beta}_{ML2}^{T}$	$\Delta H^{c)}$	$T\Delta S^{c)}$
***T* = 298.15 K**			
$I \rightarrow 0^{a)}$	5.06±0.05 [d) e)]	126±29 [d) e)]	155±30 [d) e)]
C[b)]	-2.26±0.15		

a) $\log\beta_{pqr}$ refer to eqs. (4.1 – 4.2); b) parameter for the dependence on I/mol dm^{-3}; c) enthalpy and entropy change values of formation in kJ/mol ; d) ±Std.Dev. ; e) calculated at I = 0.15 mol dm^{-3} and T = 298.15 K .

Chapter 5

The Sequestering Ability

As a further investigation on the speciation of the biological molecules taken into account, the sequestering ability towards some metal ions were studied in NaCl aqueous solution at different ionic strengths. The metals investigated are Ca^{2+}, Cd^{2+}, Cu^{2+} Mg^{2+}, Mn^{2+}, Sn^{2+}, UO_2^{2+}, Zn^{2+} CH_3Hg^+ and DET^{2+}. All the metals are very important from a biological point of view, while some have wide application in many fields, and consequently can be present in high quantities in natural systems, and therefore assimilated by different organisms.

5.1 Sequestering ability of Dopamine systems

In chelation therapy, and in many other fields where binding equilibria are involved in crucial processes, several aspects must be taken into account in the choice of the "best" chelant. Among them, from the chemical point of view, the ideal "chelant" should form very stable complexes "in competition with the stability of endogenous ligands in the body" and should be selective "toward the target metal ion" [157]. Obviously, these characteristics are strictly dependent on the stability of the complexes formed by the potential chelant and the target metal ion, but also on that of "side species", *i.e.* those formed by other endogenous ligands with the target ion and those by the potential chelant with other ions. The efficacy of the chelation depends, from the chemical side, also on the competitive reactions, involving simultaneous equilibria in different conditions [2]: even considering a very simple one metal-one ligand system in aqueous solution (and this is never the case of real systems), one must at least take into account the competition of H^+ with the ligand and OH- with the metal. This means that the selectivity and the whole "sequestering" ability of a chelant toward a cation, as well as the comparison between two or more chelants, cannot be easily assessed by the simple analysis of single sets of stability constants of metal/ligand complexes in real conditions, especially if "different complex species are formed rather than a single prevailing one" [158, 159]. In the past, some procedures were proposed for the quantification of the sequestering ability of a given ligand toward metal ions; as an example, the free metal concentration in solution at equilibrium, expressed as pM, is one of the most used parameters in chelation therapy to assess the binding ability of various chelants toward a given metal. Nevertheless, it has been frequently pointed out that the use of pM for comparisons may be, sometimes, "problematic", so that its use by "non experts" should be discouraged.

To overcome this problem, our research group introduced many years ago the $pL_{0.5}$ parameter [117], that is an easy-to-use and easy-to-get instrument to make fast and reliable quantifications of the sequestering ability of a ligand toward a given component (not necessarily a metal cation). The $pL_{0.5}$

parameter, represents the total ligand concentration necessary to sequester 50% of a given metal ion present as trace in given conditions, even in the presence of other components. It is rapidly calculated in a very simple way by the most common programs used to plot the speciation diagrams.
The $pL_{0.5}$ is then obtained graphically, or by fitting plotted data to Eq. (5.1).

$$X = \frac{1}{1+10^{(pL-pL_{0.5})}} \tag{5.1}$$

where x is the fraction of the metal M (presents in trace) complexed by the ligand. The parameter $pL_{0.5}$, calculated by least squares analysis, gives the conditions for which 50% of metal is complexed by the ligand ($[L]_{tot} = 10^{-pL0.5}$) and can be calculated once the conditions (pH, ionic strength, supporting electrolyte, temperature) are fixed and gives an objective representation of the binding ability This function is assimilable to a sigmoid curve (or a dose response curve) with asymptotes of 1 for pL → -∞ and 0 for pL → +∞. It is important to note that: this property varies with the experimental conditions, but it is independent of the analytical concentration of the metal ion when this is present as a trace amount in the system.
It can be easily demonstrated that $pL_{0.5}$, determined as above described, in particular cases, are numerically equivalent to other parameters used for the same purposes, like the intrinsic median binding concentration, BC_{50} [160-163], or the historical Schwarzenbach's apparent formation constant [164].
Despite the apparent redundancy and uselessness of a new parameter to quantify the sequestering ability of a ligand toward a metal cation, it must be underlined here that $pL_{0.5}$ shows some advantages in its use, which enable it to be of more immediate use for not-specialists. For example, like any other stability constant, the higher the $pL_{0.5}$, the higher the sequestering ability of the ligand, and this is usually of more immediate comprehension, while this is not the case for BC_{50}, which specifically designed to be similar to the median inhibitory concentration IC_{50}. However, the greatest advantage of the use of $pL_{0.5}$ is probably that related to its determination: i) as already pointed out, $pL_{0.5}$ can be calculated easily by means of very common programs and does not require any particular skills in the treatment of simultaneous equilibria and/or the solution of systems of mass balance equations.
Using this approach, the sequestering ability of the ligands here investigated against the metal cations were evaluated at the different experimental conditions (I / mol dm^{-3}, pH, T / K). The following Tables report the $pL_{0.5}$ values determined at the experimental conditions experimentally investigated.

Table 5.1. Sequestering ability of dopamine towards the metals at I = 0.15 mol dm^{-3}, pH = 7.4 and different temperatures.

Metal	T/K	$pL_{0.5}$
Ca^{2+}	288.15	0.81
	298.15	1.15
	310.15	1.86
Cd^{2+}	288.15	2.17
	298.15	1.08
	310.15	1.73
Cu^{2+}	288.15	5.07
	298.15	4.64
	310.15	5.35
	318.15	5.10
Mg^{2+}	288.15	2.23[a)]
	298.15	2.27[a)]
	310.15	2.94[a)]
Mn^{2+}	288.15	1.92
	298.15	1.58
	310.15	1.39
Sn^{2+}	288.15	3.74
	298.15	3.46
	310.15	3.75
UO_2^{2+}	288.15	7.00
	298.15	7.58
	310.15	8.87
	318.15	9.02
Zn^{2+}	288.15	3.02
	298.15	2.77
	310.15	3.48
CH_3Hg^{+}	288.15	2.36
	298.15	2.63
	310.15	3.74
	318.15	4.50
DET^{2+}	288.15	4.26
	298.15	4.64
	310.15	6.10

a) Calculated at pH = 9.5

Table 5.2. Sequestering ability of dopamine towards the metals at T = 298.15 K, pH = 7.4 and different ionic strengths.

Metal	I/ mol dm^{-3}	$pL_{0.5}$
Ca^{2+}	0.15	1.15
	0.50	1.19
	0.75	1.68
	1.00	2.58
Cd^{2+}	0.15	1.08
	0.50	1.40
	0.75	1.52
	1.00	1.65
Cu^{2+}	0.15	4.63
	0.50	4.64
	0.75	4.76
	1.00	4.82
Mg^{2+}	0.15	2.27[a)]
	0.50	2.11[a)]
	0.75	2.04[a)]
	1.00	2.10[a)]
Mn^{2+}	0.15	1.58
	0.50	1.38
	0.75	1.26
	1.00	1.14
Sn^{2+}	0.15	3.74
	0.50	3.70
	0.75	3.12
	1.00	2.60
UO_2^{2+}	0.15	7.58
	0.50	7.76
	0.75	8.01
	1.00	8.13
Zn^{2+}	0.15	2.77
	0.50	2.61
	1.00	2.42
CH_3Hg^{+}	0.15	2.63
	0.50	2.90
	0.75	3.02
	1.00	3.12
DET^{2+}	0.15	4.64
	0.50	4.83
	0.75	4.92
	1.00	5.01

a) Calculated at pH = 9.5

Table 5.3. Sequestering ability of dopamine towards the metals at I = 0.15 mol dm^{-3}, T = 298.15 K and different pHs.

Metal	pH	$pL_{0.5}$
Ca^{2+}	7.4	1.15
	8.2	2.00
	9.0	3.03
	9.5	3.65
	10.5	4.72
Cd^{2+}	7.4	1.08 [a]
	8.0	1.99 [a]
	9.0	3.56 [a]
Cu^{2+}	5.5	1.57
	7.4	5.19
	9.5	8.46
Mg^{2+}	7.4	0.08
	8.2	1.06
	9.0	1.31
	9.5	2.27
	10.5	3.97
Mn^{2+}	7.4	1.58
	8.5	2.99
Sn^{2+}	5	1.30
	6	2.33
	7.4	3.74
	8.2	4.31
	9	5.07
UO_2^{2+}	5	3.90[a]
	6	6.20 [a]
	7.4	8.60 [a]
Zn^{2+}	7.4	2.77
	8.2	4.31
	9	5.43
CH_3Hg^+	7.4	2.63
	8.2	3.46
	9.0	4.51
	9.5	5.23
	10.5	6.16
DET^{2+}	4.40	3.47
	7.4	4.64
	9.0	5.50

a) Calculated at T = 310.15K

From the sequestering diagrams below reported, it is possible to observe how the sequestering ability of dopamine towards the different metals it is strictly dependent on the experimental conditions employed, namely ionic strength, temperature, and pH.

The increase of $pL_{0.5}$ with increasing pH is clearly correlated to the increasing deprotonation of the ligand with increasing pH since, being an electrostatic interaction, the stability of the species that are

formed is strictly dependent on the charges involved in the reactions that lead to the formation of complexes.

At the same pH, the dependence of the dopamine sequestering ability on the ionic strength is closely linked both to the acid-base property of the metal and ligand, and to the strength of the metal binding species, and to the tendency of the metal to form weak species with the anion of the ionic medium.

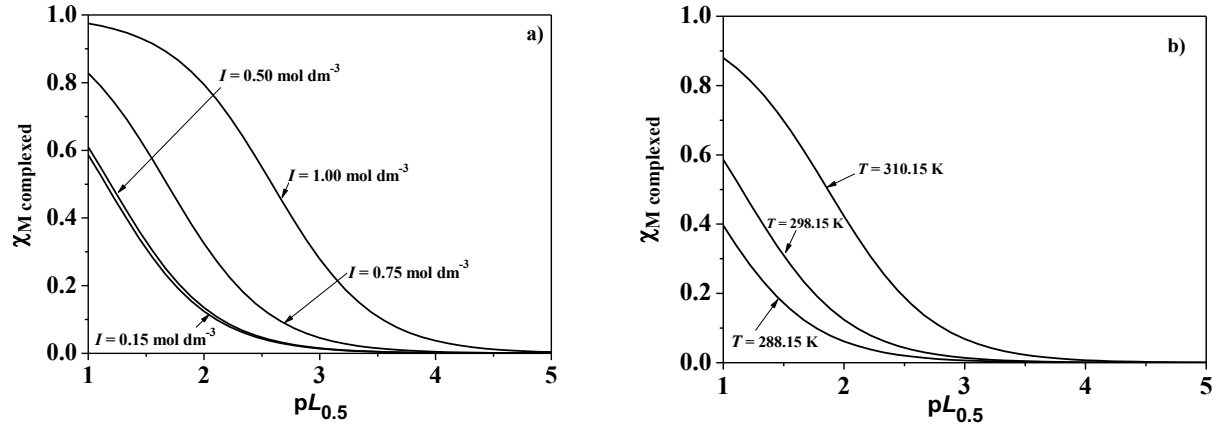

Figure 5.1. Sequestering ability of dopamine towards Ca^{2+}.
a) T = 298.15 K, pH = 7.4 at different ionic strengths; b) I = 0.15 mol dm^{-3}, pH = 7.4 at different temperatures.
$pL_{0.5}$ values: a) 1.15 (I = 0.15 mol dm^{-3}) < 1.19 (I = 0.50 mol dm^{-3}) < 1.68 (I = 0.75 mol dm^{-3}) < 2.58 (I = 1.0 mol dm^{-3}).
b) 0.81 (T = 288.15 K) < 1.15 (T = 298.15 K) < 1.86 (T = 318.15 K).

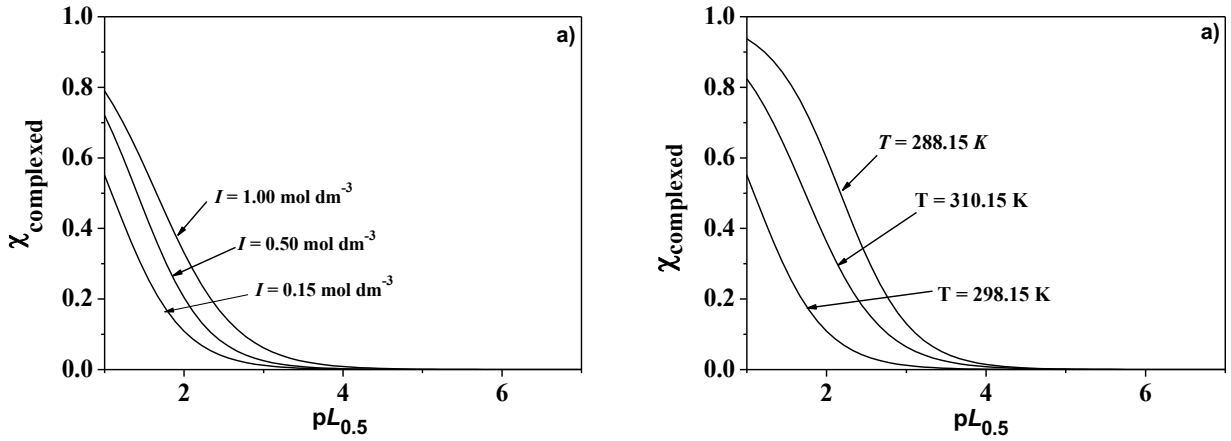

Figure 5.2. Sequestering ability of dopamine towards Cd^{2+}.
a) T = 298.15 K, pH = 7.4 at different ionic strengths; b) I = 0.15 mol dm^{-3}, pH = 7.4 at different temperatures.
$pL_{0.5}$ values: a) I = 0.15 mol dm^{-3}, 1.08; I = 0.50 mol dm^{-3}, 1.40; I = 1.0 mol dm^{-3}, 1.65.
b) $pL_{0.5}$: T = 288.15 K, 2.17; T = 298.15 K, 1.08; T = 310.15 K, 1.73.

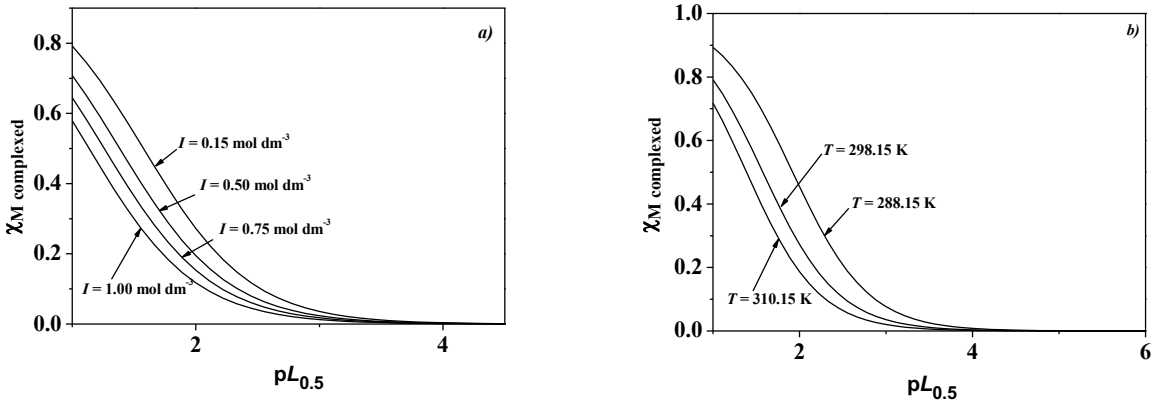

Figure 5.3. Sequestering ability of dopamine towards Mn^{2+}.
a) T = 298.15 K, pH = 7.4 at different ionic strengths; b) I = 0.15 mol dm^{-3}, pH = 7.4 at different temperatures.
$pL_{0.5}$ values: a) I = 0.15 mol dm^{-3}, 1.58; I = 0.50 mol dm^{-3}, 1.38; I = 0.75 mol dm^{-3}, 1.26; I = 1.0 mol dm^{-3}, 1.14.
b) $pL_{0.5}$: T = 288.15 K, 1.92; T = 298.15 K, 1.58; T = 310.15 K, 1.39.

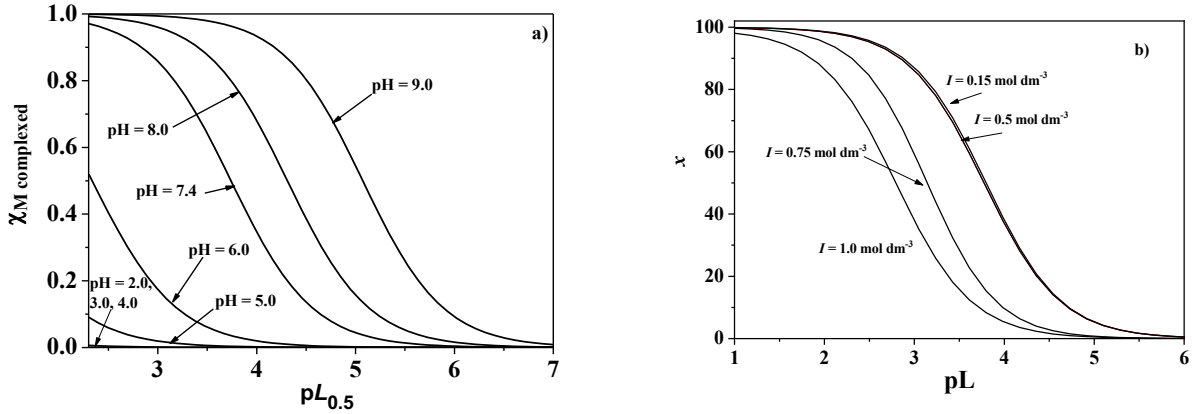

Figure 5.4. Sequestering ability of dopamine towards Sn^{2+}.
a) T = 298.15 K, I = 0.15 mol dm^{-3} and different pH values. b) T = 298.15 K, pH = 7.4 and different ionic strengths.
$pL_{0.5}$ values: a) 1.30 (pH = 5.0); 2.33 (pH = 6.0); 3.74 (pH = 7.4); 4.31 (pH = 8.0); 5.07 (pH = 9.0).
b) 3.74 (I = 0.15 mol dm^{-3}) < 3.70 (I = 0.50 mol dm^{-3}) < 3.12 (I = 0.75 mol dm^{-3}) < 2.60 (I = 1.0 mol dm^{-3}).

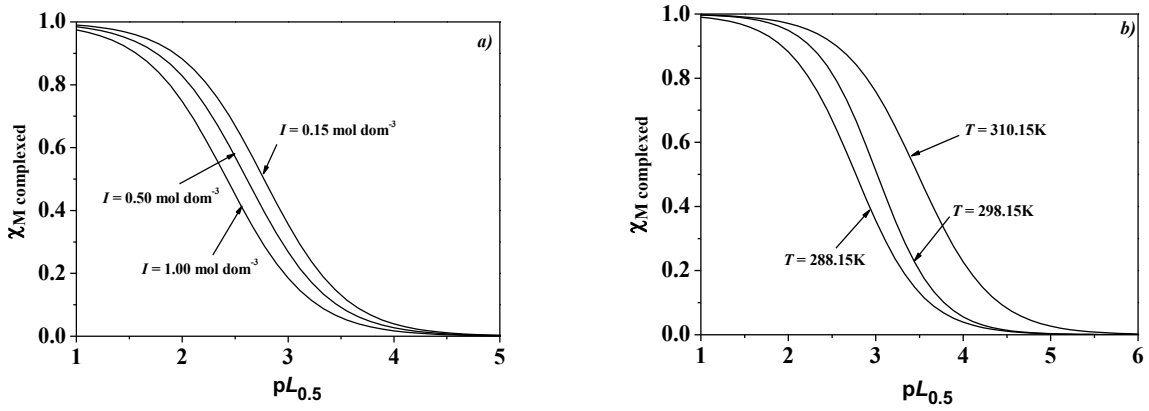

Figure 5.5. Sequestering ability of dopamine towards Zn^{2+}.
a) I = 0.15 mol dm^{-3}, pH = 7.4 at different temperatures b) T = 298.15 K, pH = 7.4 at different ionic strengths.
$pL_{0.5}$ values: a) I = 0.15 mol dm^{-3}, 2.77; I = 0.50 mol dm^{-3}, 2.61; I = 1.0 mol dm^{-3}, 2.42.
b) $pL_{0.5}$: T = 288.15 K, 3.02; T = 298.15 K, 2.77; T = 310.15 K, 3.48.

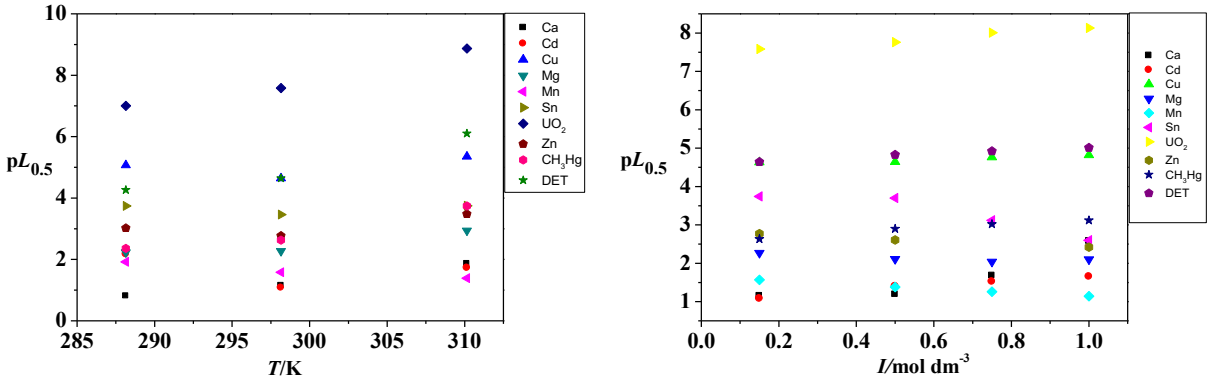

Figure 5.6. Trend of $pL_{0.5}$ vs T/K, I/mol dm^{-3}.
A. Experimental conditions: I = 0.15 mol dm^{-3} and pH = 7.4.
B. Experimental conditions: T = 298.15 K and pH = 7.4.

Figure 5.6. reports two different diagrams, where the values of the $pL_{0.5}$ parameter are reported at the different temperatures investigated and at different ionic strength (at I = 0.15 mol dm^{-3} and pH = 7.4).

The knowledge of the $pL_{0.5}$ parameter is essential for this kind of investigation, since it gives a simple way to effectively quantify the ability of a given ligand to interact with the metal. The simple comparison of a common species between different metal-ligand systems cannot be sufficient to obtain this information. As an example, for the dopamine systems here investigated and containing in the corresponding speciation model the ML species, a comparison of the $\log K_{ML}$ values determined at the same experimental condition gives the following trend of stability.

$$\log \beta_{ML}: Mg^{2+}(3.03) < Ca^{2+}(4.83) < Mn^{2+}(5.42) < Cd^{2+}(6.48) < Zn^{2+}(7.4) < DET^{2+}(15.11)$$

However, this approach, many times used by the researchers, is incorrect because does not give the correct evaluation of the cumulative strength of the interaction, since it does not take into account the many other variables (*i.e* the contribution of the other species, the effect of the pH and ionic strength, and the temperature).

If the same comparison is done by using the $pL_{0.5}$ parameter, calculated at the same experimental condition (at $T = 298.15$, $I = 0.15$ mol dm^{-3} and pH = 7.4), we have:

$$pL_{0.5}: Mg^{2+} < Cd^{2+} \sim Ca^{2+} < Mn^{2+} < Zn^{2+} < DET^{2+}$$

It can be observed that by using the $pL_{0.5}$ parameter, a different trend, in term of sequestering ability of dopamine towards the metal ions has been obtained.

Hence, trend for the sequestering capacity of dopamine towards all the investigated metal ions is:

$$pL_{0.5}: Mg^{2+} < Cd^{2+} \sim Ca^{2+} < Mn^{2+} < CH_3Hg^{+} < Zn^{2+} < Sn^{2+} < DET^{2+} < Cu^{2+} < UO_2^{2+}$$

This trend has been obtained at $T = 298.15$K, $I = 0.15$ mol dm^{-3} and pH = 7.4, but significant variations can be determined if the experimental conditions are changed (i.e. pH, T / K or I / mol dm^{-3}).

For example, **Figure 5.7** shows the sequestering curves of dopamine towards the metal ions at $T = 298.15$K, $I = 0.15$ mol dm^{-3} and pH = 7.4, except for Mg^{2+} and Cd^{2+}, where $pL_{0.5}$ the values were calculated at pH = 9.5, owing to the very low sequestering ability of dopamine at pH = 7.4.

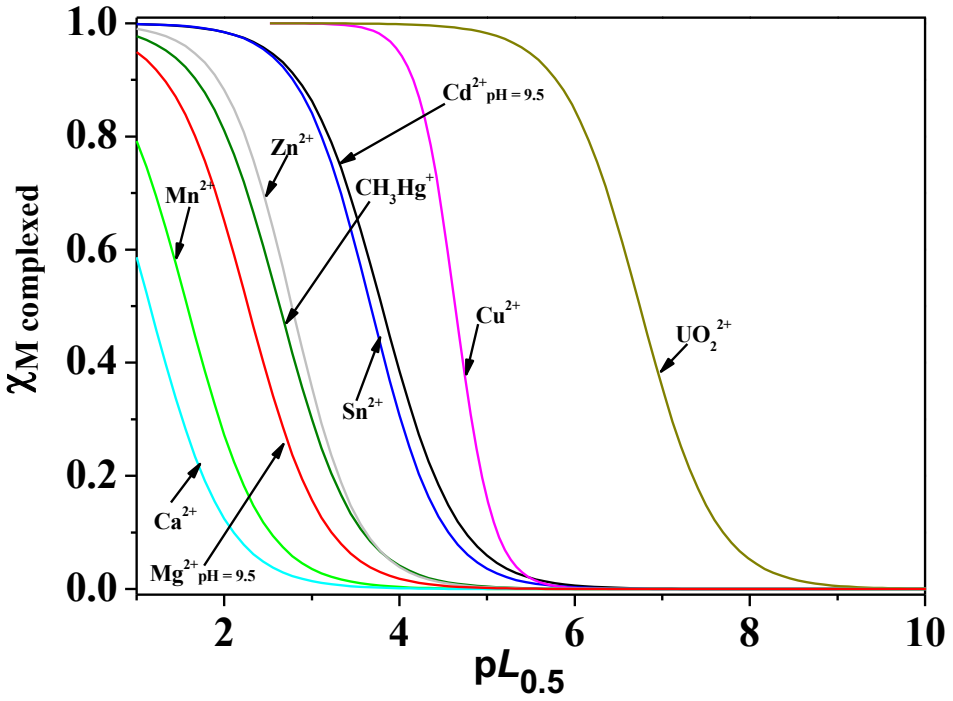

Figure 5.7 Sequestering ability of dopamine towards different metals ions, at T = 298.15 K, pH = 7.4 and I = 0.15 mol dm^{-3}

5.2 Sequestering ability of Ofloxacin

The sequestering ability of ofloxacin towards calcium and zinc was also quantified by means of the $pL_{0.5}$ parameter, and the corresponding values are reported in **Tables 5.4-5.6**.

Table 5.4. Sequestering ability of Ofloxacin towards the metals at I = 0.15 mol dm^{-3}, pH = 7.4 and different temperatures.

Metal	T/K	$pL_{0.5}$
Ca^{2+}	288.15	2.23
	298.15	2.28
	310.15	2.34
Zn^{2+}	288.15	3.88
	298.15	3.88
	310.15	3.92

Table 5.5. Sequestering ability of Ofloxacin towards the metals at T = 298.15 K, pH = 7.4 and different ionic strengths.

Metal	I/ mol dm^{-3}	$pL_{0.5}$
Ca^{2+}	0.15	2.28
	0.50	2.40
	0.75	2.52
	1.00	2.63
Zn^{2+}	0.15	3.88
	0.50	3.77
	0.75	3.73
	1.00	3.70

Table 5.6. Sequestering ability Ofloxacin towards the metals at I = 0.15 mol dm^{-3} , T = 298.15 K and different pHs.

Metal	pH	$pL_{0.5}$
Ca^{2+}	7.4	2.28
	8.2	2.51
	9.0	2.69
Zn^{2+}	5.0	2.98
	7.4	3.88
	8.0	4.63
	9.0	5.28

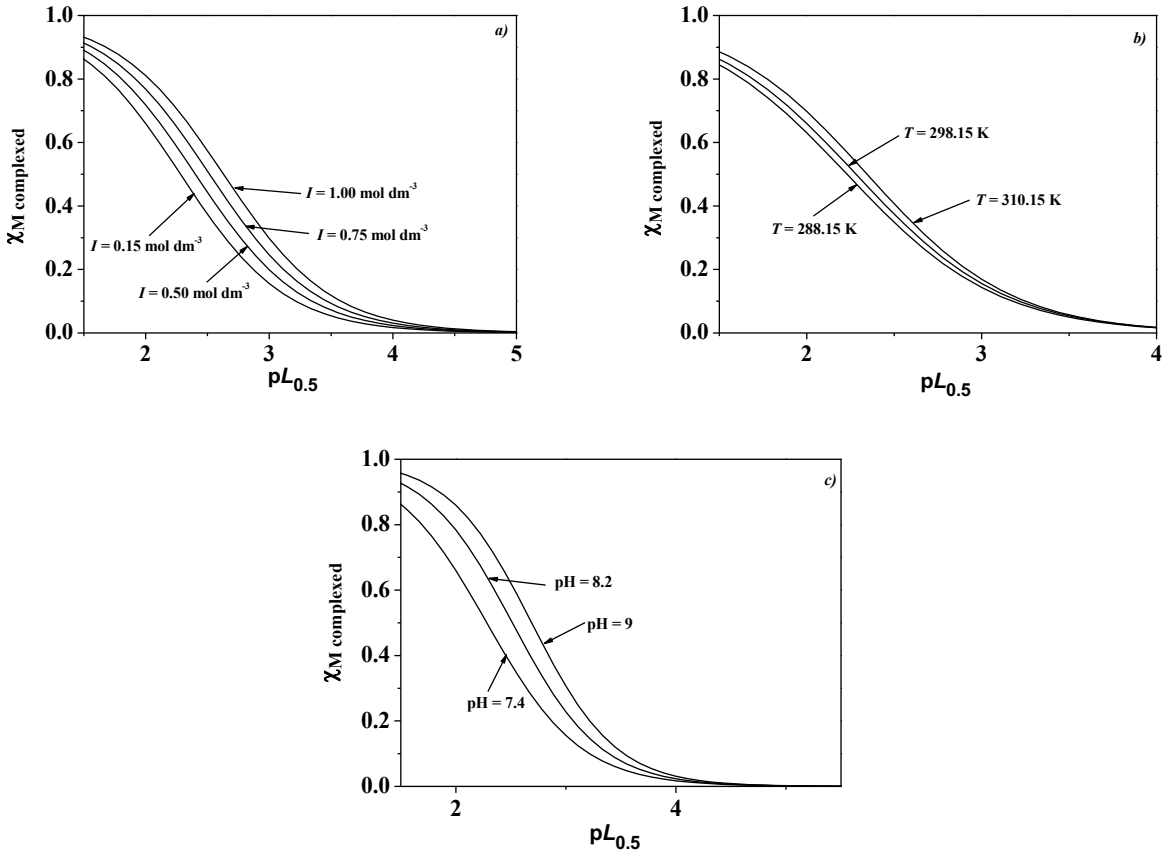

Figure 5.8. Sequestering ability of Ofloxacin towards Ca^{2+}.
a) T = 298.15 K, pH = 7.4 at different ionic strengths; b) I = 0.15 mol dm^{-3}, pH = 7.4 at different temperatures c) T = 298.15 K, I = 0.15 mol dm^{-3} at different pHs.
$pL_{0.5}$ values: a) 2.28 (I = 0.15 mol dm^{-3}) < 2.40 (I = 0.50 mol dm^{-3}) < 2.52 (I = 0.75 mol dm^{-3}) < 2.63 (I = 1.0 mol dm^{-3}).
b) 2.23 (T = 288.15 K) < 2.28 (T = 298.15 K) < 2.34 (T = 318.15 K).
c)2.28 (pH = 7.4) <2 .51 (pH = 8.2) < 2.69 (pH = 9)

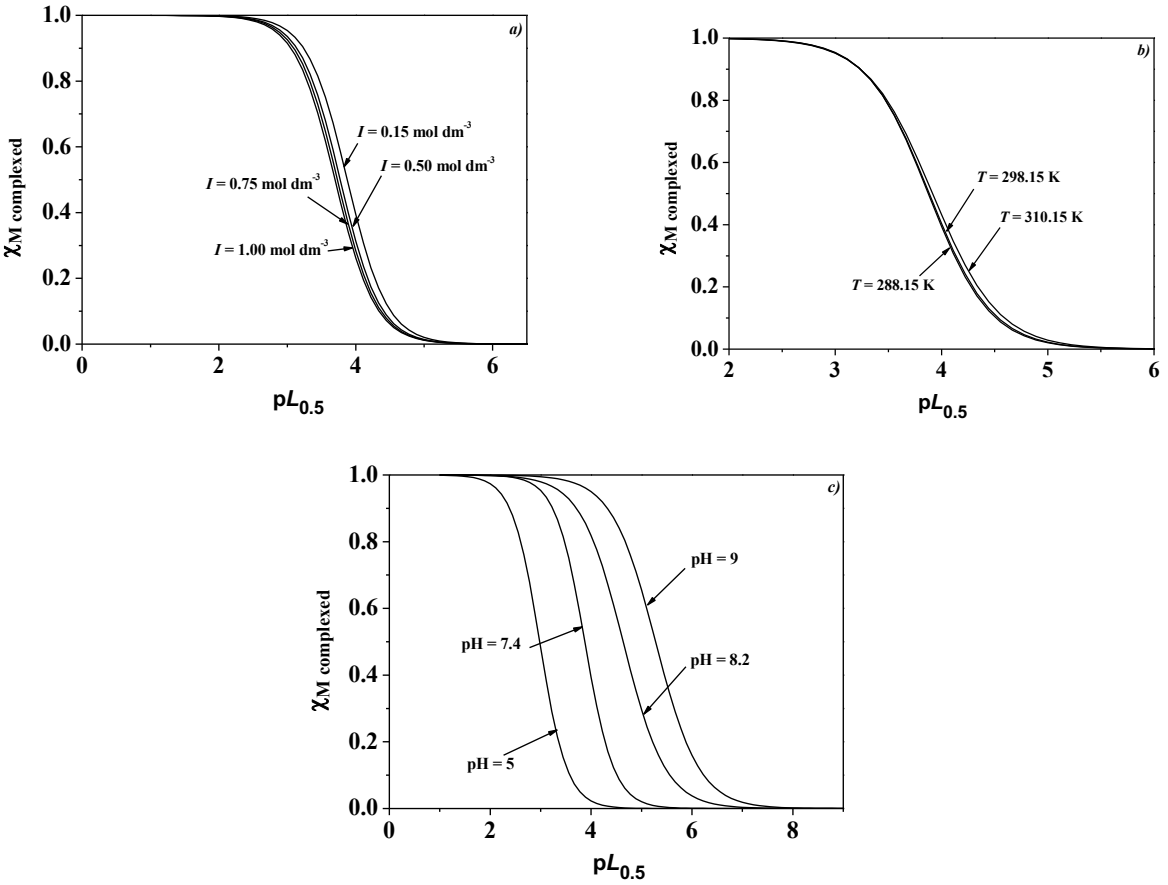

Figure 5.9. Sequestering ability of Ofloxacin towards Zn^{2+}.
a) T = 298.15 K, pH = 7.4 at different ionic strengths; b) I = 0.15 mol dm^{-3}, pH = 7.4 at different temperatures c) T = 298.15 K, I = 0.15 mol dm^{-3} at different pHs.
$pL_{0.5}$ values: a) 3.88 (I = 0.15 mol dm^{-3}) > 3.77 (I = 0.50 mol dm^{-3}) > 3.73 (I = 0.75 mol dm^{-3}) > 3.70 (I = 1.0 mol dm^{-3}).
b) 3.88 (T = 288.15 K) < 3.88 (T = 298.15 K) < 3.92 (T = 318.15 K).
c) 2.98 (pH = 5) < 3.88 (pH = 7.4) <4 .63 (pH = 8.2) < 5.28 (pH = 9)

For a better evaluation of the sequestering ability of ofloxacin towards Ca^{2+} and Zn^{2+}, the diagrams reported in the **Figures 5.8** and **5.9** were drawn. It can be observed that ofloxacin behaves similarly with respect of dopamine, for the effect of pH and temperature on the sequestering ability. For the dependence on I / mol dm^{-3}, an opposite effect was observed between Ca^{2+} and Zn^{2+}, as also observed for dopamine.

A further consideration can be made by considering the sequestering ability of the three ligands studied, towards Zn^{2+}. The $pL_{0.5}$ has been calculated at T = 298.15 K, pH = 7.4 and I = 0.15 mol dm^{-3}, and the results are reported in Figure 5.10, where it is possible to see how ofloxacin has, at these conditions, a greater sequestering abilities towards zinc, with respect to the two other ligands.

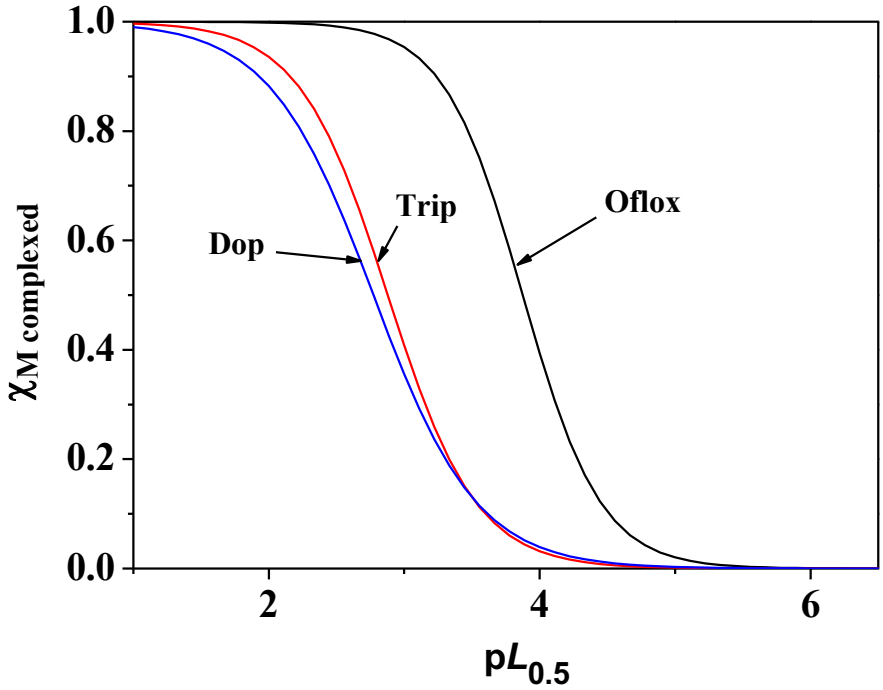

Figure 5.10. Sequestering ability of Dopamine, Tryptophan and Ofloxacine towards Zn^{2+} at $T = 298.15$ K, pH = 7.4 and $I = 0.15$ mol dm^{-3}.
$pL_{0.5}$ Values: 3.88 (Oflox) > 2.88 (Trip) > 2.77(Dop)

5.3 Literature comparison

For the purposes of evaluating the results obtained for this thesis, it is particularly important to make a comparison with the literature data. The research carried out led first of all to carry out the following assessments:

- The main difficulty for a direct comparison with the results here obtained is bound to the determination of the acid-base properties of dopamine.
  In some cases, the ligand was considered as a triprotic ligand (L^{2-}), calculating the third protonation constant with a $\log K^{H}$ value of about 13-14, outside the pH range of physiological interest. In other cases, only the protonation constants of a phenolic group and of the amino group of the alkyl chain have been taken into consideration [165-177].
- Investigations are very often carried out in ionic media that do not simulate the behavior of the components in natural systems (waters and biological fluids) or in mixed solvent media[169, 178-183].
- The different speciation models and the different stability of the species, bound also to the acid-base properties of the metal, dependent on the charges involved in the complex formation reactions.

- The possible limit for the comparison between the results here obtained and the literature ones is due to the neglection from many authors of the hydrolysis of the metal cation in the speciation model used as input. The experimental evidences show instead that in many cases the hydrolytic species of the metal coexist with the complex species and therefore cannot be neglected.

Table 5.7. Literature data for the complexation of dopamine towards metal ions

I/mol dm^{-3}	*T*/K	Metal	Medium	logβ_{ML}	logβ_{MLH}	logβ_{ML_2}	log$\beta_{M(LH)_2}$	logβ_{ML_2H}	logβ_{MLOH}	logβ_{MLOH}	Ref.
0.1	298.15	Cu^{2+}	$HClO_4$	20.56	26.91	-	48.26	-	-	-	[184]
0.2	298.15	Y^{3+}	KCl	7.95	-	14.84	-	-	-	-	[174]
		La^{3+}		6.35	-	11.7	-	-	-	-	[185]
0.2	288.15	Mg^{2+}	NaCl	4.57	-	-	-	-	-	-	[186]
0.2	298.15			4.50	-	-	-	-	-	-	
0.2	308.15			4.49							
0.2	288.15	Zn^{2+}	NaCl	-	-	-	52.94	-	-	-	[176]
	298.15			-	-	-	52.14	-	-	-	
	308.15			-	-	-	51.22	-	-	-	
0.15	310.15	Cu^{2+}	$NaClO_4$	15.44	22.07	23.25	-	-	-	-	[187]
		Ni^{2+}		9.66	18.12	26.07	-	-	-	-	
		Zn^{2+}		11.43	18.89	-	-	-	-	-	
0.2	288.15	MoO_4^{2-}	NaCl	-	-	-	51.48	-	-	-	[188]
	298.15			-	-	-	51.08	-	-	-	
	308.15			-	-	-	50.66	-	-	-	
0.2	298.15	Cu^{2+}	KCl	16.60	24.22	24.78	45.83	35.66	-	-	[165]
		Ni^{2+}		9.42	19.38	14.81	35.66	25.61	-	-	
		Zn^{2+}		-	20.21	18.05	38.93	28.67	-	-	
0.37	293.15	Ni^{2+}	$NaNO_3$	-	18.373	13.86	34.05	-	-	-	[189]
		Cu^{2+}		16.01	23.29	23.47	44.26	-	-	-	
		Zn^{2+}		-	19.33	-	-	-	-	-	
		Cd^{2+}		-	17.991	-	-	-	-	-	
		Pb^{2+}		-	22.23	-	-	-	-	-	

The literature stability constants reported in **Table 5.7**, refer to low ionic strength values (≤ 0.2 mol dm^{-3}), and this does not allow a comparison with the stability constants here reported up to I = 1.0 mol dm^{-3} and for both the dependence on the ionic strength and temperature.

From **Table 5.7,** the only attempt of comparison can be done between the literature metal/dopamine systems and those here reported regards the speciation. We can observe that the speciation models are formed mainly of simple mononuclear species (ML, MLH_i or ML_2).

For the systems reported in the literature, we do not observe the formation of metal polynuclear species, such as M_2L_2 and M_2LOH, here obtained for Sn^{2+}.

A good agreement between our and the literature data there is for Mg^{2+}, $\log\beta_{ML}$ = 4.57-4.49 at I = 0.2 mol dm^{-3} in NaCl aqueous solution and different temperatures (from T = 288.15 to 308.15 K)[186].

As an example, from our investigation we obtained at I = 0.15 mol dm^{-3} and T = 298.15 K, $\log\beta_{ML}$ = 3.034±0.044. The difference with respect the literature value can be explained considering that our speciation model also includes the MLOH species, which become significant at pH values higher than 8.5, and cannot be neglected in the speciation of the system. The formation constant of the ternary hydrolytic species we determined is: $\log\beta_{MLOH}$ = -6.111±0.016 at I = 0.15 mol dm^{-3} and T = 298.15 K.

Concerning Cd^{2+}, Cu^{2+}, Mn^{2+} and Zn^{2+} only simple mononuclear species are reported, and considering the stoichiometry of the species, seems that investigations were limited only to the acid pH range, especially for Cu^{2+}, that as well know, tends to form ternary hydrolytic species [165, 184, 187, 189, 190].

In the case of Cd^{2+}, authors reported only a single Cd^{2+}/Dop^- species, namely the MLH.

Another attempt of comparison to estimate the stability of the complexes of different systems, can be made for the CH_3Hg^+/Dop complexes here determined, and those already reported in a previous investigation for the CH_3Hg^+/Eph (Adrenaline) interactions [191]. A similar speciation model has been obtained; if we compare as a pure example the stability of the complex species at I = 0.15 ml dm^{-3} and T = 298.15 K in NaCl aqueous solution, we have for adrenaline the following values: log β_{ML} = 8.56 (10.43 for Dop); log β_{MLH} = 17.33 (19.43 for Dop); log β_{MLOH} = -0.79 (1.99 for Dop) and log β_{MLCl} = 9.17 (11.21 for Dop). It is possible to observe as dopamine form more stable complexes with CH_3Hg^+ with respect to adrenaline, with a difference of about of two orders of magnitude.

However, the difficulty to carry an accurate comparison between our and literature systems, in terms of different stability of the species, is also due, as already mentioned, to the apparent neglection from the different authors of the hydrolysis of the metals investigated. In fact, in those papers, authors report and discuss about the acid-base properties of dopamine, but no information on the hydrolysis

of the metal and their hydrolytic constants is reported. From our investigation, we have evidenced that the metal hydrolytic species coexist in some cases with the metal/dopamine complexes, as observed for Sn^{2+}, where the $Sn(OH)^{+}$ and $Sn_3(OH)_4^{2+}$ species reach about 10 and 20% of formation in pH range values where the formation of the Sn^{2+}/Dop^{-} complexes occur.

Interesting is also the comparison between the speciation model and the species stability of the Sn^{2+}/Dop^{-} and $(CH_3CH_2)_2Sn^{2+}$/Dop^{-} systems. We observe that the obtained speciation models are similar, except for the binary species; in fact, while $(CH_3CH_2)_2Sn^{2+}$ tends to form an ML species, Sn^{2+} tends to form a M_2L_2 species.

The comparison between the stability of the different species can be made by calculating the stepwise formation constants considering the equilibria reported in **Table 5.8**.

Table 5.8. Stepwise formation constants of the species of the systems $(CH_3CH_2)_2Sn^{2+}$/Dop^{-} and Sn^{2+}/Dop^{-} at I = 0.15 mol dm^{-3} and T = 298.15 K

	log K_{pqr}		**log K_{pqr}**
System	**$(CH_3CH_2)_2Sn^{2+}$**		**Sn^{2+}**
M + L = ML	15.11	2 ML = M_2L_2	~17.42
MOH + L = MLOH	10.89	MOH + L = MLOH	13.27
ML + L = ML_2	5.83	ML + L = ML_2	6.70
ML + MOH = M_2LOH	3.84	ML + MOH = M_2LOH	2.03
		M_2OH_2 + 2 L = M_2L_2 + 2 OH	39.91

Stepwise formation constants were calculated according to the equilibria shown in the table; in the case of the Sn^{2+}/Dop^{-} system, the absence of the ML species in the speciation model complicates the calculation of the partial constants. Neglecting the possible extrastability involved in the formation processes of polynuclear species, it is possible to calculate from M_2L_2 an approximate value of ML according to the simple equilibrium: 2 ML = M_2L_2, and then calculate for the $\log K_{ML}$ a value of approximately 34.83 / 2 = 17.42.

Starting from these data it is possible to calculate for the other species the value of the stepwise constants, which are higher than the analogous ones for the (CH_3CH_2) $2Sn^{2+}$/Dop^{-} system, with the exception of M_2LOH species.

There is no evidence, however, of literature data for the complexes with UO_2^{2+} in aqueous solution.

Considering that the literature reports different speciation models for the different metal-ligand systems, also determined in different experimental conditions, it is particularly difficult to make a comparison only based on the formation constants.

The use of the $pL_{0.5}$ values (at a given experimental conditions), already described, can turn useful to estimate the different sequestering ability of dopamine towards the metal ions.

The $pL_{0.5}$ parameter was calculated at $T = 298.15K$, $I = 0.15$ mol dm^{-3} and pH = 7.4, for some selected metals, taking into account in the speciation model: the protonation constants of dopamine, the hydrolytic constants of the metal, the eventual stability constants of the species formed by the interaction of the metal with the anion of the supporting electrolyte (namely Cl^-) and the stability constants of the metal/dopamine species.

The obtained $pL_{0.5}$ values are reported in Table 5.9; some aspects can be evidenced; the first one is that dopamine has at the same experimental condition, a significant different sequestering ability toward the different metal ions.

This behavior is due to the different acid-base properties of the metal ions that tend to hydrolyze in different pH range and form mono- and/or polynuclear species of different stability, reducing proportionally the amount of free metal able to interact at those conditions with the ligand. Another factor that influences the sequestering ability and the amount of free metal, is the possibility to form complexes with the anion of the supporting electrolyte stable, often stabilized by the amount of the salt in solution.

Table 5.9. $pL_{0.5}$ data comparison

	$pL_{0.5}$	
Metals	**Literature Data**	**Experimental Data**
Cd^{2+}	0.23	1.08
Cu^{2+}	6.60	4.63
Mn^{2+}	1.61	1.58
Sn^{2+}	3.67	3.74
Zn^{2+}	2.61	2.77

As regards the Ofloxacin the only accurate comparison between our and literature ptotonation constants can be made with those published by Ross et al. in NaCl aqueous solution at I = 0.15 mol·dm^{-3} and T = 298.15 K [192]. Authors report the following values, log K^{H}_{1} = 8.22 and log K^{H}_{2} = 6.05, that fit perfectly with our experimental data determined in the same experimental conditions by potentiometric and spectrophotometric titrations. The influence of the ionic strength on the acid-base properties of Ofloxacin in aqueous solutions containing sodium chloride or other supporting electrolytes is difficult to quantify for the absence of data at different ionic strength values.

Table 5.10 Literature data for the hydronation of Ofloxacin in different media

log K^{H}_{1}	log β_{2}^{H}	log K^{H}_{2}	P.I.[a)]	Ref.
8.00	14.00	6.00		[193]
8.11	14.16	6.05		[156]
8.28	14.25	5.97		[155]
8.22	14.27	6.05	7.14	[153]
8.25	13.94	5.69	6.97	[194][b)]
8.21	14.34	6.13		[154]
7.81	14.03	6.22		[195]
8.19	14.34	6.15		[195]
8.20	14.05	5.85		[196][c)]

a)Isoelectric point (calculated from the average value of logK^{H}_{1} and log K^{H}_{2}); b) log K^{H}_{3} = - 0.43; c) log K^{H}_{3} = - 0.45

As regards the medium effect and from the literature data reported in **Table 5.10**, it seems that the different solvents exert a significant influence on the acid-base properties of Ofloxacin; as an example a comparison can be made between the protonation constants reported by Babic et al. in sodium acetate solution at I = 0.05 mol·dm^{-3} (log K^{H}_{1} = 8.28 and log K^{H}_{2} = 5.97) and Barbosa et al. in H_2O/Acetonitrile (log K^{H}_{1} = 8.11 and log K^{H}_{2} = 6.05), respectively [155, 156]. Similar consideration can made with the hydronation constants reported by Völgyl et al. [195] in water/methanol and water/cosolvent mixture (consisting of equal volumes of methanol, dioxane and acetonitrile, as organic solvents). In this paper, authors report the following hydronation constants: log K^{H}_{1} = 7.81 and log K^{H}_{2} = 6.22 in water/methanol mixture, and log K^{H}_{1} = 8.19 and log K^{H}_{2} = 6.15 in the cosolvent mixture. These differences can be justified taking into account the different dielectric constants and polarity of the solvents.

Interesting are also the papers published by Lin et al. [196] and Sasz et al. [194], that report data in H_2O/methanol mixture. Also in this case we observed, especially for the log K_{2}^{H} value, a significant

difference on the constant between the different solvents. Furthermore, in these two papers, the authors report for the hydronation of Ofloxacin, a third protonation constant, which is attributed to the second dehydrogenation of the piperazine substituent, with a log K^{H} value of about -0.4 (see footnote of Table 5.10).

As highlighted in some other literature papers, we also observed a decrease of the hydronation constants increasing the temperature, with a fairly linear variation[192, 197, 198].

Similar results were obtained for the solubility investigations. Also in this case, our experimental results are in very good agreement with the literature data in pure water reported by Baluja et al. and Zhang et al.: $x = 0.000181$ ($T = 295.15$ K) and $x = 0.000143$ ($T = 298.15$ K), that are comparable with our data at $T = 295.15$ K in NaCl $I = 0.15$ mol·dm^{-3}: $x = 0.000184$. The only available data for the concentration of Ofloxacin neutral species in saturated solutions is reported by Ross et al., that report: $S^0 = 0.00764$ mol·dm^{-3} (data adjusted at $I = 0.15$ mol·dm^{-3}). This data is consistent with ours, experimentally obtained by means of spectrophotometric measurements and from mass balance equations, by using the log K^{H}_{n} and the pH values of dissolution: $S^0 = 0.00881$ mol·dm^{-3}.

For Ornidazole, the lack of data in the literature did not allow to make a comparison on the protonation constants. The only available data on the protonation of ornidazole is reported in ref [45], that proposes a log $K^{H} = 2.29$.

Chapter 6

Conclusions

6.1 Conclusions

The work carried out for this PhD thesis concerned the study of the thermodynamic properties in NaCl aqueous solutions of molecules of biological and pharmacological interest.

These studies were performed in wide concentration ranges of the components at different ionic strength and temperature values.

The investigated ligands were dopamine, ofloxacin and ornidazole. Furthermore, in order to investigate also the ternary interactions of the MM'L and MLL 'type, histidine was also considered.

The main results can be summarized as follows:

1. As regards the metal-dopamine systems, applying the criteria for the selection of the best speciation model, the proposed models generally consist of binary and ternary mononuclear species (protonated and/or hydrolytic) having different stability depending on the different acid-base properties of the metals;
2. A different behavior was observed for Cu^{2+} and Sn^{2+}, whose speciation models are characterized by a prevalence of binuclear species with significantly higher stability than the other systems;
3. The Cd^{2+} and CH_3Hg^+/dopamine systems are also worthy of attention; in this case, since the investigations were carried out in aqueous solutions of sodium chloride, the interactions with the anion of the ionic medium, namely Cl^-, assume a fundamental role both on the speciation of the system and on the stability of the metal-ligand species. In fact, while in the first case the $CdCl_i$ complexes and the CdOHCl species avoid the hydrolysis of the metal up to pH values ~ 7, for CH_3Hg^+, the stability of the CH_3HgCl species leads to the formation of a $CH_3HgDopCl^0$ ternary species, which is formed in high percentages of formation and for a wide pH range is the main species;
4. Concerning the UO_2^{2+}/Dop^- system, since the studies were carried out starting from the $UO_2(ac)_2$ product, the speciation of the system is much simpler than that of similar systems studied starting from the $UO_2(NO_3)_2$ salt; also in this case we observed the formation of a highly stable UO_2AcDop^0 ternary complex;
5. The thermodynamic properties of formation of the complex species at different ionic strengths and temperatures were modelled by means of an extended Debye-Hückel equation, containing an additional parameter that based on the Van't Hoff equation allowed the calculation of the standard enthalpy change values of formation; from the obtained results it was observed that the main thermodynamic function for the formation reactions is generally the entropy.

6. The conversion of the ionic strength and formation constants from the molar to the molal concentration scale allowed the application of the Specific ion Interaction Theory (S.I.T.), and the determination of the specific ion interaction coefficient for the ionic species and the Setschenow coefficient for the neutral ones;
7. The different speciation models obtained for the metal/dopamine systems does not allow to make a comparison between them in terms of the different capacity/strength of interaction of dopamine towards the metals. To overcome this problem, it is useful to use the $pL_{0.5}$ parameter, which allowed to quantify the effective sequestrating ability of dopamine against metals, under different experimental conditions: pH, I / mol dm^{-3} and T. The data obtained allowed to obtained at I = 0.15 mol dm^{-3}, T = 298.15 K and pH = 7.4 the following sequestration trend:

   $pL_{0.5}$: $Mg^{2+} < Cd^{2+} \sim Ca^{2+} < Mn^{2+} < CH_3Hg^{+} < Zn^{2+} < Sn^{2+} < DET^{2+} < Cu^{2+} < UO_2^{2+}$

   Obviously, changing the experimental conditions, the trend of the $pL_{0.5}$ can change.
8. The same difficulty was also encountered for the attempt of comparison of the literature data; also, in this case the use of $pL_{0.5}$ was fundamental;
9. Since the components here studied can coexist in multicomponent solutions such as biological fluids, we considered important to study the possible interactions of dopamine with UO_2^{2+}/Cd^{2+} and UO_2^{2+}/Cu^{2+}, and of the same dopamine with Zn^{2+}/ Histidine. Different speciation models were obtained, featured by ternary species of different stoichiometry and stability. These species are characterized by an extrastability with respect to the homologous binary species, avoiding in some case the formation of sparingly soluble species. The high formation percentages of the ternary species highlight that they cannot be neglected for a correct speciation study in multicomponent systems;
10. The further steps of our investigations were the studies of the acid base properties of ofloxacin and ornidazole in aqueous solutions of NaCl at different ionic strength and temperature and the determination of the solubility and concentration of the neutral species. For ofloxacin, two different protonation steps were obtained, the first one bound to the piperazine group and the second to the carboxylic one. From the knowledge of the solubility at the investigated experimental conditions and of the pH of the saturated solution, it was possible by means of simple mass balance equations to calculate the concentration and percentage of the neutral species at each investigated temperature. This allowed the calculation of the enthalpy change values of protonation and of dissolution of ofloxacin.

11. Concerning ornidazole, only a single protonation step has been determined, at from the mass balance equation it was verified that at the pH of dissolution, the ligand is totally presents in neutral form.
12. The interactions of ofloxacin and ornidazole with Ca^{2+} and Zn^{2+} were investigated, and also in this case different speciation models were obtained with different stability of the species.

Supplementary material

Table S.1 Experimental formation constants in molal scale of the Ca^{2+}/Dop^- species in NaCl aqueous solutions at different ionic strengths and temperatures.

T/K	*I*/mol dm^{-3}	logβ_{ML} [a)]	logβ_{MLH} [a)]	logβ_{MLOH} [a)]
288.15	0.150	-	13.60	-6.97
298.15	0.144	4.82	13.42	-5.78
298.15	0.483	3.64	13.26	-7.78
298.15	0.714	2.394	13.62	-6.69
298.15	0.972	5.24	14.40	-6.49
310.15	0.150	-	13.50	-5.60

*a)*logβ_{pqr} refer to Eqs. 4.1 – 4.2

Table S.2 Experimental formation constants in molal scale of the Mg^{2+}/Dop^- species in NaCl aqueous solutions at different ionic strengths and different temperatures.

I/mol dm^{-3}	logβ_{ML} [a)]	logβ_{MLOH} [a)]
	***T* = 288.15 K**	
0.151	3.46	-6.28
0.505	3.26	-6.68
0.760	3.26	-6.91
1.019	3.46	-7.34
	***T* = 298.15 K**	
0.151	3.03	-6.11
0.506	2.79	-6.53
0.763	2.77	-6.83
1.022	2.94	-7.32
	***T* = 310.15K**	
0.151	2.56	-5.93
0.508	2.27	-6.37
0.766	2.22	-6.74
1.027	2.36	-7.31

*a)*logβ_{pqr} refer to Eqs. 4.1 – 4.2

Table S.3 Experimental formation constants in molal scale of the Sn^{2+}/Dop^- species in NaCl aqueous solutions at different ionic strengths and temperatures.

T/K	*I*/mol dm^{-3}	logβ_{M2L2} [a)]	logβ_{ML2} [a)]	logβ_{MLOH} [a)]	logβ_{M2LOH} [a)]
288.15	0.151	35.20	24.50	9.53	15.42
298.15	0.148	34.82	24.11	9.49	15.67
298.15	0.477	34.33	23.09	9.1	15.54
298.15	0.720	33.93	22.50	8.74	15.95
298.15	0.974	31.65	20.73	7.63	15.59
310.15	0.151	32.53	20.88	8.46	14.89

*a)*logβ_{pqr} refer to Eqs. 4.1 – 4.2;

Table S.4 Experimental formation constants in molal scale of the Cd^{2+}/Dop^- species in NaCl aqueous solutions at different ionic strengths and temperatures.

I /mol dm^{-3}	log β_{ML} [a)]	log β_{MLH} [a)]	log β_{ML2} [a)]
	***T*=288.15 K**		
0.150	6.65	14.89	11.61
	***T*=298.15 K**		
0.149	6.48	14.08	10.88
0.494	6.05	14.17	10.30
0.742	6.40	14.70	10.34
0.976	6.29	14.08	9.11
	***T*=310.15 K**		
0.150	4.60	12.55	9.25

*a)*logβ_{pqr} refer to Eqs. 4.1 – 4.2;

Table S.5 Experimental formation constants in molal scale of the Cu^{2+}/Dop^- species in NaCl aqueous solutions at different ionic strengths and temperatures.

	logβ					
***I*/mol dm^{-3}**	**ML_2 [a)]**	**M_2L [a)]**	**M_2L_2 [a)]**	**$M_2L_2(OH)_2$ [a)]**	**M_2LOH [a)]**	**ML_2OH [a)]**
			***T* = 288.15 K**			
0.162	21.02	15.21	27.33	13.40	8.87	11.38
0.496	20.49	15.32	26.85	12.67	9.02	11.24
0.753	20.20	15.41	26.59	12.26	9.20	11.21
1.013	19.94	15.50	26.35	11.88	9.41	11.20
			***T* = 298.15 K**			
0.172	19.35	14.57	25.66	11.72	8.86	11.01
0.480	18.87	14.68	25.20	11.04	9.00	10.88
0.750	18.55	14.77	24.92	10.60	9.19	10.84
0.985	18.31	14.85	24.71	10.26	9.37	10.83
			***T* = 310.15 K**			
0.146	17.58	13.84	23.86	9.94	8.85	10.62
0.490	17.01	13.96	23.33	9.16	8.98	10.46
0.743	16.71	14.05	23.06	8.73	9.15	10.42
1.008	16.44	14.14	22.82	8.35	9.36	10.40
			***T* = 318.15 K**			
0.163	16.39	13.40	22.66	8.73	8.84	
0.515	15.81	13.52	22.12	7.93	8.98	10.18
0.750	15.54	13.60	21.88	7.54		
1.024	15.26	13.69	21.62	7.14	9.34	10.13

a) logβ_{pqr} refer to Eqs. (4.1 – 4.2)

Table S.6 Experimental formation constants in molal scale of the Mn^{2+}/Dop^- species in NaCl aqueous solutions at different ionic strengths and temperatures.

I /mol dm^{-3}	log β_{ML}	log β_{MLH}	log β_{ML2}
		***T*=288.15 K**	
0.140	6.65	14.40	11.4
		***T*=298.15 K**	
0.145	5.42	13.86	10.8
0.464	5.08	13.21	9.53
0.696	5.12	13.53	9.86
0.938	4.57	12.96	8.71
		***T*=310.15 K**	
0.139	4.48	12.33	8.95

a) logβ_{pqr} refer to Eqs. (4.1 – 4.2)

Table S.7 Experimental formation constants in molal scale of the Zn^{2+}/Dop^- species in NaCl aqueous solutions at different ionic strengths and temperatures.

I /mol Kg^{-1}	log β_{ML}	log β_{MLH}	log β_{MLOH}	log β_{ML2H}
		***T*=288.15 K**		
0.148	7.22	14.80	-1.32	22.20
		***T*=298.15 K**		
0.149	7.40	14.50	-0.64	21.63
0.476	6.93	14.23	-1.23	21.24
0.948	6.639	13.83	-1.61	20.21
		***T*=310.15 K**		
0.151	6.60	13.12	-1.31	19.21

a) logβ_{pqr} refer to Eqs. (4.1 – 4.2)

Table S.8 Experimental formation constants in molal scale of the UO_2^{2+}/Dop^- system in NaCl aqueous solutions at different ionic strengths and temperatures.

I /mol dm^{-3}	log β_{ML2} [a)]	log β_{MLAc} [a)]	log β_{MLOH} [a)]
		***T*=288.15 K**	
0.162	21.50	16.10	6.66
0.531	21.87	15.87	6.71
0.752	22.24	15.82	6.83
1.012	22.65	15.80	6.96
		***T*=298.15 K**	
0.166	21.68	16.13	7.09
0.510	21.24	15.65	6.83
0.752	21.21	15.42	6.73
1.013	21.12	15.23	6.64
		***T*=310.15 K**	
0.162	22.14	16.57	7.48
0.513	21.86	16.26	7.29
0.754	21.78	16.15	7.23
1.016	21.72	16.07	7.20
		***T*=318.15 K**	
0.161	22.11	17.21	7.49
0.512	21.96	16.79	7.51
0.757	21.96	16.60	7.60
1.018	21.99	16.45	7.71

a) logβ_{pqr} refer to Eqs. (4.1 – 4.2)

Table S.9 Experimental formation constants in molal scale of the CH_3Hg^+/Dop^- species in NaCl aqueous solutions at different ionic strengths and temperatures

I /mol dm^{-3}	log β_{ML} [a)]	log β_{MLOH} [a)]
	***T*=288.15 K**	
0	3.895	-5.291
0.151	3.458	-6.278
0.505	3.255	-6.676
0.760	3.261	-6.905
1.019	3.459	-7.336
	***T*=298.15 K**	
0	3.559	-5.366
0.151	3.032	-6.111
0.506	2.792	-6.531
0.763	2.770	-6.825
1.022	2.942	-7.324
	***T*=310.15 K**	
0	3.004	-4.796
0.151	2.557	-5.926
0.508	2.274	-6.369
0.766	2.223	-6.736
1.027	2.364	-7.311

a) logβ_{pqr} refer to Eqs. (4.1 – 4.2)

Table S.10 Experimental formation constants in molal scale of the $(CH_3CH_2)_2Sn^{2+}$/Dop^- species in NaCl aqueous solutions at different ionic strengths and temperatures

I /mol Kg^{-1}	log β_{ML}	log β_{MLOH}	log β_{ML2}	log β_{M2LOH}
		***T*=288.15 K**		
0.139	15.96	8.37	22.30	15.55
		***T*=298.15 K**		
0.149	15.11	7.32	20.94	15.38
0.473	14.88	7.38	20.87	13.76
0.713	14.58	6.96	19.77	12.09
0.955	14.18	6.62	18.88	10.04
		***T*=310.15 K**		
0.139	14.32	7.04	19.74	14.07

a) logβ_{pqr} refer to Eqs. (4.1 – 4.2)

Table S.11. Formation constants at infinite dilution and enthalpy change values of the Zn^{2+}/$Tryp^{-}$ species.

	$\log \beta^{T}_{ML}$ b)	$\log \beta^{T}_{ML(OH)2}$ b)	$\log \beta^{T}_{ML2}$ b)
***T* = 298.15 K**			
$I \rightarrow 0$ a)	5.06±0.03 e)	-11.46±0.08 e)	9.68±0.03 e)
C c)	0.45±0.04	0.52±0.12	0.34±0.05
ΔH d)	70.8±13.7	135.1±22.1	155.4±6.4

a) *I*/mol dm^{-3}; b)refers to the Eqs. (4.1 – 4.2); c)parameter for the dependence of $\log\beta_{pqr}$ on *I*/mol dm^{-3}.; d) enthalpy and entropy change values of formation in kJ/mol at *I* = 0.15 mol dm^{-3} ; e) ±Std.Dev

Bibliography

1. Templeton, D. M.; Ariese, F.; Cornelis, R.; Danielsson, L.-G.; Muntau, H.; van Leeuwen, H. P.; Lobinski, R., Guidelines for terms related to chemical speciation and fractionation of elements. Definitions, structural aspects, and methodological approaches (IUPAC Recommendations 2000). *Pure and applied chemistry* **2000,** 72, (8), 1453-1470.
2. Kot, A.; Namieśnik, J., The role of speciation in analytical chemistry. *TrAC Trends in Analytical Chemistry* **2000,** 19, (2), 69-79.
3. Stoecker, B.; Chromium, I., Elements and their Compounds in the Environment, Edited by Merian E., Anke M., Ihnat M., Stoepler M. Wiley-VCH, Weinheim: 2004.
4. Fitzgerald, P. A., *Adrenal Medulla and Paraganglia. Greenspan's Basic & Clinical Endocrinology*. 9th edition ed.; McGraw-Hill: New York, 2011.
5. California, S. D. U. O., *Catecholamines. Health Library*.
6. Fahn, S. In *The History of Levodopa as it Pertains to Parkinson's disease*, The Movement Disorder Society's 10th International Congress of Parkinson's Disease and Movement Disorders, 2006.
7. Benes, F. M., Carlsson and the discovery of dopamine. *Trends Pharmacol. Sci.* **2001,** 22, (1), 46-7.
8. S., B. J., *Ann. Chem.* **1934,** 513, 196.
9. Hahn G.; K., S., *Chem. Ber.* **1936,** 69, 2640.
10. Ben-Jonathan, N.; Hnasko, R., Dopamine as a prolactin (PRL) inhibitor. *Endocr. Rev.* **2001,** 22, (6), 724-63.
11. Cinelli, A. R.; Efendiev, R.; Pedemonte, C. H., Trafficking of Na-K-ATPase and dopamine receptor molecules induced by changes in intracellular sodium concentration of renal epithelial cells. *American Journal of Physiology-Renal Physiology* **2008,** 295, (4), F1117-F1125.
12. Gildea, J. J., Dopamine and angiotensin as renal counterregulatory systems controlling sodium balance. *Curr Opin Nephrol Hypertens* **2009,** 18, (1), 28-32.
13. Shen, H., Illustrated Pharmacology Memory Cards: PharMnemonics. Minireview. 2008. *Back to cited text*, (36), 5.
14. Goldman-Rakic, P. S.; Castner, S. A.; Svensson, T. H.; Siever, L. J.; Williams, G. V., Targeting the dopamine D 1 receptor in schizophrenia: insights for cognitive dysfunction. *Psychopharmacology* **2004,** 174, (1), 3-16.
15. Davis, K. L.; Kahn, R. S.; Ko, G.; Davidson, M., Dopamine in schizophrenia: A review and reconceptualization. *The American Journal of Psychiatry* **1991,** 148, (11), 1474-1486.
16. Gasco, A.; Gualtieri, F.; Melchiorre, C., *Chimica Farmaceutica* 2015.
17. Fromm, H. J.; Hargrove, M. S., Introduction to Biomolecules. In *Essentials of Biochemistry*, Springer: 2012; pp 5-34.
18. Hopkins, F. G.; Cole, S. W., A contribution to the chemistry of proteids: Part I. A preliminary study of a hitherto undescribed product of tryptic digestion. *J Physiol* **1901,** 27, (4-5), 418-428.
19. Kilbourne, E. M.; Philen, R.; Kamb, M.; Falk, H., Tryptophan produced by Showa Denko and epidemic eosinophilia-myalgia syndrome. *The Journal of rheumatology. Supplement* **1996,** 46, 81-8; discussion 89.
20. Cox, G.; King, H., l-Tryptophane. *Org. Synth* **1943,** 2, 612-616.
21. Radwanski, E. R.; Last, R. L., Tryptophan biosynthesis and metabolism: biochemical and molecular genetics. *The Plant Cell* **1995,** 7, (7), 921-934.
22. Kanai, Y.; Segawa, H.; Miyamoto, K.-i.; Uchino, H.; Takeda, E.; Endou, H., Expression Cloning and Characterization of a Transporter for Large Neutral Amino Acids Activated by the Heavy Chain of 4F2 Antigen (CD98) *. *Journal of Biological Chemistry* **1998,** 273, (37), 23629-23632.
23. D.;, B. C. A. J. N., Tryptophan depletion and its implications for psychiatry. *British J. Psyc.* **2001,** 178, ((5)), 399-40.

24. Markus, C. R.; Olivier, B.; de Haan, E. H., Whey protein rich in α-lactalbumin increases the ratio of plasma tryptophan to the sum of the other large neutral amino acids and improves cognitive performance in stress-vulnerable subjects. *The American Journal of Clinical Nutrition* **2002,** 75, (6), 1051-1056.
25. Levkovitz, Y.; Ophir-Shaham, O.; Bloch, Y.; Treves, I.; Fennig, S.; Grauer, E., Effect of L-Tryptophan on Memory in Patients With Schizophrenia. *Journal of Nervous and Mental Disease* **2003,** 191, (9), 568-573.
26. Liao, S.-M.; Du, Q.-S.; Meng, J.-Z.; Pang, Z.-W.; Huang, R.-B., The multiple roles of histidine in protein interactions. *Chemistry Central Journal* **2013,** 7, (1), 44.
27. Vickery, H. B.; Leavenworth, C. S., On the separation of histidine and arginine IV. The preparation of histidine. *Journal of biological chemistry* **1928,** 78, (3), 627-635.
28. Bornhorst, J. A.; Falke, J. J., [16] Purification of proteins using polyhistidine affinity tags. In *Methods in Enzymology*, Academic Press: 2000; Vol. 326, pp 245-254.
29. Watly, J.; Simonovsky, E.; Barbosa, N.; Spodzieja, M.; Wieczorek, R.; Rodziewicz-Motowidlo, S.; Miller, Y.; Kozlowski, H., African Viper Poly-His Tag Peptide Fragment Efficiently Binds Metal Ions and Is Folded into an α-Helical Structure. *Inorganic Chemistry* **2015,** 54, (16), 7692-7702.
30. Ntountoumi, C.; Vlastaridis, P.; Mossialos, D.; Stathopoulos, C.; Iliopoulos, I.; Promponas, V.; Oliver, S. G.; Amoutzias, G. D., Low complexity regions in the proteins of prokaryotes perform important functional roles and are highly conserved. *Nucleic Acids Research* **2019,** 47, (19), 9998-10009.
31. Bisacchi, G. S., Origins of the Quinolone Class of Antibacterials: An Expanded "Discovery Story". *Journal of Medicinal Chemistry* **2015,** 58, (12), 4874-4882.
32. Liu, H.; Mulholland, S. G., Appropriate antibiotic treatment of genitourinary infections in hospitalized patients. *The American Journal of Medicine* **2005,** 118, (7, Supplement), 14-20.
33. Lesher, G. Y.; Froelich, E. J.; Gruett, M. D.; Bailey, J. H.; Brundage, R. P., 1,8-Naphthyridine Derivatives. A New Class of Chemotherapeutic Agents. *Journal of Medicinal and Pharmaceutical Chemistry* **1962,** 5, (5), 1063-1065.
34. Piddock, L. J.; Johnson, M.; Ricci, V.; Hill, S. L., Activities of new fluoroquinolones against fluoroquinolone-resistant pathogens of the lower respiratory tract. *Antimicrobial agents and chemotherapy* **1998,** 42, (11), 2956-2960.
35. Mitscher, L. A., Bacterial Topoisomerase Inhibitors: Quinolone and Pyridone Antibacterial Agents. *Chemical Reviews* **2005,** 105, (2), 559-592.
36. Hooper, D. C., Emerging mechanisms of fluoroquinolone resistance. *Emerg Infect Dis* **2001,** 7, (2), 337-341.
37. K. Naber and D. Adam, *International Journal of Antimicrobial Agents* **1998,** 10, 255–257.
38. Sharma, P. C.; Jain, A.; Jain, S., Fluoroquinolone antibacterials: a review on chemistry, microbiology and therapeutic prospects. *Acta Pol Pharm* **2009,** 66, (6), 587-604.
39. Alhajhusain, A. A. E. S. a. A., *Journal of Antimicrobial Chemotherapy* **2009,** 64, 229– 238.
40. Kuhlmann, F.; Fleckenstein, J., Antiparasitic Agents in Infectious Diseases. Cohen, J.; Powderly, W. G; Opal, SM, Eds. Elsevier: 2017.
41. Nagel, J. L.; Aronoff, D. M., 28 - Metronidazole. In *Mandell, Douglas, and Bennett's Principles and Practice of Infectious Diseases (Eighth Edition)*, Bennett, J. E.; Dolin, R.; Blaser, M. J., Eds. W.B. Saunders: Philadelphia, 2015; pp 350-357.e2.
42. Wilcox, M. H., Nitroimidazoles, metronidazole, ornidazole and tinidazole; and fidaxomicin. In *Infectious Diseases*, Elsevier: 2017; pp 1261-1263. e1.
43. Salo, J. P. K.; Yli-Kauhaluoma, J.; Salomies, H., On the hydrolytic behavior of tinidazole, metronidazole, and ornidazole. *Journal of Pharmaceutical Sciences* **2003,** 92, (4), 739-746.
44. Zameeruddin, M.; Solanke, S.; Kalyankar, S.; Jadhav, S.; Kadam, V.; Bharkad, V., Review on analytical method validation of nitro-imidazoles. *World J Pharm Pharm Sci* **2014,** 3, 557-577.

45. Sanli, S.; Basaran, F.; Sanli, N.; Akmese, B.; Bulduk, I., Determination of Dissociation Constants of Some Antifungal Drugs by Two Different Methods at 298 K. *Journal of Solution Chemistry* **2013,** 42.
46. Rutgeerts, P.; van Assche, G.; Vermeire, S.; D'Haens, G.; Baert, F.; Noman, M.; Aerden, I.; de Hertogh, G.; Geboes, K.; Hiele, M.; D'Hoore, A.; Penninckx, F., Ornidazole for prophylaxis of postoperative Crohn's disease recurrence: A randomized, double-blind, placebo-controlled trial. *Gastroenterology* **2005,** 128, (4), 856-861.
47. Hermann, C. S., Noch ein Schreiben über das neue Metall. *Annalen der Physik* **1818,** 59, (5), 113-116.
48. Peterlik, M.; Stoeppler, M., Calcium. In *Elements and Their Compounds in the Environment*, Merian, E.; Anke, M.; Ihnat, M.; Stoeppler, M., Eds. Wiley-VCH Verlag GmbH: 2008; pp 599-618.
49. Anke, M.; Kramer-Beselia, K.; Losch, E.; Muller, R.; Muller, M.; Seifert, M., Calcium supply, intake, balance and requirement of man. First information: Calcium content of plant food. In *Macro and Trace Elements.*, Schubert, V. H., Ed. Leipzig, 2002; pp 1386-1391.
50. Weaver, C. M., Calcium. *American Society for Nutrition* **2011,** 2, 290–292.
51. Weaver, C. M.; Heaney, R. P., Calcium. In *Modern nutrition in health disease.*, 10th ed ed.; Shils, M. E.; Shike, M.; Ross, A. C.; Caballero, B.; Cousins, R. J., Eds. Lippincott Williams & Wilkins: Baltimore (MD), 2006; pp 194-210.
52. Peacock, M., Calcium Metabolism in Health and Disease. *Clinical Journal of the American Society of Nephrology* **2010,** 5, S23-S30.
53. Anke, M.; Ihnat, M.; Stoeppler, M., Elements and their compounds in the environment. Wiley-VCH, Weinheim: 2004.
54. Bidlack, W. R., Handbook of Nutritional Essential Mineral/Elements. *Journal of the American College of Nutrition* **1997,** 16, (5), 443-443.
55. Flink, E. B., Magnesium deficiency syndrome in man. *Journal of the American Medical Association* **1956,** 160, 1406-1409.
56. Kontani, M.; Hara, A.; Ohta, S.; Ikeda, T., Hypermagnesemia induced by massive cathartic ingestion in an elderly woman without pre-existing renal dysfunction. *Internal Medicine* **2005,** 44, (5), 448-452.
57. Emsley, J., *Nature's building blocks: an AZ guide to the elements*. Oxford University Press: 2011.
58. Sayre, E. V.; Smith, R. W., Compositional categories of ancient glass. *Science* **1961,** 133, (3467), 1824-1826.
59. Ullrich, S. M.; Tanton, T. W.; Abdrashitova, S. A., Mercury in the aquatic environment: a review of factors affecting methylation. *Critical reviews in environmental science and technology* **2001,** 31, (3), 241-293.
60. Kerper, L. E.; Ballatori, N.; Clarkson, T. W., Methylmercury transport across the blood-brain barrier by an amino acid carrier. *American Journal of Physiology-Regulatory, Integrative and Comparative Physiology* **1992,** 262, (5), R761-R765.
61. Guallar, E.; Sanz-Gallardo, M. I.; Veer, P. v. t.; Bode, P.; Aro, A.; Gómez-Aracena, J.; Kark, J. D.; Riemersma, R. A.; Martín-Moreno, J. M.; Kok, F. J., Mercury, fish oils, and the risk of myocardial infarction. *New England Journal of Medicine* **2002,** 347, (22), 1747-1754.
62. Cigala, R. M.; Crea, F.; De Stefano, C.; Lando, G.; Milea, D.; Sammartano, S., The inorganic speciation of tin(II) in aqueous solution. *Geochim. Cosmochim. Acta* **2012,** 87, 1-20.
63. Anger, J. P., Tin. In *Elements and Their Compounds in the Environment*, Merian, E.; Anke, M.; Ihnat, M.; Stoeppler, M., Eds. Wiley-VCH Verlag GmbH: 2008; pp 1113-1124.
64. Lantzy, R. J.; Mackenzie, F. T., Atmospheric trace metals: global cycles and assessment of man's impact. *Geochimica et Cosmochimica Acta* **1979,** 43, (4), 511-525.

65. Senesil, G. S.; Baldassarre, G.; Senesi, N.; Radina, B., Trace element inputs into soils by anthropogenic activities and implications for human health. *Chemosphere* **1999,** 39, (2), 343-377.
66. Howe, P.; Watts, P., *Tin and inorganic tin compounds*. World health organization: 2005.
67. Eisler, R., *Tin hazards to fish, wildlife, and invertebrates: a synoptic review*. Fish and Wildlife Service, US Department of the Interior: 1989.
68. Ichihashi, H.; Nakamura, Y.; Kannan, K.; Tsumura, A.; Yamasaki, S., Multi-elemental concentrations in tissues of Japanese common squid (Todarodes pacificus). *Archives of environmental contamination and toxicology* **2001,** 41, (4), 483-490.
69. Maguire, R.; Tkacz, R.; Chau, Y.; Bengert, G.; Wong, P., Occurrence of organotin compounds in water and sediment in Canada. *Chemosphere* **1986,** 15, (3), 253-274.
70. Blunden, S.; Wallace, T., Tin in canned food: a review and understanding of occurrence and effect. *Food and Chemical Toxicology* **2003,** 41, (12), 1651-1662.
71. Kimbrough, R. D., Toxicity and health effects of selected organotin compounds: a review. *Environmental Health Perspectives* **1976,** 14, 51-56.
72. Guard, H. E.; Cobet, A. B.; Coleman, W., Methylation of trimethyltin compounds by estuarine sediments. *Science* **1981,** 213, (4509), 770-771.
73. Bowen, H.; Blunden, S.; Hobbs, L.; Smith, P., The environmental chemistry of organotin compounds. In *Environmental chemistry*, 1984; pp 49-77.
74. Appel, K. E., Organotin compounds: toxicokinetic aspects. *Drug metabolism reviews* **2004,** 36, (3-4), 763-786.
75. Peganova, S.; Eder, K., Zinc. In *Elements and Their Compounds in the Environment*, Wiley-VCH Verlag GmbH: 2008; pp 1203-1239.
76. Adriano, D. C., Zinc. In *Trace Elements in the Terrestrial Environment*, Springer New York: New York, NY, 1986; pp 421-469.
77. Malle, K. G., Zink in der Umwelt. *Acta hydrochimica et hydrobiologica* **1992,** 20, (4), 196-204.
78. Yeats, P. A., The distribution of trace metals in ocean waters. *Science of The Total Environment* **1988,** 72, 131-149.
79. Siegert, E.; Anke, M.; Szentmihalyi, S.; Regius, A.; Lokay, D.; Powel, J.; Gruen, M., The zinc supply of plants and animals in Middle Europe. In *Trace Element Symposium*, University of Leipzig-Jena, Germany, 1986; pp 487-493.
80. Wastney, M. E.; Aamodt, R. L.; Rumble, W. F.; Henkin, R. I., Kinetic analysis of zinc metabolism and its regulation in normal humans. *The American Journal of Physiology* **1986,** 251, (2), R398-408.
81. Kaltenberg, J.; Plum, L. M.; Ober-Blöbaum, J. L.; Hönscheid, A.; Rink, L.; Haase, H., Zinc signals promote IL-2-dependent proliferation of T cells. *European Journal of Immunology* **2010,** 40, (5), 1496-1503.
82. Agren, M. S., Studies on zinc in wound healing. *Acta dermato-venereologica. Supplementum* **1990,** 154, 1-36.
83. Powell, S. R., The antioxidant properties of zinc. *The Journal of Nutrition* **2000,** 130, (5S Suppl), 1447S-1454S.
84. Tuerk, M. J.; Fazel, N., Zinc deficiency. *Current Opinion in Gastroenterology* **2009,** 25, (2), 136-143.
85. Health, N. I. o., Zinc - Fact Sheet for Health Professionals. *Office of Dietary Supplements* **2013**.
86. Rouessac, F.; Rouessac, A., *Chemical analysis: modern instrumentation methods and techniques*. John Wiley & Sons: 2013.
87. Robinson, J. W.; Frame, E. M. S.; Frame, G. M.; Eileen, M.; Skelly, F., Undergraduate instrumental analysis. **2005**.

88. De Stefano, C.; Foti, C.; Giuffrè, O.; Mineo, P.; Rigano, C.; Sammartano, S., Binding of Tripolyphosphate by Aliphatic Amines: Formation, Stability and Calculation Problems. *Ann. Chim. (Rome)* **1996,** 86, 257-280.
89. De Stefano, C.; Mineo, P.; Rigano, C.; Sammartano, S., Ionic Strength Dependence of Formation Constants. XVII. The Calculation of Equilibrium Concentrations and Formation Constants. *Ann. Chim. (Rome)* **1993,** 83, 243-277.
90. Daniele, P. G.; De Robertis, A.; De Stefano, C.; Sammartano, S.; Rigano, C., On the Possibility of Determining the Thermodynamic Parameters for the Formation of Weak Complexes Using a Simple Model for the Dependence on Ionic Strength of Activity Coefficients. Na^+, K^+ and Ca^{2+} Complexes of Low Molecular Weight Ligands in Aqueous Solution. *J. Chem. Soc. Dalton Trans.* **1985**, 2353-2361.
91. De Stefano, C.; Princi, P.; Rigano, C.; Sammartano, S., Computer Analysis of Equilibrium Data in Solution. ESAB2M: An Improved Version of the ESAB Program. *Ann. Chim. (Rome)* **1987,** 77, 643-675.
92. De Stefano, C.; Sammartano, S.; Mineo, P.; Rigano, C., Computer Tools for the Speciation of Natural Fluids. In *Marine Chemistry - An Environmental Analytical Chemistry Approach*, Gianguzza, A.; Pelizzetti, E.; Sammartano, S., Eds. Kluwer Academic Publishers: Amsterdam, 1997; pp 71-83.
93. Gans, P.; Sabatini, A.; Vacca, A., Investigation of equilibria in solution. Determination of equilibrium constants with the HYPERQUAD suite programs. *Talanta* **1996,** 43, 1739-1753.
94. Flaschka, H. A., *EDTA (ethylenediamine Tetra-acetic) Titrations: An Introduction to Theory and Practice*. Pergamon: 1964.
95. Davies, C., Ion association.,(Butterworths: London). *Ion association. Butterworths, London.* **1962**, -.
96. De Robertis, A.; Foti, C.; Sammartano, S.; Gianguzza, A., Chemical Speciation of Some Classes of Low Molecular Weight Ligands in Seawater. In *Marine Chemistry - An Environmental Analytical Chemistry Approach*, Gianguzza, A.; Pelizzetti, E.; Sammartano, S., Eds. Kluwer Academic Publishers: Amsterdam, 1997; pp 59-69.
97. McCutcheon, S. C. M., J.J.; Barnwe, l.T.O., *Water Quality*. New York, NY, USA, 1993.
98. Apruzzese, F.; Bottari, E.; Festa, M. R., Protonation equilibria and solubility of l-cystine. *Talanta* **2002,** 56, (3), 459-469.
99. McMaster, L.; Bender, E.; Weil, E., The solubility of phthalic acid in water and sodium sulfate solutions. *Journal of the American Chemical Society* **1921,** 43, (5), 1205-1207.
100. Rivett, A.; Rosenblum, E., The influence of a second solute on the solubility of ortho-phthalic acid. *Transactions of the Faraday Society* **1914,** 9, 297-309.
101. Viçoso, C.; Lito, M.; Camoes, M., Solubility and osmotic coefficient of phthalic acid aqueous solutions from isopiestic measurements. *Analytica chimica acta* **2004,** 514, (1), 131-135.
102. Pitzer, K. S., Thermodynamics of electrolytes. I. Theoretical basis and general equations. *The Journal of Physical Chemistry* **1973,** 77, (2), 268-277.
103. Bromley, L. A., Thermodynamic properties of strong electrolytes in aqueous solutions. *AIChE Journal* **1973,** 19, (2), 313-320.
104. G., B., Ionic Media. *Dahlem workshop on the nature of seawater, Dahelem Konferenzen: Berlin* **1975**, 339.
105. Brønsted, J., Calculation of the osmotic and activity functions in solutions of uni-univalent salts. *Journal of the American Chemical Society* **1922,** 44, (5), 938-948.
106. Ciavatta, L., The specific interaction theory in evaluating ionic equilibria. *Ann. Chim.(Rome)* **1980,** 70, 551.
107. Garrels, R.; Thompson, M., A chemical model for sea water at 25 degrees C and one atmosphere total pressure. *American Journal of Science* **1962,** 260, (1), 57-66.

108. Guggenheim, E., L. The specific thermodynamic properties of aqueous solutions of strong electrolytes. *The London, Edinburgh, and Dublin Philosophical Magazine and Journal of Science* **1935,** 19, (127), 588-643.
109. Setschenow, J., Über die Konstitution der Salzlösungen auf Grund ihres Verhaltens zu Kohlensäure. *Zeitschrift für Physikalische Chemie* **1889,** 4U, (1), 117-125.
110. Bretti, C.; Crea, F.; De Stefano, C.; Foti, C.; Materazzi, S.; Vianelli, G., Thermodynamic Properties of Dopamine in Aqueous Solution. Acid-Base Properties, Distribution, and Activity Coefficients in NaCl Aqueous Solutions at Different Ionic Strengths and Temperatures. *J. Chem. Eng. Data* **2013,** 58, 2835-2847.
111. Baes Jr, C.; Mesmer, R., The Hydrolysis of cations. *Willey, New-York* **1976**.
112. Cigala, R. M.; Crea, F.; De Stefano, C.; Sammartano, S.; Vianelli, G., Thermodynamic Parameters for the Interaction of Amoxicillin and Ampicillin with Magnesium in NaCl Aqueous Solution, at Different Ionic Strengths and Temperatures. *Journal of Chemical and Engineering Data* **2017,** 62, (3), 1018-1027.
113. Crea, F.; Foti, C.; Milea, D.; Sammartano, S., Speciation of Cadmium in the Environment. In *Cadmium: From Toxicity to Essentiality*, Sigel, A.; Sigel, H.; Sigel, R. K. O., Eds. Springer Science + Business Media B.V.: Dordrecht, 2013; Vol. 11, pp 63-83.
114. De Stefano, C.; Gianguzza, A.; Leggio, T.; Sammartano, S., Dependence on ionic strength of hydrolysis constants for dioxouranium(VI) in $NaCl_{(aq)}$ and $NaNO_{3(aq)}$, at pH < 6 and t = 25°C. *J. Chem. Eng. Data* **2002,** 47, (3), 533-538.
115. Crea, F.; De Robertis, A.; Sammartano, S., Dioxyuranium carboxylate complexes. Formation and stability of acetate species at different ionic strengths in $NaCl_{aq}$. *Ann. Chim. (Rome)* **2003,** 93, 1027-1035.
116. Brown, P. L.; Ekberg, C., *Hydrolysis of metal ions*. John Wiley & Sons: 2016.
117. Crea, F.; De Stefano, C.; Foti, C.; Milea, D.; Sammartano, S., Chelating agents for the sequestration of mercury(II) and monomethyl mercury(II). *Curr. Med. Chem.* **2014,** 21, (33), 3819-3836.
118. De Robertis, A.; Foti, C.; Patanè, G.; Sammartano, S., Hydrolysis of $(CH_3)Hg^+$ in Different Ionic Media: Salt Effects and Complex Formation. *J. Chem. Eng. Data* **1998,** 43, 957-960.
119. Foti, C.; Gianguzza, A.; Sammartano, S., Interaction of alkyltin(IV) compounds with ligands of interest in the speciation of natural fluids: carboxylate and hydroxycarboxylate complexes of monomethyltin(IV) trichloride. *Ann. Chim. (Rome)* **2002,** 92, (7-8), 705-715.
120. Foti, C.; Gianguzza, A.; Milea, D.; Sammartano, S., Hydrolysis and chemical speciation of $(C_2H_5)_2Sn^{2+}$, $(C_2H_5)_3Sn^+$ and $(C_3H_7)_3Sn^+$ in aqueous media simulating the major composition of natural waters. *Appl. Organomet. Chem.* **2002,** 16, 34-43.
121. Crea, F.; De Stefano, C.; Irto, A.; Lando, G.; Materazzi, S.; Milea, D.; Pettignano, A.; Sammartano, S., Understanding the Solution Behavior of Epinephrine in the Presence of Toxic Cations: A Thermodynamic Investigation in Different Experimental Conditions. *Molecules* **2020,** 25, (3), 511.
122. Cigala, R. M.; Crea, F.; De Stefano, C.; Lando, G.; Milea, D.; Sammartano, S., Thermodynamics of binary and ternary interactions in the tin(II)/phytate system in aqueous solutions, in the presence of Cl^- or F^-. *J. Chem. Thermodyn.* **2012,** 51, 88–96.
123. Cigala, R. M.; Crea, F.; De Stefano, C.; Lando, G.; Manfredi, G.; Sammartano, S., Quantitative study on the interaction of Sn^{2+} and Zn^{2+} with some phosphate ligands, in aqueous solution at different ionic strengths. *J. Mol. Liquids* **2012** 165, 143-153.
124. Cigala, R. M.; Crea, F.; De Stefano, C.; Milea, D.; Sammartano, S.; Scopelliti, M., Speciation of tin(II) in aqueous solution: thermodynamic and spectroscopic study of simple and mixed hydroxocarboxylate complexes. *Monatsh. Chem.* **2013,** 144, (6), 761-772.
125. Bretti, C.; Foti, C.; Sammartano, S., A new approach in the use of SIT in determining the dependence on ionic strength of activity coefficients. Application to some chloride salts of interest in the speciation of natural fluids. *Chem. Spec. Bioavail.* **2004,** 16, (3), 105-110.

126. Grenthe, I. P. I., *Modelling in Aquatic Chemistry*. OECD: Paris, France, 1997.
127. Berto, S.; Crea, F.; Daniele, P. G.; Gianguzza, A.; Pettignano, A.; Sammartano, S., Advances in investigation of dioxouranium(VI) complexes of interest for natural fluids. *Coord. Chem. Rev.* **2012,** 256, 63-81.
128. Crea, F.; Milea, D.; Sammartano, S., Enhancement of hydrolysis through the formation of mixed hetero-metal species: dioxouranium(VI)-cadmium(II) mixtures. *Ann. Chim. (Rome)* **2005,** 95, 767-778.
129. Beck, M. T.; Nagypal, I.; Williams, D., *Chemistry of complex equilibria*. Horwood Chichester, New York: 1990.
130. De Robertis, A.; De Stefano, C.; Gianguzza, A., Salts Effects On The Protonation of L-Histidine and L-Aspartic Acid: A Complex Formation Model. *Thermochim. Acta* **1991,** 177, 39-57.
131. Bretti, C.; Crea, F.; De Stefano, C.; Sammartano, S.; Vianelli, G., Some thermodynamic properties of DL-Tyrosine and DL-Tryptophan. Effect of the ionic medium, ionic strength and temperature on the solubility and acid–base properties. *Fluid Phase Equilibria* **2012,** 314, 185– 197.
132. Altun, Y.; Köseoĝlu, F., Stability of copper (II), nickel (II) and zinc (II) binary and ternary complexes of histidine, histamine and glycine in aqueous solution. *Journal of solution chemistry* **2005,** 34, (2), 213-231.
133. Arena, G.; Call, R.; Cucinotta, V.; Musumeci, S.; Rizzarelli, E.; Sammartano, S., Thermodynamics of metal complexes with ligand–ligand interaction. Mixed complexes of copper (II) and zinc (II) with adenosine 5′-triphosphate and L-histidine or histamine. *Journal of the Chemical Society, Dalton Transactions* **1984**, (8), 1651-1658.
134. Bottari, E.; Festa, M., Histidine and ornithine as ligands towards zinc (II). *Journal of coordination chemistry* **1990,** 22, (3), 237-248.
135. Perrin, D.; Sharma, V., Histidine complexes with some bivalent cations. *Journal of the Chemical Society A: Inorganic, Physical, Theoretical* **1967**, 724-728.
136. Pettit, L. D.; Powell, K., The IUPAC stability constants database. *Chemistry international* **2006**.
137. Bergen Jr, R.; Long, F., The salting in of substituted benzenes by large ion salts. *The Journal of Physical Chemistry* **1956,** 60, (8), 1131-1135.
138. Choi, M. Y.; Chan, C. K., Continuous measurements of the water activities of aqueous droplets of water-soluble organic compounds. *The Journal of Physical Chemistry A* **2002,** 106, (18), 4566-4572.
139. Czeisler, J. L.; Schrier, E. E., Activity coefficients in aqueous carboxylic acid-sodium carboxylate solutions. *Journal of Chemical and Engineering Data* **1969,** 14, (1), 6-9.
140. Dolar, D.; Bester, M., Activity coefficient of a polyelectrolyte from solubility measurements. *The Journal of Physical Chemistry* **1995,** 99, (13), 4763-4767.
141. Grabnar, I.; Bogataj, M.; Mrhar, A., Influence of chitosan and polycarbophil on permeation of a model hydrophilic drug into the urinary bladder wall. *International journal of pharmaceutics* **2003,** 256, (1-2), 167-173.
142. Han, N.; Zhu, L.; Wang, L.; Fu, R., Aqueous solubility of m-phthalic acid, o-phthalic acid and p-phthalic acid from 298 to 483 K. *Separation and purification technology* **1999,** 16, (2), 175-180.
143. Kwak, J. C.; Morrison, N. J.; Spiro, E. J.; Iwasa, K., Mean activity coefficients for the simple electrolyte in aqueous mixtures of polyelectrolyte and simple electrolyte. The mixed counterion system sodium (1+), calcium (2+), chloride (1-), polystyrenesulfonate. *The Journal of Physical Chemistry* **1976,** 80, (25), 2753-2761.
144. Larson, W., The The Activity Coefficients of the Undissociated Part of Weak Acids. III. Orthophos-phoric A cid. *The Journal of Physical Chemistry* **1950,** 54, (3), 310-315.

145. Larson, W.; Tomsicek, W., The Activity Coefficients of the Undissociated Part of Weak Acids. I. Acetic Acid in Potassium Acetate Solutions. *Journal of the American Chemical Society* **1939,** 61, (1), 65-67.
146. Larson, W.; Tomsicek, W., The Activity Coefficients of the Undissociated Part of Weak Acids. II. Oxalic Acid. *Journal of the American Chemical Society* **1941,** 63, (12), 3329-3331.
147. Lewis, G. N.; Randall, M., *Thermodynamics and the free energy of chemical substances*. McGraw-Hill: 1923.
148. Xie, W.-H.; Shiu, W.-Y.; Mackay, D., A review of the effect of salts on the solubility of organic compounds in seawater. *Marine Environmental Research* **1997,** 44, (4), 429-444.
149. Carta, R., Solubilities ofL-cystine, L-tyrosine, L-leucine, and glycine in sodium chloride solutions at various pH values. *The Journal of Chemical Thermodynamics* **1998,** 30, (3), 379-387.
150. Carta, R.; Tola, G., Solubilities of L-cystine, L-tyrosine, L-leucine, and glycine in aqueous solutions at various pHs and NaCl concentrations. *Journal of Chemical & Engineering Data* **1996,** 41, (3), 414-417.
151. Apelblat, A.; Manzurola, E., Solubility of oxalic, malonic, succinic, adipic, maleic, malic, citric, and tartaric acids in water from 278.15 to 338.15 K. *The Journal of Chemical Thermodynamics* **1987,** 19, (3), 317-320.
152. Guo, Y.; Yin, Q.; Hao, H.; Zhang, M.; Bao, Y.; Hou, B.; Chen, W.; Zhang, H.; Cong, W., Measurement and correlation of solubility and dissolution thermodynamic properties of furan-2-carboxylic acid in pure and binary solvents. *Journal of Chemical & Engineering Data* **2014,** 59, (4), 1326-1333.
153. Okeri, H. A.; Arhewoh, I. M., Analytical profile of the fluoroquinolone antibacterials. I. Ofloxacin. *African Journal of Biotechnology* **2008,** 7, (6).
154. Rusu, A.; Tóth, G.; Szőcs, L.; Kökösi, J.; Kraszni, M.; Gyéresi, Á.; Noszál, B., Triprotic site-specific acid–base equilibria and related properties of fluoroquinolone antibacterials. *Journal of pharmaceutical and biomedical analysis* **2012,** 66, 50-57.
155. Babić, S.; Horvat, A. J.; Pavlović, D. M.; Kaštelan-Macan, M., Determination of pKa values of active pharmaceutical ingredients. *TrAC Trends in Analytical Chemistry* **2007,** 26, (11), 1043-1061.
156. Barbosa, J.; Bergés, R.; Toro, I.; Sanz-Nebot, V., Protonation equilibria of quinolone antibacterials in acetonitrile-water mobile phases used in LC. *Talanta* **1997,** 44, (7), 1271-1283.
157. Crisponi, G.; M Nurchi, V.; Crespo-Alonso, M.; Toso, L., Chelating agents for metal intoxication. *Current medicinal chemistry* **2012,** 19, (17), 2794-2815.
158. Bazzicalupi, C.; Bianchi, A.; Giorgi, C.; Clares, M. P.; García-España, E., Addressing selectivity criteria in binding equilibria. *Coordination Chemistry Reviews* **2012,** 256, (1-2), 13-27.
159. Sigel, A.; Sigel, H.; Sigel, R. K., *Cadmium: from toxicity to essentiality*. Springer: 2013; Vol. 11.
160. Vacca, A.; Nativi, C.; Cacciarini, M.; Pergoli, R.; Roelens, S., A new tripodal receptor for molecular recognition of monosaccharides. A paradigm for assessing glycoside binding affinities and selectivities by 1H NMR spectroscopy. *Journal of the American Chemical Society* **2004,** 126, (50), 16456-16465.
161. Roelens, S.; Vacca, A.; Venturi, C., Binding of ionic species: A general approach to measuring binding constants and assessing affinities. *Chemistry–A European Journal* **2009,** 15, (11), 2635-2644.
162. Nativi, C.; Francesconi, O.; Gabrielli, G.; Vacca, A.; Roelens, S., Chiral Diaminopyrrolic Receptors for Selective Recognition of Mannosides, Part 1: Design, Synthesis, and Affinities of Second-Generation Tripodal Receptors. *Chemistry–A European Journal* **2011,** 17, (17), 4814-4820.

163. Vacca, A.; Francesconi, O.; Roelens, S., BC50: A generalized, unifying affinity descriptor. *The Chemical Record* **2012,** 12, (6), 544-566.
164. Schwarzenbach, G., " Complexometric Titrations" translated by H. *Irving, Methuen & Co. Ltd., London* **1957**, 78.
165. Kiss, T.; Gergely, A., Complexes of 3, 4-dhydroxyphnyl derivatives, III. Equilibrium study of parent and some mixed ligand complexes of dopamine, alanine and pyrocatechol with nickel (II), copper (II) and zinc (II) ions. *Inorganica Chimica Acta* **1979,** 36, 31-36.
166. Rajan, K.; Davis, J.; Colburn, R., METAL CHELATES IN THE STORAGE AND TRANSPORT OF NEUROTRANSMITTERS: INTERACTIONS OF METAL IONS WITH BIOGENIC AMINES 1. *Journal of neurochemistry* **1971,** 18, (3), 345-364.
167. Palomar-Pardavé, M.; Alarcón-Angeles, G.; Ramírez-Silva, M.; Romero-Romo, M.; Rojas-Hernández, A.; Corona-Avendaño, S., Electrochemical and spectrophotometric determination of the formation constants of the ascorbic acid-β-cyclodextrin and dopamine-β-cyclodextrin inclusion complexes. *Journal of Inclusion Phenomena and Macrocyclic Chemistry* **2011,** 69, (1), 91-99.
168. Zelano, V.; Zerbinati, O.; Ostacoli, G., Ternary Cu (II) complex-formation with L-dopa or dopamine and valine, leucine, phenylalanine and threonine in aqueous-solution. *ANNALI DI CHIMICA* **1988,** 78, (5-6), 273-283.
169. Bard, B.; Martel, S.; Carrupt, P.-A., High throughput UV method for the estimation of thermodynamic solubility and the determination of the solubility in biorelevant media. *European journal of pharmaceutical sciences* **2008,** 33, (3), 230-240.
170. Kiss, T.; Sovago, I.; Martin, R. B., Complexes of 3, 4-dihydroxyphenyl derivatives. 9. Aluminum (3+) binding to catecholamines and tiron. *Journal of the American Chemical Society* **1989,** 111, (10), 3611-3614.
171. Sedeh, I. F.; Sjöberg, S.; Öhman, L.-O., Equilibrium and structural studies of silicon (IV) and aluminum (III) in aqueous solution. 31. Aqueous complexation between silicic acid and the catecholamines dopamine and L-DOPA. *Journal of inorganic biochemistry* **1993,** 50, (2), 119-132.
172. Gerard, C.; Chehhal, H.; Hugel, R., Complexes of iron (III) with ligands of biological interest: dopamine and 8-hydroxyquinoline-5-sulphonic acid. *Polyhedron* **1994,** 13, (4), 541-597.
173. Kiss, T.; Jakusch, T.; Kilyén, M.; Kiss, E.; Lakatos, A., Solution speciation of bioactive Al (III) and VO (IV) complexes. *Polyhedron* **2000,** 19, (24-25), 2389-2401.
174. Aydin, R., Study on the interaction of Yttrium (III) with adrenaline, noradrenaline, and dopamine. *Journal of Chemical & Engineering Data* **2007,** 52, (6), 2400-2404.
175. Corona-Avendano, S.; Alarcon-Angeles, G.; Rosquete-Pina, G. A.; Rojas-Hernandez, A.; Gutierrez, A.; Ramírez-Silva, M. T.; Romero-Romo, M.; Palomar-Pardave, M., New insights on the nature of the chemical species involved during the process of dopamine deprotonation in aqueous solution: theoretical and experimental study. *The Journal of Physical Chemistry B* **2007,** 111, (7), 1640-1647.
176. Bagheri Gh, A., Thermodynamic complexation of dopamine with zinc (II) in media with different dielectric constants. *Chinese Journal of Chemistry* **2009,** 27, (6), 1073-1078.
177. Mohamed, G. G.; El-Dien, F. N.; El-Nahas, R., New copper (II) complexes with dopamine hydrochloride and vanillymandelic acid: Spectroscopic and thermal characterization. *Spectrochimica Acta Part A: Molecular and Biomolecular Spectroscopy* **2011,** 81, (1), 489-497.
178. Antikainen, P. J. W., U., A Comparative Study on the Ionization of Catechol Amines in Aqueous Solutions. *Acta Chemica Scandinavica* **1973,** 27, 2075-2082.
179. Nagy, P. I.; Takács-Novák, K., Tautomeric and conformational equilibria of biologically important (hydroxyphenyl) alkylamines in the gas phase and in aqueous solution. *Physical Chemistry Chemical Physics* **2004,** 6, (10), 2838-2848.

180. Corona-Avendaño, S.; Alarcón-Angeles, G.; Ramírez-Silva, M. T.; Rosquete-Pina, G.; Romero-Romo, M.; Palomar-Pardavé, M., On the electrochemistry of dopamine in aqueous solution. Part I: The role of [SDS] on the voltammetric behavior of dopamine on a carbon paste electrode. *Journal of Electroanalytical Chemistry* **2007,** 609, (1), 17-26.
181. Liu, X.; Kang, J.; Wang, Y.; Li, W.; Guo, H.; Xu, L.; Guo, X.; Zhou, F.; Jia, X., Amine-Triggered Dopamine Polymerization: From Aqueous Solution to Organic Solvents. *Macromolecular rapid communications* **2018,** 39, (12), 1800160.
182. Djozan, D.; Amir-Zehni, M., Determination of L-dopa and L-dopamine in aqueous solutions using in-loop SPME coupled with LC. *Chromatographia* **2005,** 62, (3), 127-132.
183. Milovanović, B.; Ilić, J.; Stanković, I. M.; Popara, M.; Petković, M.; Etinski, M., A simulation of free radicals induced oxidation of dopamine in aqueous solution. *Chemical Physics* **2019,** 524, 26-30.
184. Verastegui-Omaña, B.; Palomar-Pardavé, M.; Rojas-Hernández, A.; Avendaño, S. C.; Romero-Romo, M.; Ramírez-Silva, M., Spectrophotometric quantification of the thermodynamic constants of the complexes formed by dopamine and Cu (II) in aqueous media. *Spectrochimica Acta Part A: Molecular and Biomolecular Spectroscopy* **2015,** 143, 187-191.
185. Aydin, R. I., D., Potentiometric and Spectrophotometric Studies of the Complexation of Lanthanum(III) with Adrenaline, Noradrenaline, and Dopamine. *J. Chem. Eng. Data* **2012,** 57, 967-973.
186. Bagheri, A.; Boghaei, D.; Monajjemi, M., Thermodynamic Complexation of Dopamine with Magnesium (II) in Media with Different Dielectric Constants. *Main Group Metal Chemistry* **2008,** 31, (1-2), 81-92.
187. Mansoor, S. S., Mixed Metal complexes of Copper (II), Nickel (II) and Zinc (II) Involving Dopa and Dopamine. *International Journal of Chem Tech Research* **2010,** 2, (1), 640-645.
188. Gh Bagheri, A., Thermodynamic Complexation of Dopamine with Molybdenum (VI) in Media with Different Dielectric Constants. *Journal of Chemical & Engineering Data* **2009,** 54, (11), 2981-2985.
189. Grgas-Kužnar, B.; Simeon, V.; Weber, O., Complexes of adrenaline and related compounds with Ni2+, Cu2+, Zn2+, Cd2+ and Pb2+. *Journal of Inorganic and Nuclear Chemistry* **1974,** 36, (9), 2151-2154.
190. Sheik Mansoor, S., Mixed metal complexes of Copper(II), Nickel(II) and Zinc(II) involving Dopa and Dopamine. *Int. Journal of ChemTech research* **2010,** 2, 640-645.
191. Crea, F.; De Stefano, C.; Irto, A.; Lando, G.; Materazzi, S.; Milea, D.; Pettignano, A.; Sammartano, S., Understanding the Solution Behavior of Epinephrine in the Presence of Toxic Cations: A Thermodynamic Investigation in Different Experimental Conditions. *Molecules* **2020,** 25, (3).
192. Ross, D. L.; Riley, C. M., Aqueous solubilities of some variously substituted quinolone antimicrobials. *International Journal of Pharmaceutics* **1990,** 63, (3), 237-250.
193. Azeem, W.; John, P.; Nazar, M. F.; Ashfaq, M.; Khan, I. U.; Sharif, S.; Riaz, A., Fixed-Dose combination antibiotics interacting with a quaternary ammonium disinfectant: insights from spectral and chromatographic measurements. *Journal of Solution Chemistry* **2018,** 47, (6), 1048-1059.
194. Szász, G.; Takácsné, N.; Budváriné, B.; Hermecz, I.; Jozan, M.; Lore, A.; Noszal, B., Correlation between the structures and physicochemical properties of chemotherapeutic fluoroquinolone agents. *Acta Pharmaceutica Hungarica* **1993,** 63, (3), 105-114.
195. Völgyi, G.; Ruiz, R.; Box, K.; Comer, J.; Bosch, E.; Takács-Novák, K., Potentiometric and spectrophotometric pKa determination of water-insoluble compounds: validation study in a new cosolvent system. *Analytica chimica acta* **2007,** 583, (2), 418-428.

196. Lin, C.-E.; Deng, Y.-J.; Liao, W.-S.; Sun, S.-W.; Lin, W.-Y.; Chen, C.-C., Electrophoretic behavior and pKa determination of quinolones with a piperazinyl substituent by capillary zone electrophoresis. *Journal of Chromatography A* **2004,** 1051, (1-2), 283-290.
197. Baluja, S.; Gajera, R.; Bhatt, M.; Bhalodia, R.; Vekariya, N., Solubility of Ofloxacin in 1, 2-Dichloromethane, Chloroform, Carbon Tetrachloride, and Water from (293.15 to 313.15) K. *Journal of Chemical & Engineering Data* **2010,** 55, (2), 956-958.
198. Zhang, C.-L.; Wang, Y., Aqueous solubilities for ofloxacin, norfloxacin, lomefloxacin, ciprofloxacin, pefloxacin, and pipemidic acid from (293.15 to 323.15) K. *Journal of Chemical & Engineering Data* **2008,** 53, (6), 1295-1297.